BIOREMEDIATION OF PHENOLIC COMPOUNDS IN CIRCULATING PACKED BED BIOREACTOR

A Thesis Submitted to the College of

Graduate and Postdoctoral Studies

In Partial Fulfillment of the Requirements

For the Degree of Ph.D.

In the School of Environment and Sustainability

University of Saskatchewan

Saskatoon

By

Yi Zhou

PERMISSION TO USE

In presenting this thesis in partial fulfillment of the requirements for a Ph.D. degree from the University of Saskatchewan, I agree that the Libraries of this University may make it freely available for inspection. I further agree that permission for copying of this thesis in any manner, in whole or in part, for scholarly purposes may be granted by the professor or professors who supervised my thesis work or, in their absence, by the Head of the Department or the Dean of the College in which my thesis work was done. It is understood that any copying or publication or use of this thesis/dissertation or parts thereof for financial gain shall not be allowed without my written permission. It is also understood that due recognition shall be given to me and to the University of Saskatchewan in any scholarly use which may be made of any material in my thesis.

Requests for permission to copy or to make other uses of materials in this thesis in whole or part should be addressed to:

Executive Director
School of Environment and Sustainability
University of Saskatchewan
Room 329, Kirk Hall
117 Science Place
Saskatoon, Saskatchewan S7N 5C8

OR

Dean
College of Graduate and Postdoctoral Studies
University of Saskatchewan
116 Thorvaldson Building, 110 Science Place
Saskatoon, Saskatchewan S7N 5C9
Canada

ABSTRACT

Wastewaters containing phenolic compounds such as phenol and cresols pose a high risk to human health and natural environment. Compared to physicochemical methods, bioremediation is an attractive alternative for removal of phenolic compounds from contaminated waters. This research aimed to evaluate bioremediation of phenolic compounds in batch systems and in continuously operated circulating packed bed bioreactors (CPBBs).

The biodegradation of individual phenol, o-cresol, and p-cresol and mixtures of these compounds (binary and ternary mixtures) were studied. In addition to creating kinetic data on biodegradation of these contaminants, toxicity of the treated effluents generated under various conditions were assessed. Effects of initial concentrations and temperatures were investigated in batch system. Work in continuous flow CPBBs focused on the impact of phenols concentration and loading rate on the removal percentage and removal rate for influents containing individual and mixture of phenols (binary and ternary) for a wide range of conditions. The toxicity of treated effluent samples generated under various conditions was determined and compared with the employed influents to evaluate the potential risk of releasing the effluents into natural water bodies.

In batch systems, a linear relationship between biodegradation rate and initial concentration of p-cresol or o-cresol was observed for the range of initial concentrations evaluated. The optimum temperature for biodegradation of p-cresol and o-cresol were 35 and 25 °C, respectively. In a binary mixture, the presence of phenol enhanced p-cresol biodegradation. During both binary- and

ternary-biodegradation, p-cresol was the preferred substrate and utilized first, while phenol and o-cresol were used simultaneously (if both were present) upon complete exhaustion of p-cresol. The interaction of phenols in the ternary mixture was more complicated, as a result, polynomial models were used to describe the impact of initial concentration on biodegradation rate. It was shown that increase in p-cresol and o-cresol initial concentrations had positive effects on biodegradation rate of all three phenols, but their interaction appeared to impact the biodegradation rate negatively. In batch system the maximum observed biodegradation rates for phenol, p-cresol, and o-cresol were 17.8, 8.9, and 7.2 mg L^{-1} h^{-1}, respectively.

In continuous flow CPBBs, the maximum removal rates of phenol, p-cresol, and o-cresol were 82.6, 107.2, and 73.8 mg L^{-1} h^{-1} at the loading rates of 104.7 (residence time: 4.7 h), 183.9 (residence time: 2.8 h), and 163.9 mg L^{-1} h^{-1} (residence time: 1.8 h), respectively under mono-substrate biodegradation. For binary-substrate biodegradation, the presence of o-cresol had a negative impact on phenol removal rate, while p-cresol did not impose the same effect. The maximum removal rates of phenol and p-cresol during binary-substrate biodegradation were 89.2 and 78.4 mg L^{-1} h^{-1} at their respective loading rates of 137.9 and 123.9 mg L^{-1} h^{-1}. The maximum removal rates of phenol and o-cresol during binary-substrate biodegradation were 119.9 and 70.3 mg L^{-1} h^{-1} at the respective loading rates of 209.8 and 112.9 mg L^{-1} h^{-1}. When all three substrates were present in the influent, the maximum removal rates of phenol, p-cresol, and o-cresol were 129.2, 135.3, and 108.0 mg L^{-1} h^{-1} at their corresponding loading rates of 179.3, 195.9, and 165.7 mg L^{-1} h^{-1}. It was also shown that p-cresol was the preferred substrate, followed by phenol and o-cresol. In case of untreated influents, p-cresol presented the most toxicity, followed by o-cresol, with phenol presenting the least toxicity among these three compounds. Toxicity evaluation of

effluents obtained under various operating conditions revealed that overall treatment in CPBBs reduced the toxicity of influent containing phenolic compounds, although the decrease in toxicity differed pending on the operating conditions such as nature of phenolic compound, its influent concentration and loading rate.

ACKNOWLEDGEMENTS

I would like to acknowledge my sincere gratitude to my supervisor, Dr. Mehdi Nemati for his tireless help and guidance throughout my Ph.D. Without his encouragement, patience, and detail-oriented comments, I simply would not make it to the end. In addition, I would want to express my appreciation to my committee members, Dr. Wonjae Chang, Dr. Jafar Soltan, and Dr. Paul Jones. I also want to say thanks to Richard Blondin, who provided technical supports and suggestions. I also wish to express my thanks to our lab member, Fangzhou Dong, Guadalupe Valdes Labrada, Suraj Kumar, and Lyman Moreno for their recommendation and help when I encountered problems.

I would also like to express my appreciation to the University of Saskatchewan, School of Environment and Sustainability, Chinese Scholarship Council (CSC), and Natural Sciences and Engineering Research Council of Canada (NSERC) for their financial support during my studies as a Ph.D. student.

DEDICATION

To my parents, sister, and brother in law for their endless love and support.

TABLE OF CONTENTS

Page

PERMISSION TO USE i
ABSTRACT ii
ACKNOWLEDGEMENTS v
DEDICATION vi
TABLE OF CONTENTS vii
LIST OF TABLES x
LIST OF FIGURES xiii
1 INTRODUCTION 1
2 LITERATURE REVIEW AND RESEARCH OBJECTIVES 7
2.1 Phenol and Cresols 7
2.2 Health Issues Associated with Phenols 9
2.3 Exiting Methods to Remove Phenols from Contaminated Waters 10
2.3.1 Chemical Oxidation 11
2.3.2 Adsorption 12
2.3.3 Solvent Extraction 13
2.3.4 Electrochemical Incineration 15
2.3.5 Bioremediation 16
2.4 Different Types of Bioremediation 19
2.4.1 In-situ Bioremediation 20
2.4.2 Ex-situ Bioremediation 20
2.4.3 Factors Affecting Bioremediation 21
2.4.4 Advantages and Disadvantages of Bioremediation 21
2.5 Bioreactors 22
2.5.1 Stirred Tank Bioreactors 24
2.5.2 Membrane Bioreactors 25
2.5.3 Airlift Bioreactors 27
2.6 Existing Studies of Bioremediation of Phenols 29
2.6.1 Phenols Biodegradation Pathway 29

2.6.2 Recent Studies of Phenols Biodegradation 30
2.7 Knowledge Gap and Research Objectives 32
3 MATERIALS AND METHODS 34
3.1 Chemicals 34
3.2 Culture and Medium 35
3.3 Batch Experiments 36
3.3.1 Effect of the Initial Concentration of Phenolic Compounds 36
3.3.2 Effect of Temperature 38
3.3.3 Co-biodegradation of Phenolic compounds (binary and ternary substrates) 38
3.3.4 Control Experiments 40
3.4 Experimental Set-up for continuous biodegradation of phenolic compounds in Circulating Packed Bed Bioreactors (CPBB) 41
3.4.1 Biofilm Development 43
3.4.2 Continuous Experiments 44
3.5 Analytical Methods 50
3.6 Toxicity Test Procedures 52
3.7 Statistical Analysis 52
4 RESULTS AND DISCUSSION – BATCH SYSTEM 54
4.1 Batch Biodegradation of p-cresol 54
4.1.1 Effects of p-cresol Initial Concentration 54
4.1.2 Effects of Temperature on Biodegradation of p-cresol 58
4.2 Batch Biodegradation of o-cresol 62
4.2.1 Effects of o-cresol Initial concentration 62
4.2.2 Effects of Temperature on Biodegradation of o-cresol 65
4.3 Comparison of the Biodegradation Process of p-cresol and o-cresol in Batch System 68
4.4 Binary-substrate Biodegradation 70
4.4.1 Co-biodegradation of Phenol and p-cresol 70
4.4.2 Co-biodegradation of Phenol and o-cresol 74
4.5 Ternary Biodegradation of phenol, p-cresol, and o-cresol 79
5 RESULTS AND DISCUSSION – CONTINUOUS SYSTEM 95
5.1 Biodegradation of Phenol 95
5.1.1 Toxicity Evaluation of Influents and Effluents 101

5.2 Biodegradation of p-cresol 107
5.2.1 Toxicity Evaluation of Influent and Effluent 112
5.3 Biodegradation of o-cresol 116
5.3.1 Toxicity Evaluation of Influent and Effluent 121
5.4 Comparison of Biodegradation of phenol, p-cresol, and o-cresol 124
5.5 Co-biodegradation of Phenol and p-cresol 130
5.5.1 Toxicity Assessment for Co-biodegradation of Phenol and p-cresol 137
5.6 Co-biodegradation of Phenol and o-cresol 140
5.6.1 Toxicity Assessment for Co-biodegradation of Phenol and o-cresol 148
5.7 Ternary Biodegradation of phenol, p-cresol, and o-cresol 152
5.7.1 Toxicity Assessment for ternary biodegradation of phenol, p-cresol, and o-cresol…..……..…….176
6 CONCLUSIONS 184
7 RECOMMENDATIONS FOR FUTURE WORK 189
REFERENCE LIST 192
APPENDICES 207
Appendix A Conference Contribution 207
Appendix B Sample Calculations 208
Appendix C HPLC Chromatogram 209
Appendix D Calibration Curves and Experimental Data Uncertainties 210
D1 Biomass Calibration Curve 210
D2 Phenols Calibration Curve (Spectrophotometeric method) 211
D3 HPLC Calibration Curves 213
D4 Control Experiments and Calculation of Data Uncertainty……215

LIST OF TABLES

Table 2.1 Chemical and physical properties of phenol and cresols (Verschueren, 1983) 9

Table 2.2 Examples of biodegradation studies reported in the literature 31

Table 3.1 Initial concentrations used in mono-substrate batch biodegradation experiments..... 37

Table 3.2 Initial concentrations of phenols in binary-substrate batch biodegradation experiments 39

Table 3.3 Initial concentrations of phenols used in ternary-substrate batch biodegradation experiments 40

Table 3.4 Specifications of 1st and 2nd circulating packed bed bioreactors (CPBB)..... 42

Table 3.5 Concentration of phenolic compounds, flow rates and corresponding residence time of ternary-substrate biodegradation in CPBB 49

Table 4.1 Effect of initial concentration of p-cresol on its biodegradation rate..... 58

Table 4.2 Effect of temperature on biodegradation rate of p-cresol 61

Table 4.3 Effect of initial concentration of o-cresol on its biodegradation rate..... 65

Table 4.4 Effect of temperature on biodegradation rate of o-cresol 68

Table 4.5 Paired t-test results of effect of temperature on the biodegradation rate of p-cresol and o-cresol 70

Table 4.6 Summary of the biodegradation rates of phenol and p-cresol in binary-substrate system 73

Table 4.7 Summary of the biodegradation rates of phenol and o-cresol in binary-substrate system 78

Table 4.8 Results of paired t-test of effect of the initial concentration of p-cresol and o-cresol on phenol biodegradation..... 79

Table 4.9 Summary of the biodegradation rates of phenol, p-cresol, and o-cresol in ternary-substrate batch system..... 85

Table 4.10 Results of ANOVA test for significance of various coefficients in Equation 4.4 87

Table 4.11 Results of ANOVA test for significance of various coefficients in Equation 4.5…..90

Table 4.12 Results of ANOVA test for significance of various coefficients in Equation 4.6…..91

Table 5.1 Results of normality checking and paired t-test..... 106

Table 5.2 Results of normality checking and paired t-test..... 116

Table 5.3 Results of normality checking and paired t-test..... 124

Table 5.4 Comparison of toxicity of influent and effluents of various phenolic compounds after 2 h exposure..... 130

Table 5.5 Experimental results for co-biodegradation of phenol and p-cresol in CPBB under steady state conditions 134

Table 5.6 Experimental results for co-biodegradation of phenol and o-cresol in CPBB under steady state conditions 146

Table 5.7 Experimental results for ternary biodegradation of phenol, p-cresol, and o-cresol in CPBBs under steady state conditions 159

Table 5.8 Experimental results for ternary biodegradation of phenol, p-cresol, and o-cresol in CPBB under steady state conditions..... 167

Table 5.9 Experimental results for ternary biodegradation of phenol, p-cresol, and o-cresol in CPBB under steady state conditions 174

Table D.1 Standard deviation calculation for biomass concentration..... 217

Table D.2 Standard deviation calculation for circulating packed bed bioreactor data 218

LIST OF FIGURES

Figure 2.1 Schematic diagram of continuous stirred-tank bioreactor 25

Figure 2.2 Schematic diagram of hollow fiber membrane bioreactor 26

Figure 2.3 Schematic diagram of Circulating Packed Bed Bioreactor 28

Figure 3.1 Schematic diagram of an experimental set-up 42

Figure 3.2 Photograph of experimental set-up 43

Figure 3.3 Photograph of biofilm development. Photo in the left shows the bioreactor at the early stage of biofilm formation, while the right photo represents the biofilm toward the end of 8 weeks. 44

Figure 4.1 Biomass growth and substrate biodegradation profiles obtained with various initial concentrations of p-cresol at room temperature (24 ± 1 °C). (A): 100 mg L^{-1}, (B): 200 mg L^{-1}, (C): 300 mg L^{-1}, (D): 500 mg L^{-1}. Error bars represent one standard deviation and may not be visible in some cases. 56

Figure 4.2 Biomass growth and p-cresol concentrations obtained at various temperatures. (A): 10 °C, (B): 15 °C, (C): 20 °C, (D): 30 °C, (E): 35 °C. Error bars represent one standard deviation and may not be visible in some cases. 61

Figure 4.3 Biomass growth and substrate biodegradation profile obtained with various initial o-cresol concentration at room temperature (24 ± 2 °C). (A): 100 mg L^{-1}, (B): 200 mg L^{-1}, (C) 300: mg L^{-1}, (D): 500 mg L^{-1}. Error bars represent one standard deviation and may not be visible in some cases. 64

Figure 4.4 Biomass growth and o-cresol concentrations observed at various temperatures. (A): 10 °C, (B): 15 °C, (C): 20 °C, (D): 30 °C, (E): 35 °C. Error bars represent one standard deviation and may not be visible in some cases. 67

Figure 4.5 Biodegradation rate of p-cresol and o-cresol as a function of initial concentration (left panel) and temperature (right panel). 69

Figure 4.6 Co-biodegradation of phenol and p-cresol in mixtures of different compositions. Phenol concentration 500 mg L^{-1} and p-cresol concentration of 100 (A), 200 (B), 300 (C-1), 300 (C-2), 400 (D), and 500 mg L^{-1} (E). Duplicate experimental results are presented in panels C-1 and C-2. Error bas represent standard deviation and may not be visible in some cases..... 72

Figure 4.7 Biodegradation rates of p-cresol at different initial concentrations in the presence and absence of phenol. 74

Figure 4.8 Co-biodegradation of phenol and o-cresol. Phenol concentration: 500 mg L^{-1} and o-cresol concentration: 100 (A), 200 (B), 300 (C-1), 300 (C-2), 400 (D), 500 mg L^{-1} (E). Duplicate experimental results are presented in panels C1 and C-2 at an o-cresol concentration of 300 mg L^{-1}. Error bars represent standard deviation and may not be visible in some cases. ... 76

Figure 4.9 Biodegradation rates of o-cresol at different initial concentrations in the presence and absence of phenol. 78

Figure 4.10 Co-biodegradation of phenol, p-cresol, and o-cresol in mixtures of different compositions. Phenol concentration of 500 mg L^{-1} and p-cresol concentration of 100 mg L^{-1} with 100 (A), 200 (B), 300 (C), 400 (D) mg L^{-1} o-cresol; phenol concentration of 500 mg L^{-1} and p-cresol concentration of 200 mg L^{-1} with 100 (E), 200 (F), 300 (G), 400 (H) mg L^{-1} o-cresol; phenol concentration of 500 mg L^{-1} and p-cresol concentration of 300 mg L^{-1} with 100 (I), 200 (J), 300 (K), and 400 (L) mg L^{-1} o-cresol; phenol concentration of 500 mg L^{-1} and p-cresol concentration of 400 mg L^{-1} with 100 (M), 200 (N) mg L^{-1} o-cresol. Error bas represent one standard deviation and may not be visible in some cases. 83

Figure 4.11 Contour plot of phenol biodegradation rate with respect to p-cresol and o-cresol initial concentration. 88

Figure 4.12 Parity chart for the experimental data against the predicted values by the modified response model (Equation 4.4) 89

Figure 4.13 Contour plot for p-cresol biodegradation rate with respect to p-cresol and o-cresol intial concentrations. 91

Figure 4.14 Parity chat for the experimental data against the values predicted by the modified response model (Equation 4.5) 91

Figure 4.15 Contour plot for o-cresol biodegradation rate with respect to p-cresol and o-cresol initial concentration. 94

Figure 4.16 Parity chat for the experimental data against the values predicted by the modified response model (Equation 4.6) 94

Figure 5.1 Residual concentration of phenol as a function of its loading rate for influents containing 100, 300 and 500 mg L^{-1} phenol. Each point represents the average value of the data obtained over an extended period equal to at least three residence times after the establishment of steady state. Error bars represent standard deviations and might not be visible in some cases..... 97

Figure 5.2 The effect of phenol loading rate on the performance of the CPBB. Panel (A): 98.6 ± 1.9 mg L^{-1} phenol, Panel (B): 295.4 ± 10.2 mg L^{-1} phenol, Panel (C): 496.3 ± 9.3 mg L^{-1} phenol. Each point represents the average value of the data obtained over an extended period of operation equal to at least three residence times after the establishment of steady state. Error bars represent standard deviation and may not be visible in some cases..... 100

Figure 5.3 Comparison of phenol removal rate as a function of its loading rate for the influents containing different phenol concentrations..... 101

Figure 5.4 Results of toxicity test on the CPBB influent and treated effluent. Panel (A): Toxicity of influent with different levels of phenol; Panel (B): Toxicity results of effluents with the maximum removal rate. Error bars represent standard deviation and may not be visible in some cases..... 103

Figure 5.5 Boxplot of the difference of death percentage score between influent and effluent at different exposure time. 106

Figure 5.6 Residual concentration of p-cresol as a function of its loading rate for influents containing 100, 300 and 500 mg L^{-1} p-cresol. Each point represents the average value of the data obtained over an extended period after the establishment of steady state. Error bars represent standard deviation and may not be visible in some cases. 108

Figure 5.7 The effect of p-cresol loading rate on the performance of the CPBB. Panel (A): 98.6 ± 1.9 mg L^{-1} p-cresol, Panel (B): 294.3 ± 3.6 mg L^{-1} p-cresol, Panel (C): 485.9 ± 10.3 mg L^{-1} p-cresol. Each point represents the average value of the data obtained over an extended period of operation after the establishment of steady state. Error bars represent standard deviation and may not be visible in some cases. 111

Figure 5.8 Comparison of p-cresol removal rate as a function of its loading rate with influents containing different p-cresol concentrations..... 112

Figure 5.9 Results of p-cresol toxicity test. Panel (A): Influent toxicity; Panel (B): Toxicity results of effluents with the maximum removal rate. Error bars represent standard deviation and may not be visible in some cases. 114

Figure 5.10 Boxplot of the difference of death percentage score between influent and effluent at different exposure time. 115

Figure 5.11 Residual concentration of o-cresol as a function of its loading rate for influents containing 100, 300 and 500 mg L^{-1} o-cresol. Each point represents the average value after the establishment of steady state. Error bars represent standard deviation and may not be visible in some cases..... 117

Figure 5.12 The effect of o-cresol loading rates on the performance of the CPBB. Panel (A): 95.6 ± 7.3 mg L^{-1} o-cresol, Panel (B): 302.6 ± 9.3 mg L^{-1} o-cresol, Panel (C): 506.9 ± 5.7 mg L^{-1} o-cresol. Each point represents the average value after the establishment of steady state. Error bars represent standard deviation and may not be visible in some cases. 119

Figure 5.13 Comparison of o-cresol removal rate as a function of its loading rate with influents containing different o-cresol concentrations..... 120

Figure 5.14 Results of o-cresol toxicity test. Panel (A): Influent toxicity; Panel (B): Toxicity results of effluents with the maximum removal rate. Error bars represent standard deviation and may not be visible in some cases. 122

Figure 5.15 Boxplot of the difference of death percentage score between influent and effluent at different exposure time. 124

Figure 5.16 Removal rate as a function of loading rate in the CPBBs fed with different phenolic substrate with influent concentrations of (A): 100 mg L^{-1}; (B): 300 mg L^{-1}; and (C) 500 mg L^{-1}..... 127

Figure 5.17 Toxicity comparison of phenolic compounds influent with different concentration: (A): 100 mg L^{-1}; (B): 300 mg L^{-1}; and (C): 500 mg L^{-1}..... 130

Figure 5.18 Residual concentration as a function of loading rate obtained with various combinations of phenol and p-cresol in the influent. Panel (A): phenol; Panel (B): p-cresol. Each point represents the average value of the data obtained after the establishment of steady state. Error bars represent standard deviation and may not be visible in some cases..... 132

Figure 5.19 Removal percentages and removal rates and of phenol and p-cresol as a function of their respective loading rates in the CPBB fed with various combinations of phenol and p-cresol in the feed. Panel (A): phenol removal percentage vs. loading rate; Panel (B): p-cresol removal percentage vs. its loading rate; Panel (C): phenol removal rate vs. its loading rate; Panel (D): p-cresol removal rate vs. its loading rate. Each point represents the average value of the data obtained after the establishment of steady states. Error bars represent standard deviation and may not be visible in some cases. 135

Figure 5.20 Results of toxicity test for co-biodegradation of binary-substrate (500 mg L^{-1} phenol and p-cresol). Panel (A): Toxicity of influent solution (untreated); Panel (B): Toxicity of effluents obtained with maximum removal rate of phenol; (C): Toxicity of effluents with maximum removal rate of p-cresol. Error bars represent standard deviation of repeated tests and may not be visible in some cases. 140

Figure 5.21 Residual concentrations of phenol and o-cresol as a function of their loading rate obtained with various combinations of phenol and o-cresol in the influent. Panel (A): phenol; Panel (B) o-cresol. Each point represents the average value of the data obtained after the establishment of steady state. Error bars represent standard deviation and may not be visible in some cases..... 142

Figure 5.22 Removal percentages and removal rates and of phenol and o-cresol as a function of their respective loading rates in the CPBB fed with various combinations of phenol and o-cresol in the feed. Panel (A): phenol removal percentage vs. its loading rate; Panel (B): o-cresol removal percentage vs. its loading rate; Panel (C): phenol removal rate vs. its loading rate; Panel (D): o-cresol removal rate vs. its loading rate. Each point represents the average value of the data obtained after the establishment of steady state. Error bars represent standard deviation and may not be visible in some cases. 147

Figure 5.23 Results of toxicity test for co-biodegradation of 500 mg L^{-1} phenol and o-cresol of different concentrations. Panel (A): Toxicity of influent solution (untreated); Panel (B): Toxicity of effluents obtained when maximum removal rate of phenol was reached; (C): Toxicity of effluents obtained when maximum removal rate of o-cresol was reached. Error bars represent standard deviation of repeated tests and may not be visible in some cases..... 151

Figure 5.24 Residual concentration as a function of loading rate obtained with various combinations of phenol, p-cresol, and o-cresol influent concentrations. Panel (A): phenol; Panel (B) p-cresol; Panel (C): o-cresol. Each point represents the average value of the data obtained after the establishment of steady state. Error bars represent standard deviation and may not be visible in some cases. 154

Figure 5.25 Removal percentages and removal rates of phenol, p-cresol and o-cresol as a function of their respective loading rates in the CPBB fed with 500 mg L^{-1} phenol and 100 mg L^{-1} p-cresol and various concentration of o-cresol in the influent. Panel (A): phenol removal percentage vs. its loading rate; Panel (B): p-cresol removal percentage vs. its loading rate; Panel (C): o-cresol removal percentage vs. its loading rate; Panel (D): phenol removal rate vs. its loading rate; Panel (E): p-cresol removal rate vs. its loading rate; Panel (F): o-cresol removal rate vs. its loading rate. Each point represents the average value of the data obtained after the establishment of steady states. Error bars represent standard deviation and may not be visible in some cases. 160

Figure 5.26 Residual concentration as a function of loading rate obtained with various combinations of phenol, p-cresol, and o-cresol influent concentrations. Panel (A): phenol; Panel (B) p-cresol; Panel (C): o-cresol. Each point represents the average value of the data obtained after the establishment of steady state. Error bars represent standard deviation and may not be visible in some cases. 162

Figure 5.27 Removal percentages and removal rates and of phenol, p-cresol and o-cresol as a function of their respective loading rates in the CPBB fed with 500 mg L^{-1} phenol and 300 mg L^{-1} p-cresol and various concentration of o-cresol in influent. Panel (A): phenol removal percentage vs. its loading rate; Panel (B): p-cresol removal percentage vs. its loading rate; Panel (C): o-cresol removal percentage vs. its loading rate; Panel (D): phenol removal rate vs. its loading rate; Panel (E): p-cresol removal rate vs. its loading rate; Panel (F): o-cresol removal rate vs. its loading rate. Each point represents the average value of the data obtained after the establishment of steady states. Error bars represent standard deviation and may not be visible in some cases. 168

Figure 5.28 Residual concentration as a function of loading rate obtained with various combinations of phenol, p-cresol, and o-cresol influent concentrations. Panel (A): phenol;

Panel (B) p-cresol; Panel (C): o-cresol. Each point represents the average value of the data obtained after the establishment of steady state. Error bars represent standard deviation and may not be visible in some cases. 170

Figure 5.29 Removal percentages and removal rates and of phenol, p-cresol and o-cresol as a function of their respective loading rates in the CPBB fed with 500 mg L^{-1} phenol and 500 mg L^{-1} p-cresol and various concentration of o-cresol in influent. Panel (A): phenol removal percentage vs. its loading rate; Panel (B): p-cresol removal percentage vs. its loading rate; Panel (C): o-cresol removal percentage vs. its loading rate; Panel (D): phenol removal rate vs. its loading rate; Panel (E): p-cresol removal rate vs. its loading rate; Panel (F): o-cresol removal rate vs. its loading rate. Each point represents the average value of the data obtained after the establishment of steady states. Error bars represent standard deviation and may not be visible in some cases. 175

Figure 5.30 Toxicity results for influent containing 500 mg L^{-1} phenol, 100 mg L^{-1} p-cresol and various concentration of o-cresol. 176

Figure 5.31 Toxicity of effluent samples when 500 mg L^{-1} phenol and 100 mg L^{-1} p-cresol was in influent. Panel (A): under phenol maximum removal rate; Panel (B): under p-cresol maximum removal rate; Panel (C): under o-cresol maximum removal rate. Error bars represent standard deviation and may not be visible in some cases. B in the bracket indicates best performance (under maximum removal rate) for the compound. 179

Figure 5.32 Toxicity of effluent samples when 500 mg L^{-1} phenol and 300 mg L^{-1} p-cresol was in influent. Panel (A): under phenol maximum removal rate; Panel (B): under p-cresol maximum removal rate; Panel (C): under o-cresol maximum removal rate. Error bars represent standard deviation and may not be visible in some cases. B in the bracket indicates best performance (under maximum removal rate) for the compound. 181

Figure 5.33 Toxicity of effluent samples when 500 mg L^{-1} phenol and 500 mg L^{-1} p-cresol was in influent. Panel (A): under phenol maximum removal rate; Panel (B): under p-cresol maximum removal rate; Panel (C): under o-cresol maximum removal rate. Error bars represent standard deviation and may not be visible in some cases. B in the bracket indicates best performance (under maximum removal rate) for the compound. 183

Figure C.1 The representative HPLC chromatogram of phenols. 209

Figure D.1 Biomass calibration curve..... 210

Figure D.2 Calibration curve developed for various phenol concentrations. 211

Figure D.3 Calibration curve developed for various p-cresol concentrations. 212

Figure D.4 Calibration curve developed for various o-cresol concentrations. 212

Figure D.5 HPLC calibration curve for phenol (A), p-cresol (B), and o-cresol (C)……...210

Figure D.6 Control experiments results: (A) phenol; (B) p-cresol; (C) o-cresol……216

1 INTRODUCTION

Water contamination has become a serious problem around the globe. For instance, in 2010, United States produced 720 kg per capita municipal wastewater (USEPA, 2017). According to the US Environmental Protection Agency (USEPA) report, until 2004, there have been approximately 40,000 sites contaminated with various kinds of chemicals. Toxic chemicals, especially heavy metals and toxic organic compounds such as polycyclic aromatic hydrocarbons (PAHs) can enter the food chain. If not appropriately treated, pollution will continue to affect the ecological system and human health, causing diseases in respiratory, cardiovascular, gastrointestinal, dermal and other systems (Das, 2014).

Petroleum is one of the most important energy sources in the world as human activities and livelihood heavily dependent on fossil fuels. However, the recovery and conversion of petroleum to valuable products can result in the generation of toxic contaminants, thus causing the disturbance in the air, soil and groundwater (Gogoi et al., 2003). World crude oil production reached 4.4 billion metric tons in 2015 (World Energy Council, 2016). Wastewaters produced during the process of petroleum production and refinery poses a serious threat to the ecological environment. Severe pollution of water bodies can happen as a result of oils spills from the rupture of the pipes, sudden release from oil wells, and leakage from storage tanks and other processing equipment (Kumar, 2010). The recent Saskatchewan oil spills is an example. The rupture of a section of Husky Energy pipeline caused the discharge of oil into North Saskatchewan River, which had a major impact on thousands of residents in communities downstream of the leak (CBC, 2016). Spills such as these could release large quantities of toxic compounds into the aquatic

environment. Some of these compounds can persist in the natural environment for a long time, as it is challenging for them to be naturally degraded. Xenobiotic and recalcitrant compounds such as chlorophenol are typical examples (Jernberg and Jansson, 2002).

Other than altering present way of industrial development, improving education, having ecological identity work (Thomashow, 1996), having more strict law enforcement towards pollution, and developing highly advanced pollution prevention technologies could also help to mitigate the existing problems and prevent future contamination (Head et al., 2003). The lack of awareness about the consequences of pollution is one of the contributing reasons to environmental pollution (Hoque and Clarke, 2013). In the process of globalization, environmental social justice and advanced technology are highly demanded with the trend towards a more rational path to achieve economic growth (Moss, 2008). Pollution prevention has been used to reduce costs, improve efficiency, reduce risk, and reduce liability; therefore, it could and should be promoted to be incorporated into the management practices of industrial firms (Moss, 2008).

Wastewaters are categorized as domestic and industrial wastewaters. Domestic wastewaters are from domestic and household activities as well as commercial and business buildings and institutions, while industrial wastewaters originate from various manufacturing processes. Compared to industrial wastewaters, domestic wastewaters usually have predictable quality and quantity; thus, domestic wastewaters require relatively standard treatment techniques. Examples of these techniques include physical (sedimentation, screening, aeration, filtration, etc.), chemical (chlorination, ozonation, coagulation, etc.), and biological treatment (aerobic and anaerobic bioremediation) (Muralikrishna and Manickam, 2017).

By contrast, industrial wastewaters usually have compositions that are more complex and are difficult to treat and require industry-by-industry examination and treatment technology (Muralikrishna and Manickam, 2017). The successful design of treatment plants for industrial wastewaters depends on a thorough investigation of the characteristics of the wastewaters and a study of the best choice of the specific method of treatment (Muralikrishna and Manickam, 2017). The techniques for industrial wastewaters treatment are discussed in the next chapter.

One group of the highly toxic compounds in industrial wastewaters are phenolic compounds. Phenolic compounds have been reported to be highly stable due to the difficulty of cleavage of the benzene ring (Das and Chandran, 2011). The aromatic structure of phenols contributes to their resistance to natural biodegradation. Most industrial wastewater contains more than one type of toxic organic compounds, so investigation on the biodegradation of multi-substrates will help to gain a better understanding of the degradation and treatment processes. Phenol and cresols are examples of the most widely occurring types of toxic compounds that can persist in the environment for a long time. Furthermore, they are common intermediates of degradation of other compounds such as toluene (Basha et al., 2010). Therefore, in this study, they were identified as suitable model candidates for studying the biodegradation process in batch and continuous systems. Specifically, we chose phenol, p-cresol, and o-cresol as the target contaminants in this study with the rationale for this choice is given in the relevant section of Materials and Methods.

Among the wastewater treatment methods, bioremediation appears as a cost-effective approach with minimal environmental impacts. The continuous endeavor to improve this technique helps to

reduce the cost of wastewater treatments and overall efficiency. The concepts of bioremediation shaped the way in which one could view sustainability within the framework and definition from the report *Our Common Future* (Brundtland, 1987). Economic development and industrial production are inevitable for humanity; therefore, the treatment of wastes and decontamination play a critical role in preventing the large-scale pollution and restoring the ecological function of polluted sites. Maintaining manufacturing and industrial process while avoiding contamination as much as possible is an urgent topic in academic and industrial research since it fits into the definition of sustainability. Though there are still many barriers and restraints for bioremediation to be fully applied in contaminated sites, it is a prominent technique due to its low cost and less destructive nature. Bioremediation shares many principles with sustainability, one of which is to ensure that inputs and outputs – including materials, energy, and budgeting – are as safe as possible (Kirchhoff, 2003). Sustainable Environmental Remediation (SER) is a critical concept that keeps in view both the social and economic issues (Fortina et al., 2011). Sustainable remediation is broadly defined as "a remedy or combination of remedies whose net benefit on human health and the environment is maximized through the careful use of limited resources" (Mohee and Mudhoo, 2012). One of the objectives of remediation systems is to keep the function of the ecological system, human health and safety as well as to minimize adverse impact during and post application of a remediation system besides consuming limited resources (Mulligan et al., 2009). Bioremediation could serve to achieve the goal of environmental sustainability if thorough investigation of polluted sites is conducted. (Pandey et al., 2009).

The development of biodegradation technologies has provided a low-cost, low energy method of transforming organic contaminants and immobilizing inorganic contaminants in soil, groundwater,

and shorelines. The application of bioremediation is considered as an environmental-friendly and economical approach to restoring contaminated sites. It offers a potential possibility that we can tackle contamination and prevent the devastating consequences while maintaining economic development. It has contributed to the pollution remediation realistically over the last 50-100 years (Lynch et al., 2005).

The current research should be viewed from broader and interdisciplinary perspectives since successful bioremediation of contaminated sites should take information from various disciplines into account and apply them in developing an efficient treatment process (Head and Singleton, 2003). The optimization of microbial transformation of organic contaminants demands the collaboration of many scientific and engineering disciplines (Brar et al., 2006). While microbiology is the primary driver of bioremediation, a treatment based on microbial conversion is inherently interdisciplinary, involving microbiology, engineering, geology, ecology, chemistry as well as the collaboration of these disciplines (Rittmann, 1994). Also, it is essential to analyze the economic aspect of the bioremediation considering the high cost of conventional remediation treatment techniques. Due to the complex nature of contamination and pollutions, it is helpful to analyze the problem through the lenses of various disciplines and to have a holistic understanding of the issues. This research mainly focused on bioremediation process analysis, toxicity assessment, and biodegradation efficiency determination that included utilization of a bioreactor design. Toxicity assessment is especially relevant from the sustainability perspectives as it would provide details about how the treated sites impact on ecological system and what could be the potential risks (García et al., 2013).

This thesis presented here is divided into five chapters. The first chapter is Introduction, which provides the background and significance of this work. The second one is the Literature Review. The physical and chemical characteristics of phenol and cresols, as well as various types of treatment techniques for phenolic compounds are discussed in this chapter. Besides, three bioreactor configurations and their respective advantages and disadvantages were reviewed. Knowledge gap and Objectives are also presented in this chapter. The next chapter is the Materials and Methods in which the detailed procedures for all the experiments conducted in this project are presented in a sequence that corresponds to the actual experimental work (i.e. batch experiments with mono-, binary-, and ternary-substrates and then continuous system experiments with mono-, binary-, and ternary-substrates). The fourth chapter is the results and discussion for the batch systems. The fifth chapter is results and discussion of CPBB results. The toxicity of the untreated feed and treated effluent samples are also examined. The following chapter is Conclusions and Recommendation for Future Work. References and Appendix are the last parts of this thesis.

2 LITERATURE REVIEW AND RESEARCH OBJECTIVES

2.1 Phenol and Cresols

Physical and chemical properties of phenol and cresols are discussed in this section. Phenol is the common name of hydroxybenzene, an aromatic compound having one hydroxyl group attached to the benzene ring. It is a colorless, hygroscopic crystalline solid at room temperature with a melting point of 40.9 °C, which is very soluble in water and many organic solvents such as ethanol, ethers, chloroform and some other polar solvents. When molten, phenol is a colorless liquid. However, it can rapidly turn to pink color if exposed to certain trace impurities such as iron and copper that may be present in production or storage. Phenol is denser than water, so it would sink to the bottom of water basins when the concentration is high, which can lead to slow dissolution and continuous toxicity (Krastanov et al., 2013). It can be extracted from coal tar by distillation and can be synthesized through cumene oxidation (Jordan et al. 1991). Phenol is widely used to produce caprolactam, bisphenol-A, disinfectants, and to disinfect production equipment in pharmaceutical and medical industry (ATSDR, 1989). In 2008, production of bisphenol-A was the primary consumption of phenol (44%). Other uses of phenol include producing phenolic resins (26%), cyclohexanone /caprolactam (12%), and alkylphenols (4%) (Pilato, 2010). The concentration of phenolic compounds can be as high as 6800 mg L^{-1} in wastewaters generated in petrochemical industry (Busca et al., 2008). In the study of phenol removal from petroleum refinery wastewater conducted by El-Naas et al. (2010), phenol concentrations up to 88 mg L^{-1} were evaluated. Phenol has been used as a model aromatic compound in treatment studies. It is a prevalent pollutant. It is also the intermediate produced in the degradation pathway of complex compounds such as

polycyclic aromatic hydrocarbons (PAHs), pesticide, and depolymerization products of lignin (Karigar and Rao, 2011).

Cresols are phenol derivatives that include three isomers: *m*-cresol, *o*-cresol, and *p*-cresol depending on the relative positions of hydroxyl and methyl group. Cresols originate from both anthropogenic and natural sources. Anthropogenic sources are auto exhaust coal, roadway runoffs, asphalt runoffs, petroleum distillates as well as oil and lubricants. On the other hand, cresols can be traced back to petroleum, wood constituents, and natural waterbodies (natural sources). The melting point of *m*-cresol, *o*-cresol, and *p*-cresol are 35.5, 29.8, and 11.8 °C, respectively. Cresols are less soluble in water than phenol under the same temperature due to their more complicated molecular structure (Verschueren, 1983). Phenols (the name for phenol and its derivatives) can be extracted from organic solutions in combination with aqueous sodium hydroxide, which is the preferred method to recover phenol and cresols from coal tar. Direct oxidation of benzene for synthesizing phenol has also been explored during the past two decades. Table 2.1 provides the summary of physical and chemical properties of phenol and cresols.

Table 2.1 Chemical and physical properties of phenol and cresols (Verschueren, 1983)

Property	phenol	o-cresol	m-cresol	p-cresol
Chemical structure	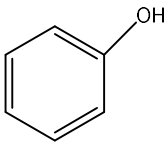	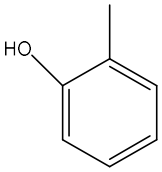	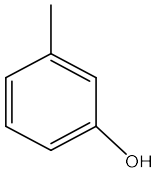	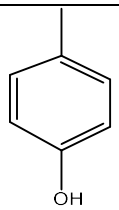
Molecular weight (g mol^{-1})	94.1	108.1	108.1	108.1
Water solubility (g L^{-1} at 25 °C)	87.0	25.0	24.0	19.0
Dielectric constant	11.0	5.8	5.0	5.6
Melting point (°C)	43.0	31.0	11.0	35.5
Boiling point (°C)	181.8	191.0	202.8	201.8
flash point (°C)	87.0	81.0	86.0	86.1
pk_a	10.0	10.3	10.09	10.3

2.2 Health Issues Associated with Phenols

Phenol and its derivatives have negative impacts on the ecological system, human health, and quality of life. In addition to unintentional spillage, various industrial activities generate wastewaters containing phenolic compounds. The effluent from industries such as oil refineries, paper mills, olive oil mills, wood processing, coal gasification, textiles, resins, and agro-industrial wastes discharge phenols at concentrations higher than the toxic level set for these compounds. Phenols are toxic to most organisms. For example, when concentration higher than 2 mg L^{-1} they are considered toxic to fish (Environment and Climate Change Canada, 2016). The phenol LD_{50} for fish in an aquatic environment in 48h is 13.1 mg L^{-1} (Tisler and Zagorc-koncan, 1997). The concentrations between 10 to 100 mg L^{-1} could result in the death of most aquatic life (Huang et al., 2007). Most of these phenolic compounds are also recognized as carcinogens. Many

organizations and documents including Environment and Climate Change Canada and United State Environmental Protection Agency define phenol and its derivatives as priority pollutants. Drinking water contaminated by phenol causes elevated cases of diarrhea, nausea, mouth sores, dark urine, paralysis of the central nervous system and kidney damage (Senturk et al., 2009). The guideline level of phenol in fresh water in Canada is 4.0 $\mu g\ L^{-1}$ (Canadian Council of Ministers of the Environment, 2017). US Environmental Protection Agency defined Oral Reference Doses of 600 $\mu g\ kg^{-1}\ d^{-1}$ for phenol, 500 $\mu g\ kg^{-1}\ d^{-1}$ for *o*- and *m*-cresol, and 5 $\mu g\ kg^{-1}\ d^{-1}$ for *p*-cresol (US EPA, 2016). The Oral Reference Dose refers to "an estimate, with uncertainty spanning perhaps an order of magnitude, of a daily oral exposure to the human population (including sensitive subgroups) that is likely to be without an appreciable risk of deleterious effects during a lifetime" (US EPA, 2016).

2.3 Exiting Methods to Remove Phenols from Contaminated Waters

A wide range of approaches has been studied to remove phenol and cresols from wastewaters. Depending on the end products of the process, these methods can be classified as a destructive or recuperative process, including chemical oxidation, adsorption, solvent extraction, incineration, and bioremediation (Dutta et al., 1998). Single treatment or combination of these methods have been applied to treat waters contaminated with phenols. The choice of the treatment depends upon the concentration of contaminants, geographic location, available equipment, and cost of treatment. These treatment methods are discussed in more details below.

2.3.1 Chemical Oxidation

Chemical oxidation of phenols involves utilizing oxidants such as hydrogen peroxide and peroxymonosulfate (PMS) to degrade phenols to less or harmless compounds in the wastewater. Using hydrogen peroxide as an oxidant to remove phenol is considered as a "clean technology" (Qiao et al., 2012). Advanced oxidation processes (AOPs) are one example of chemical oxidation used to treat wastewater contaminated by phenols. This process removes phenols with oxidants, catalysts, radiation, or combination of these for the generation of radicals such as hydroxyl and sulfate radicals. Catalytic oxidation of phenol would generate catechol and hydroquinone. Bansal et al. (2008) synthesized and characterized a catalyst, $[Cu\{Me_4Bzo_2[14]aneN_4\}]Cl_2$, which was found to be able to catalyze the oxidation of phenol by H_2O_2 to dehydroxylate benzenes with 42.2% conversion at 80 °C. Based on the results and proposed mechanism, they concluded that the chemical catalysis process was fitting for the stereoselective transformation of mono-hydroxy aromatic compounds to *ortho*-dihydroxy derivatives. In another study, Kavitha and Palanivelu (2005) used Fenton reagent to oxidize cresols (200 mg L^{-1}) into lower molecular weight aliphatic acids. The mineralization rate for cresols follows the sequence: *m*-, *p*-, and *o*-cresol. The optimal condition was achieved at 30 °C. A more advanced method was developed in a study conducted by Olmez-Hanci and Arslan-Alatan (2013). They managed to achieve complete phenol degradation at a rate of $0.069 \pm 0.002 – 0.382 \pm 0.003$ min^{-1} with UV-C photo-assisted persulfate (PS), hydrogen peroxide (H_2O_2) and peroxymonosulfate (PMS) oxidation process.

It is important to note that the selectivity and the cost of chemical oxidants limit the application of chemical and advanced oxidations.

2.3.2 Adsorption

Phenolic compounds can be removed using adsorbents such as activated carbons (ACs) or bentonite. Activated carbon has been widely used to treat phenolic compounds due to high adsorption capability for organic compounds and the high surface area per unit mass (Dabrowski, 2005). ACs can be classified as granular, powder-like, fiber or others depending on the physical form. The sources of ACs include primarily mineral carbons, lignocellulose from biomass, wood, and agricultural waste (Alslaibi et al., 2013). Gupta et al. (2014) conducted phenols adsorption study using rubber tire activated carbon modification (RTACMC) and rubber tire activated carbon (RTAC). The results showed that with RTAC, the maximum adsorption capability was 71.4 and 47.6 mg g^{-1} for p-cresol and phenol, respectively, while with RTACMC, 250.0 and 100.0 mg g^{-1} adsorption capability was achieved for *p*-cresol and phenol, respectively. In another study, an activated carbon packed bed was evaluated for the adsorption of phenols from petroleum refinery wastewater (El-Naas et al., 2017). With the initial concentration of 178 mg L^{-1} phenol and 15 g AC mass, the system managed to remove 88.4% of phenol at the flow rate of 10 mL min^{-1}. The adsorption capability was reported as 63 mg g^{-1}.

However, ACs and its regeneration are relatively costly. Thus, naturally occurring adsorbents such as montmorillonite, kaolinite, and bentonite have gained more attention due to their lower cost. These adsorbents can adsorb both organic and inorganic compounds (Sdiri et al., 2011). Hank et al. (2014) compared the capability of activated carbon (F400) and bentonite for adsorption of phenol. Both adsorbents took about 30 min to reach the equilibrium. Powdered activated carbon had the adsorption capability of 17.3 mg g^{-1}, while bentonite capacity was 9.7 mg g^{-1}. The reason

that activated carbon possesses higher adsorption capability might be the presence of macropores and micropores on the surface.

Other adsorbents used for phenol removal are industrial wastes or by-products such as coal, coal fly ash, red mud, and waste sludge (Lin and Juang, 2009). The phenol-adsorption capacity of Samla coal reached 13.3 mg g^{-1} (Ahmaruzzaman and Sharma, 2005). As a comparison, the adsorption capacities of coal fly ash (Sarkar and Acharya, 2006), red mud (Gupta et al., 2004), and activated sewage sludge (Otero et al., 2003) were 17.1, 59.2, and 42.0 mg g^{-1}, respectively. These materials are inexpensive and locally available. Adsorption of phenols can reach the desired results in a short period. However, the cost of these methods and the required further treatment (i.e., regeneration of adsorbent and secondary treatment of released phenolic compounds) limits their application.

2.3.3 Solvent Extraction

Solvent extraction is mainly applied in the treatment of wastewater containing high concentrations of phenol, cresols, and other phenolic acids. It is widely used as a unit operation in chemical and petrochemical industries for the separation of aromatics, the extraction of heavy metals, etc. (Kiezyk and Mackay, 1971).

Solvent extraction is one of the most important techniques used in high phenol-concentrated wastewater pre-treatment. When the concentration of phenols is more than 3000 mg L^{-1}, biological treatment is not feasible generally, as most microorganisms would not survive under such extreme conditions. Also, some dihydric and trihydric phenols are highly resistant to natural oxidation. As a result, a pre-treatment is vital for the subsequent process (Yang et al., 2005). Solvents used for

phenols removal include octanol (Rao et al., 2009), N-octanoylpyrrolidine (Li et al., 2004), cyanex 923 (Reis et al., 2007), diethyl carbonate (Olejniczak et al., 2005), methyl isobutyl ketone (MIBK) (Palma et al., 2007), tributyl of phosphate (TBP) (Balasubramania and Venkatesan, 2012), and ionic liquids (Zhao et al., 2005). In a study of phenol removal using cumene, which is one of the most widely used extractants in industry, 59.2% extraction efficiency was achieved at 25.1 °C with the initial concentration of phenol as 100 mg L^{-1} (Liu et al., 2013). In the next step using 0.1 mol L^{-1} NaOH, 99% of phenol was stripped from the organic phase. In another work by Yang et al. (2005), the performance of 4 alternative solvents including di-isopropyl ether, butyl acetate, methyl isobutyl ketone, and 30% tributyl phosphate – kerosene was investigated. According to the results, 30% TBP-kerosene had the highest distribution coefficient of 171.9 at 25 °C, which is the indicator of the performance of an extracting solvent. After three stages of batch extraction, 5000 mg L^{-1} phenols was reduced to around 300 mg L^{-1}, which would be suitable for subsequent biological treatment. An on-site trial showed that 93% phenol and 80% COD were removed (Yang et al., 2005). This study eventually helped to develop a process to remove phenol at concentrations as high as 5000 mg L^{-1} and CODs up to 20, 000 mg L^{-1}.

The Advantages of solvent extraction include its feasibility for wastewater treatment with concentrated phenol, the effectiveness of this method includes removing and recovering phenols from the wastewater (Liu et al., 2013). However, like adsorption, further treatment is also required for the removal of residual phenol.

2.3.4 Electrochemical Incineration

Electrochemical incineration is a process that completely oxidizes the organic pollutants such as phenols to CO_2 by physisorbed hydroxyl radicals. The electrode material must have high electrocatalytic activity towards the oxidation of organics to CO_2 and H_2O. Electrodes with high overpotential for oxygen including Ti/PbO_2, Ti/SnO_2-Sb, and Ti/boron-doped diamond (BDD) have been used for complete removal of organic pollutants and their immediate products (Yavuz et al., 2011).

The reactions involved in the process can be expressed as follow:

$$H_2O \rightarrow \cdot OH + H^+ + e^- \quad (2.1)$$

$$R + M(\cdot OH) \rightarrow M + m\ CO_2 + n\ H_2O + H^+ + e^- \quad (2.2)$$

The important parameters for electrochemical treatment include electrode support materials, coating materials, pH, current density, and temperature. Electrochemical incineration has been studied for restaurant wastewater treatment (Klamklang, 2007) and color removal of pulp and paper mill wastewater (Mahesh, 2006). In case of pulp mill wastewater, 95-99% colour removal was attained. In another work, 62% of COD removal efficiency was reached using SnO_2 film with the thickness of 3.6 micron (Puzyn and Mostrag-Szlichtyng, 2012).

Medel et al. (2012) studied the effect of boron-doped diamond as anode on the electrochemical incineration of phenolic compounds in samples obtained from a refinery. The results showed that 99.5% of the phenolic compounds were mineralized, while 97% of TOC were removed under acidic condition (pH=1) using a current of 2 A at 25 °C (Medel et al., 2012). Flox et al. (2009)

compared the effect of PbO_2 and boron-doped diamond anodes on the electrochemical incineration of cresols. Cresols at concentrations of 5M were completely mineralized after 480 min (pH = 4.0, T = 298 K) at batch mode. Boron doped diamond led to higher energy consumption. DOC removal was lower using PbO_2 (139 kW h m^{-3}) compared to a BDD anode (165 kW h m^{-3}). The initial cell voltage values of 9.0 and 7.3 V for BDD and PbO_2 anodes were determined at 40 mA cm^{-2}, respectively.

Electrical incineration is a clean, versatile, and powerful tool to eliminate recalcitrant organic contaminants in wastewater (Kapalka et al., 2009). It is also simple and robust in structure and operation. It is potentially useful for the low-volume application (Li et al., 2005). However, it has high power consumption, which makes it economically less feasible for wastewater treatment.

2.3.5 Bioremediation

Bioremediation is defined as "the process using various biological agents, primarily microorganisms to degrade the environmental contaminants into less toxic form" (Lynch et al., 2005). Microbial biodegradation was first recognized for the ability of naturally occurring microbes in the soil to biodegrade hydrocarbons more than 100 years ago. Follow-up research found out that a wide range of indigenous microbes in the soil, groundwater, and marine ecosystem are capable of biodegrading a variety of contaminants such as aromatic compounds (Koukkou, 2011). The capability of microbes to degrade toxic organic compounds or absorb heavy metal encouraged researcher to develop the bioremediation technology. "Bioremediation" was eventually termed in 1990 with the aim of developing rapid and complete biodegradation of toxic organic compounds (Chapelle, 1999). Research works in bioremediation are mainly falling into

three categories: biostimulation, bioaugmentation, and monitored natural attenuation. Biostimulation is carried out by addition of water-based solutions with nutrients, electron acceptors, or other amendments. By contrast, if there are no locally available degradative microbes or the process is too slow, inoculates may be added to enhance the biodegradation process. The process is, therefore, called bioaugmentation. Natural attenuation is a proactive approach that focuses on the verification and monitoring the natural bioremediation process (Mohee and Mudhoo, 2012). Biostimulation has been moderately successful compared to bioaugmentation. Biostimulation has provided the foundation for bioremediation methods such as biopiling, bioventing, in situ biobarriers, and biosparging. Bioaugmentation also had successful application when it was used to treat contamination in an environment where no indigenous pollutant degrading microbes exists or no active degraders are available. Monitored natural attenuation is especially applicable to hydrocarbon plume in groundwater (Koukkou, 2011). Microbial bioremediation has been applied in Sun Oil pipeline spill in ambler in Pennsylvania in 1972, which is the first commercial application (Li et al., 2002). During the 1970s, Richard Raymond of Sun Oil continued bioremediation projects. However, the initial emphasis on bioengineering organism failed its goal in mid-1980. Afterwards, researchers focused more on natural microorganisms (Li et al., 2002). Successful application of bioremediation in the cleanup of oil tanker spill in Prince William in 1989 and the Gulf of Alaska attracted attention on biodegradation and bioremediation (Atlas and Bartha, 1998). Although bioremediation has been used to treat oil-contaminated shorelines, most of the applications have been field-scale research and development (Head and Singleton, 2003).

Biological treatment of wastewater containing organic pollutants is an alternative compared to other treatment options. The cost of biodegradation of organic contaminants is reported to be 5 to

20 times less than chemical treatments such as ozonation and the use of hydrogen peroxide (Agarry et al., 2008). Bioremediation usually have three major processes: 1) transformation or alteration of the molecule; 2) fragmentation or degradation of the molecule to simpler compounds; and 3) mineralization or conversion of complex compounds into simpler ones such as CO_2, H_2, NH_3, CH_4, H_2O and others (Krastanov et al., 2013). The microorganisms need carbon as a source of energy and inorganic salts or nutrients to reproduce and to carry out their metabolic activities. The organic contaminants in wastewater serve as carbon and energy sources for the microorganisms. The primary nutrients used to maintain the microbial activity are nitrogen (N), sulphur (S), potassium (K), magnesium (Mg) and calcium (Ca). Many biotic and abiotic factors could affect the degradation ability or metabolism of microbes through preventing or stimulating the growth of the organisms (Trigo, et al. 2008). Biodegradation of an organic pollutant is also dependent on factors such as pH, temperature, oxygen targeted pollutants, and the design of the system in which biodegradation occurs (Agarry, et al., 2008). The microorganisms may destroy the contaminants or convert them to harmless or simple inorganic compounds such as CO_2 and water. When culture is used in bioreactors, the degradation rate will depend on biomass development and hold-up, feed concentration, liquid flow rate (or residence time) and aeration rate (Basha et al., 2010).

The use of cell immobilization in bioreactors has also been proposed to improve the performance of the biodegradation process and to overcome substrate inhibition (Singh et al., 2006). Cell immobilization can be defined as the “confinement or localization of viable microbial cells to a certain defined region of space in such a way as to exhibit hydrodynamic characteristics which differ from those of surrounding environments” (Webb and Dervakos 1996; Nemati and Webb, 2011). The immobilization process affects the performance of the bioreactors through various

mechanisms. The first advantage of immobilization is the retention of active biomass on support particles, allowing shorter hydraulic retention times and no biomass washout (Bajaj et al., 2008). The second advantage is the flexibility of reactor design and the improved thermal and operational stability. Because of biomass, a large volume of wastewater can be continuously treated using a defined quantity of immobilized cells (Aksu and Bülbül, 1998).

However, the extensive use of biodegradation technologies is still under debate. The complete biodegradation of pollutants by microorganism requires the combination of aerobic and anaerobic degradations, which is very hard to manipulate and control in situ. Another problem is the unwillingness of the public to accept genetically engineered organisms, which has negatively affected the progress of this technology (Richardson, 2008). Furthermore, the potential of biodegradation practice has not been well assessed for environmental and human health risks, especially those relying on genetically engineered organisms. Also, it is very difficult to find suitable consortium for mixed contaminants and biofouling may occur after the degradation of microbial biomass (Das, 2014).

2.4 Different Types of Bioremediation

Based on where the practice happens, bioremediation can be broadly classified as in-situ and ex-situ. Although the following classification has been used in many classic texts, one should not overlook the potential overlap that might exist among the described in situ and ex situ processes.

2.4.1 In-situ Bioremediation

In situ bioremediation is the practice of biological treatment to remove or transform toxic compounds present in the environment. Examples of the in-situ bioremediation practices include: biosparging bioventing, and bioaugmentation.

Biosparging is a process that increases microbial biodegradation rate of contaminants through increasing oxygen concentration in the saturated zone by injecting air under pressure below the water table. This technique helps to improve the contact of soil and water in the saturated zone (Johnson et al., 2001). Bioventing is a bioremediation application to stimulate in-situ aerobic biodegradation by providing oxygen to the microorganism in the subsurface, which can be accomplished by injecting or extracting air through the unsaturated soil in a passive system. Microbial activities are enhanced by the slow airflow rate on sites. Therefore, the adsorbed pollutant residuals are biodegraded and volatile compounds are also biodegraded due to the slow movement of vapors through the soil (Rubin et al., 2012). Bioaugmentation is a technology to introduce non-indigenous microorganisms to increase the biodegradation rate. Municipal wastewater treatment adopts this approach to restart activated sludge aeration basins (Tyagi et al., 2011)

2.4.2 Ex-situ Bioremediation

Ex-situ bioremediation technologies are bioremediation applications involving the physical removal of the contaminated soil or water and their transfer to a controlled environment such as a bioreactor, possibly within sites, for further treatment. Although the in-situ approach could be less

expensive and be the only option in some instances, the ex-situ approach usually provides higher efficiencies due to the carefully controlled conditions in the bioreactor (Carberry and Wik, 2001). The ex-situ approach has been found to be more predictable and to be controlled more easily than in-situ bioremediation (Carberry and Wik, 2001). Examples of ex situ bioremediation are composting, controlled solid phase biotreatment, slurry phase bioremediation (bioreactors), and landfarming.

2.4.3 Factors Affecting Bioremediation

The optimization and control of bioremediation process is more complicated compared to physicochemical methods and many factors should be considered. These include microbial culture, bioavailability of contaminant, soil moisture, oxygen, redox potential, nutrients, pH, temperature, and the presence of heavy metals (Das, 2014).

2.4.4 Advantages and Disadvantages of Bioremediation

There are several advantages associated with bioremediation when compared with other techniques. It can be done on-site, which could help to eliminate transportation costs. Manufacturing and industrial use of the site is likely not to be interrupted by microbial bioremediation. In other words, bioremediation is less destructive to the original sites. Finally, it can be coupled with physical and chemical treatment technologies to achieve a better efficiency (Erdogan and Karaca, 2011).

The disadvantages of bioremediation are also noticeable. Degradation of some toxic compounds such as highly chlorinated compounds and heavy metals is not easy. Some biodegradation process could even produce more harmful compounds. The biodegradation of trichloroethenes (TCE) is a typical example (Schmidt et al., 2014). The biodegradation of TCE through anaerobic reductive dichlorination risks the formation of high concentration of 1,1-dichloroethene (cDCE) or vinyl chloride (VC), both of which are on the priority list of hazardous substances (ATSDR, 2012). A thorough investigation of bioremediation for each site is essential to minimize the environmental and kinetic constraints, which could make the initial cost higher than conventional technologies. The continuous monitoring of bioremediation sites is also required to assess the effectiveness. The last disadvantage is the implementation of bioremediation could be restrained by regulatory due to the introduction of new species of microbes or uncertainties associated with the process and the public acceptance of such practice (Romeela and Ackmez, 2012).

2.5 Bioreactors

One of the most common approaches in ex-situ bioremediation is the use of bioreactors. Bioreactors exist in a variety of configurations and various modes of operations. The design of bioreactors has often been used to enhance the biodegradation rate of contaminants especially in wastewaters (Huang, 2011). Determination of bioreactor configurations is dependent on bioremediation purposes. Configurations of bioreactors include stirred tanks, fixed bed reactors, fluidized bed and membrane bioreactors depending on biomass particle characteristics, reaction kinetics and cost, etc. (Nemati and Webb, 2011). Packed-bed bioreactor, stirred tank, fluidized-bed bioreactors were used to increase the efficiency of phenolic compounds biodegradation in past studies (Bajaj et al., 2008). For aerobic biodegradation, microorganisms can aggressively degrade

the water-soluble toxic organic with sufficient oxygen present in the environment. Utilizing these bioreactors has several advantages such as enhancing mass transfer of oxygen and providing an extended surface for cells immobilization (Huang, 2011).

Ex-situ techniques relying on bioreactor can be highly efficient to remove petroleum contaminants under controlled environment. A bioreactor is a vessel utilizing biological catalyst(s) to obtain the desired chemical transformation, such as the removal of organic compounds or absorption of inorganic compounds like heavy metals (Singh et al., 2014). Bioreactors can be categorized into three types: batch, continuous and semi-continuous or fed batch depending on the feeding strategy into the bioreactor (McNeil and Harvey, 2008). The fundamental features of a bioreactor are volume, agitator system, oxygen delivery system, foam control, temperature & pH control system, sampling ports, and lines for charging or emptying the reactor (Singh et al., 2014). The controlled environment in bioreactor determines the cell growth rate, reaction rate, and process stability (Chen et al., 2006). The factors, which influence the design and mode of operation of bioreactors, include the production of organisms, required optimum conditions, product values, and the scale of production (Singh, Kaushik, and Biswas, 2014). Among all the bioreactors, immobilized cell bioreactors have been proved beneficial in environmental remediation due to the possibility of operating the bioreactors at short residence time and high loading rates without concern about the cell washout (Nemati and Webb, 2011). Other advantages include prolonged stability, enhanced biomass hold-up, improved mass transfer in the bulk liquid, reaction selectivity, increased product yield, and simplified downstream processing.

Several immobilized cell bioreactors configurations have been utilized for bioremediation purposes: stirred tanks, airlift bioreactor, fluidized bed bioreactors, and membrane bioreactors (Nemati and Webb, 2011; Singh et al., 2014). They are discussed below regarding their advantages and disadvantages.

2.5.1 Stirred Tank Bioreactors

The stirred tank bioreactors, comprised of a tank, a rotating impeller, and baffles, are a common type of aerobic bioreactors. They could be operated under both batch and continuous modes. The main advantages of this bioreactor are its high volumetric mass-transfer coefficient for gas transfer and adaptability to a wide range of conditions (Shuler et al., 2002). The microbial cells in the reactor are resistant to the inhibition effect of high concentration of contaminants because the influent solution is diluted upon entering the bioreactor

However, there are also drawbacks for stirred tank bioreactors. The shear forces from the impellers especially the conventional flat blade turbines and propeller could damage the particles in the bioreactor (Nemati and Webb, 2011). Foaming problem associated with stirred tank bioreactor could increase the pressure drop, reduce flow rate, and make contaminating cells enter the system. For shear sensitive cells, the presence of mechanical agitation will limit their growth (Huang, 2011). Saravanan et al. (2008) used a batch stirred tank bioreactor (BSTR) to removal phenol with *Pseudomonas spp*. The results showed that BSTR achieved phenol removal rate of 0.5 g day^{-1}. In comparison, a continuous stirred tank bioreactor (CSTB) achieved the maximum phenol degradation capacities of 3.2 g day^{-1} with suspended cells of *Pseudomonas putida* ATCC 17484 (Gonzalez et al., 2000). Schematic diagram of stirred tank bioreactor is shown below in Figure 2.1.

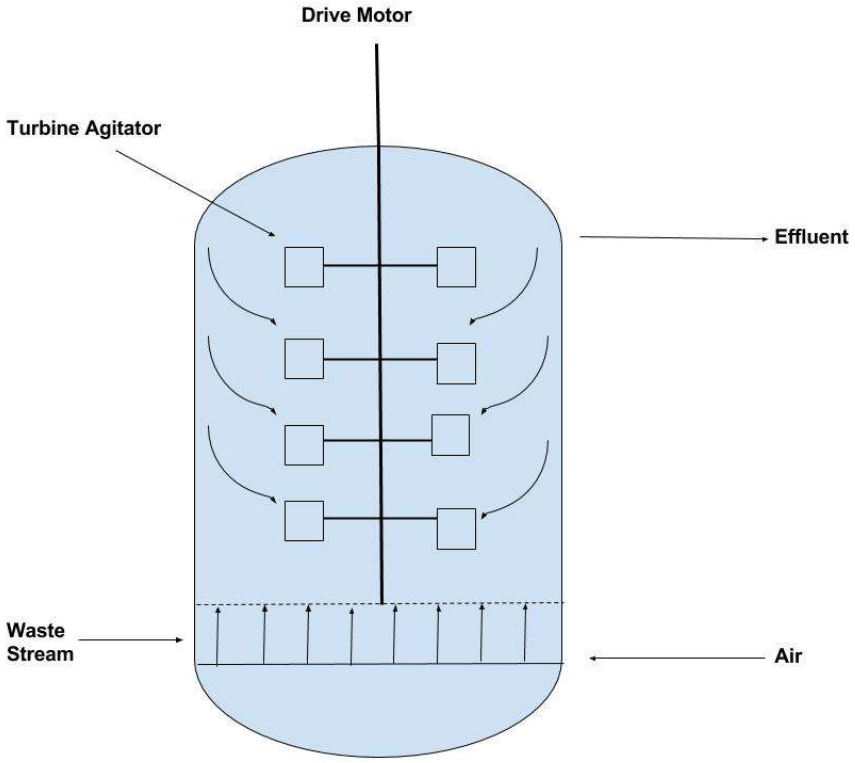

Figure 2.1 Schematic diagram of continuous stirred-tank bioreactor

2.5.2 Membrane Bioreactors

Membrane bioreactors (MBR) deploy membrane separation of activated sludge and biochemical components of the reaction cell. They are designed either as a flat sheet or hollow fiber modules. Microbial cells in MBR are protected against the shear forces and bubble bursting by the membrane. Compared to other conventional bioreactors, they are more expensive due to the high cost of the membrane (Nemati and Webb, 2011). These reactors are a hybrid system combining membrane separation with biological treatment. Biological treatment involves biochemical reactions such as fermentation and denitrification. A membrane separator is used for subsequent solids and liquid separation (Fazal et al., 2015). When waste streams contain toxic compounds or heavy metals, MBRs are preferred. The advantages of membrane bioreactor include robustness,

high organic loadings, and capability of removing inhibitory compounds (Klinkow et al., 1998). However, microbial selection process is heavily influenced by industrial wastewater due to the inhibition effects of refractory compounds. In addition, the type of industrial process also affects the removal of organic load, measured by the quantity of non-biodegradable compounds (Fazal et al., 2015).

Hollow fiber membrane bioreactors are the most widely used type of MBR. In most membrane bioreactor designs, cells grow on the shell side, while substrate flows through the tube bundle with the stream flows (Nemati and Webb, 2011). Praveen et al. (2015) used a forward osmotic fiber bioreactor coupled with a chemostat (FOHFMB) to treat high strength saline phenolic wastewater. The results showed that bacterial (*P. putida* cells) could tolerate up to 0.5 M salinity with phenol concentration up to 600 mg L^{-1} in FOHFMB. Phenol in chemostat was rapidly removed to the concentration of zero (within 20 h), reaching the steady state at biomass of 170 mg L^{-1} (Praveen et al., 2012). A hollow fiber membrane bioreactor is shown in Figure 2.2.

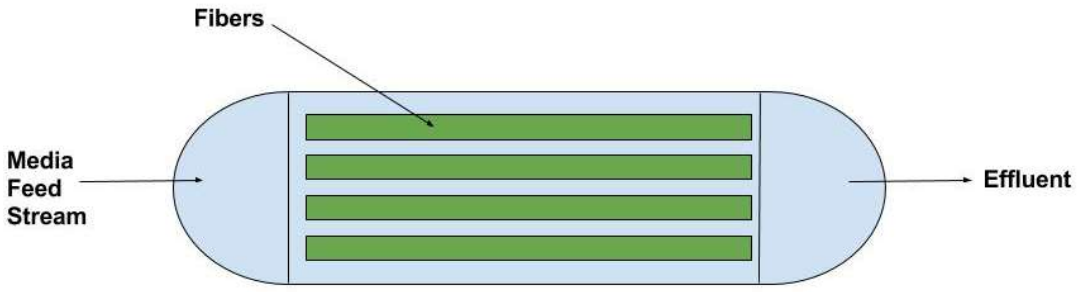

Figure 2.2 Schematic diagram of hollow fiber membrane bioreactor

2.5.3 Airlift Bioreactors

Airlift bioreactor is a tower reactor that uses the flow of compressed gas (in most cases air) for mixing (Christi, 1989). Both free and immobilized cells can be applied in the configuration. Airlift bioreactors can be classified as internal and external type. The bioreactors contain a draft tube arranged either inside of the column or outside attached to the column. The tube that induces mixing is used for controlling the oxygen transfer and mixing of the medium, as well as equalizing and moderating the shear forces in the reactor (Veera and Josh, 1999). Due to the absence of agitation, the system is energy efficient. The system could increase mass transfer because oxygen solubility is enhanced in tanks with controlled flow and efficient mixing with a good residence time (Singh et al., 2014). Moreover, it has capability to handle viscous fluids and maintain a homogeneous environment especially under continuous mode. The potential of airlift bioreactor for scaling up also broadens its application (Merchuk, 2003)

Circulating packed bed bioreactor is a modified external loop airlift bioreactor (ELAB). The packing material is put in the riser section. The improved mass transfer rate can provide sufficient oxygen for microorganism attached on packing material to degrade the targeted organic contaminants in an efficient manner (Huang, 2011). The packing materials, which have been investigated for the potential to improve mass transfer of oxygen, include nylon, crushed glass, stainless mesh, porcelain, and acrylic Raschig rings (Meng et al., 2002).

The packing material also provides a stable surface for microbes to attach to, as a consequence, biomass hold-up in the bioreactor is also improved (Huang, 2011). Loh and Liu (2001) used an external loop fluidized bed airlift bioreactor (EIFBAB) for treatment of high strength phenolic

wastewater. Circulating packed bed bioreactor have been used for the treatment of other recalcitrant organics such as naphthenic acids and managed to achieve the highest removal rate of a surrogate NA of 209 mg L^{-1} h^{-1}, which is about 22 times faster than a CSTR and 3.8 times faster than a packed bed bioreactor (Huang, 2011). D'Souza (2014) reported the maximum removal rate of octanoic acid in CPBB was 410.1 mg L^{-1} h^{-1}. The potential of biofouling, aeration cost, and difficulties of maitainance are some of drawbacks associated with CPBBs. The configuration of Circulating Packed Bed Bioreactor is shown below.

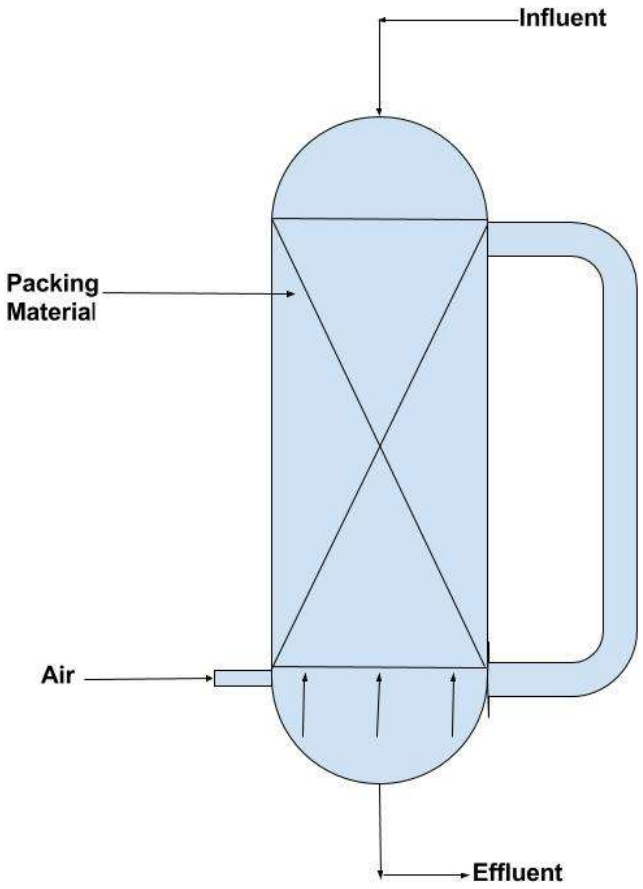

Figure 2.3 Schematic diagram of Circulating Packed Bed Bioreactor

2.6 Existing Studies of Bioremediation of Phenols

2.6.1 Phenols Biodegradation Pathway

The biodegradation of phenols demands the presence of molecular oxygen under aerobic condition or other electron acceptors such as nitrate, manganese, iron, or sulfate under anaerobic conditions. For phenol aerobic pathway, molecular oxygen is utilized by enzyme - phenol hydroxylase or monooxygenase - to add an extra hydroxyl group in ortho-position to the one already present. This process required a reduced pyridine nucleotide ($NADH_2$). Catechol (1, 2 - dihydroxybenzene) molecule is generated as a result. Two alternative pathways for the subsequent degradation are followed depending on the responsible microorganisms. The first one is ortho- or beta-ketoadipate pathway in which the aromatic ring is cleaved between the catechol hydroxyls by a catechol 1, 2 – dioxygenase that in turn produces cis-cis muconate for further metabolism (Harwood and Parales, 1996; Stanier and Ornston, 1973). The second pathway is meta-pathway, in which catechol 2, 3 – dioxygenase transforms catechol to 2-hydroxymuconic semialdehyde. Both pathways generate products which can be further metabolized to intermediates of the krebs cycle. *P. putida* utilize phenol by aerobic pathway and employ ortho-pathway (Cerniglia, 1984). Anaerobic pathway of phenol is less advanced than aerobic process, in which phenol is carboxylated in the para position to 4-hyroxy benezoate by the enzyme, 4-hydroxy benezoate carboxylase (Basha et al., 2010).

For p-cresol, the pathway involves oxidation to 4-hydroxybenzoate and hydroxylation to protocatechuate as a ring-fission substrate while m-cresol can be metabolized either by oxidation to 3-hydroxybenzoate followed by hydroxylation to gentisate (ring-fission substrate) or by meta cleavage involving a methyl-substituted catechol and ring-fission (Hopper and Taylor, 1974). In

terms of o-cresol biodegradation pathway, the first step identified by Masunaga et al. (1985) was hydroxylation to form three dihydroxytolunes, among of which are 3-methylcatechol (3MeC), 4-methylresorcinol (4MeR) and methylhydroquinone (MeHQ). 3MeC is the central pathway. It was shown to be metabolized via 2 meta-cleavage pathways, distal and proximal.

Other enzymes that are involved in the bioremediation process of phenols include monooxygenase, dioxygenase, laccase, versatile peroxidase, manganese peroxidase, etc. (Karigar and Rao, 2011).

2.6.2 Recent Studies of Phenols Biodegradation

Various studies have been conducted on the biodegradation of individual phenolic compounds or their combinations in either batch or continuous systems. Table 2.2 provides some of the results from existing studies and their respective operating conditions applied. High removal efficiency was achieved in several systems even under high saline or alkaline conditions. Majority of these studies utilized *P. putida* as the microorganisms to degrade phenols. However, there is only limited information regarding ternary biodegradation of phenol and cresols even in the batch systems. The information is also less available in continuous systems such as circulating packed-bed bioreactors (CPBB) that have been shown to be advantageous when compared with other bioreactor configurations.

Table 2.2 Examples of biodegradation studies and process conditions reported in the literature

Contaminant(s)	Microorganism	Type of reactor	Concentration (mg L^{-1})	pH	Temperature (°C)	Removal Efficiency (%)	Degradation time (h)	Reference
phenol	*Acinetobacter sp.* BS8Y	Batch	600-1200	7.2	30	96% - 99.2%	24-30	Jiang et al., 2012
phenol	*P. fluorescens*	Inverse Fluidized Bed Biofilm reactor	1200	6.5	28	98.50%	48	Sabarunisha and Radha, 2013
phenol and p-cresol	*Halomonas*	Batch	up to 1100	11-Aug	30	64% (7 % NaCl) - 95% (18 % NaCl)	up to 168	Haddadi and Shavandi, 2013
o-cresol	*Arthrobacter sp.*	Batch	100-1000	8.3 ± 0.2	30 ± 1	100%	20-55	Jemaat et al., 2014
phenol and 4-chlorophenol (4-CP)	*P. putida* LY1	Batch	phenol (20 - 400); 4-CP (15 and 40)	09-Mar	5-35	100%	40 - 115	Wang et al., 2014
o-cresol	*Arthrobacter sp.*	Continuous Airlift reactor	100-1000	8.3 ± 0.2	30 ± 1	100%	20-55	Jemaat et al., 2014
o-cresol and ammonia	activated sludge	Continuous Airlift reactor	ammonia (950 ± 25); o-cresol (300 and 1000)	8.3 ± 0.2	30 ± 1	100%	20 – 55	Jemaat et al., 2014
phenol	*P. putida* ATCC 11172	Osmotic Membrane Bioreactor	600-2500	NA	room temperature	100%	2.8 – 14	Praveen and Loh, 2015
Phenol	*P. putida* ATCC 11172	Osmotic Hollow Fiber membrane	1000	NA	NA	100%	7-20	Praveen et al., 2015

2.7 Knowledge Gap and Research Objectives

Given that real wastewaters such as tailing pond wastewater from oil sands processing (Allen, 2006) and wastewater from pharmaceutical production processes (Yoong et al., 1999) contain more than one phenolic compound, it is imperative to study the biodegradation process with the mixture of phenolic compounds and to understand the interaction among these compounds that could potentially influence the overall biodegradation process. It is also important to note that the concentration of phenolic compounds and temperature are two of the most important factors influencing the bacterial activity and biodegradation process (Mohee and Mudhoo, 2012). Therefore, these two factors were studied as part of batch experiments with individual (concentration and temperature) and mixture of phenolic compounds (concentration). Biodegradation study in batch system generated detailed and specific kinetic data that could be used in the development of kinetic expressions with utility in the modeling and design of continuous flow bioreactors for large scale applications.

Given the unique characteristics of circulating packed bed bioreactors that combine the promising features of CSTR and packed-bed bioreactors such as efficient mixing and mass transfer, as well as high biomass hold-up and the fact that the biodegradation cresols and mixture of phenol and cresols have not been studied in such system part of this research was dedicated to biodegradation of phenol, p-cresol, and o-cresol as individual or mixtures of various combinations in the CPPBs. The study in CPBB focused not only on biodegradation but also as the toxicity of the treated effluent.

The specific objectives of this research were:

1. To evaluate biodegradation of individual o- and p-cresol, as well as mixture of o-, p-cresol and phenol of different combinations in batch systems; to understand the effects of initial concentration of phenolic compounds and temperature on the biodegradation process.

2. To evaluate biodegradation of individual o- and p-cresol, as well mixture of o-, p-cresol and phenol of different combination in the continuously operated CPBBs, and specifically to investigate the effects of concentration and loading rate of phenolic compounds, as well as composition of the mixture on the biodegradation process (residual concentration, removal percentage, and removal rate).

3. To assess the toxicity of the treated effluent obtained in CPBBs under various operating conditions to have a better understanding of the potential application of CPBBs for the treatment of waters contaminated with phenolic compounds at large scale.

3 MATERIALS AND METHODS

Experimental works in this research were divided into two parts: biodegradation studies in batch systems and biodegradation studies in continuous mode using Circulating Packed Bed Bioreactors. For the batch system, biodegradation of individual phenols, and co-biodegradations of phenolic compounds (binary and ternary mixtures) with different initial concentrations and different combinations, as well as different temperatures have been investigated. In a similar fashion in continuous bioreactors (CPBB), biodegradation of individual phenols, and co-biodegradations of phenolic compounds (binary and ternary mixtures) with different initial concentrations and different combinations under different loading rates were investigated.

3.1 Chemicals

Pure phenol (99% purity, CAS No.108-95-2), o-cresol (99% purity, CAS No. 95-48-7) and p-cresol (ACROS Organics, 99+% purity, CAS No. 106-44-5) were obtained from BDH Inc., and ACROS Organics, respectively and used in biodegradation experiments. The selection of these compounds as candidate pollutants was based on their physical properties and chemical structure as presented in Table 2.1. Phenol and cresols differ structurally due to absence or presence of a methyl group. Thus, choice of phenol and cresols was justified. Among the three cresol isomers the solubility of p-cresol is different from those of o- and m- cresols, thus p-cresol was a certain choice. Given the closeness of physical properties of m-cresol and o-cresol, we chose the o-cresol as it represented the most distinct difference in chemical structure with p-cresol in terms of relative location of branched groups of -OH and -CH_3.

3.2 Culture and Medium

A pure culture of *Pseudomonas putida*, obtained from the American Type Culture Collection, Virginia, USA (ATCC 17484) was used in biodegradation experiments. *P. putida* is a gram-negative, rod shaped bacteria which can move using flagella. *P. putida* has been used extensively by others for phenols biodegradation in various bioreactors (Al-Khalid and El-Naas, 2010; Moreno et al., 2018; Chung et al., 2003; Kumar et al, 2005). Thus, selection of this pure culture would allow comparison of the biodegradation data obtained in the batch and CPBBs with previous studies in other conventional bioreactors with *P. putida* as the bacterial species (D'Souza, 2012; Kumar, 2010; Huang, 2011). Additionally, *P. putida* has been identified as one of the main species of activated sludge that is commonly used in wastewater treatment plant (Marrot et al., 2006).

Modified McKinney's medium was used as growth medium and culture maintenance (Hill and Robinson, 1975, Paslawski et al., 2009). Modified McKinney's medium containing phenolic compounds was used in all experimental runs. Modified McKinney's medium had the following composition: 840 mg L^{-1} KH_2PO_4 ;750 mg $L^{-1}K_2HPO_4$; 474 mg L^{-1} $(NH_4)_2SO_4$; 60 mg L^{-1} NaCl ; 60 mg L^{-1} $CaCl_2$; 60 mg L^{-1} $MgSO_4.7H_2O$; 2.6 mg L^{-1} $Fe(NH_4)_2(SO_4)$; 20 mg L^{-1} H_2O, and 0.1% v/v trace medium solution. Trace medium solution was composed of 600 mg L^{-1} H_3BO_3; 400 mg L^{-1} $CoCl_3$; 200 mg L^{-1} $ZnSO_4$.; 60 mg L^{-1} $MnCl_2$; 60 mg L^{-1} $NaMoO_4.2H_2O$; 40 mg L^{-1} $NiCl_2$; and 20 mg L^{-1} $CuCl_2$. The medium was sterilized in an autoclave at 121ºC and a pressure of 15 psi for 30 minutes prior to use.

P. putida was initially grown in 500 mL Erlenmeyer flasks (shaken at 200 rpm) containing 200 mL sterilized modified McKinney's medium with 500 mg L^{-1} of phenol. When the bacteria biomass reached a maximum concentration around 0.18 mg dry weight cell mL^{-1}, 20 mL of culture (10% v/v) was transferred to a second shake flask containing modified McKinney's medium and 500 mg L^{-1} of phenol, or 300 mg L^{-1} of o-cresol, or 300 mg L^{-1} p-cresol. Sub-culturing was carried out on a weekly basis. It takes 6-8 days to reach maximum biomass concentration for subsequent biodegradation experiments.

3.3 Batch Experiments

Batch experiments were conducted to study the microbial growth and biodegradation of o-cresol and p-cresol as single substrates, and co-biodegradation of cresols (either p-cresol or o-cresol) and phenol as binary-substrate, and co-biodegradation of phenol, p-cresol, and o-cresol as ternary-substrate in the mixture of different initial concentrations and combinations. Experiments were carried out in duplicates to assess the uncertainty and variation of data.

3.3.1 Effect of the Initial Concentration of Phenolic Compounds

The first set of experiment aimed to determine the biodegradation of individual o-cresol and p-cresols. Phenol biodegradation was not investigated because there are sufficient studies found in literature (Table 2.2). Effect of initial concentration of phenolic compounds was determined through batch experiments with p-cresol and o-cresol having initial concentration ranging from 100 to 500 mg L^{-1} (Table 3.1). The concentration range was chosen for quantifying the relationship between concentration and biodegradation rate. Each flask was loaded with 150 mL sterile

modified McKinney's medium containing either 100, 200, 300, or 500 mg L^{-1} of o-cresol or p-cresol. These flasks were then inoculated (10% v/v) with a 5-day old *P. putida* culture grown in modified McKinney's medium containing either o-cresol or p-cresol depending on the experiments. The culture age was chosen based on the experimental observation that *P. putida* could reach the maximum growth rate in batch system around 5 days. The experiments were conducted at room temperature (24 ± 2 °C). Flasks were capped with sponge and was completely covered with aluminum foil and placed on the gyratory shaker (New Brunswick Scientific Co., Inc, Edison, N.J. U.S.A) operated at 140 rpm. Samples were taken at regular intervals (either once a day, twice, or three times a day, depending on the growth rate of P. putida) using stainless steel needles and hypodermic syringes and were analyzed for phenolic compound concentration. Optical density was also measured for each sample. The optical density was converted to biomass or dry cell weight concentration using a calibration curve developed for this purpose (the procedures of developing the calibration curve and the figure are given in the appendix).

Table 3.1 Initial concentrations used in mono-substrate batch biodegradation experiments

	p-cresol (mg L^{-1})	**o-cresol (mg L^{-1})**
1	100	100
2	200	200
3	300	300
4	500	500

3.3.2 Effect of Temperature

The effect of temperature was studied by conducting biodegradation of individual o-cresol or p-cresol at different temperatures of 10, 15, 20, 30, and 35 °C. The results could help to quantify the relationship between temperature and biodegradation rate. For room temperature (24 ± 2 °C), the batch experiments have been conducted in previous section, thus it was not repeated here. All the biodegradation experiments were performed in the temperature-controlled chambers to maintain the desired temperatures (one was used for temperatures below room temperature and the other for the higher temperatures). All experiments were carried in 250 mL flasks with modified Mckinney's medium containing either 300 mg L^{-1} p-cresol or 300 mg L^{-1} o-cresol. The inoculum for experiments at 20 °C and 30 °C was a 5-day old stock culture grown in at room temperature (24 ± 2 °C). The resulting culture at 20 °C was subsequently used for the experiments at 15 °C, and the culture developed at 15 °C was then used as inoculum for 10°C. Similarly, culture developed at 30 °C was used as inoculum for experiment at 35 °C. Sampling and analyses procedures were the same as those described in the preceding section.

3.3.3 Co-biodegradation of Phenolic Compounds (binary and ternary substrates)

These biodegradation experiments were conducted using mixtures of phenol and cresols (binary and ternary) at various combinations. Experimental procedures were similar to those described earlier. For binary-substrate co-biodegradation, each flask was charged with 150 mL sterile modified McKinney's medium containing 500 mg L^{-1} phenol and either 100, 200, 300, 400, or 500 mg L^{-1} o-cresol or 500 mg L^{-1} phenol with either 100, 200, 300, 400, or 500 mg L^{-1} p-cresol.

Experiments were conducted at room temperature (24 ± 2 °C). The initial concentrations of phenolic compounds used in various combinations have been given in Table 3.2.

Table 3.2 Initial concentrations of phenols in binary-substrate batch biodegradation experiments

Combination	phenol	p-cresol	phenol	o-cresol
1	500	100	500	100
2	500	200	500	200
3	500	300	500	300
4	500	400	500	400
5	500	500	500	500

For ternary substrate biodegradation, the initial concentration of phenol was kept at 500 mg L^{-1}, the concentration of p-cresol and o-cresol ranged from 100 to 400 mg L^{-1} with different combinations as shown in Table 3.3.

Table 3.3 Initial concentrations of phenolic compounds used in ternary-substrate batch biodegradation experiments

Combination	phenol concentration (mg L^{-1})	p-cresol concentration (mg L^{-1})	o-cresol concentration (mg L^{-1})
1	500	100	100
2	500	200	100
3	500	300	100
4	500	400	100
5	500	100	200
6	500	200	200
7	500	300	200
8	500	400	200
9	500	100	300
10	500	200	300
11	500	300	300
12	500	400	300
13	500	100	400
14	500	200	400
15	500	300	400
16	500	400	400

3.3.4 Control Experiments

Control experiments were carried out using modified McKinney's medium containing either 500 mg L^{-1} phenol, 500 mg L^{-1} p-cresol, and 500 mg L^{-1} o-cresol without inoculum at room temperature to examine the potential for abiotic degradation. Samples were taken to be measured for biomass concentration and phenols concentration every two days for 20 days. Control experiments were conducted only at 500 mg L^{-1} as the potential for spontaneous degradation is more likely at high concentrations.

3.4 Experimental Set-up for continuous biodegradation of phenolic compounds in Circulating Packed Bed Bioreactors (CPBB)

Two identical experimental systems were set up and run in parallel. A schematic diagram of a typical experimental set-up is shown in Figure 3.1. Representative photograph of the experimental set-up (Figure 3.2) is shown as well.

Both CPBBs were made of clear glass. Each CPBB had inlet and outlet ports which allowed continuous operation of the bioreactor. Stainless steel mesh was used as carrier matrix for the establishment of biofilm. The steel packing material used in CPBBs has a porosity of around 80%. In all experiments, sterilized modified McKinney's medium, autoclaved at 121 ºC for 60 minutes, was used. The specifications of 1st and 2nd CPBB were listed in Table 3.4. During the continuous experiments, sterile medium containing phenols at the desired concentrations was fed continuously into the upper part of CPBB by a peristaltic pump and effluent was removed from the bottom of the reactor through overflow tube. The effluent port was elevated to maintain sufficient liquid in the bioreactor. Air was introduced into the reactor from the bottom through a flow meter. The air flow rate was maintained at 0.3-0.5 L min^{-1} (Huang, 2012). Feed container was placed on a magnetic stirrer to make sure the dissolve of phenols or cresols in the feed stream before being connected to the continuous system. The bioreactor columns, tubes, as well as feed containers were sterilized using both bleach and ethanol prior to the experiments.

Table 3.4 Specifications of 1st and 2nd circulating packed bed bioreactors (CPBB)

Parameter	1st CPBB	2nd CPBB
Riser height (cm)	35	31
Riser diameter (cm)	4.5	4.1
Down comer height (cm)	32	29
Down comer diameter (cm)	0.5	0.5
Porosity	0.8	0.8
Void Volume (mL)	450	375
Total reactor volume (without packing) (mL)	562	468

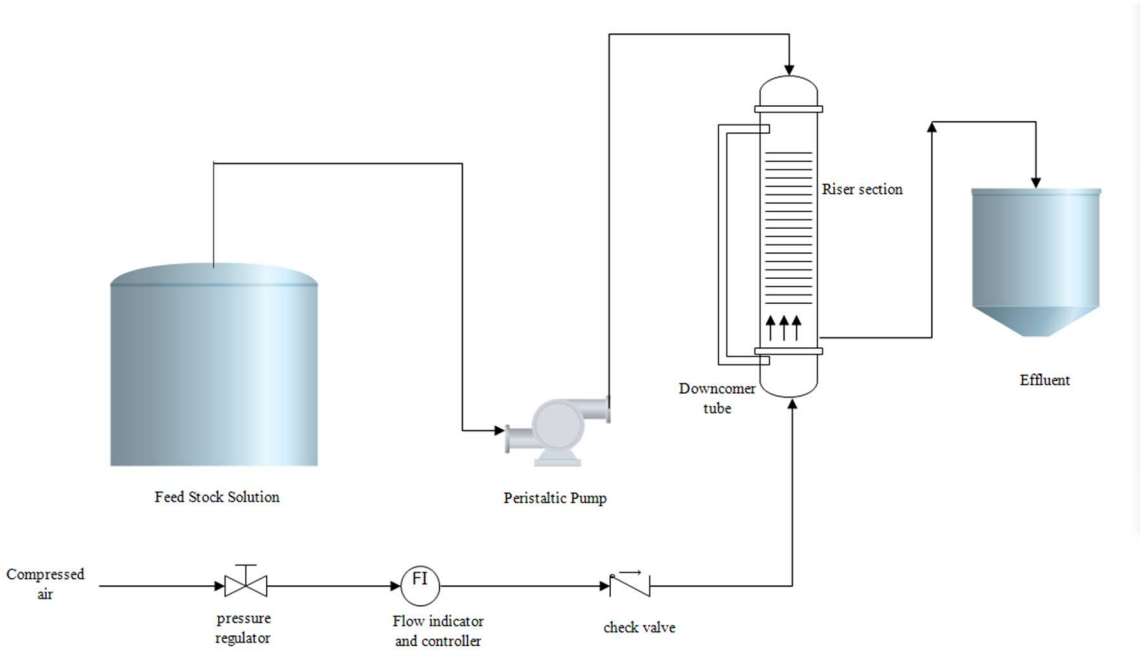

Figure 3.1 Schematic diagram of an experimental set-up

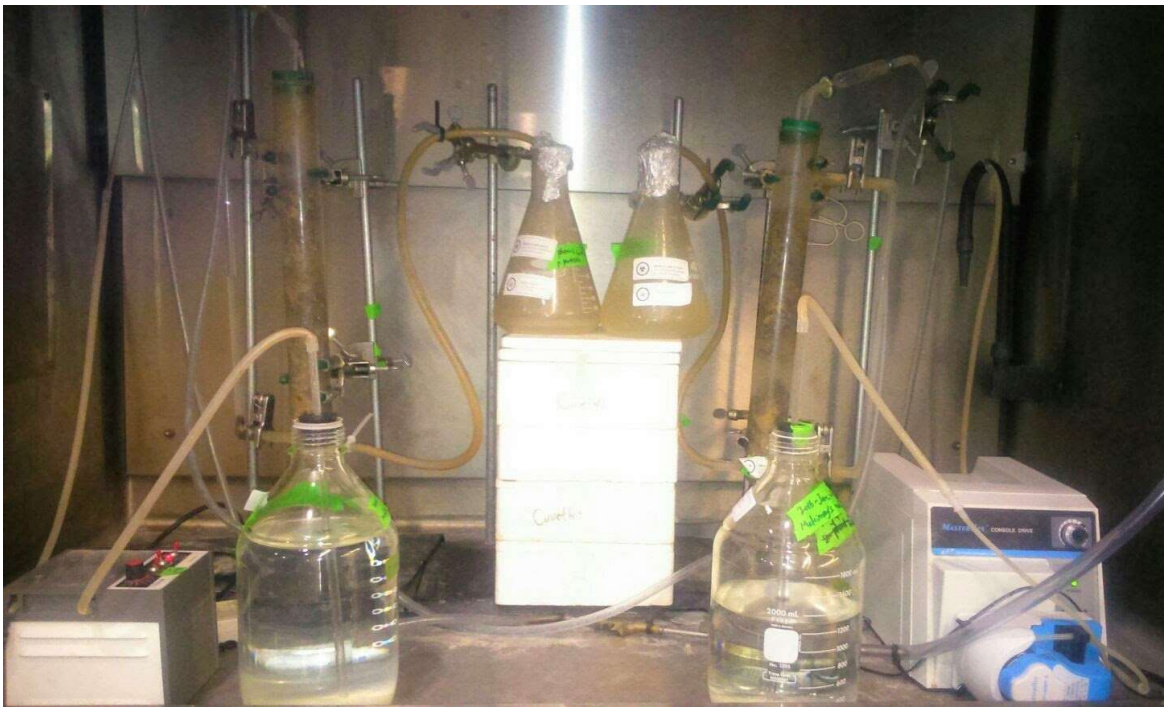

Figure 3.2 Photograph of experimental set-up

3.4.1 Biofilm Development

The biofilm in the first bioreactor was developed over a period of 8 weeks by trickling sterile modified McKinney's medium containing 100 mg L^{-1} phenol and 10% (v/v) inoculum at a flow rate of around 10 mL h^{-1} over the stainless-steel mesh packing (Huang et al., 2012). Upon the formation of a significant amount of biofilm in the bioreactor that was quite visible (8 weeks), the continuous experiments were initiated by draining the reactor and supplying fresh medium containing the phenolic compound at the designated concentration. For the second bioreactor, the inoculum was the effluent of 1st CPBB. The feed concentration, 300 mg L^{-1} phenol, was higher than the first one to allow a faster formation of biofilm. The setting of trickling liquid and its flow rate was the same as the first CPBB. The biofilm in the second CPBB formed within three weeks. Residual phenolic compound concentrations were monitored on a regular basis to examine the

performance of the biofilm system under different volumetric loading rates. The stability of the residual concentration in the effluents verified the establishment of steady state condition (i.e. when residual concentration varied by less than 10% over an extended period equal to three or more residence time). The photographs of biofilm development at different stages are presented in Figure 3.3.

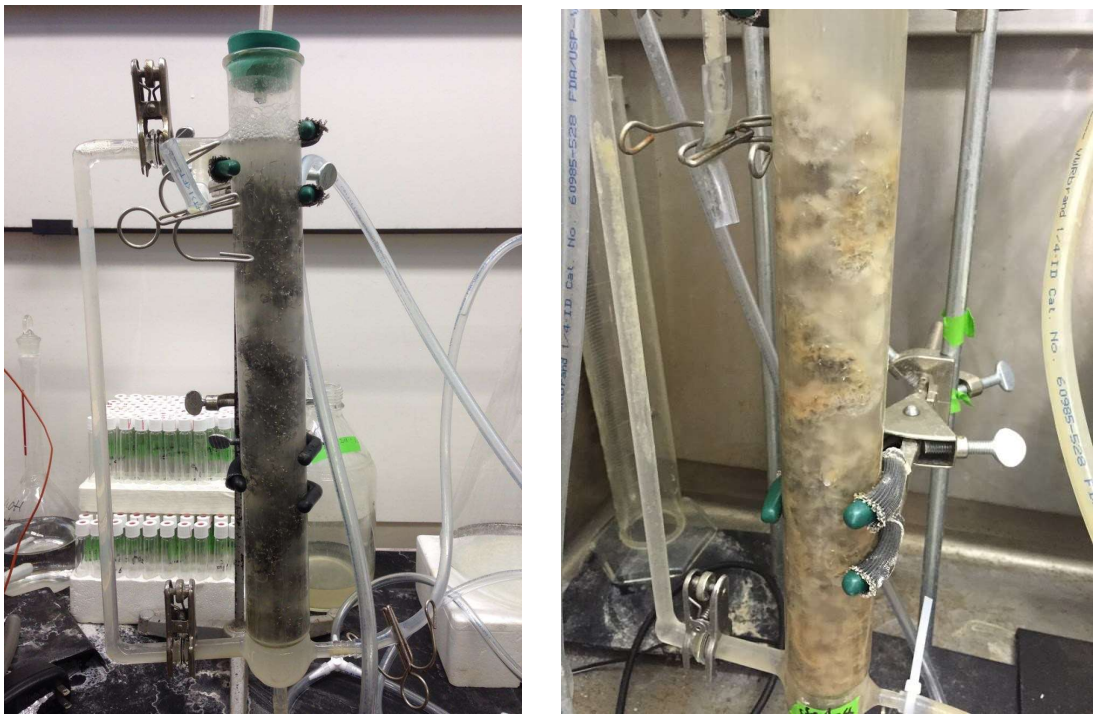

Figure 3.3 Photograph of biofilm development. The photo in the left shows the bioreactor at the early stage of biofilm formation, while the right photo represents the biofilm toward the end of 8 weeks.

3.4.2 Continuous Experiments

The continuous biodegradation of phenolic compounds was studied at room temperature (24 ± 2 °C) and under aerobic conditions in two Circulating Packed Bed Bioreactor. The pump provided

the desired flow rates. The flow rates were determined by measuring the volume of the effluent collected over a specific period of time. During continuous operation, sterile medium containing phenols was fed into the top of CPBB by a peristaltic pump. Effluents were removed from the bottom of the bioreactor through overflow tube into an effluent collecting container. Effect of phenolic compound concentration and loading rate on biodegradation and performance of the bioreactors was investigated by varying the flow rate of the feed and concentration of phenolic compounds in the feed. Overall, flow rates in the range of 5 to 1300 mL h^{-1} were evaluated through the incremental increase of flow rate. At each flow rate, adequate time was given to achieve steady-state conditions. Steady state conditions were assumed by stable readings in the residual concentration of substrate(s) in the effluent (i.e., variation in the residual substrate concentration less than 10%). Samples were taken at regular intervals from the effluent and analyzed by a spectrophotometer (for mono-substrate) or by an HPLC (for binary- or ternary-substrate) to determine the residual concentration of phenolic compounds. Samples were drawn at regular intervals from the inlet port of the bioreactor and the feed tank to ensure that desired feed concentration is maintained throughout the study and contamination did not occur. The concentrations of phenol and cresols in mono-substrate, binary-substrate, and ternary-substrate used in these experiments were consistent with the range used in the batch system and based on the results obtained in the batch experiments. The composition of various feeds investigated in the continuous experiments is given in Table 3.5. All the experiments on the left side of the table were conducted in the 1st CPBB while those on the right side were performed in the 2nd CPBB to run experiments in parallel.

3.4.2.1 Individual substrate biodegradation in CPBB

In the first set of experiments, the CPBB was operated with sterile modified McKinney's medium containing 100 mg L^{-1} phenol at increasing flow rates of 5.22, 11.82, 15.46, 23.01, 50.16, 76.32, 145.01, 195.44, 303.02, 409.21, 497.32, 735.40, and 1105.45 ml h^{-1} with corresponding residence times of 86.21, 38.07, 29.11, 19.55, 8.97, 5.90, 3.10, 2.30, 1.48, 1.10, 0.91, 0.61, and 0.41 h. For 300 mg L^{-1} phenol, flow rates tested were 14.40, 79.24, 152.36, 276.95, and 467.32 ml h^{-1}, with the corresponding residence times of 31.25, 5.68, 2.95, 1.62, and 0.96 h. Then the concentration of phenol in effluent was increased to 500 mg L^{-1}, the flow rates were 11.02, 21.03, 96.33, 157.36, and 201.79 ml h^{-1} with the residence times of 40.83, 21.40, 4.67, 2.86, and 2.23 h.

The second set of experiments in CPBB was for p-cresol degradation. Similar to phenol, the experiments started with 100 mg L^{-1} p-cresol, at increasing flow rates of 59.33, 63.33, 99.67, 154.02, 227.20, 226.52, 312.01, 451.32, 689.51, and 1015.00 ml h^{-1} with the corresponding residence times of 6.32, 5.92, 3.76, 2.44, 1.65, 1.66, 1.20, 0.83, 0.54, and 0.37 h, respectively. For 300 mg L^{-1} p-cresol, flow rates tested were 8.87, 69.65, 153.69, 301.38, 375.74, and 498.182 ml h^{-1}, with the corresponding residence times of 50.73, 6.46, 2.93, 1.49, 1.20, and 0.90 h. As for 500 mg L^{-1} p-cresol, the flow rates were 14.57, 23.98, 106.33, 159.37, and 212.39 ml h^{-1} with the residence times of 30.89, 18.77, 4.23, 2.82, and 2.12 h.

The third set of experiments was to determine the effect of loading rate of the biodegradation process of o-cresol. The experiments started with 100 mg L^{-1} o-cresol, at increasing flow rates of 11.32, 49.35, 99.34, 220.11, 326.32, and 510.02 ml h^{-1} with the corresponding residence times of

33.13, 7.60, 3.77, 1.70, 1.15, and 0.74 h, respectively. For 300 mg L^{-1} o-cresol, flow rates tested were 15.69, 32.35, 56.39, 102.76, 184.17, and 342.37ml h^{-1}, with the corresponding residence times of 28.68, 13.91, 7.98, 4.38, 2.44, and 1.31 h. As for 500 mg L^{-1} o-cresol, the flow rates were 11.32, 44.16, 140.62, 249.67, and 380.99 ml h^{-1} with the residence times of 39.75, 10.19, 3.20, 1.80, and 1.18 h, respectively.

3.4.2.1 Binary-substrate biodegradation in CPBB

The fourth set of experiments was to examine the effect of loading rate and the interaction between phenol and p-cresol as well as the interaction between phenol and o-cresol on biodegradation of binary-substrate. For phenol and p-cresol co-biodegradation, the initial concentration was set to 500 and 100 mg L^{-1}, 500 and 300 mg L^{-1}, as well as 500 and 500 mg L^{-1}, respectively. The applied flow rates and residence time for the biodegradation of 500 and 100 mg L^{-1} phenol and p-cresol in CPBB were 9.56, 53.23, 113.39, 225.19, 296.17, 458.39 ml h^{-1} and 47.07, 8.45, 3.97, 2.03, 1.52, 0.98 h respectively. For 500 and 300 mg L^{-1} phenol and p-cresol biodegradation in CPBB, the flow rates and corresponding residence time were 11.29, 80.83, 124.50, 178.60, 275.60, 312.26 ml h^{-1} and 39.86, 5.57, 3.61, 2.52, 1.63, 1.44 h, respectively. For 500 and 500 mg L^{-1} phenol and p-cresol biodegradation, the flow rates were 11.34, 25.36, 50.39, 86.36, 150.39, and 250.97 ml h^{-1} with the residence times of 39.68, 17.74, 8.93, 5.21, 2.99, and 1.79 h. The initial concentration for phenol and o-cresol co-biodegradation was also set to 500 and 100 mg L^{-1}, 500 and 300 mg L^{-1}, as well as 500 and 500 mg L^{-1}. The applied flow rates and residence time for the biodegradation of 500 and 100 mg L^{-1} phenol and o-cresol in CPBB were 11.34, 27.39, 61.02, 107.36, 189.37, 293.04 ml h^{-1} and 39.68, 16.43, 7.37, 4.19, 2.38 1.54 h respectively. For 500 and 300 mg L^{-1} phenol and p-

cresol biodegradation in CPBB, the flow rates and corresponding residence time were 11.29, 80.83, 124.50, 178.60, 275.60, 312.26 ml h^{-1} and 39.86, 5.57, 3.61, 2.52, 1.63, 1.44 h, respectively. For 500 and 500 mg L^{-1} phenol and p-cresol biodegradation, the flow rates were 11.34, 25.36, 50.39, 86.36, 150.39, and 250.97 ml h^{-1} with the residence times of 39.68, 17.74, 8.93, 5.21, 2.99, and 1.79 h.

3.4.2.2 Ternary-substrate biodegradation in CPBB

The experimental procedures for ternary-substrate biodegradation in CPBB were identical to mono- and binary-substrate biodegradation except for the difference of initial substrates combination. Table 3.5 summarizes the concentration of phenolic compounds of different combinations, applied flow rates and corresponding residence time during the biodegradation of ternary-substrate in CPBB.

Table 3.5 Concentration of phenolic compounds, flow rates and corresponding residence time of ternary-substrate biodegradation in CPBB

phenol Concentration (mg L^{-1})	p-cresol concentration (mg L^{-1})	o-cresol concentration (mg L^{-1})	Flow rates (mL h^{-1}) with corresponding residence time (h) given in the bracket
500	100	100	16.98 (26.50), 54.39 (8.27), 156.32 (2.88), 257.31 (1.75), 431.85 (1.04)
500	100	300	10.31 (43.65), 45.32 (9.93), 99.41 (4.53), 156.39 (2.88), 329.38 (1.37)
500	100	500	11.24 (40.04), 46.67 (9.64), 75.40 (5.97), 144.85 (3.11), 279.31 (1.61), 325.35 (1.38)
500	300	100	14.39 (31.27), 57.64 (7.81), 121.36 (3.71), 250.36 (1.80), 329.36 (1.37)
500	300	300	9.01 (49.98), 36.27 (12.41), 55.39 (8.12), 143.75 (3.13), 256.96 (1.75)
500	300	500	8.35 (53.89), 36.32 (12.39), 73.02 (6.16), 199.10 (2.26), 212.32 (2.12)
500	500	100	9.87 (45.59), 36.27 (12.41), 93.33 (4.82), 147.83 (3.04), 212.50 (2.12)
500	500	300	14.08 (31.96), 33.19 (13.56), 75.40 (5.97), 132.01 (3.41), 173.75 (2.59)
500	500	500	12.39 (36.32), 51.39 (8.76), 110.95 (4.06), 170.96 (2.63), 210.39 (2.14)

3.4.2.3 Toxicity tests

Toxicity tests were carried out on all feed combinations (individual, binary, and ternary) and treated effluent from the continuous CPBB system under selected operating conditions. In case of the treated effluent samples, effluent corresponded to the maximum removal rate were selected for toxicity tests as they were representing the optimal operating conditions in the CPBBs in terms of phenolic compound removal rate. By comprising the difference of toxicity between the untreated feed solution and treated effluent using a paired t-test, it was then possible to examine the efficiency of CPBB and potential application of this configuration for the treatment of industrial wastewater containing phenols. The results could also help to assess the potential risk of releasing the treated effluents under the optimal operation condition in CPBB into the ecological environment. The untreated feed solution was obtained by mixing phenolic compounds with reverse osmosis water (RO water). The effluent samples were taken from the continuous system and were stored in the -80 °C Freezer prior to the tests.

3.5 Analytical Methods

Optical density was used as an indication of biomass concentration in the batch system. A Mini Shimadzu (model 1240) ultraviolet (UV) spectrophotometer at a wavelength of 620 nm was utilized to determine the optical density (OD). Samples were centrifuged for 5 minutes at 10000 rpm prior to analysis by HPLC and before being tested by ultraviolet spectrophotometer. The modified McKinney's medium was used as the blank. A calibration curve was developed and used to convert the OD to biomass concentration (Figure A.1). The procedures for developing this curve

are provided in the appendix. The correlation coefficients of biomass calibration curves were 99.97%.

As indicated earlier, concentration of phenols in case of mono-substrate were determined by a spectrophotometer. These were done by conducting a full scan over the wavelength range of 190 nm to 1100 nm to identify the wavelengths at which peak for each phenolic compound appeared. The concentration of samples used was 100 mg L^{-1}. The spectrophotometric scan identified 269 nm, 269 nm, and 277 nm as the peak wavelength for phenol, o-cresol, and p-cresol, respectively. Calibration curves developed using standard solutions of phenol, o-cresol or p-cresol and used to convert the optical density to substrate concentrations (Figure A.2, A.3, and A.4). The concentration of the standard solutions used for developing the calibration curve were 10, 12.5, 25, 50, and 100 mg L^{-1} for all three chemicals. When the concentration of substrate in the samples was over 100 mg L^{-1}, it was diluted before being tested. Concentrations of phenol and cresols in binary-substrate and ternary-substrate systems were determined by HPLC (Alexieva et al., 2008). An Agilent HPLC 1100 with a Diode Array Detector equipped with a reversed phase C18 column (Nova pack: 4.6 x 150 mm: 4μm) was used for this purpose. The mobile phase was a mixture of methanol and water (50:50) with a flow rate of 1.0 mL min^{-1}. Detection was carried out using an ultraviolet detector at a wavelength of 220 nm (Alexieva et al., 2008). Samples used for phenol and cresols concentration measurements were centrifuged for 5 minutes at 10000 rpm prior to analysis by HPLC. The calibration curve was developed by analyzing a series of standard solutions. These solutions contained all three substrates (phenol, p-cresol, o-cresol) with their respective concentration of each compound being 10, 12.5, 25, 50, and 100 mg L^{-1} (Figure A.6).

3.6 Toxicity Test Procedures

The procedure for toxicity tests as described by Toussaint et al. (1995) are provided as follow. First, one gram of brine shrimp eggs (Ocean Star International, Inc. Snowville, USA) was added to a flask containing 100 ml of reverse osmosis (RO) water with 20 g L^{-1} NaCl. The NaCl concentration was maintained at 20 g L^{-1} to keep shrimps live. The flask was kept at room temperature and was aerated for 24 hours to allow shrimps to hatch. After 24 hours, 0.5 mL aliquots of the solution were poured into each of six watch glasses. For the first 2 watch glasses, 2 mL of RO water was added as the sample (control). This was followed by adding 2 mL of sample to 4 other watch glasses. The toxicity of each sample was carried out in duplicates. The watch glasses were monitored for the number of live/motile shrimps. A 7X magnification Optivisor headset was used to count all motile shrimps. Counting was carried out at times 0, 0.5, 1, and 2 hours with time zero representing the time when samples were added to watch glasses.

Before the tests, the stored samples (treated effluents) were re-analyzed by HPLC and the obtained results were compared with those obtained with fresh samples during the experiments in CPBBs to ensure the substrates were not degraded during the storage.

3.7 Statistical Analysis

For batch experiments, selective set of experiments were run in duplicates to assess the reproducibility of results and associated errors. The measurement average (three times) of experiments have been presented as the results and associated standard deviations as error bars.

For continuous experiments in CPBBs, the system was maintained at each flow rate for minimum three residence times after the establishment of steady state. At least three samples were taken during this period. The results were represented as the average value of the data obtained during this period and associated standard deviation as the error bar.

For toxicity test, the goal was to examine the efficiency of CPBB in reducing the toxicity of phenols in wastewater. Hence, a paired t-test was used to determine whether there was significant difference between the untreated feed solution and the treated effluent samples (Box et al., 2005).

4 RESULTS AND DISCUSSION – BATCH SYSTEM

This chapter presents the results of aerobic biodegradation of phenolic compounds in the batch system. The effect of initial concentration and temperature on the biodegradation of individual compound is discussed first, followed by the results for co-biodegradation of binary-substrate and ternary-substrate. For binary- and ternary-substrate systems, the effect of initial concentrations and interaction among different substrate compounds are discussed. Biodegradation of phenol as a single substrate in batch was excluded because of the abundant literature information (Al-Kahlid et al., 2012; Agarry et al., 2008).

4.1 Batch Biodegradation of p-cresol

The effects of two variables were investigated for p-cresol biodegradation: initial concentration of p-cresol and temperature. The presented results are the average values. The error-bars indicates the associated standard deviations.

4.1.1 Effects of p-cresol Initial Concentration

Biodegradation of p-cresol was studied using various initial concentrations of p-cresol ranging from 100 to 500 mg L^{-1} (100, 200, 300, and 500 mg L^{-1}). Figure 4.1 shows the biodegradation profiles at different initial concentrations of p-cresol. The experiments were started in the evening thus there is scarce data in the beginning.

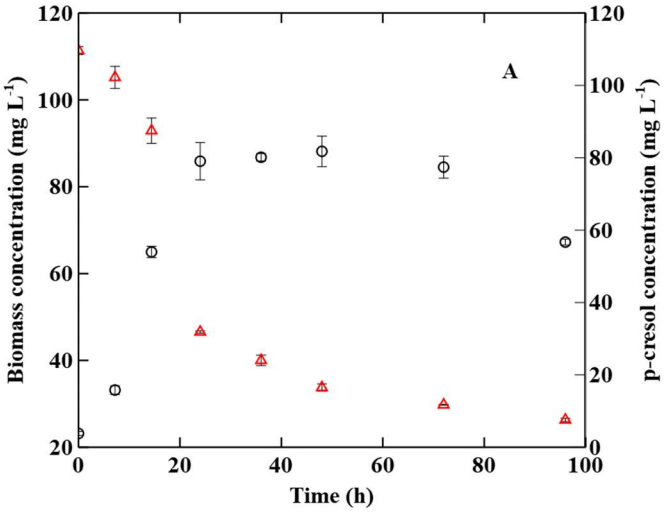
A
Biomass concentration (mg L-1)
p-cresol concentration (mg L-1)
Time (h)
120
100
80
60
40
20
0
0
20
40
60
80
100

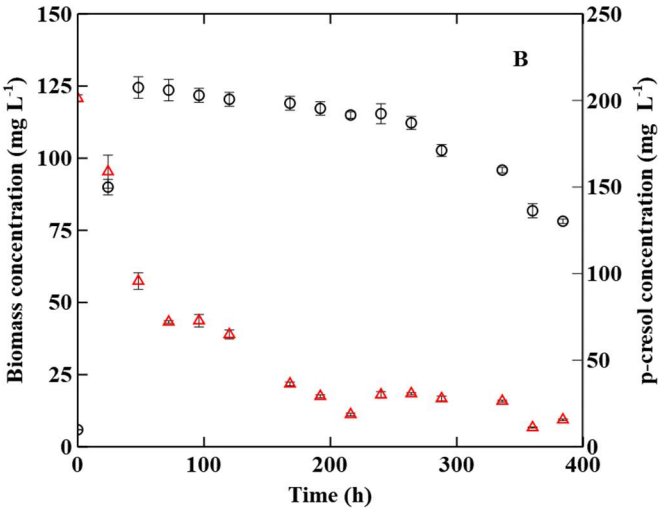
B
Biomass concentration (mg L-1)
p-cresol concentration (mg L-1)
Time (h)
150
125
100
75
50
25
0
250
200
150
100
50
0
0
100
200
300
400

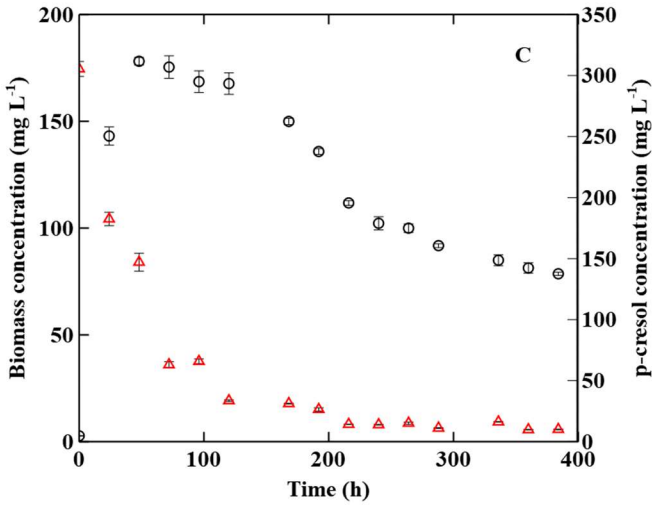
C
Biomass concentration (mg L-1)
p-cresol concentration (mg L-1)
Time (h)
200
150
100
50
0
350
300
250
200
150
100
50
0
0
100
200
300
400

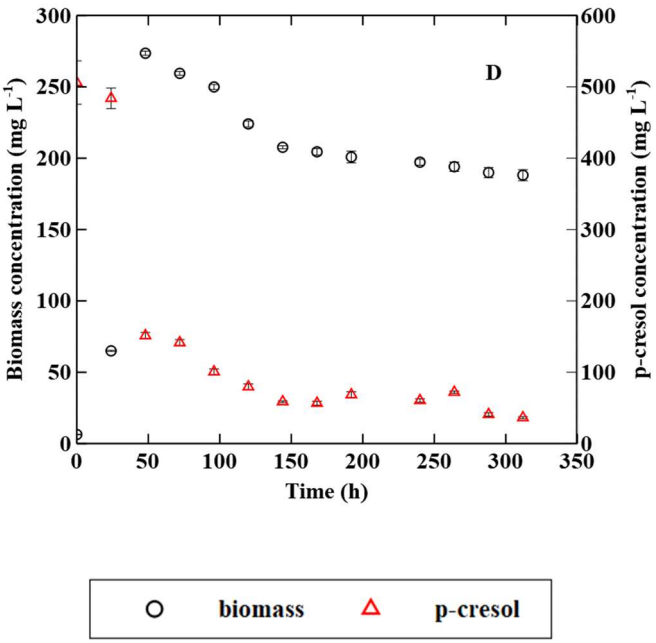

Figure 4.1 Biomass growth and substrate biodegradation profiles obtained with various initial concentrations of p-cresol at room temperature (24 ± 1 °C). (A): 100 mg L^{-1}, (B): 200 mg L^{-1}, (C): 300 mg L^{-1}, (D): 500 mg L^{-1}. Error bars represent one standard deviation and may not be visible in some cases.

The potential of microbial culture in biodegradation of p-cresol was verified through cultivating the microbial culture in a wide range of p-cresol concentrations in the batch system. Regardless of p-cresol initial concentration, there was a direct relationship between the microbial growth and p-cresol biodegradation. Bacteria consumed p-cresol as their carbon and energy source, thus an increase in biomass concentration and a decrease in p-cresol concentration co-occurred and correlated with each other. An increase of p-cresol initial concentration resulted in higher maximum biomass concentration and more extended period for completion of biodegradation. As indicated in Figure 4.1, when the p-cresol initial concentration was 100 mg L^{-1}, the maximum biomass concentration was 88.1 mg L^{-1}; while with 500 mg L^{-1} p-cresol (the highest initial concentration employed), the maximum biomass concentration was 273.5 mg L^{-1}. Complete

biodegradation of 100 and 500 mg L^{-1} p-cresol took 36 h and 312 h, respectively. The lag phases in all cases were negligible. Bacterial growth started immediately after inoculation, indicating p-cresol, even at the highest concentration tested, did not have a strong inhibitory effect. Another observation was that biomass concentration reached to a maximum and then leveled off, but p-cresol concentrations kept decreasing. The reason could be continued biodegradation by a stationary (non-growing) population or that the death rate balanced the slow growth of population due to the lack of enough substrate.

Through calculating the slope of linear part of p-cresol concentration profiles, average biodegradation rate of p-cresol was determined at different initial concentrations and summarized in Table 4.1.

As shown in Table 4.1, the increase of initial concentration led to the elevated biodegradation rate. The highest biodegradation rate of p-cresol was 6.8 mg L^{-1} h^{-1} and obtained with an initial concentration of 500 mg L^{-1}. These results indicated that biodegradation rate was dependent on the initial concentration of p-cresol in the experimental range (100 - 500 mg L^{-1}). The highest concentration of p-cresol tested did not impose inhibition on the microbial activity.

Table 4.1 Effect of initial concentration of p-cresol on its biodegradation rate

p-cresol initial concentration ($mg\ L^{-1}$)	Biodegradation rate of p-cresol ($mg\ L^{-1}\ h^{-1}$)
100	1.7 (0.99) *
200	1.9 (0.95)
300	3.2 (0.94)
500	6.8 (0.84)

*Numbers in the parentheses indicates regression coefficient.

4.1.2 Effects of Temperature on Biodegradation of p-cresol

The effect of temperature on biodegradation of p-cresol was also evaluated because temperature is one of the most important factors influencing biodegradation process. Some experiments were conducted in duplicates to verify the reproducibility (10, 15, 30, and 35 °C). The results for biodegradation of 300 mg L^{-1} at five different temperatures of 10, 15, 20, 30, and 35°C are shown in Figure 4.2. In all evaluated temperatures, p-cresol biodegradation trends were similar. Besides, an increase in biomass concentration was accompanied by a decrease of p-cresol concentration. The results also indicated that temperature influenced the length of lag phase. To be specific, the lag phase at 10, 15, and 20 °C was negligible but at higher temperatures of 30 and 35 °C, longer lag phases were observed.

The required time for complete biodegradation of p-cresol varied by temperature. Data in Figure 4.2 show that at 10 and 15 °C, microbial culture took up to 600 and 320 hours for the complete biodegradation of p-cresol. By contrast, at higher temperature of 30 and 35 °C less than 200 hours was required. In other words, higher temperature enhanced the ability of bacteria to utilize p-cresol. The maximum biomass concentrations achieved at 10 and 15 °C were 144 and 147 mg L^{-1},

respectively, while at 30 and 35 °C, the maximum biomass concentrations were 275 and 136 mg L^{-1}. These results together with calculated biodegradation rates, presented in the following section, suggested the optimum temperature was 35 °C.

A

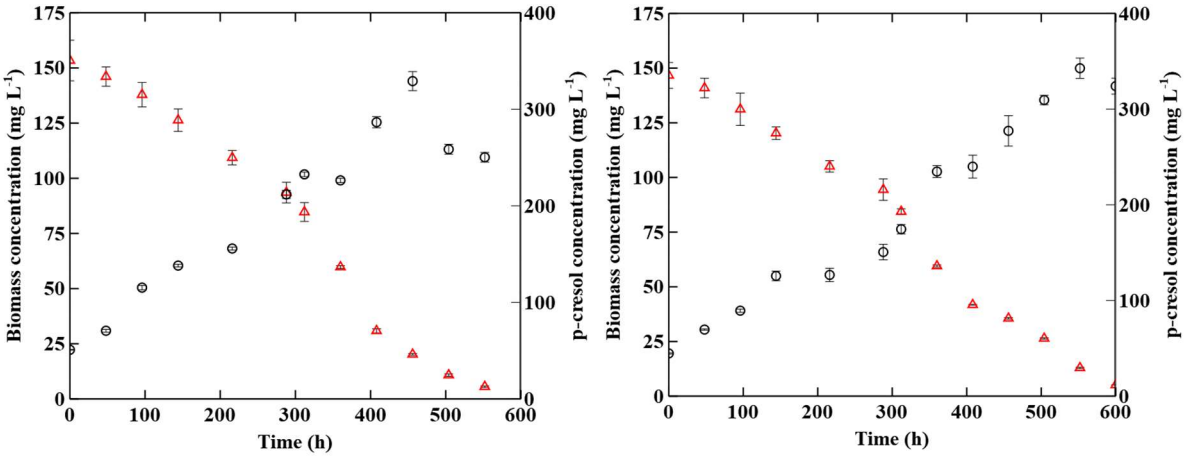

B

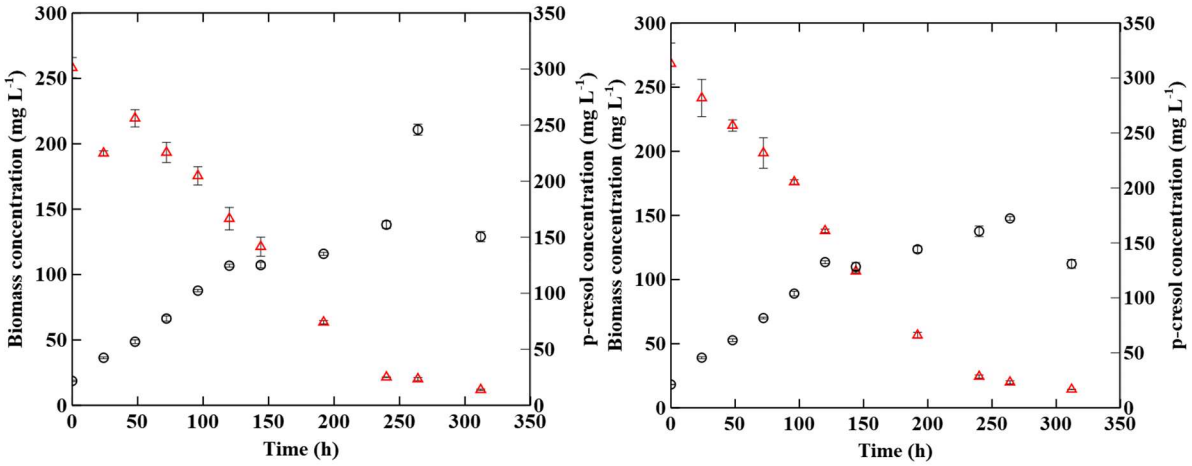

C

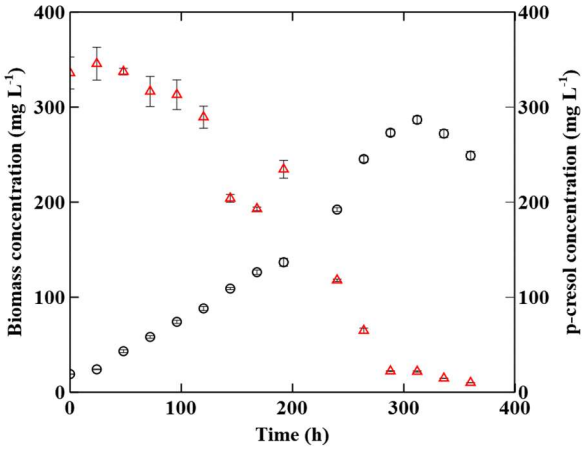
Biomass concentration (mg L-1)
p-cresol concentration (mg L-1)
Time (h)
0
100
200
300
400

D

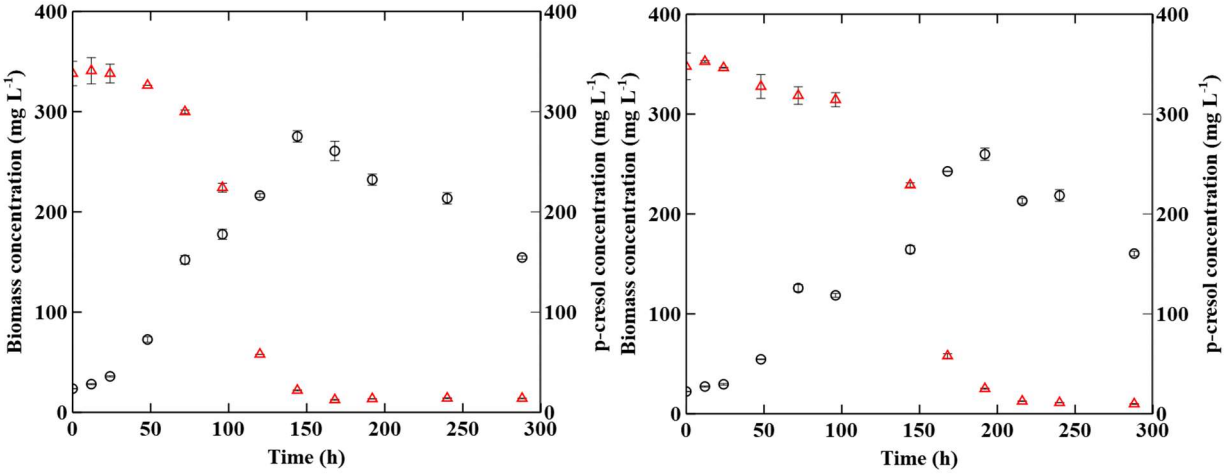
Biomass concentration (mg L-1)
p-cresol concentration (mg L-1)
Time (h)
0
50
100
150
200
250
300

E

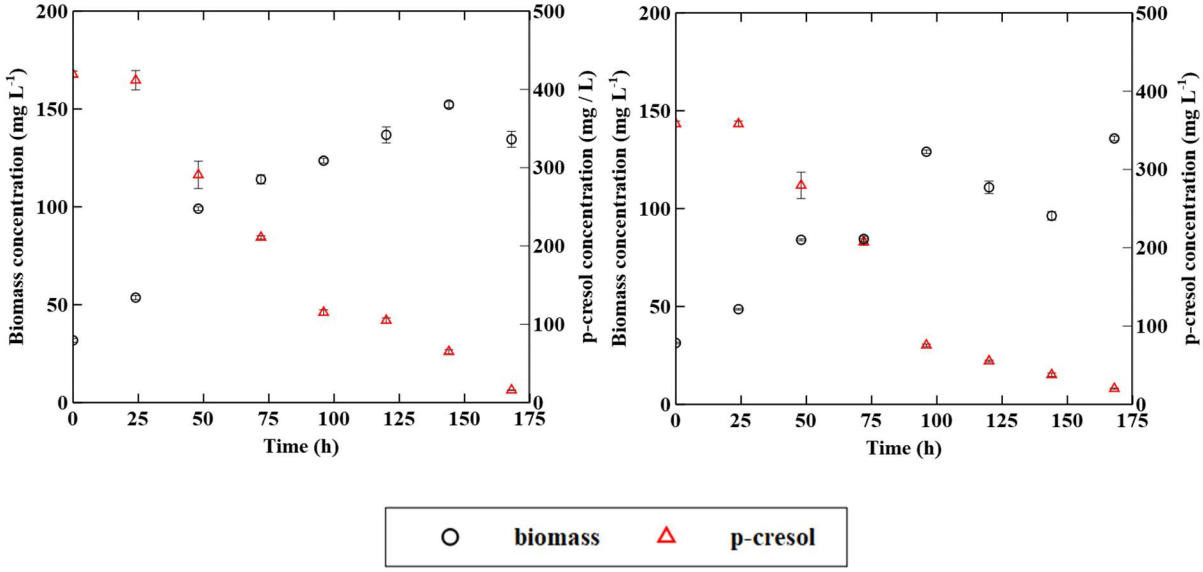

Figure 4.2 Biomass growth and p-cresol concentrations obtained at various temperatures. (A): 10 °C, (B): 15 °C, (C): 20 °C, (D): 30 °C, (E): 35 °C. Error bars represent one standard deviation and may not be visible in some cases.

Table 4.2 summarizes biodegradation rates of p-cresol at various temperatures. Data presented here revealed that increase of temperature in the range 10 to 35 °C increased the biodegradation rate from 1.0 to 4.0 mg L^{-1} h^{-1}, respectively.

Table 4.2 Effect of temperature on p-cresol biodegradation rate

Temperature (°C)	**Biodegradation rate of p-cresol (mg L^{-1} h^{-1})**
10	1.0 ± 0.2 (0.96) *
15	1.6 ± 0.1 (0.99)
20	2.0 (0.95)
24 ± 1	3.2 ± 0.7 (0.92)
30	3.6 ± 0.6 (0.93)
35	4.0 ± 0.1 (0.99)

*Numbers in parentheses are the Regression coefficients

4.2 Batch Biodegradation of o-cresol

4.2.1 Effects of o-cresol Initial Concentration

Figure 4.3 presents the profiles of biodegradation of o-cresol at different initial concentrations. Similar to p-cresol biodegradation, there was a correlation between microbial growth and o-cresol biodegradation. An increase of biomass concentration corresponded a decrease of o-cresol concentration. An increase of o-cresol initial concentration caused a longer period for complete biodegradation. For instance, biodegradation of 100 mg L^{-1} o-cresol finished within 48 hours, while for initial concentration of 500 mg L^{-1} the required time was 216 hours. For initial concentration up to 300 mg L^{-1}, the lag phase was negligible. However, when initial concentration was increased to 500 mg L^{-1}, the lag phase was 72 hours, indicating potential inhibition of bacterial growth. An increase of maximum biomass concentration from 63.1 to 248.1 mg L^{-1} was also observed with the corresponding increase of initial concentration from 100 to 500 mg L^{-1}.

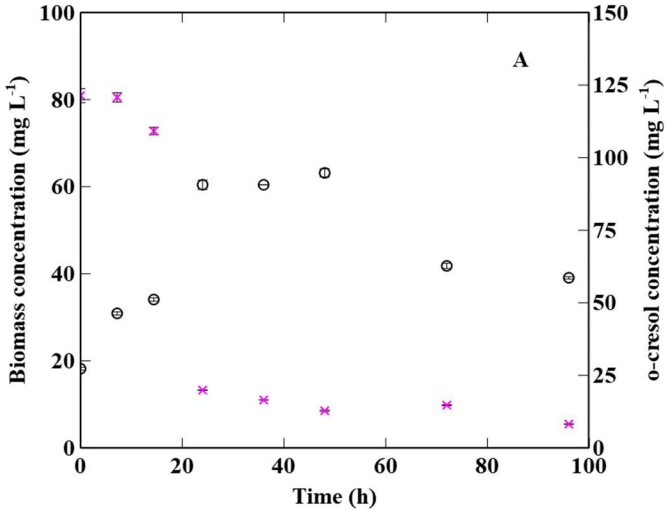

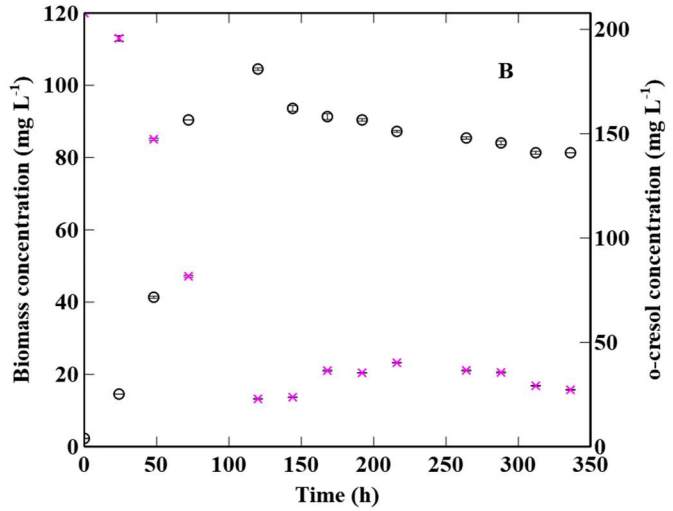
B
Biomass concentration (mg L-1)
o-cresol concentration (mg L-1)
Time (h)
0
20
40
60
80
100
120
0
50
100
150
200
0
50
100
150
200
250
300
350

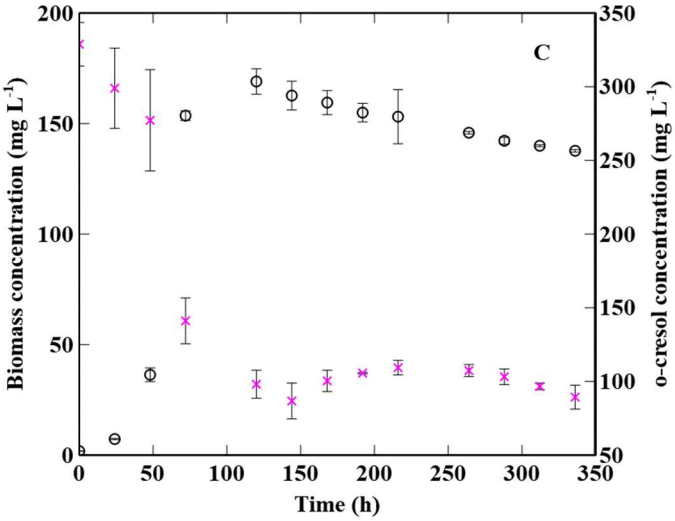
C
Biomass concentration (mg L-1)
o-cresol concentration (mg L-1)
Time (h)
0
50
100
150
200
50
100
150
200
250
300
350
0
50
100
150
200
250
300
350

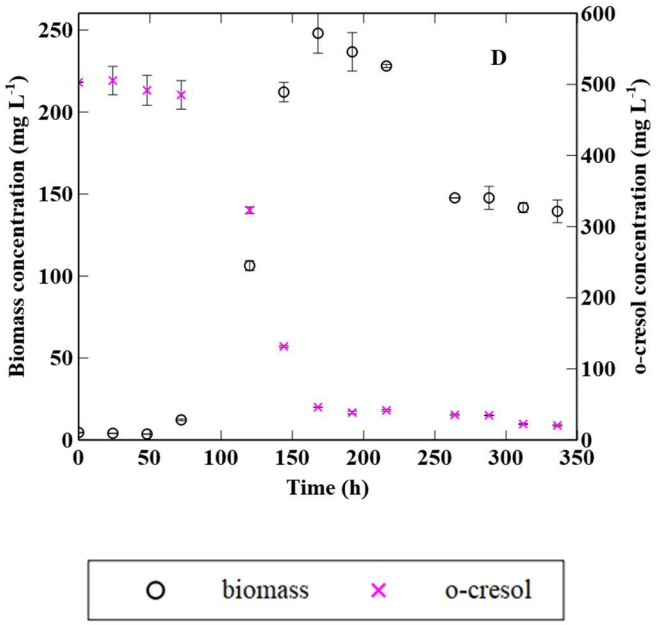

Figure 4.3 Biomass growth and substrate biodegradation profile obtained with various initial o-cresol concentration at room temperature (24 ± 2 °C). (A): 100 mg L^{-1}, (B): 200 mg L^{-1}, (C) 300: mg L^{-1}, (D): 500 mg L^{-1}. Error bars represent one standard deviation and may not be visible in some cases.

The biodegradation rates of o-cresol at different initial concentrations are shown in Table 4.3. The calculated biodegradation rates ranged from 0.7 to 4.2 mg L^{-1} h^{-1} when the initial concentration was increased from 100 to 500 mg L^{-1}. The results demonstrated that application of higher initial concentration of o-cresol up to 500 mg L^{-1} increased biodegradation rate and there was a positive correlation between biodegradation rate and increase in initial concentration. Similar to p-cresol biodegradation, o-cresol at high concentrations did not impose strong inhibition on bacterial growth during the exponential phase of growth but caused a longer lag phase during the early stage of growth.

Table 4.3 Effect of initial concentration of o-cresol on its biodegradation rate

o-cresol initial concentration (mg L^{-1})	Biodegradation rate of o-cresol (mg L^{-1} h^{-1})
100	0.7 (0.92) *
200	1.7 (0.99)
300	3.4 (0.99)
500	4.2 (0.89)

*Numbers in the parentheses are regression coefficients.

4.2.2 Effects of Temperature on Biodegradation of o-cresol

The results for biodegradation o-cresol (300 mg L^{-1}) at five different temperatures are shown below in Figure 4.4. As seen in this figure, the lag phase was negligible in all temperatures with the exception of 10 °C in which no bacterial activity or biodegradation occurred. In this case, the concentration of o-cresol remained the same even after 500 hours. Application of different temperatures resulted in different period for completion of biodegradation. For instance, at 15 °C the required time was 500 hours, while at 30 and 35 °C biodegradation was complete at 288 and 312 hours, respectively. The maximum biomass concentration achieved at 30 °C was higher than any other temperatures (10, 15, 20, 25, and 30 °C).

A

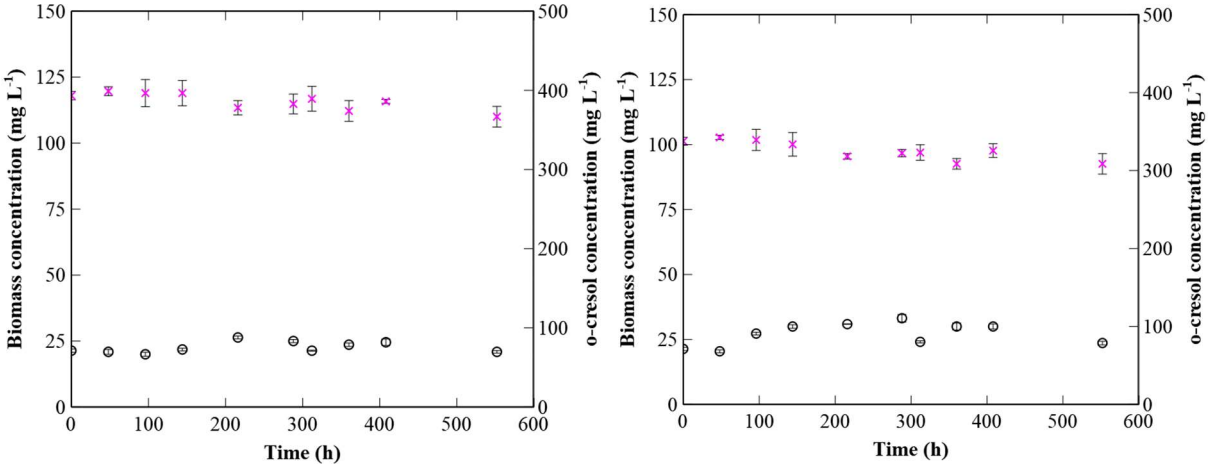
Biomass concentration (mg L-1)
o-cresol concentration (mg L-1)
Time (h)
Biomass concentration (mg L-1)
o-cresol concentration (mg L-1)
Time (h)

B

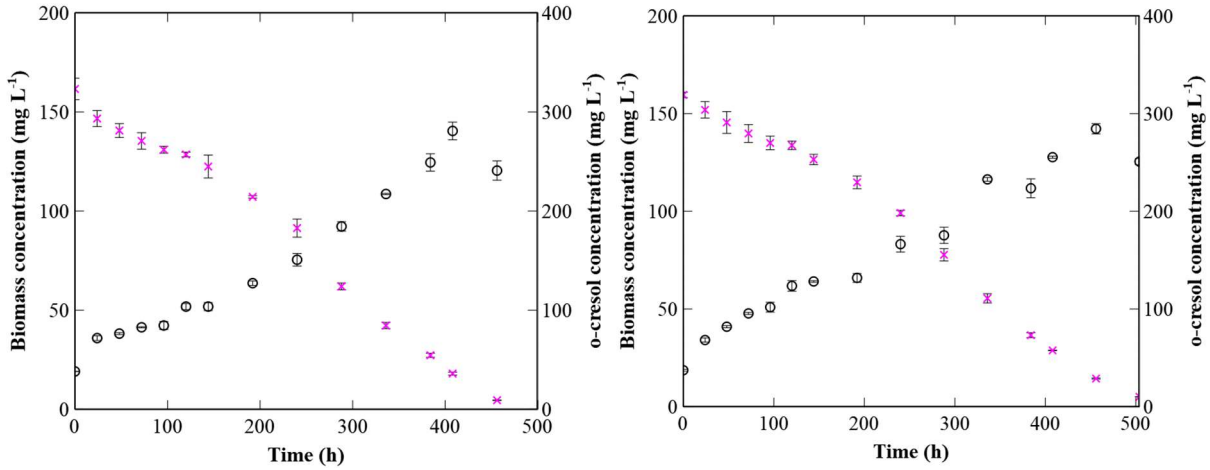
Biomass concentration (mg L-1)
o-cresol concentration (mg L-1)
Time (h)
Biomass concentration (mg L-1)
o-cresol concentration (mg L-1)
Time (h)

C

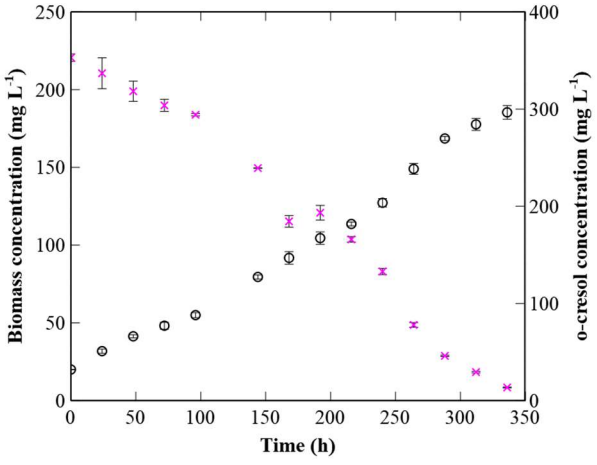
Biomass concentration (mg L-1)
o-cresol concentration (mg L-1)
Time (h)

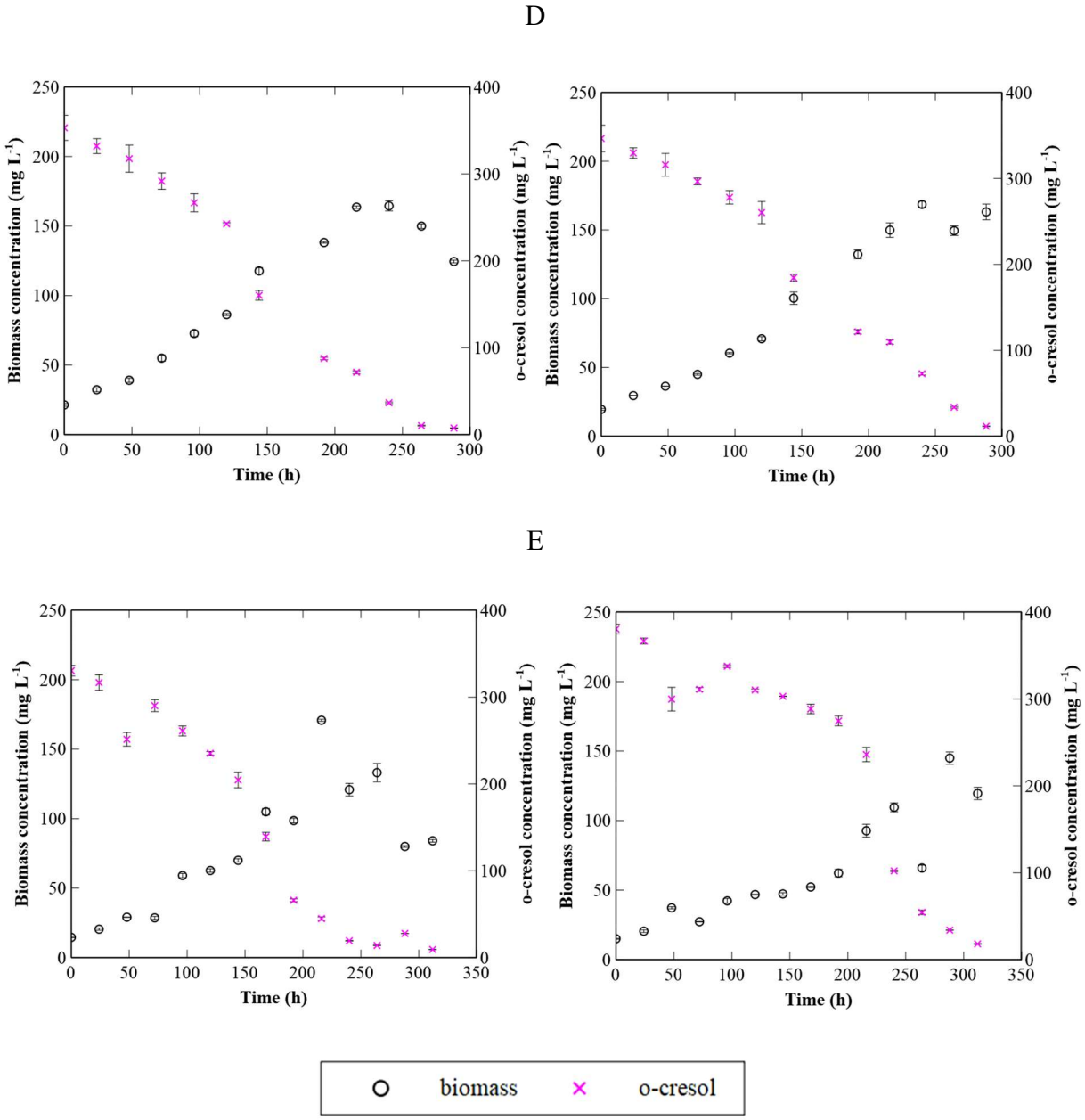

Figure 4.4 Biomass growth and o-cresol concentrations observed at various temperatures. (A): 10 °C, (B): 15 °C, (C): 20 °C, (D): 30 °C, (E): 35 °C. Error bars represent one standard deviation and may not be visible in some cases.

Table 4.4 summarizes the biodegradation rate of o-cresol at different temperatures. As seen, the highest rate (3.4 mg L^{-1} h^{-1}) was observed at 24 °C. Biodegradation rate was lower at the temperature above or below 24 °C. Low temperature had a marked impact on the growth of

bacteria and their utilization of o-cresol, which was indicated by low biodegradation rates. At 35 °C, bacterial has a long adaptation stage (lag phase) even though the biodegradation rate appeared to be high. The optimum temperature for o-cresol biodegradation seems to be around 24 °C.

Table 4.4 Effect of temperature on biodegradation rate of o-cresol

Temperature (°C)	**Biodegradation rate of o-cresol ($mg\ L^{-1}\ h^{-1}$)**
10	0 *
15	0.7 ± 0.1 (0.98)
20	1.1 (0.96)
24 ± 1	3.4 ± 0.7 (0.89)
30	1.9 ± 0.6 (0.91)
35	1.7 ± 0.1 (0.97)

*Numbers in parentheses are the Regression coefficients

4.3 Comparison of the Biodegradation process of p-cresol and o-cresol in Batch System

The differences between the biodegradation of p-cresol and o-cresol are compared.. The biodegradation rates of p-cresol and o-cresol as a function of their initial concentration are presented in Figure 4.5 (left panel). Biodegradation rate increased with an increase of initial concentration for both p-cresol and o-cresol and the linear trend can be expressed by Equations 4.1 and 4.2 where r is the biodegradation rate and S_i is the initial concentration. The value of rate constants for p-cresol and o-cresol (0.0126 vs. 0.0091) indicated that biodegradation rate of p-cresol was slightly higher than that of o-cresol in the batch system.

$$r_{p-cresol} = 0.0126\, S_{i-p-cresol} \qquad (R^2 = 0.93) \tag{4.1}$$

$$r_{o-cresol} = 0.0091\, S_{i-o-cresol} \qquad (R^2 = 0.92) \tag{4.2}$$

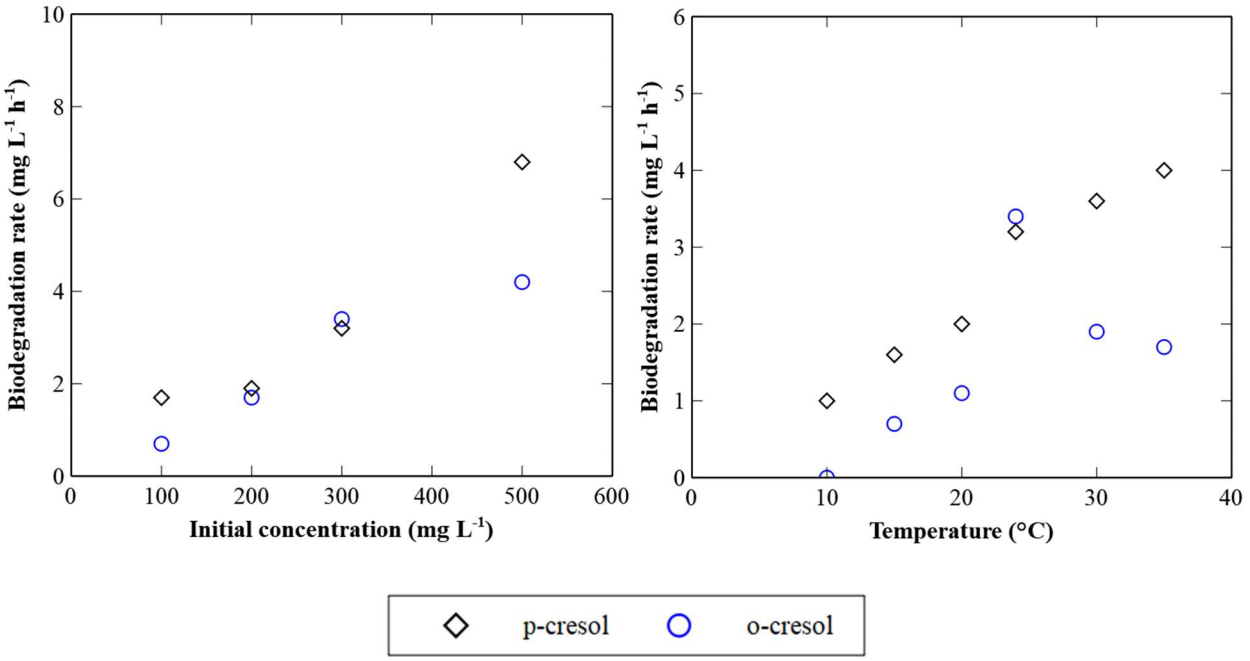

Figure 4.5 Biodegradation rate of p-cresol and o-cresol as a function of initial concentration (left panel) and temperature (right panel).

The right panel in Figure 4.5 represents biodegradation rates of 300 mg L^{-1} p-cresol and o-cresol as a function of temperature. As sees the optimum temperature for o-cresol biodegradation is 25 °C and higher temperatures lead to lower rates. Similar trends have been reported for biodegradation of substrates such as trans-4-methyl-1-cyclohexane carboxylic acid (*trans*-4MCHCA) under aerobic (Paslawski, 2008) and anaerobic (Gunawan, 2013) conditions, as well as 1, 4 – hydroquinone (Kumar, 2010) by *Pseudomonas putida*. However, the pattern for p-cresol was different and higher temperatures (up to 35 °C) did not hamper the microbial activity and biodegradation process. The optimum temperature was 35 °C.

Moreover, under most temperatures, biodegradation rate of p-cresol was higher than o-cresol at the same temperature. A paired t-test was conducted to verify it statistically and the results are

presented in Table 4.5. The mean of biodegradation rate difference at different temperatures is 1.10 mg L^{-1} h^{-1} and p-value is 0.024 (< 0.05). Therefore, the assumption that the biodegradation rate of p-cresol is higher than o-cresol at similar temperature is valid. The bacterial culture used in this study can degrade p-cresol in a broader range of temperature.

Table 4.5 Paired t-test results of the effect of temperature on the biodegradation rate of p-cresol and o-cresol

	biodegradation rate of p-cresol	**biodegradation rate of o-cresol**
Mean	2.567	1.467
Variance	1.447	1.371
Observations	6	6
Pearson Correlation	0.746	
Hypothesized Mean Difference	0.000	
df	5.000	
t Stat	3.184	
P(T<=t)	0.024	

4.4 Binary-substrate Biodegradation

4.4.1 Co-biodegradation of Phenol and p-cresol

Upon completion of biodegradation experiments with individual compounds, experiments were conducted to examine co-biodegradation of phenol and p-cresol in the batch system. -Co-biodegradations of 500 mg L^{-1} phenol and p-cresol at various initial concentrations (100, 200, 300, 400, and 500 mg L^{-1}) were evaluated. Duplicate experiments were also included with phenol and p-cresol at their respective concentrations of 500 mg L^{-1} and 300 mg L^{-1} to assess the reproducibility of the results.

Figure 4.6 shows the results of biomass growth and substrates biodegradation at various combinations of phenol and p-cresol. Data for the repeated experiments are presented in panels (C-1) and (C-2). When the initial concentration of p-cresol was around 500 mg L^{-1}, no biodegradation activity was detected, likely due to the inhibition effect of high concentrations of both substrates, especially p-cresol. In other cases, regardless of mixture compositions, biodegradation of p-cresol occurred first, and only after complete consumption of p-cresol, phenol biodegradation occurred. This trend hints that p-cresol was the preferred substrate for bacterial culture (*P. putida*) when compared to phenol.

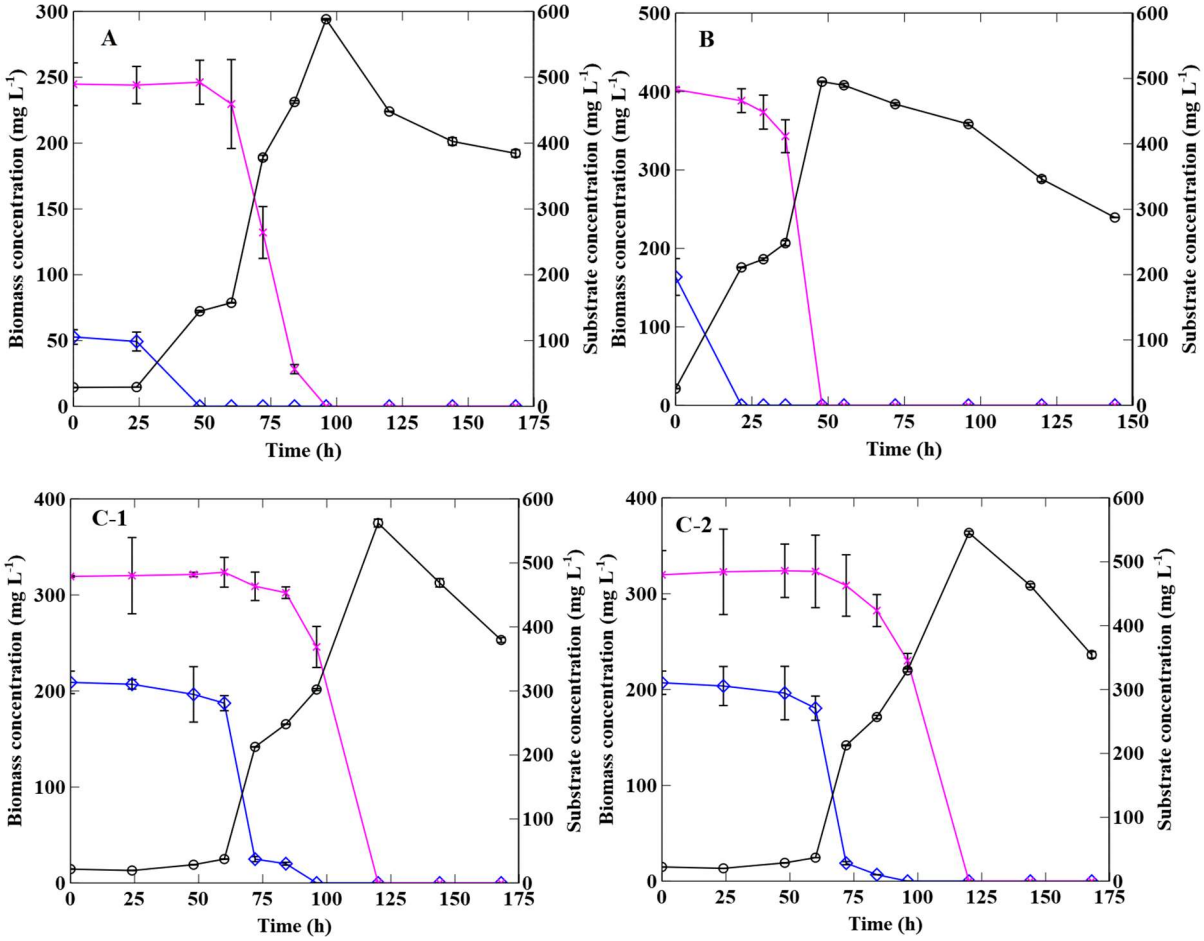

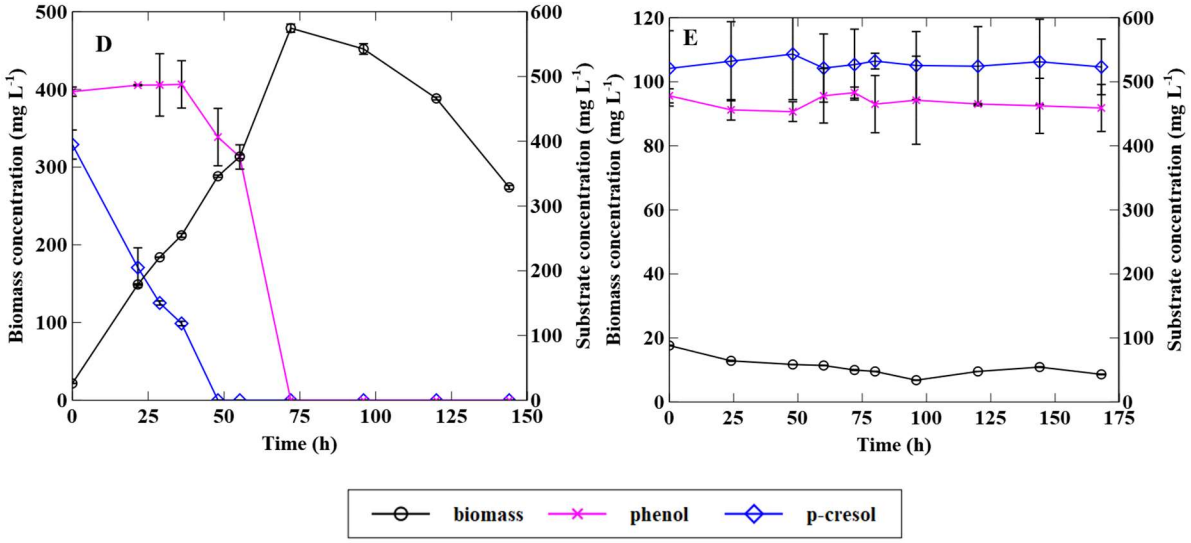

Figure 4.6 Co-biodegradation of phenol and p-cresol in mixtures of different compositions. Phenol concentration 500 mg L^{-1} and p-cresol concentration of 100 (A), 200 (B), 300 (C-1), 300 (C-2), 400 (D), and 500 mg L^{-1} (E). Duplicate experimental results are presented in panels C-1 and C-2. Error bars represent standard deviation and may not be visible in some cases.

Calculated biodegradation rates of phenol and p-cresol are shown in Table 4.6. As indicated in the table, when p-cresol concentration was in the range 100 - 200 mg L^{-1}, an increase in initial concentration led to the higher biodegradation rate of both p-cresol and phenol. However, the further increase resulted in the decrease of biodegradation rate of both substrates. Thus, the optimum initial concentrations resulting in the maximum biodegradation rates were 500 and 200 mg L^{-1} for phenol and p-cresol, respectively. The maximum biodegradation rate of phenol and p-cresol was 17.8 mg L^{-1} h^{-1} and 9.1 mg L^{-1} h^{-1}, respectively. The data in Table 4.6 also indicates that p-cresol posed inhibition effect of the growth of *P. putida* at high concentrations (>200 mg L^{-1}) when phenol was present. Biodegradation rates of phenol were calculated as 10.1 and 9.9 mg L^{-1} h^{-1} for the duplicate experiments (Panels C-1and C-2, Figure 4.6), which represented as 2% variation in the experimental results. This variation in the biodegradation rates of p-cresol was 3%. Overall these results showed the reproducibility of the experimental results.

Table 4.6 Summary of the biodegradation rates of phenol and p-cresol in binary-substrate system

Concentration of phenol ($mg\ L^{-1}$)	Concentration of p-cresol ($mg\ L^{-1}$)	Biodegradation rate of phenol ($mg\ L^{-1}\ h^{-1}$)	Biodegradation rate of p-cresol ($mg\ L^{-1}\ h^{-1}$)
500	100	11.6 (0.95)*	4.1
500	200	17.8 (0.84)	9.1
500	300	10.1 (0.98)	8.7 (0.86)
500	300	9.9 (0.93)	8.9 (0.88)
500	400	9.4 (0.87)	7.7 (0.98)
500	500	0	0

*Numbers in brackets represent the regression coefficient (R^2).

Figure 4.7 represents the biodegradation rate of p-cresol as a function of its initial concentration in the presence and absence of phenol. The addition of phenol appears to stimulate bacteria to utilize p-cresol more efficiently compared to the mono-substrate counterpart when the initial concentration of p-cresol was less than 500 mg L^{-1}. In other words, phenol increased the biodegradation rates of p-cresol when the initial concentration of p-cresol was in the range of 100 to 300 mg L^{-1}. For example, p-cresol biodegradation rate at the initial concentration of 200 mg L^{-1} in the presence of phenol is 4.8 times faster than that in the absence of phenol. When p-cresol concentration was increased to 500 mg L^{-1}, however, the inhibition effect of p-cresol stopped the bacterial activity. The linear relationship between p-cresol initial concentration and its biodegradation rate did not appear when phenol was present. The enhancement of p-cresol biodegradation could be attributed to enzyme activation when a lower concentration of phenol was available. Bacteria enzyme may form a complex with phenol and in a way positively influenced the following reactions (Schugerl et al., 2012). Substrate mixture of phenol and p-cresol may

induce both ortho pathway and meta pathway. In a study which examined bacterial catabolism of phenol and p-cresol, it was revealed that phenol could induce the p-cresol protocatechuate pathway via the induction of p-cresol methylhydroxylase (Heinaru et al., 2000)

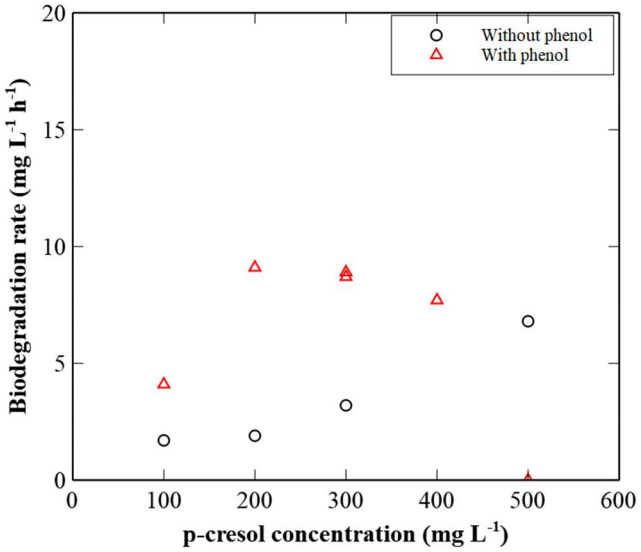

Figure 4.7 Biodegradation rates of p-cresol at different initial concentrations in the presence and absence of phenol.

4.4.2 Co-biodegradation of Phenol and o-cresol

Co-biodegradation of phenol and o-cresol was also carried out to investigate the effect of phenol on the biodegradation of o-cresol and vice versa. The initial phenol concentration was kept constant at 500 mg L^{-1}, while the initial o-cresol concentration was changed incrementally to 100, 200, 300, 400, and 500 mg L^{-1}.

The results of co-biodegradation of phenol and o-cresol in a binary-substrate batch system are presented in Figure 4.8. The first observation was that the lag phase in biomass growth increased

as the initial concentration of o-cresol was increased, especially for concentrations above 200 mg L^{-1}. For instance, the lag phase with100 mg L^{-1} was around 24 h but with 500 mg L^{-1} o-cresol, the lag phase increased to around 55 h. Similar to what was observed with p-cresol, when the o-cresol concentration was increased to 500 mg L^{-1}, no microbial activity was observed. Similar to the case with the individual substrate, the maximum biomass concentration increased as the initial concentration of o-cresol was increased, that can be explained by the availability of more substrate for bacteria to consume and grow. The most important observation was that contrary to the case of phenol and p-cresol, biodegradation of phenol and o-cresol happened simultaneously in all evaluated concentrations. This observation suggests that bacteria in the medium did not prefer phenol over o-cresol or vice versa.

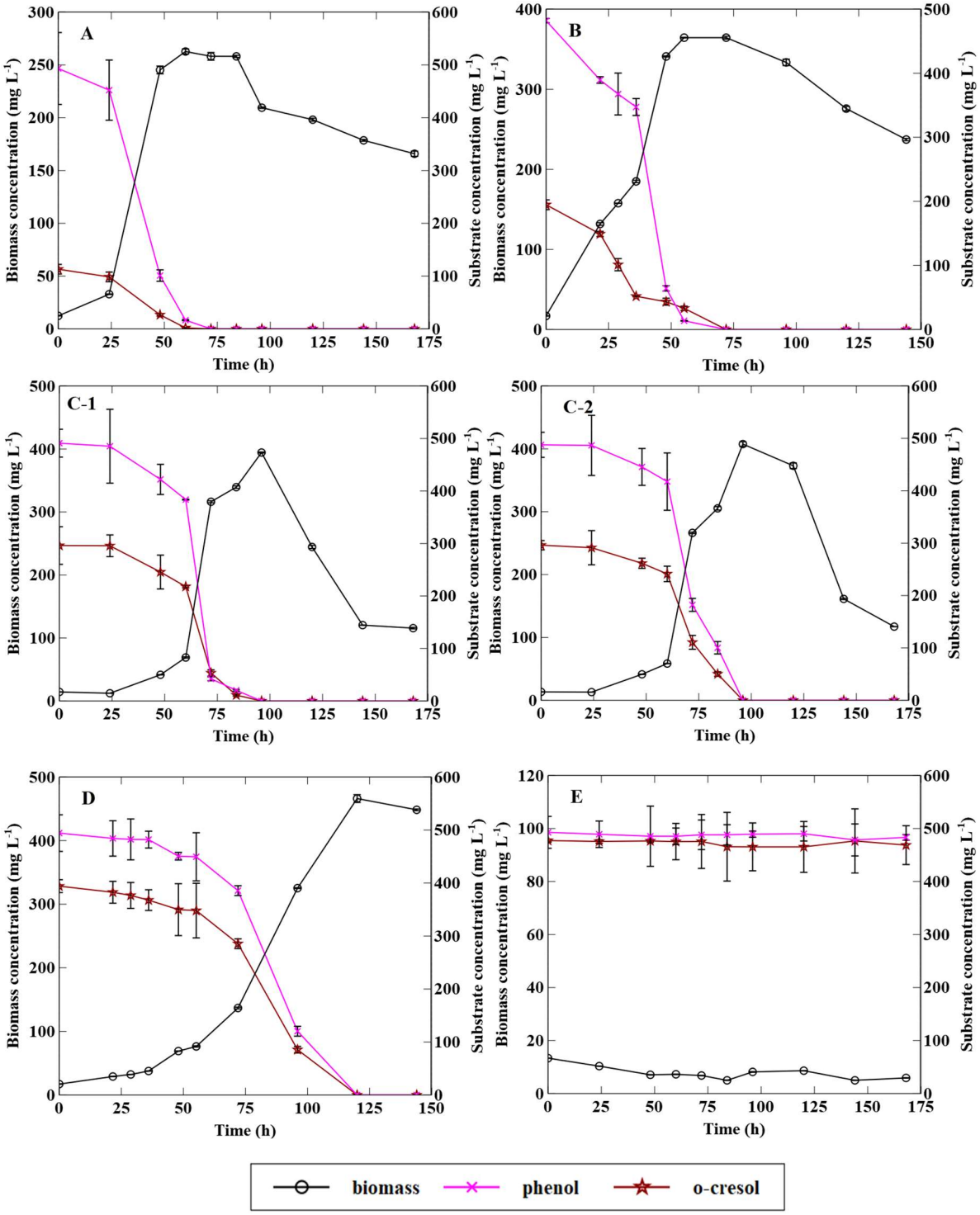

Figure 4.8 Co-biodegradation of phenol and o-cresol. Phenol concentration: 500 mg L^{-1} and o-cresol concentration: 100 (A), 200 (B), 300 (C-1), 300 (C-2), 400 (D), 500 mg L^{-1} (E). Duplicate experimental results are presented in panels C1 and C-2 at an o-cresol concentration of 300 mg L^{-1}. Error bars represent standard deviation and may not be visible in some cases.

Table 4.7 summarized biodegradation rates of phenol and p-cresol in the binary-substrate batch system. As seen, biodegradation rate of phenol increased as the initial concentration of o-cresol was increased until reaching the maximum value of 16.6 mg L^{-1} h^{-1} with an o-cresol initial concentration of 200 mg L^{-1}. Phenol biodegradation rate was then decreased as the concentration of o-cresol was further increased. The biodegradation rate of o-cresol followed the same trend. An increase of the initial concentration of o-cresol from 100 to 300 mg L^{-1} resulted in the increase in its biodegradation rate, but a further increase of o-cresol led to the decrease of biodegradation rate.

The biodegradation rates of o-cresol as a function of its initial concentration in the presence and absence of phenol are presented in Figure 4.9. Comparing the data for these two cases showed that the addition of phenol did not improve the biodegradation rate of o-cresol markedly, unlike the case of phenol and p-cresol where the addition of phenol increased the biodegradation rate of p-cresol. The exception was when o-cresol initial concentration was 200 mg L^{-1} whereby phenol improved the biodegradation rate of o-cresol by about three times. Like previous experiments, duplicate experiments were conducted to assess the reproducibility of the results (Panels C-1 and C-2). The biodegradation rates of phenol in these duplicate experiments were 12.9 and 11.1 mg L^{-1} h^{-1}, representing a 14.0% variation. For o-cresol, the biodegradation rates were 7.2 and 6.5 mg L^{-1} h^{-1}, indicating a 9.7% variation which again confirmed the experimental results were reproducible considering the biological nature of the system in which data were generated.

Table 4.7 Summary of the biodegradation rates of phenol and o-cresol during binary-substrate biodegradation

Concentration of phenol (mg L^{-1})	Concentration of o-cresol (mg L^{-1})	Biodegradation rate of phenol (mg L^{-1} h^{-1})	Biodegradation rate of o-cresol (mg L^{-1} h^{-1})
500	100	8.0 (0.92) *	2.7 (0.99)
500	200	16.6 (0.90)	6.8 (0.99)
500	300	12.9 (0.86)	7.2 (0.92)
500	300	11.1 (0.94)	6.5 (0.94)
500	400	7.4 (0.97)	5.7 (0.97)
500	500	0	0

*Numbers in brackets represent the regression coefficient (R^2).

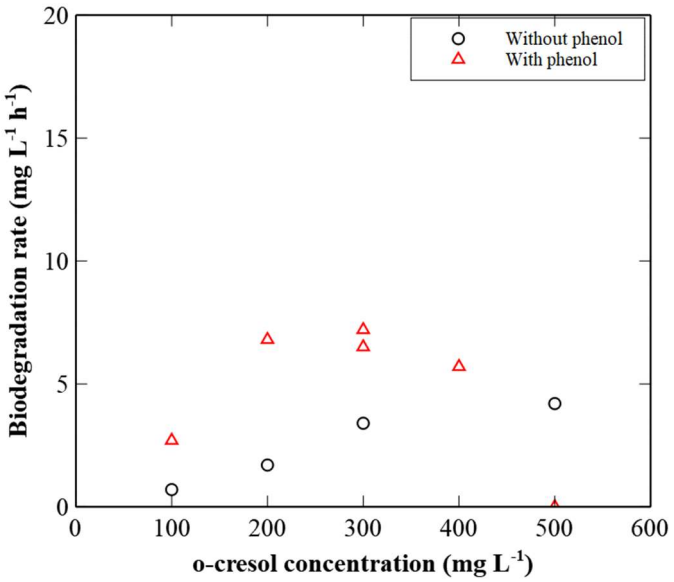

Figure 4.9 Biodegradation rates of o-cresol at different initial concentrations in the presence and absence of phenol.

A paired t-test was performed to assess the impact of the presence of p-cresol or o-cresol on biodegradation rate of phenol. Biodegradation rates of phenol in the presence of p-cresol at different initial concentration were compared with those in the presence of o-cresol with corresponding initial concentration. Results that are presented in Table 4.8 show that the P value

of the test is 0.64, which is much more than 0.05. Hence, statistically speaking the presence of o-cresol had an equivalent effect on biodegradation rate of phenol when compared to p-cresol.

Table 4.8 Results of paired t-test of effect of the initial concentration of p-cresol and o-cresol on phenol biodegradation

	Phenol biodegradation rate in the presence of p-cresol	**Phenol biodegradation rate in the presence of o-cresol**
Mean	9.83	9.33
Variance	32.71	32.25
Observations	6	6
Pearson Correlation	0.92	
Hypothesized Mean Difference	0	
Df	5	
t Stat	0.50	
P(T<=t)	0.64	

4.5 Ternary Biodegradation of Phenol, p-cresol, and o-cresol

Experiments with three phenolic compounds were performed with the fixed initial concentration of phenol (500 mg L^{-1}) and various concentrations of p-cresol and o-cresol, ranging from 100 - 400 mg L^{-1}. The combinations are described in detail in Table 3.3. The case with either p-cresol or o-cresol concentration being 500 mg L^{-1} was excluded, because under binary biodegradation with phenol, there was no microbial activity detected when either p-cresol or o-cresol concentration reached 500 mg L^{-1}. This point is further elaborated in the following discussion.

The biodegradation profiles for mixtures of different compositions are presented in Figure 4.10. Generally, an increase of biomass concentration was accompanied by a decrease of concentration of all three substrates until the biomass reached the maximum value, except in the case of no microbial activity observed in Panel L and N. When concentrations of all three substrates decreased to zero, biomass concentration started to decline. An increase of lag phase was observed as overall initial substrates concentration was increased. For example, for biodegradation of mixtures shown in panel A, B, C, and D, the same initial concentrations for phenol (500 mg L^{-1}) and p-cresol (100 mg L^{-1}) were employed. We can observe that an increase of o-cresol concentration from 100 to 400 mg L^{-1} increased the lag phase from 24 to almost 50 h Another observation from these four experimental conditions was that the higher the initial concentration of o-cresol, the longer it took for complete biodegradation of all substrates when p-cresol concentration kept constant. When initial concentration of p-cresol was high (over 400 mg L^{-1}), the inhibition effect was substantial as it took over 260 h to completely degrade all the compounds even when the concentration of o-cresol was quite low (100 mg L^{-1}). High concentration of o-cresol had stronger inhibition on overall biodegradation process compare to p-cresol with the same concentration. For example, when the initial o-cresol concentration was 400 mg L^{-1} and p-cresol was 100 mg L^{-1}, it took less than 125 h to finish the process. What's more, the biodegradation order of the three substrates is consistent with the binary-substrate biodegradation system. *P. putida* preferred consuming p-cresol to phenol and o-cresol. Concentration of p-cresol decreased to 0 before phenol and o-cresol in all cases. The simultaneous consumption of phenol and o-cresol after p-cresol suggests *P. putida* did not distinguish phenol and o-cresol regarding preference, similar to what was observed in the binary-substrate system.

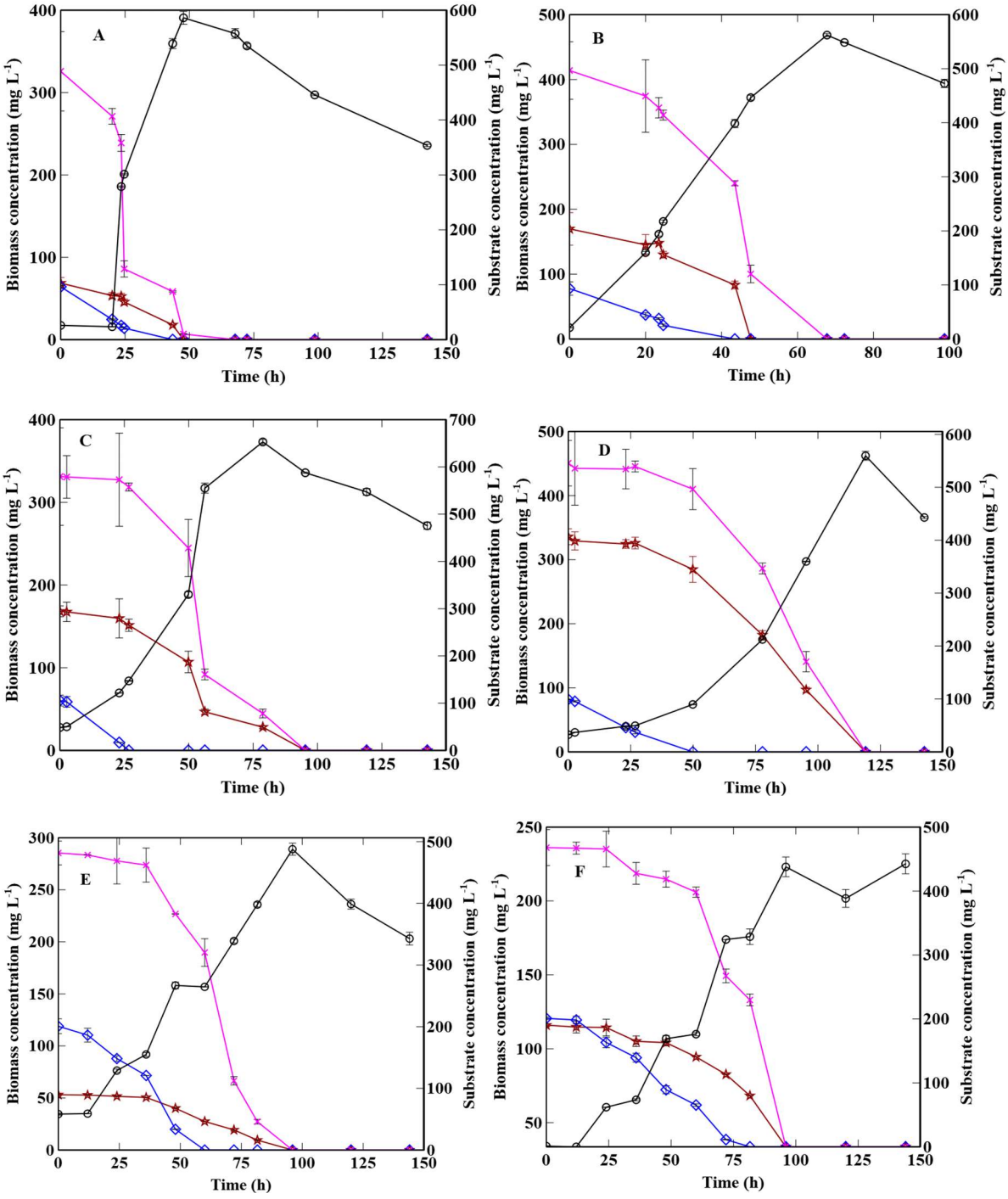
A
B
C
D
E
F
Biomass concentration (mg L-1)
Substrate concentration (mg L-1)
Time (h)

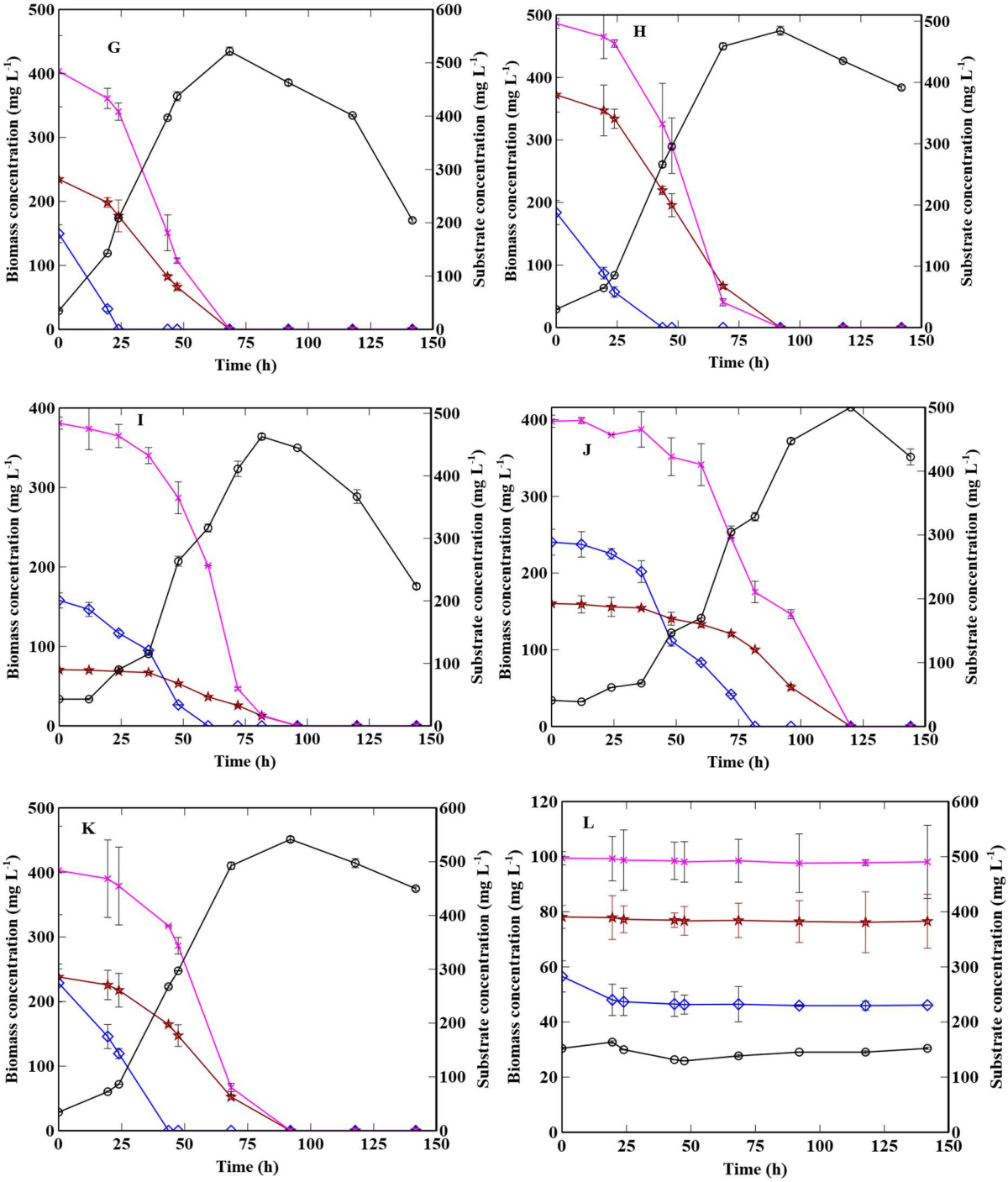
G
H
I
J
K
L
Biomass concentration (mg L-1)
Substrate concentration (mg L-1)
Time (h)

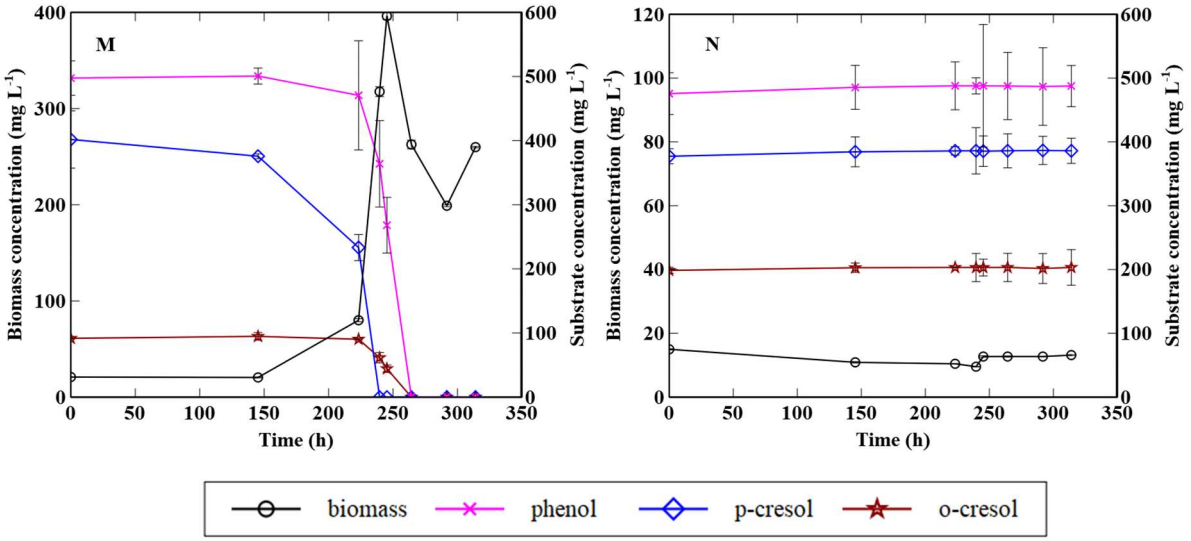

Figure 4.10 Co-biodegradation of phenol, p-cresol, and o-cresol in mixtures of different compositions. Phenol concentration of 500 mg L^{-1} and p-cresol concentration of 100 mg L^{-1} with 100 (A), 200 (B), 300 (C), 400 (D) mg L^{-1} o-cresol; phenol concentration of 500 mg L^{-1} and p-cresol concentration of 200 mg L^{-1} with 100 (E), 200 (F), 300 (G), 400 (H) mg L^{-1} o-cresol; phenol concentration of 500 mg L^{-1} and p-cresol concentration of 300 mg L^{-1} with 100 (I), 200 (J), 300 (K), and 400 (L) mg L^{-1} o-cresol; phenol concentration of 500 mg L^{-1} and p-cresol concentration of 400 mg L^{-1} with 100 (M), 200 (N) mg L^{-1} o-cresol. Error bas represent standard deviation and may not be visible in some cases.

Biodegradation rates of the phenolic compounds in the ternary-substrate batch system are presented in Table 4.9 as five subsets. Each subset comprised of fixed phenol and p-cresol concentrations with o-cresol concentration ranging from 100 to 400 mg L^{-1}. When both p- and o-cresol concentrations were 200 mg L^{-1}, respectively, phenol biodegradation rate reached the maximum, 10.7 mg L^{-1} h^{-1}. When phenol and o-cresol initial concentrations were kept the same, an increase of p-cresol led to lower phenol biodegradation rate. On the other hand, when phenol and p-cresol initial concentrations were kept the same, an increase of o-cresol also caused the decrease of phenol biodegradation rate. The simultaneous increase of the initial concentration of both p-cresol and o-cresol led to even more drastic decline of phenol biodegradation rate. This is discussed in detail in the following section.

For p-cresol biodegradation rate, the maximum value appeared when the initial concentration of p-cresol and o-cresol was 200 and 300 mg L^{-1}, respectively. When o-cresol initial concentration was kept lower than 300 mg L^{-1}, an increase of p-cresol concentration led to an increase of p-cresol biodegradation, as expected. Further increase of o-cresol led to a more drastic decline of p-cresol biodegradation rate when o-cresol initial concentration was around 300 mg L^{-1}. When p-cresol concentration was too high, the inhibition effect on bacteria activity became much stronger. Therefore, p-cresol biodegradation rate diminished. The simultaneous increase of p-cresol and o-cresol initial concentrations (<300 mg L^{-1}) caused an increase of p-cresol biodegradation rate. The dependency of p-cresol biodegradation rate on initial concentration diminished when both substrates had high initial concentrations (over 400 mg L^{-1}).

For o-cresol biodegradation rate, the maximum biodegradation rate of o-cresol was 5.8 mg L^{-1} h^{-1} when the initial concentration of p-cresol and o-cresol was 100 and 200 mg L^{-1}, respectively. Like phenol biodegradation rate, an increase of p-cresol concentration had an adverse effect on o-cresol biodegradation when the initial concentration of o-cresol was the same. However, when o-cresol concentration exceeded 300 mg L^{-1}, p-cresol up to 200 mg L^{-1} had a positive effect on its biodegradation. The simultaneous increase of concentration (<300 mg L^{-1}) of both substrates led to an increase of o-cresol biodegradation rate. Further increase had a negative effect due to strong inhibition effect on bacterial activity.

Table 4.9 Summary of the biodegradation rates of phenol, p-cresol, and o-cresol in ternary-substrate batch system

Concentration of phenol (mg L^{-1})	Concentration of p-cresol (mg L^{-1})	Concentration of o-cresol (mg L^{-1})	Biodegradation rate of phenol (mg L^{-1} h^{-1})	Biodegradation rate of o-cresol (mg L^{-1} h^{-1})	Biodegradation rate of p-cresol (mg L^{-1} h^{-1})
500	100	100	10.2 (0.82)*	2.4 (0.98)	2.3 (0.92)
500	100	200	9.8 (0.95)	5.8 (0.84)	2.6 (0.98)
500	100	300	8.4 (0.88)	4.4 (0.92)	4.2 (0.99)
500	100	400	7.3 (0.99)	4.4 (0.98)	2.1 (0.99)
500	200	100	8.6 (0.87)	1.4 (0.99)	4.1 (0.97)
500	200	200	10.7 (0.96)	3.3 (0.94)	4.8 (0.86)
500	200	300	9.3 (0.98)	5.0 (0.99)	7.4 (0.99)
500	200	400	8.7 (0.96)	5.2 (0.98)	4.3 (0.97)
500	300	100	8.2 (0.93)	1.4 (0.97)	6.7 (0.96)
500	300	200	8.9 (0.86)	2.8 (0.98)	7.4 (0.96)
500	300	300	7.4 (0.94)	3.9 (0.98)	6.3 (0.99)
500	300	400	0	0	0
500	400	100	8.6 (0.85)	2.2 (0.99)	3.3 (0.78)
500	400	200	0	0	0

*Numbers in the bracket represent the R^2.

To understand the observed patterns and to illustrate the interaction of these three substrates during co-biodegradation, the biodegradation rates of each substrate were fit into a second-order polynomial model (Equation 4.3).

$$Y = \alpha_0 + \alpha_1 X_1 + \alpha_2 X_2 + \alpha_3 X_1^2 + \alpha_4 X_2^2 + \alpha_5 X_1 X_2 \quad (4.3)$$

Where Y (response variable) is the biodegradation of the phenolic compound in mg L^{-1} h^{-1}, and X_1 and X_2 (explanatory variables) are the initial concentrations of p-cresol and o-cresol in mg L^{-1}, respectively. No term for phenol concentration was included because phenol concentration was constant.

Via fitting the experimental data for phenol biodegradation rate into eq. 4.3, the value of various coefficients was determined and included in Eq. 4.4 with the results of the ANOVA test are shown in Table 4.10 and the corresponding contour plot in Figure 4.11.

$$Y = -0.32 + 0.085X_1 + 0.038X_2 - 0.0001X_1^2 + 0.00005X_2^2 - 0.0001X_1X_2 \quad (4.4)$$

As seen in Table 4.10 the p-values associated with X_1^2, X_2^2, and X_1X_2 terms are greater than 0.05, indicating that these terms are insignificant at 95% confidence interval. However, it does not make too much sense to remove these terms because of insignificance, especially considering that only 2 explanatory variables were used in this model (Box et al., 2005). Other factors to be considered include the squared R-value and the agreement between the predicted value and experimental results. The R squared is 0.73 (reduced to less than 0.50 if dropping these insignificant terms), which means the proposed model could explain 73% variation. The dependency of phenol biodegradation rate on o-cresol and p-cresol concentrations can be seen graphically in the contour plot in Figure 4.11. The contour plot (based on Eq 4.4) indicates that there was an interaction between p-cresol and o-cresol, especially when the concentration of both substrates was lower than 300 mg L^{-1}, indicated by the curvature of the contour lines. One can observe in a wide range of concentration combination, phenol biodegradation rate was higher than 9.8 mg L^{-1} h^{-1}. It is also safe to speculate that when o-cresol concentration is lower than 100 mg L^{-1}, phenol biodegradation rate would still be as high as 9.8 mg L^{-1} as long as p-cresol concentration is lower than around 300 mg L^{-1}. Further increase of either p-cresol or o-cresol concentration led to the steep decline of phenol biodegradation rate, as indicated by the relatively dense contour lines. The fitted model showed a rather linear decrease of phenol biodegradation rate when concentrations of both p-cresol

(>300 mg L^{-1}) and o-cresol (>400 mg L^{-1}) are high, which can be demonstrated by the rather evenly distributed contour lines in that region. High concentration of p-cresol had more inhibition effect on phenol biodegradation compare to o-cresol. Under low concentration of p-cresol and high concentration of o-cresol, phenol biodegradation rate was still high (>8.6 mg L^{-1} h^{-1}). The opposite led to low biodegradation rate (around 5 mg L^{-1} h^{-1}).

Table 4.10 Results of ANOVA test for significance of various coefficients in Equation 4.4

	Df	**Sum of square**	**Mean square**	**F ratio**	**P value**
X_1	1	39.79	39.79	7.99	0.02
X_2	1	29.48	29.48	5.92	0.04
X_1^2	1	11.81	11.81	2.37	0.16
X_2^2	1	1.40	1.40	0.28	0.61
X_1X_2	1	23.34	23.34	4.69	0.06
Residuals	8	39.81	4.98		

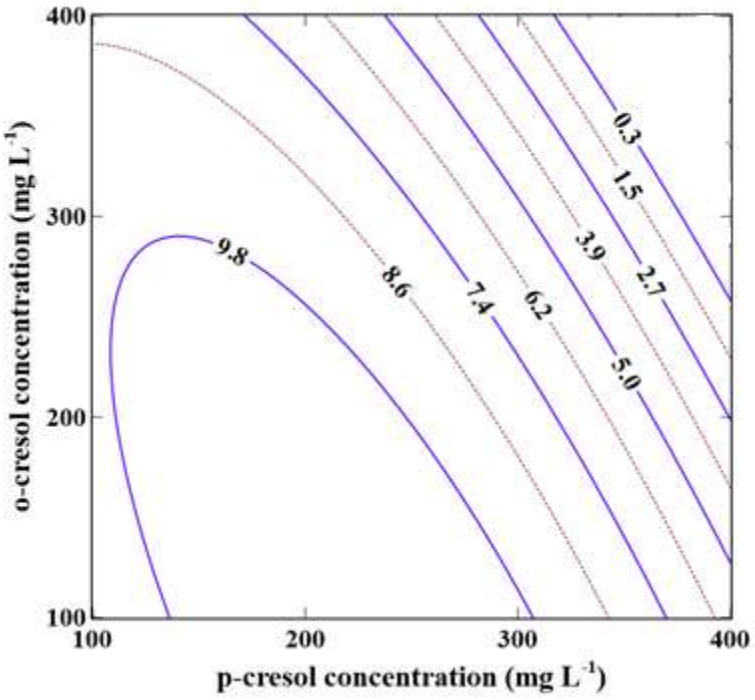

Figure 4.11 Contour plot of phenol biodegradation rate with respect to p-cresol and o-cresol initial concentration.

The experimentally determined biodegradation rate of phenol with predicated values from Eq. 4.4 are compared in the parity chart presented in Figure 4.12. Based on it, the model seems to have better prediction capability when biodegradation rate is in the range from around 7 to 11 mg L^{-1} h^{-1}. Outside of the range, an increase of variation and uncertainties is expected.

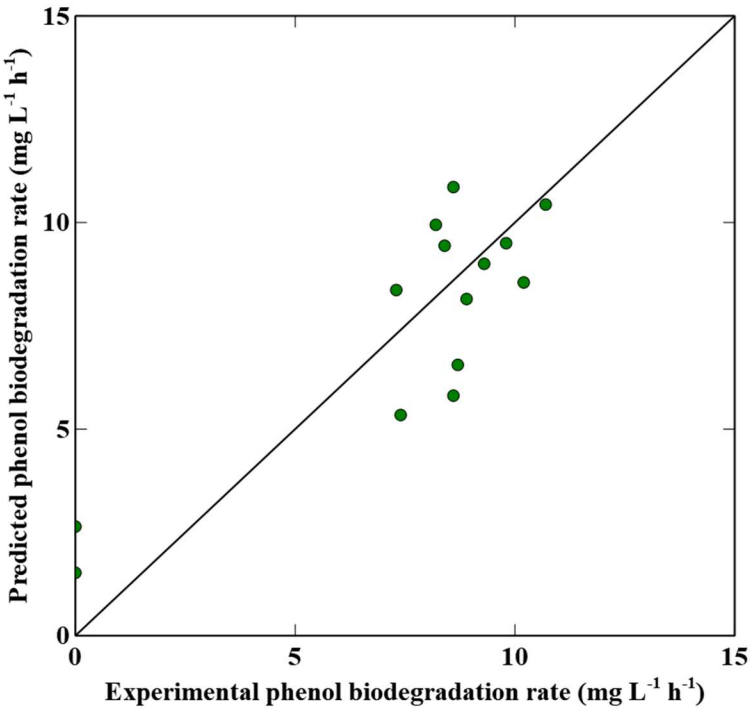

Figure 4.12 Parity chart for the experimental data against the predicted values by the modified response model (Equation 4.4)

The second response variable is p-cresol biodegradation rate. The ANOVA result (Table 4.11) for second order linear regression presents the F ratio and P value for all the terms in full model described in Equation 4.5. Similar to the previous discussion, in order to preserve some model accuracy, non-significant terms are also preserved for modeling.

$$Y = -3.328 + 0.02038X_1 + 0.05016X_2 - 0.0003X_1^2 + 0.00006X_2^2 - 0.00077X_1X_2 \qquad (4.5)$$

The coefficient of determination (R^2) for the model is 0.68, which means the model only explains 67% of the variability. Due to the complex nature of intracellular and extracellular bioreaction, some uncertainties are expected, which might be attributed to underlying microbial enzyme activities. Figure 4.13 is the contour plot of p-cresol biodegradation rate as a function of p-cresol

and o-cresol concentration. The initial concentration of p-cresol and o-cresol had different effects on p-cresol biodegradation rate. High biodegradation rates were observed when p-cresol concentration was less than 200 mg L^{-1} while o-cresol concentration was in the range of 300 to 400 mg L^{-1}, which can be demonstrated by the projected contour plot. In the examined concentration range, when o-cresol concentration was under 300 mg L^{-1}, p-cresol biodegradation rate decreased more gradually. Further increase of o-cresol led to the more drastic decline, indicated by the denser contour lines in that region. The effect of p-cresol and o-cresol concentration on p-cresol biodegradation rate is different. High concentration of o-cresol (300 to 400 mg L^{-1}) and low concentration of p-cresol led to high biodegradation rate, which means the presence of o-cresol enhanced p-cresol biodegradation. However, a high concentration of p-cresol, regardless of o-cresol concentration, led to low biodegradation rate. It seems that p-cresol had stronger inhibition effect on biodegradation process. Figure 4.14 presents the predicted values versus experimental data for p-cresol biodegradation rate.

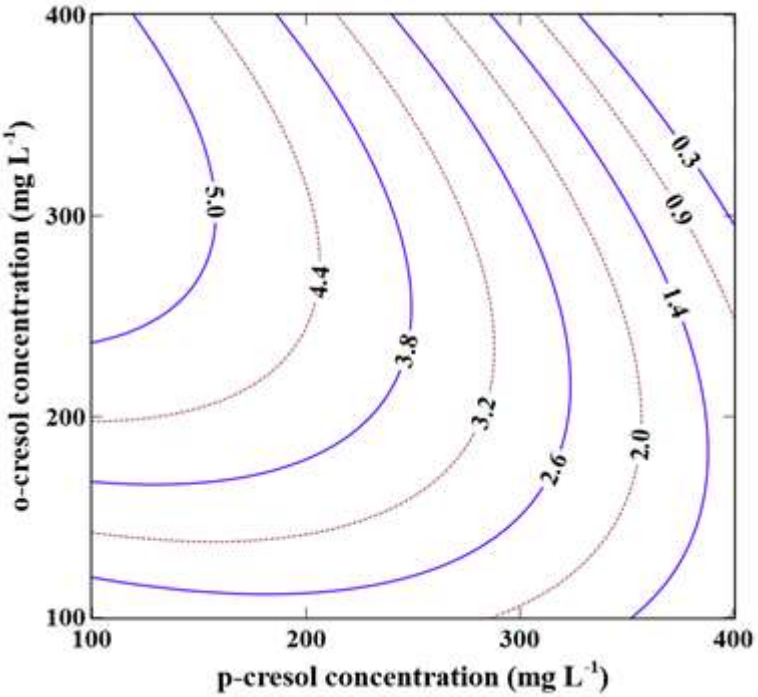

Figure 4.13 Contour plot for p-cresol biodegradation rate with respect to p-cresol and o-cresol concentrations.

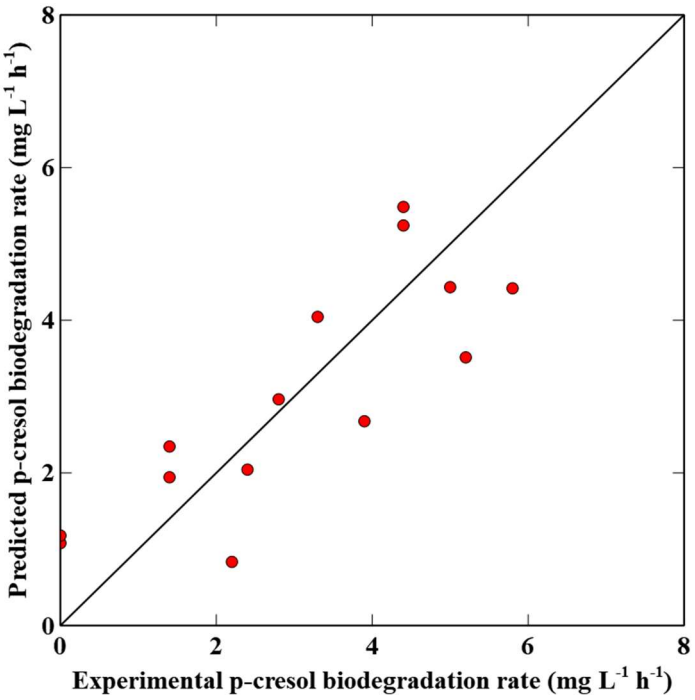

Figure 4.14 Parity chat for the experimental data against the values predicted by the modified response model (Equation 4.5)

Table 4.11 Results of ANOVA test for significance of various coefficients in Equation 4.5

	Df	**Sum of square**	**Mean square**	**F ratio**	**P value**
X_1	1	18.45	18.45	9.99	0.01
X_2	1	2.35	2.34	1.27	0.29
X_1^2	1	0.02	0.01	0.00	0.93
X_2^2	1	4.40	4.40	2.38	0.16
X_1X_2	1	5.67	5.67	3.07	0.11
Residuals	8	14.77	1.84		

The last response variable to discuss is o-cresol biodegradation rate. Table 4.12 shows the ANOVA results for full model with all the terms. The determined model is as follow:

$$Y = -0.01378 + 0.01247X_1 + 0.063X_2 - 0.0002X_1^2 + 0.00009X_2^2 - 0.0001X_1X_2 \quad (4.6)$$

The coefficient of determination (R^2) is 0.67, which only has limited power to explain the biodegradation rate of o-cresol as a function of p-cresol and o-cresol initial concentration. The projected contour plot based on the model is represented in Figure 4.15. There is an obvious interaction between the two explanatory variables. The region where high biodegradation rate of o-cresol occurred was when the p-cresol concentration is around 200 to 300 mg L^{-1} and o-cresol 100 to 300 mg L^{-1}. Outside of that range, biodegradation rate gradually decreased. When concentrations of both substrates were high, a drastic decline of biodegradation rate was observed. Similar to previous analysis, high concentrations of p-cresol had more negative effect

on o-cresol biodegradation rate. An increase of o-cresol had a less drastic effect. Figure 4.16 showed the predicted values of o-cresol biodegradation rate as a function of experimental data.

Table 4.12 Results of ANOVA test for significance of various coefficients in Equation 4.6

	Df	**Sum of square**	**Mean square**	**F ratio**	**P value**
X_1	1	0.00	0.00	0.00	0.99
X_2	1	1.87	1.86	0.78	0.40
X_1^2	1	31.18	31.18	12.99	0.007
X_2^2	1	7.96	7.96	3.32	0.10
X_1X_2	1	17.19	17.19	7.16	0.03
Residuals	8	19.21	2.40		

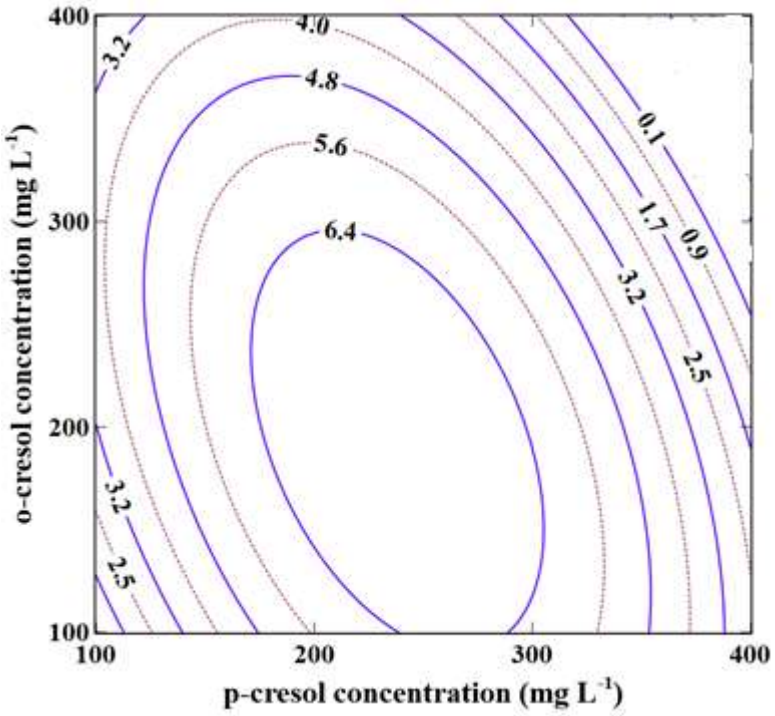

Figure 4.15 Contour plot for o-cresol biodegradation rate with respect to p-cresol and o-cresol initial concentration.

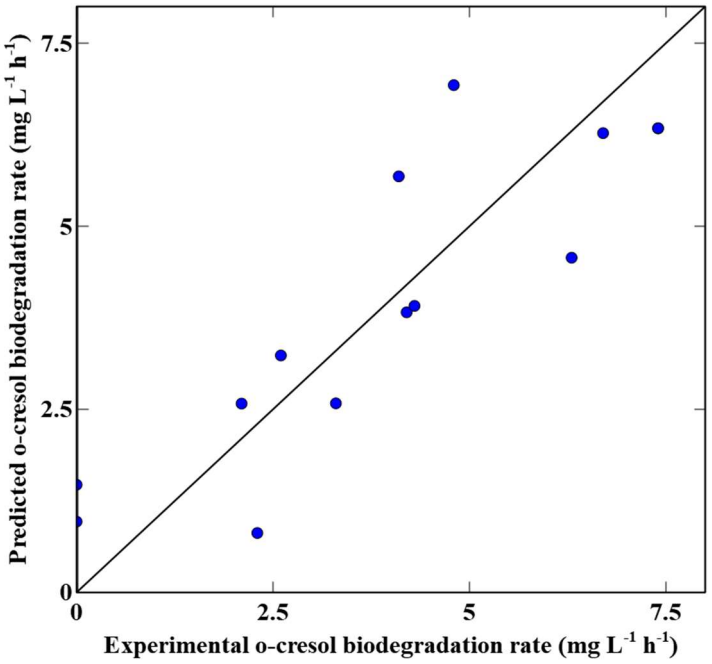

Figure 4.16 Parity chat for the experimental data against the values predicted by the modified response model (Equation 4.6)

5 RESULTS AND DISCUSSION – CONTINUOUS SYSTEM

In this chapter, results for biodegradation of each phenolic compound (i.e., phenol, p-cresol, and o-cresol) obtained in the CPBBs are presented and discussed. Biodegradation of each compound at three different initial concentration of 100, 300, and 500 mg L^{-1} was examined. The effects of volumetric loading rate of phenolic compounds on the removal rate in CPBBs were determined through increasing phenolic compound (substrate) concentration and influent flow rate. The performance of the bioreactor was assessed by determining the removal percentage and removal rate of the individual phenolic compounds as a function of its loading rate. In addition, the toxicity of influent and the treated effluent under certain conditions was determined and compared.

5.1 Biodegradation of phenol

Results for biodegradation of phenol in CPBB are shown in Figure 5.1 and 5.2. Figure 5.1 demonstrates the profile of the residual phenol concentration, while Figure 5.2 shows the patterns of phenol removal percentage and removal rate as a function of its loading rate. The results for all evaluated phenol influent concentrations (100, 300 and 500 mg L^{-1}) are included in these figures. Irrespective of the initial concentration, the residual phenol concentration increased gradually as phenol loading rate was increased. This, in turn, led to a gradual decrease of phenol removal percentage. Removal rate initially increased with the increase of loading rate until it reached a maximum value and then decreased with further increase of loading rate. As expected, the residual concentration and removal percentage varied when different initial concentration of phenol was

applied in the influent. For similar loading rate, higher initial concentrations of phenol in the influent led to higher residual concentrations.

As illustrated in Figure 5.1, the influent phenol concentration was 98.6 ± 1.9 mg L^{-1}.At the lowest loading rate (1.2 mg L^{-1} h^{-1}), the residual phenol concentration in the effluent sample was 9.1 mg L^{-1}. w At the evaluated loading rate of 253.0 mg L^{-1} h^{-1}, the residual concentration increased to 99.2 mg L^{-1} which was close to the influent concentration.. Once the first set of experiments was done, the CBPP system was used to study the biodegradation of phenol at higher initial concentrations. With an influent containing 295.4 ± 10.2 mg L^{-1} phenol, at the lowest loading rate (9.1 mg L^{-1} h^{-1}), the residual phenol concentration in CPBB effluent was 0.4 mg L^{-1}, while at the highest tested loading rate (296.5 mg L^{-1} h^{-1}), a residual concentration of 273.3 mg L^{-1} was observed. The influent concentration was then increased to the highest tested value of 496.3 ± 9.3 mg L^{-1}. With this level of phenol at the lowest loading rate (11.9 mg L^{-1} h^{-1}), the residual phenol concentration in CPBB was 5.2 mg L^{-1} which increased to 453.9 mg L^{-1} when the highest loading rate of 219.4 mg L^{-1} h^{-1} was applied.

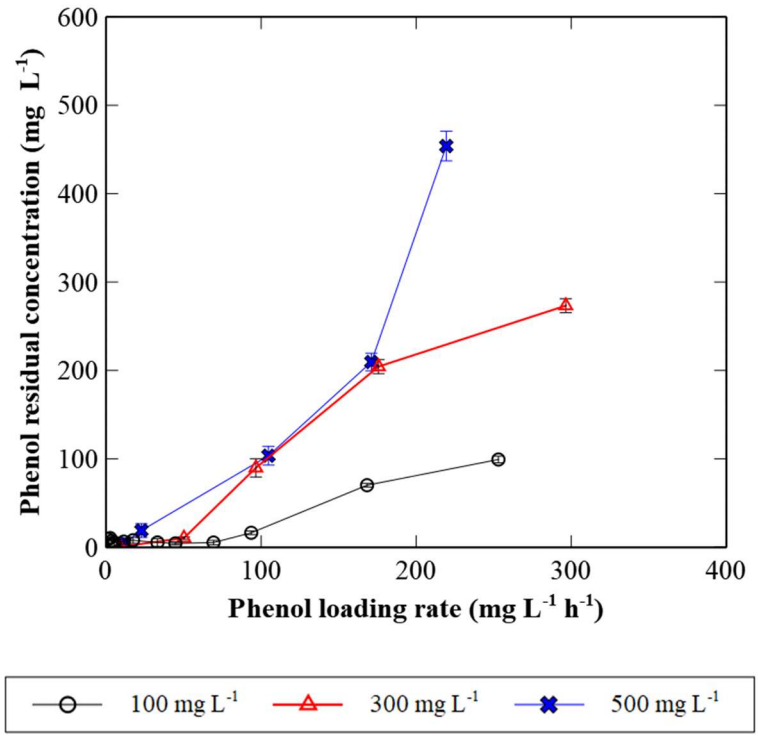

Figure 5.1 Residual concentration of phenol as a function of its loading rate for influents containing 100, 300 and 500 mg L^{-1} phenol. Each point represents the average value of the data obtained over an extended period equal to at least three residence times after the establishment of steady state. Error bars represent the standard deviations and might not be visible in some cases.

Figure 5.2 shows the dependency of phenol removal percentage and removal rate on its loading rate. For biodegradation of phenol with 98.6 ± 1.9 mg L^{-1} initial concentration, removal percentage of 90.59% was achieved at the loading rate of 1.19 mg L^{-1} h^{-1} with the corresponding removal rate being 1.08 mg L^{-1} h^{-1} (residence time: 86.2 h). With further increase in the loading rate (1.19 to 253.0 mg L^{-1} h^{-1}) the removal percentage decreased, while removal rate passed through a maximum. To be more specific, the removal percentage remained in the range of 84.2 – 95.8% for loading rates up to 93.6 mg L^{-1} h^{-1}. The maximum removal rate of 78.9 mg L^{-1} h^{-1} was obtained at a loading rate of 93.6 mg L^{-1} h^{-1} (residence time: 1.1 h), with the corresponding removal percentage

being 84.32%. Further increase of loading rate to 253.0 mg L^{-1} h^{-1} resulted in the decrease of removal rate and removal percentage to 9.32 mg L^{-1} h^{-1} and 3.7%, respectively.

A similar pattern was observed during the biodegradation of 295.4 ± 10.2 mg L^{-1} phenol, whereby when loading rate was increased, removal rate increased initially, reached the maximum value, then it gradually decreased. The initial phenol removal percentage of 99.2% was achieved at the loading rate of 9.1 mg L^{-1} h^{-1} with the corresponding removal rate of 9.1 mg L^{-1} h^{-1} (residence time: 31.25 h). The removal percentage remained in the range of 70.0 – 99.2% for loading rates up to 96.7 mg L^{-1} h^{-1}. The maximum removal rate was 67.6 mg L^{-1} h^{-1} and obtained at a loading rate of 96.7 mg L^{-1} h^{-1} (residence time: 3.0 h), with the corresponding removal percentage of 69.9%. Further increase of loading rate to 290.5 mg L^{-1} h^{-1} resulted in the decrease of removal rate and removal percentage to only 10.1 mg L^{-1} h^{-1} and 3.4%, respectively.

With influent containing 496.3 ± 9.3 mg L^{-1} phenol, in a similar manner, the initial phenol removal percentage of 98.9% was achieved at a loading rate of 12.0 mg L^{-1} h^{-1} with the corresponding removal rate of 11.9 mg L^{-1} h^{-1} (residence time: 40.8 h). The removal percentage remained in the range of 78.8 – 98.9 % for loading rates up to 104.7 mg L^{-1} h^{-1}. The maximum removal rate was 82.6 mg L^{-1} h^{-1} and observed at a loading rate of 104.7 mg L^{-1} h^{-1} (residence time: 4.7 h) with the corresponding removal percentage of 78.9%. Further increase of loading rate to 219.4 mg L^{-1} h^{-1} resulted in the decrease of removal rate and percentage to only 15.8 mg L^{-1} h^{-1} and 7.2%, respectively.

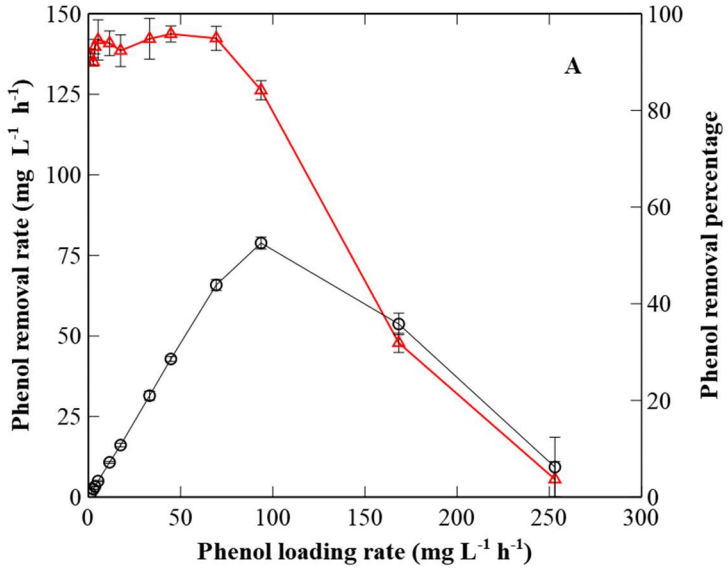
A
Phenol removal rate (mg L-1 h-1)
Phenol removal percentage
Phenol loading rate (mg L-1 h-1)
0
25
50
75
100
125
150
0
20
40
60
80
100
0
50
100
150
200
250
300

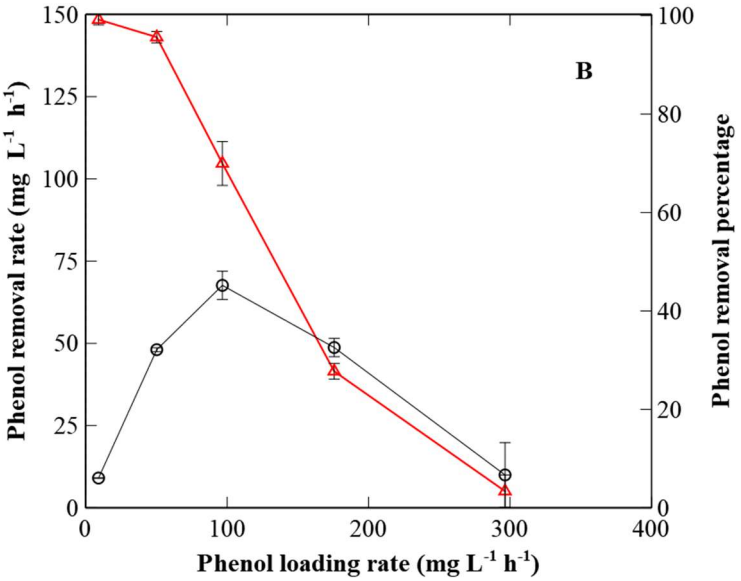
B
Phenol removal rate (mg L-1 h-1)
Phenol removal percentage
Phenol loading rate (mg L-1 h-1)
0
25
50
75
100
125
150
0
20
40
60
80
100
0
100
200
300
400

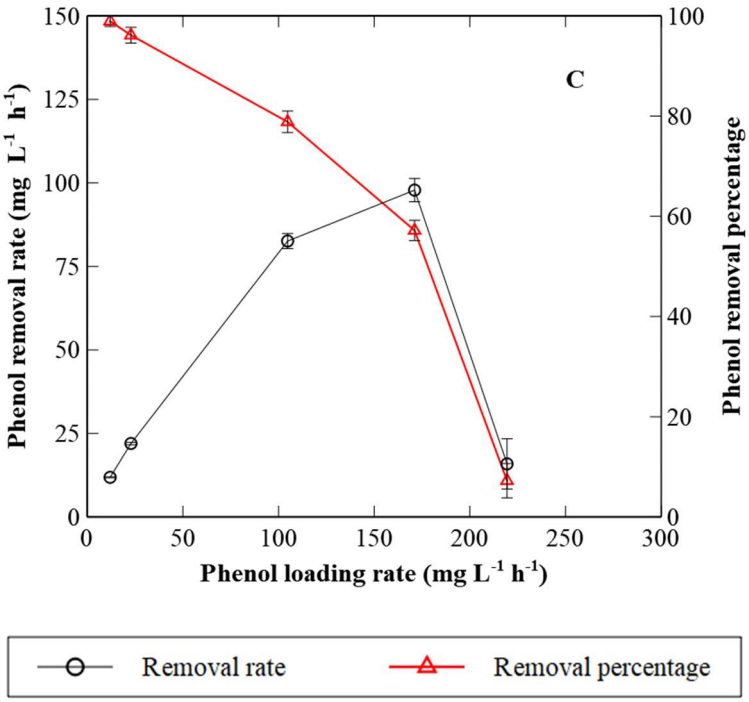

Figure 5.2 The effect of phenol loading rate on the performance of the CPBB. Panel (A): 98.6 ± 1.9 mg L^{-1} phenol, Panel (B): 295.4 ± 10.2 mg L^{-1} phenol, Panel (C): 496.3 ± 9.3 mg L^{-1} phenol. Each point represents the average value of the data obtained over an extended period of operation equal to at least three residence times after the establishment of steady state. Error bars represent standard deviation and may not be visible in in some cases.

Figure 5.3 shows the removal rates of phenol as a function of its loading rates obtained with the influent containing different concentrations of phenol. When loading rate was low (less than 50 mg L^{-1} h^{-1}), the removal rates at similar loading rates were identical and were not affected by phenol concentration. However, once the loading rate exceeds 100 mg L^{-1} h^{-1}, the difference became apparent, and the performance of the system influent containing 500 mg L^{-1} phenol achieved the highest removal rate at a high loading rate. In other words, phenol at concentrations in the range 100 - 500 mg L^{-1} did not impose inhibition on microbial activity and biodegradation process.

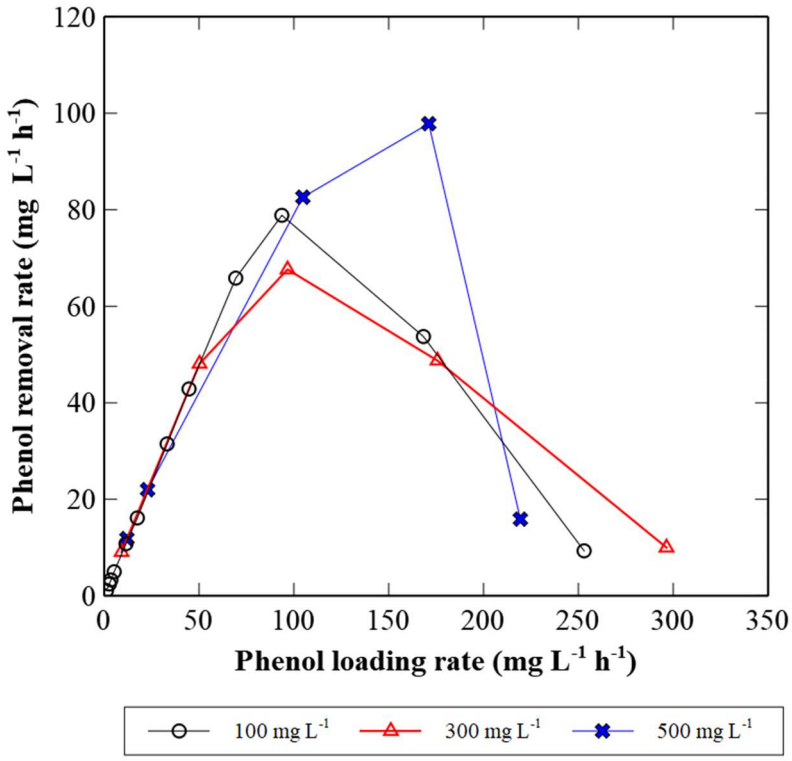

Figure 5.3 Comparison of phenol removal rate as a function of its loading rate for the influents containing different phenol concentrations.

5.1.1 Toxicity Evaluation of Influents and Effluents

Due to the potential ecological risk posed by releasing treated phenolic wastewater that might contain residual phenol in the natural environment, it is imperative to investigate the toxicity of treated effluent. The investigation in this work focused mainly on the acute toxicity of the treated effluent that was generated when CPBBs were operating at the highest phenol removal rate. Evaluation also included the toxicity of untreated influent containing various levels of phenol (100, 300 and 500 mg L^{-1}).

The results of toxicity tests are shown in Figure 5.4. The results from control experiments were used to normalize the survival percentage of shrimp larvae (in almost all cases, 100% shrimp larvae remained alive within 2 h exposure). With influent containing 100, 300, and 500 mg L^{-1} phenol and after 2 h exposure, the survival levels of shrimp larvae were 90.3, 34.3, and 0% respectively. This indicated that when phenol concentration was around or lower than 100 mg L^{-1}, the toxicity was relatively low and increase in initial concentration to 300 and 500 mg L^{-1} increased the toxicity and with 500 mg L^{-1} phenol all shrimp larvae died after 2 hours.

For the effluent generated during the biodegradation of 98.6 ± 1.9 mg L^{-1} phenol with the highest removal rate of 78.98 mg L^{-1} h^{-1} (removal percentage: 84.3%) at a loading rate of 93.7 mg L^{-1} h^{-1}, survival of shrimp larvae after 2 h was 98.3%. In case of an influent with 295.4 ± 10.2 mg L^{-1} phenol influent where the highest removal rate of 69.7 mg L^{-1} h^{-1} obtained at a loading rate of 96.7 mg L^{-1} h^{-1} (removal percentage: 69.9%), the shrimp survival was 90.2% after 2 h. Finally, with 496.3 ± 9.3 mg L^{-1} phenol, 48.8 % of shrimp larvae stayed live after 2 h with the effluent that represented the maximum removal rate of 98.6 mg L^{-1} h^{-1} at the loading rate of 171.11 mg L^{-1} h^{-1} (removal percentage: 78.9%). These results indicated to two points: 1)- the treatment of influent in the CPBBs resulted in reduced toxicity, as the survival percentage of shrimp in the treated effluent obtained at highest removal rate was substantially higher when compared to the corresponding results with untreated influent; 2)- influent decrease in toxicity was somewhat proportional to the concentration of phenol in the influent whereby increase of phenol concentration led to lower removal percentage, thus a higher phenol concentration in the effluent and subsequently higher toxicity of the effluent (lower shrimp survival percentage).

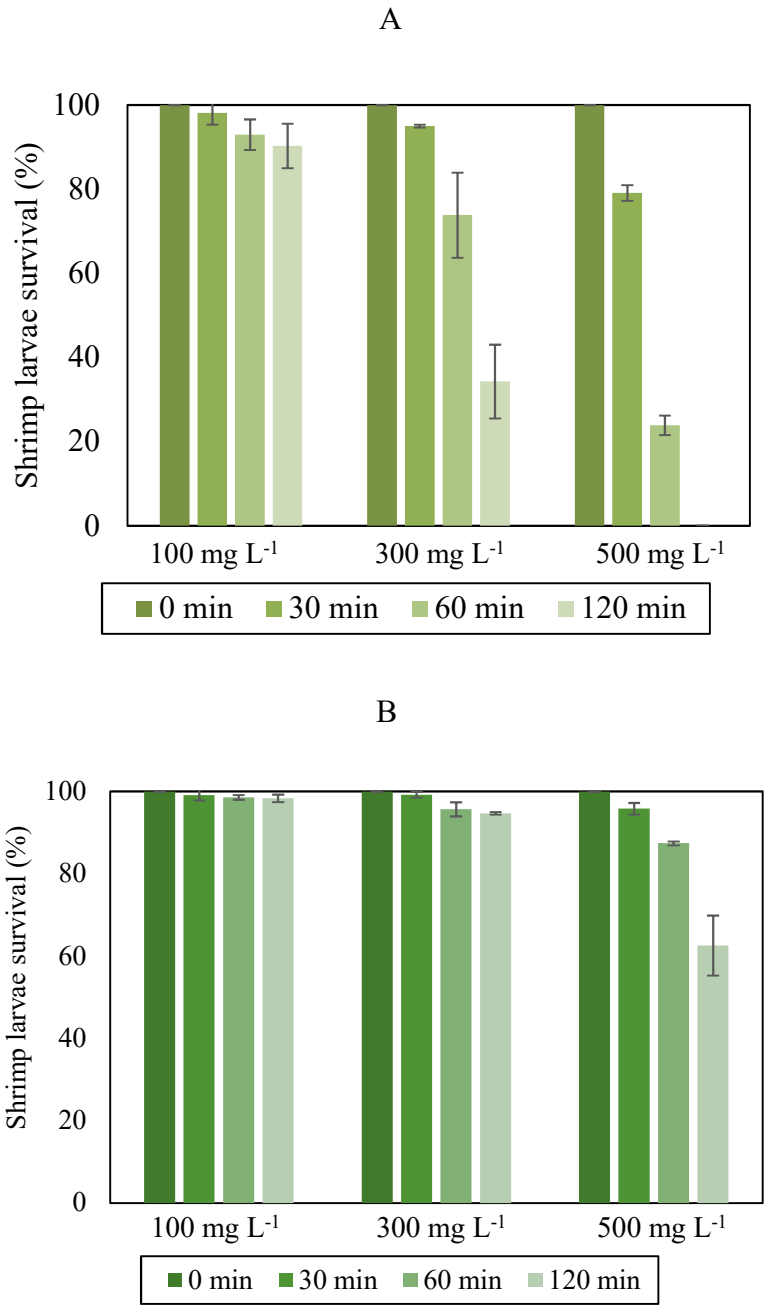

Figure 5.4 Results of toxicity test on the CPBB influent and treated effluent. Panel (A): Toxicity of influent with different levels of phenol; Panel (B): Toxicity of treated effluents representing the maximum phenol removal rate. Error bars represent standard deviation and may not be visible in some cases.

For the aim of understanding the significance of the toxicity results, a statistical analysis was used. In this context, the important question is whether treatment of water contaminated with phenol in CPBB could significantly reduce the toxicity of the treated effluent. The toxicity of phenolic solution here was quantified as the survival percentage of brine shrimp larvae. Therefore, the statistical question can be framed as a Null hypothesis stated as "there is no significant difference in percentage of live shrimps in the original phenol solution (influent) and the treated effluent"; or a corresponding hypothesis stated as "there is significant difference in the percentage of live shrimps in the original phenol solution (influent) and the treated effluent".

A paired t-test of the toxicity (expressed as the death percentage of shrimp larva) between influent and effluent, was performed. The result could verify these hypotheses. Before treating binomial proportions using t statistics, it is recommended to make a variance stabilizing transformation (Box et al., 2005). In this case, the death percentage should be transformed to "score" x given by:

$$\sin x = \sqrt{p} \tag{5.1}$$

where p is death percentage (the number of dead shrimp larvae divided by the total number of shrimp larvae).

Boxplot of the score difference between influent and effluent at different exposure time is presented in Figure 5.5. Each "box" shows the median and percentiles of calculated death percentage score. The "box" in the middle indicates the likely range of variance (IQR), which is the difference between of the first quartile and third quartile. Two "whiskers" beneath and above the "box" represent the difference between first quartile and 1.5 times of IQR and the sum of the

third quartile and 1.5 times of IQR, respectively. It also demonstrates the distribution of calculated score. One can observe that an increase of exposure time resulted in higher death percentage score. In addition, the variance of scores also increased as observed time increased. The widened range of score when exposure time is increased from 30 to 120 minutes as shown in the boxplot was possibly due to the decreased efficiency of bioreactors to remove higher concentration of phenol. Since phenol concentration in the effluent tended to be higher when the initial concentration was high. For instance, at the exposure time of 120 minutes, the death percentage score of effluent with the initial concentration of 100 mg L^{-1} was less than that with the initial concentration of 500 mg L^{-1}.

Shapiro-Wilk test was performed on the variable "score difference" at different exposure time to evaluate the normality for checking the satisfaction of the assumption of t-test, with the results compiled in Table 5.1. For normality test, the p-value of the score difference for every exposure time is higher than 0.05, so we tentatively accept the assumption that the data is normally distributed (also because of the relatively small sample size). The t-test results, however, showed a discrepancy between the short and long exposure times. At low exposure time (30 min), shrimp larva appeared to cope with the toxic environment, thus, the toxicity reduction is not significant ($p > 0.05$). However, the positive impact of treatment on reducing the toxicity is clear when one considers the data at 60 and 120 minutes, as p-value for both exposure times is less than 0.05. The mean of the difference for the toxicity between influent and effluent after 120 min exposure was 33.6%, indicating that the treatment in the bioreactor achieved the goal of reducing the toxicity of phenol under the highest performance as far as the removal rate of phenol is concerned.

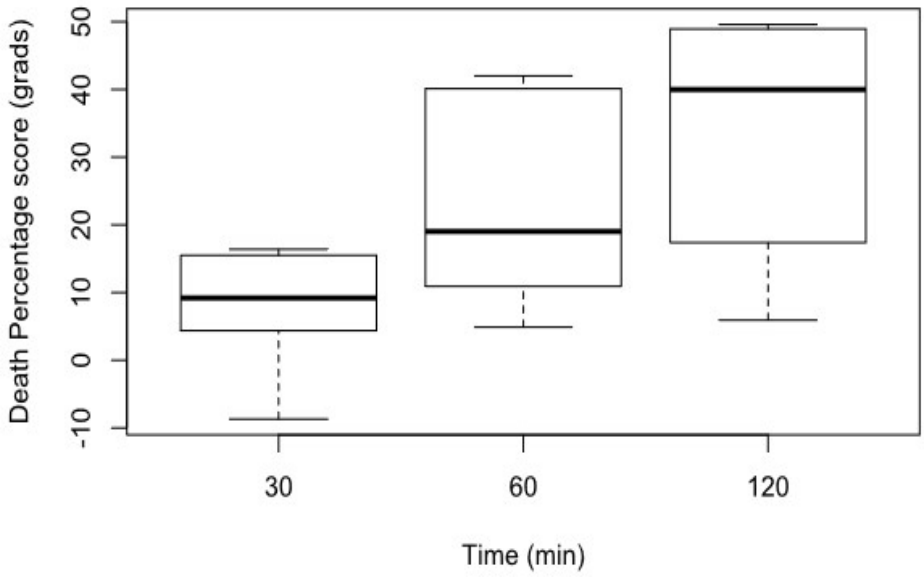

Figure 5.5 Boxplot of the difference of death percentage score between influent and effluent at different exposure time.

Table 5.1 Results of normality checking and pair t-test

Exposure time (min)	Shapiro test P value	t value	p value of t-test
30	0.31	1.99	0.102
60	0.34	3.56	0.016
120	0.22	4.56	0.006

5.2 Biodegradation of p-cresol

In this part, biodegradation results obtained with p-cresol biodegradation are presented. Specifically, the effects of loading rate of p-cresol on its residual concentration, removal rate and removal percentage of p-cresol are discussed.

Similar to what observed with phenol, an increase of loading rate increased the residual concentration of p-cresol in the effluent. Additionally, higher p-cresol concentrations in the influent resulted in higher residual concentration at the same loading rate (Figure 5.6). For biodegradation of p-cresol at the concentration of 99.2 ± 3.9 mg L^{-1} when the loading rate was gradually increased incrementally from 17.7 mg L^{-1} h^{-1} to 284.2 mg L^{-1} h^{-1}, the steady state residual concentration rose from the lowest value of 2.4 mg L^{-1} to the highest level of 88.2 mg L^{-1}. With 294.3 ± 3.6 mg L^{-1} of p-cresol, in the influent at the minimum tested loading rate was 5.6 mg L^{-1} h^{-1} that led to the lowest residual concentration of 0.5 mg L^{-1}, while with the highest loading rate of 316.1 mg L^{-1} h^{-1} a very high residual concentration of 274.0 mg L^{-1}. With the highest influent concentration of 485.9 ± 10.3 mg L^{-1}, the residual effluent concentration increased from 3.0 to 481.3 mg L^{-1} once the loading rate was increased from the lowest value of 16.8 mg L^{-1} h^{-1} to 245.1 mg L^{-1} h^{-1}. In all cases, at the highest applied loading rate, the residual effluent concentration was very close to the influent concentration.

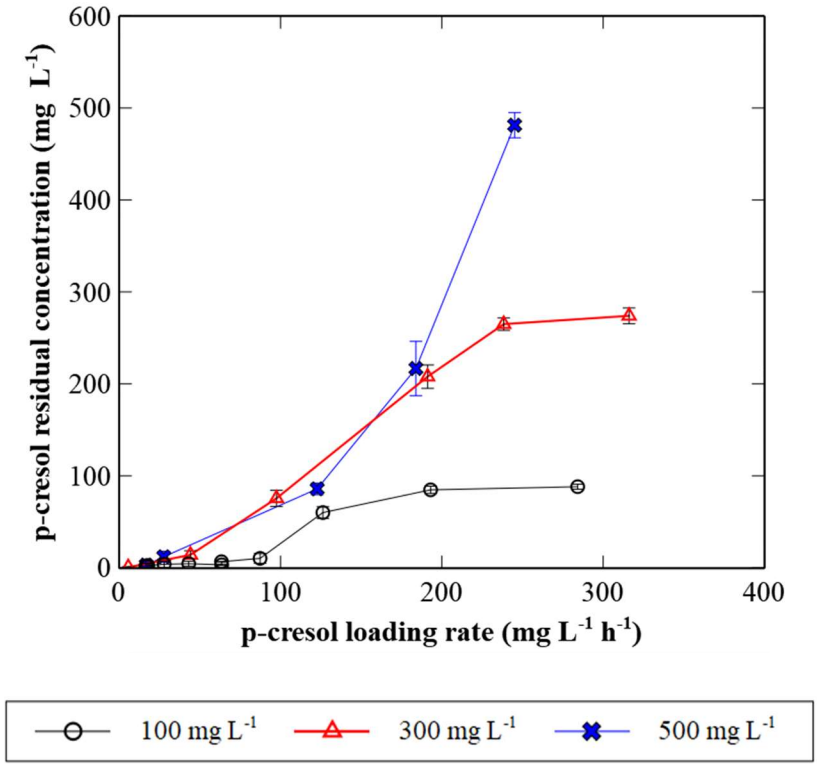

Figure 5.6 Residual concentration of p-cresol as a function of its loading rate for influents containing 100, 300 and 500 mg L^{-1} p-cresol. Each point represents the average value of the data obtained over an extended period after the establishment of steady state. Error bars represent standard deviation and may not be visible in some cases.

The effect of loading rate of p-cresol on its removal percentage and removal rate is illustrated in Figure 5.7. With influent containing 98.6 ± 1.9 mg L^{-1} p-cresol, the initial removal percentage was 98.0% at the loading rate of 16.6 mg L^{-1} h^{-1} with the corresponding removal rate being 15.6 mg L^{-1} h^{-1} (residence time: 6.3 h). Removal percentage reached the maximum value at this loading rate. The incremental increase of loading rate led to increase in the removal rate until it reached the maximum value of 77.2 mg L^{-1} h^{-1} at the loading rate of 87.4 mg L^{-1} h^{-1} with the corresponding removal percentage being 90.3% (residence time: 1.2 h). For the loading rate in the range from 16.6 to 87.3 mg L^{-1} h^{-1}, removal percentage was above 90.3%. Further increase loading rate caused

the decrease of both removal rate and removal percentage to only 40.2 mg L^{-1} h^{-1} and 16.0 %, respectively.

Upon finishing the study of the biodegradation experiment with 98.6 ± 1.9 mg L^{-1}, the influent concentration was increased to 294.3 ± 3.6 mg L^{-1}. At the initial loading rate of 5.6 mg L^{-1} h^{-1}, the removal rate was 5.6 mg L^{-1} h^{-1} with the corresponding removal percentage being 99.8% (residence time: 50.7 h). The maximum removal rate was 71.7 mg L^{-1} h^{-1} and achieved at the loading rate of 97.5 mg L^{-1} h^{-1} with the removal percentage of 73.6% (residence time: 1.5 h). The removal percentage was above 71.7% for loading rates up to 97.5 mg L^{-1} h^{-1}. However, further increase of loading rate resulted in a sharp drop of removal percentage to only 4.1% at the loading rate of 316.0 mg L^{-1} h^{-1}.

With an influent containing 485.9 ± 10.3 mg L^{-1} p-cresol the highest removal percentage of 99.5% was achieved at the lowest tested loading rate of 16.8 mg L^{-1} h^{-1} with the removal rate of 16.7 mg L^{-1} h^{-1} (residence time: 30.9 h). Similar to previous experiments, the loading rate was increased gradually to a final value of 245.1 mg L^{-1} h^{-1}. The removal rate reached 107.2 mg L^{-1} h^{-1} (the maximum) at the loading rate of 183.9 mg L^{-1} h^{-1} with the removal percentage of 58.3% (residence time: 2.8 h). The removal percentage was between 58.3% and 99.5% for loading rates ranging from 16.8 mg L^{-1} h^{-1} to 183.9 mg L^{-1} h^{-1}. The lowest removal rate was 18.0 mg L^{-1} h^{-1} at the loading rate of 245.1 mg L^{-1} h^{-1} with the lowest removal percentage of 7.3%.

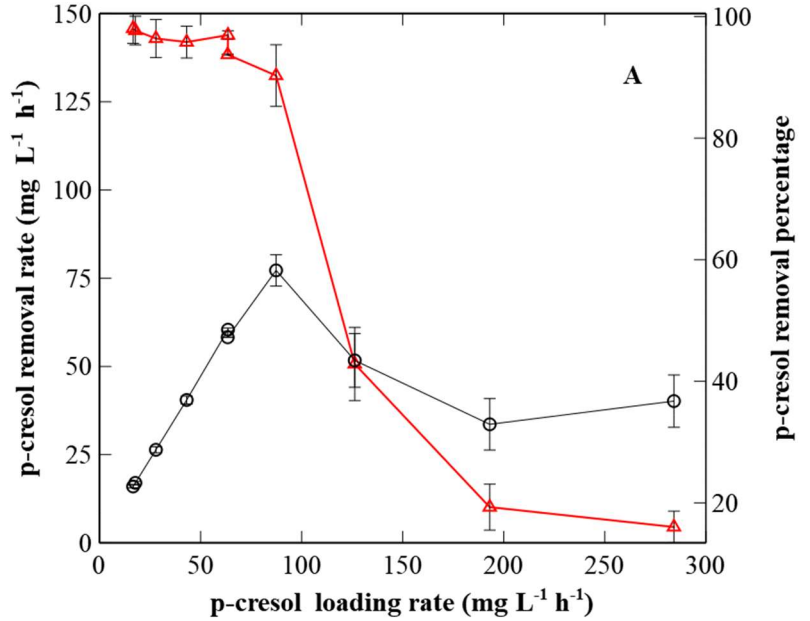
A
p-cresol removal rate (mg L-1 h-1)
p-cresol removal percentage
p-cresol loading rate (mg L-1 h-1)
0
25
50
75
100
125
150
20
40
60
80
100
0
50
100
150
200
250
300

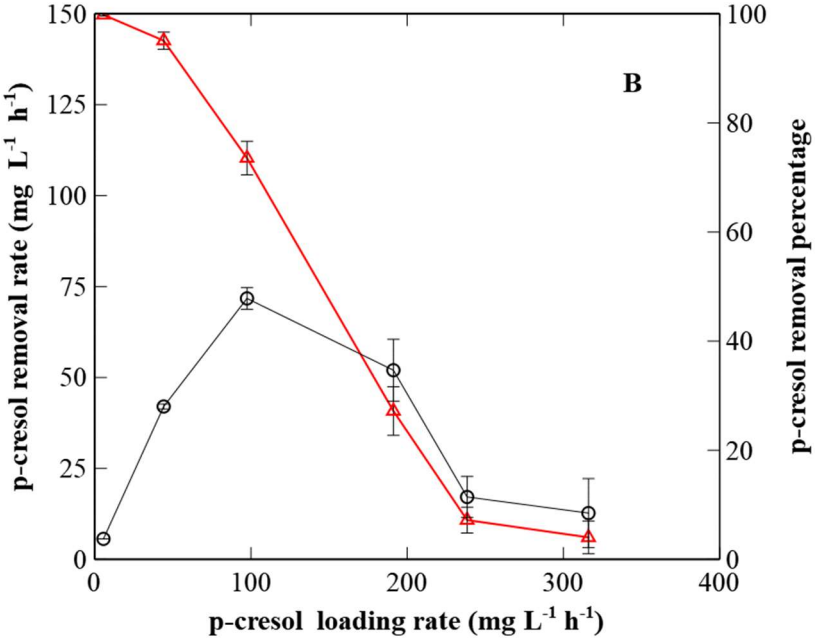
B
p-cresol removal rate (mg L-1 h-1)
p-cresol removal percentage
p-cresol loading rate (mg L-1 h-1)
0
25
50
75
100
125
150
0
20
40
60
80
100
0
100
200
300
400

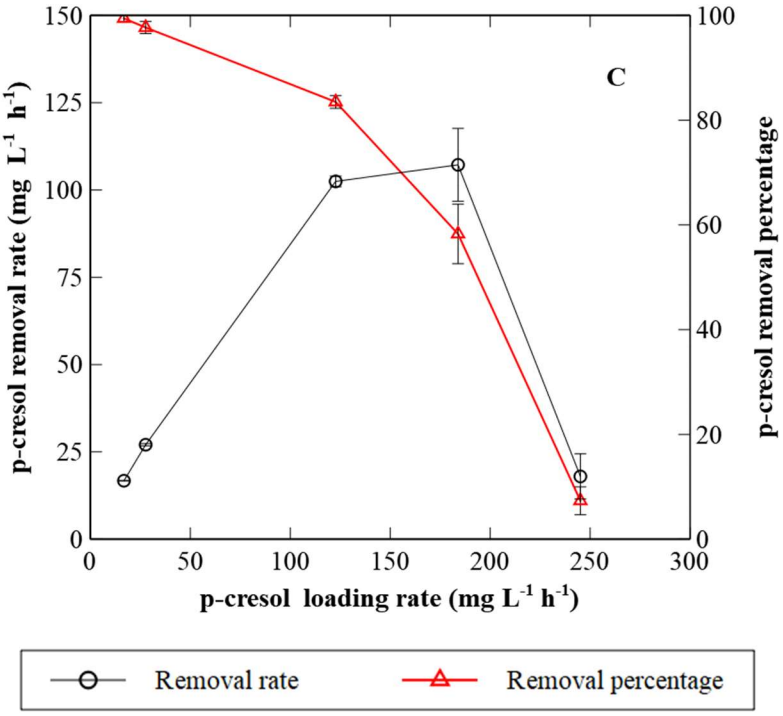

Figure 5.7 The effect of p-cresol loading rate on the performance of the CPBB. Panel (A): 98.6 ± 1.9 mg L^{-1} p-cresol, Panel (B): 294.3 ± 3.6 mg L^{-1} p-cresol, Panel (C): 485.9 ± 10.3 mg L^{-1} p-cresol. Each point represents the average value of the data obtained over an extended period of operation after the establishment of steady state. Error bars represent standard deviation and may not be visible in some cases.

Figure 5.8 presents the effect of p-cresol concentration in the influent and loading rate and on its removal rate in the CPBB. The patterns obtained with p-cresol was similar to that of phenol. Another word for the lower loading rate range, the removal rates were not affected by influent concentration and were identical. Further increase of loading rate brought about the larger differences whereby for the same loading rate higher influent concentrations led to higher removal rates compared to those with lower influent concentration.

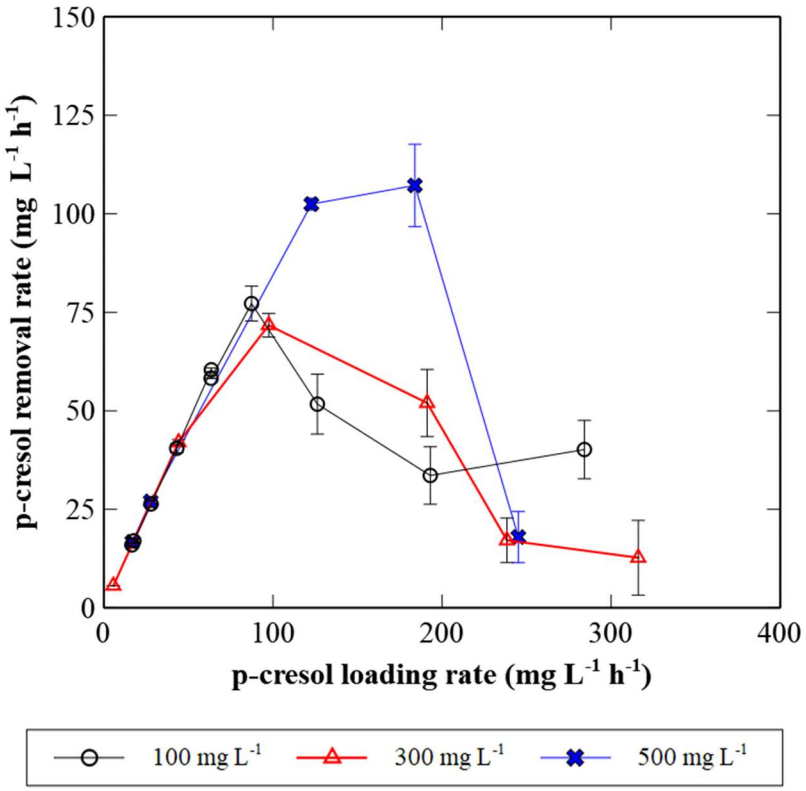

Figure 5.8 Comparison of p-cresol removal rate as a function of its loading rate with influents containing different p-cresol concentrations.

5.2.1 Toxicity Evaluation of Influent and Effluent

The results of toxicity test for influents and treated effluents are presented in Figure 5.9. For untreated p-cresol influent with p-cresol concentrations of 100, 300, and 500 mg L^{-1}, the survival percentage of shrimp larvae after 2 h exposure was 16.3%, 0%, and 0%, respectively. It is important to point out that with 300 and 500 mg L^{-1} p-cresol, even only after 30 min exposure only 16.5% and 3.3% of shrimp larvae were alive in untreated p-cresol solutions, respectively.

For treated effluent obtained with 98.6 ± 1.9 mg L^{-1} p-cresol in the influent, the percentage of live shrimps in the effluent was 98.1% after 2 h exposure. This effluent corresponded to the maximum removal rate of 77.2 mg L^{-1} h^{-1} at the loading rate of 87.4 mg L^{-1} h^{-1} (p-cresol removal percentage: 90.3%). As for the effluent obtained with 294.3 ± 3.6 mg L^{-1} p-cresol in the influent, the percentage of live shrimp larvae was 22.5%. The effluent had been collected when the removal rate was at the maximum level (71.7 mg L^{-1} h^{-1}) at the loading rate of 97.5 mg L^{-1} h^{-1} (p-cresol removal percentage: 73.6%). When the p-cresol influent concentration was increased to 485.9 ± 10.3 mg L^{-1}, the percentage of live shrimp exposed to effluent decreased to only 3.8%. This effluent corresponded to the maximum removal rate of 107.2 mg L^{-1} h^{-1} at the loading rate of 183.9 mg L^{-1} h^{-1} (removal percentage: 58.3%). Similar to the trend observed with phenol solution, survival percentage of shrimps increased due to the treatment. However, the survival percentage in the treated effluent obtained with p-cresol was markedly lower compared to those observed with treated effluent with phenol.

A

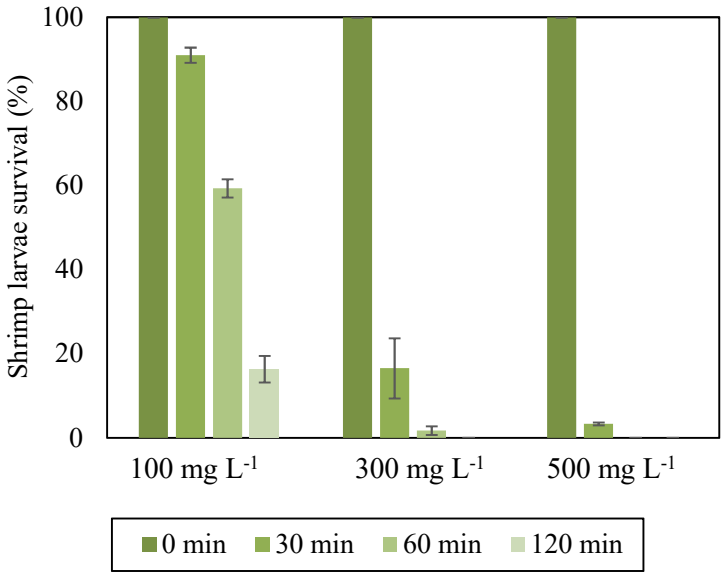

B

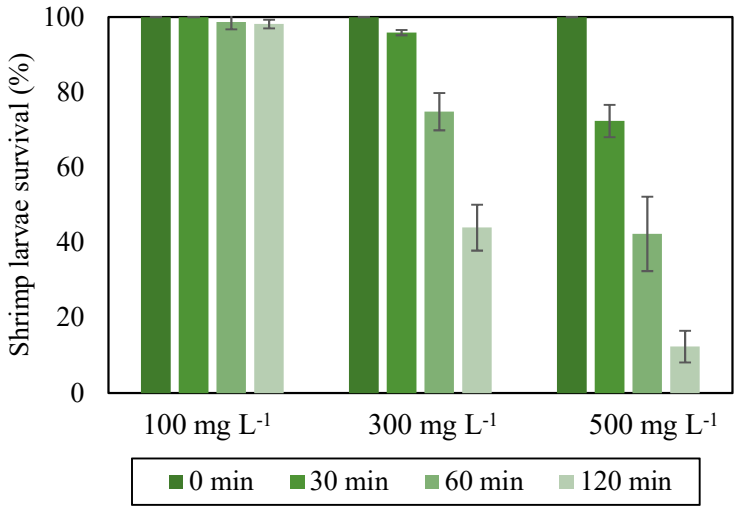

Figure 5.9 Results of p-cresol toxicity test. Panel (A): Influent toxicity; Panel (B): Toxicity results of effluents with the maximum removal rate. Error bars represent standard deviation and may not be visible in some cases.

Similar to phenol case, statistical analysis was done to verify if there was a significant difference in shrimp larvae percentage when exposed to untreated (influent) and treated (effluent) o-cresol solution.

The boxplot (Figure 5.10) indicates that the toxicity reduction at different exposure time. The median is higher at the exposure time of 30 min compared to 60 and 120-minute exposures. The reason for the higher median is that at 30 min, most shrimp larvae stayed alive in the effluent samples, while most died in the influent. By contrast with higher exposure times, the difference between the survival percentage in the effluent and influent was smaller.

Paired t-test results presented in Table 5.2 reveals that the assumption that the difference score was from a normally distributed sample is a valid one, as all Shapiro p value is high than 0.05. Paired t-test P-values for all the exposure time were much less than 0.05, which helped to answer the statistical questions raised previously. In other words, the treated effluent toxicity was significantly different from influent toxicity regardless of the exposure time.

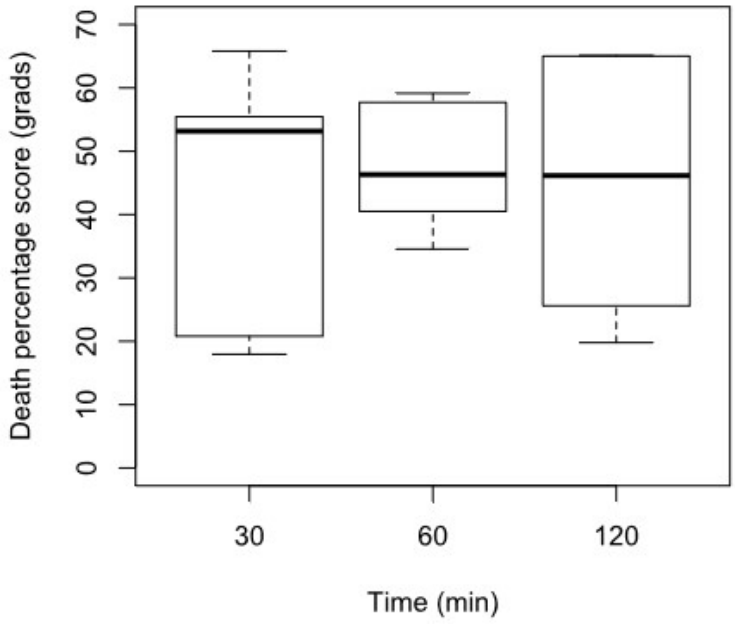

Figure 5.10 Boxplot of the difference of death percentage score between influent and effluent at different exposure time.

Table 5.2 Results of the normality checking and pair t-test

Exposure time (min)	Shapiro test P value	t value	p value of t-test
30	0.1161	5.44	0.002
60	0.6348	11.86	0.00007
120	0.3909	5.71	0.002

5.3 Biodegradation of o-cresol

During the biodegradation of o-cresol, the variation o-cresol residual concentration, removal percentage, and removal rate with its loading rate, as illustrated in Figure 5.11, were similar to those observed with phenol and p-cresol. Therefore, for the sake of brevity, the discussion of o-cresol biodegradation results has focused on the critical information.

As can be seen in Figure 5.11, with an influent containing 95.6 ± 7.3 mg L^{-1} o-cresol the lowest applied loading rate was 3.1 mg L^{-1} h^{-1} that was incrementally increased to 142.8 mg L^{-1} h^{-1}. As a result, the residual concentration of o-cresol increased from 3.2 mg L^{-1} to 96.1 mg L^{-1}. The influent concentration was then increased to 302.6 ± 9.3 mg L^{-1} and loading rate was increased from an initial value of 7.4 mg L^{-1} h^{-1} to 250.2 mg L^{-1} h^{-1}. Residual effluent concentrations were 5.5 mg L^{-1} and 274.8 mg L^{-1}, respectively. Finally, with the highest applied influent concentration of 506.9 ± 5.7 mg L^{-1}, the steady state o-cresol residual concentration in the effluent increased from 13.0 mg L^{-1} to 477.7 mg L^{-1} when loading rate was increased from 17.5 to the highest value of 382.2 mg L^{-1} h^{-1}.

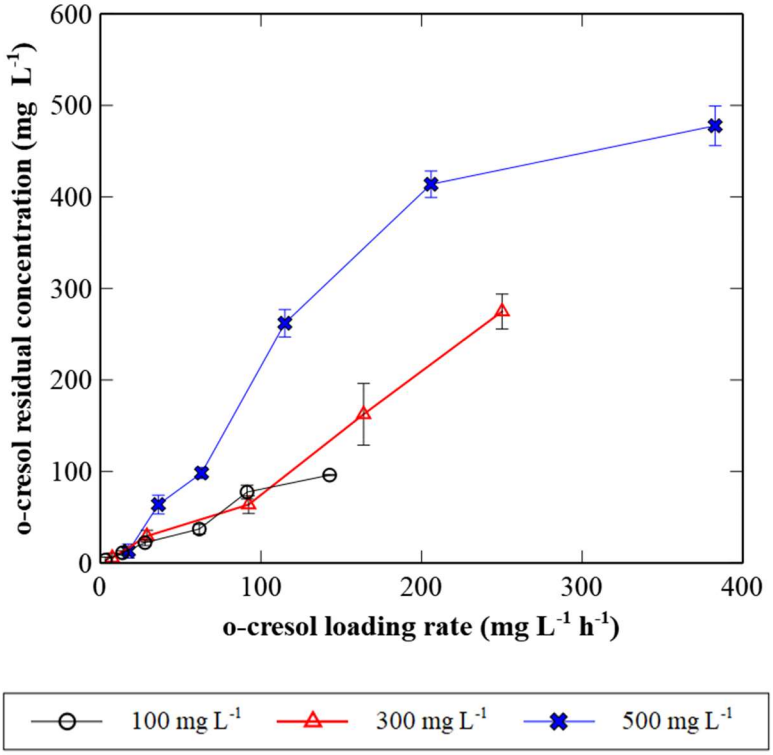

Figure 5.11 Residual concentration of o-cresol as a function of its loading rate for influents containing 100, 300 and 500 mg L^{-1} o-cresol. Each point represents the average value after the establishment of steady state. Error bars represent standard deviation and may not be visible in some cases.

The variation of o-cresol removal percentage and rate as a function of its loading rate is illustrated in Figure 5.12. With an influent o-cresol concentration of 95.6 ± 7.3 mg L^{-1}, the highest removal percentage was 96.9% and obtained at the loading rate of 3.2 mg L^{-1} h^{-1} with a removal rate of 3.0 mg L^{-1} h^{-1} (residence time: 33.1 h). The maximum removal rate was 38.7 mg L^{-1} h^{-1} at the loading rate of 61.6 mg L^{-1} h^{-1} with the removal percentage being 64.1% (1.7 h). For loading rates up to 61.7 mg L^{-1} h^{-1}, the removal percentage was above 64.0%. At the highest tested loading rate of 142.8 mg L^{-1} h^{-1}, the removal rate was only 9.5 mg L^{-1} h^{-1} with a removal percentage of 6.8%.

For an influent containing 302.6 ± 9.3 mg L^{-1} o-cresol, the loading rate varied from 7.4 to 250.2 mg L^{-1} h^{-1}. The highest removal percentage was 98.1% achieved at the loading rate of 15.6 mg L^{-1} with the removal rate of 7.3 mg L^{-1} h^{-1} (residence time: 28.7 h). The highest removal rate of 73.8 mg L^{-1} h^{-1} achieved at the loading rate of 163.9 mg L^{-1} h^{-1} with the removal percentage of 45.0% (residence time: 1.8 h). When the loading rate was increased to 250.2 mg L^{-1} h^{-1}, the removal rate dropped to 17.5 mg L^{-1} h^{-1} with a removal percentage of 7.1%.

With the highest influent concentration of 506.9 ± 5.7 mg L^{-1} h^{-1} the highest removal percentage of 97.4% was obtained at the lowest tested loading rate (17.5 mg L^{-1} h^{-1}; residence time: 28.7 h), with the removal rate being 17.1 mg L^{-1} h^{-1}. The maximum removal rate was 55.1 mg L^{-1} h^{-1} at the loading rate of 114.9 mg L^{-1} h^{-1} with the removal percentage of 47.9% (residence time: 4.4h). An increase of loading rate to 382.8 mg L^{-1} h^{-1} led to low removal rate and removal percentage of 19.4 mg L^{-1} h^{-1} and 5.1%, respectively.

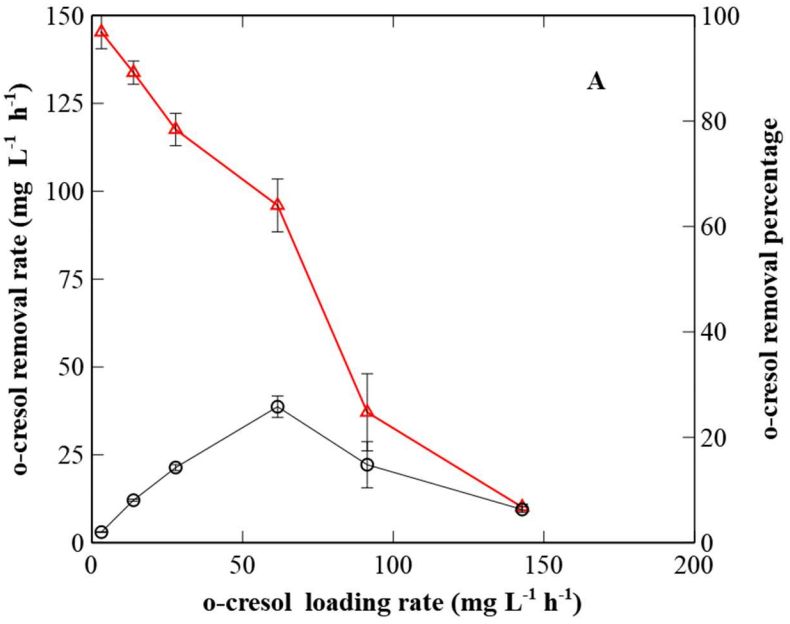

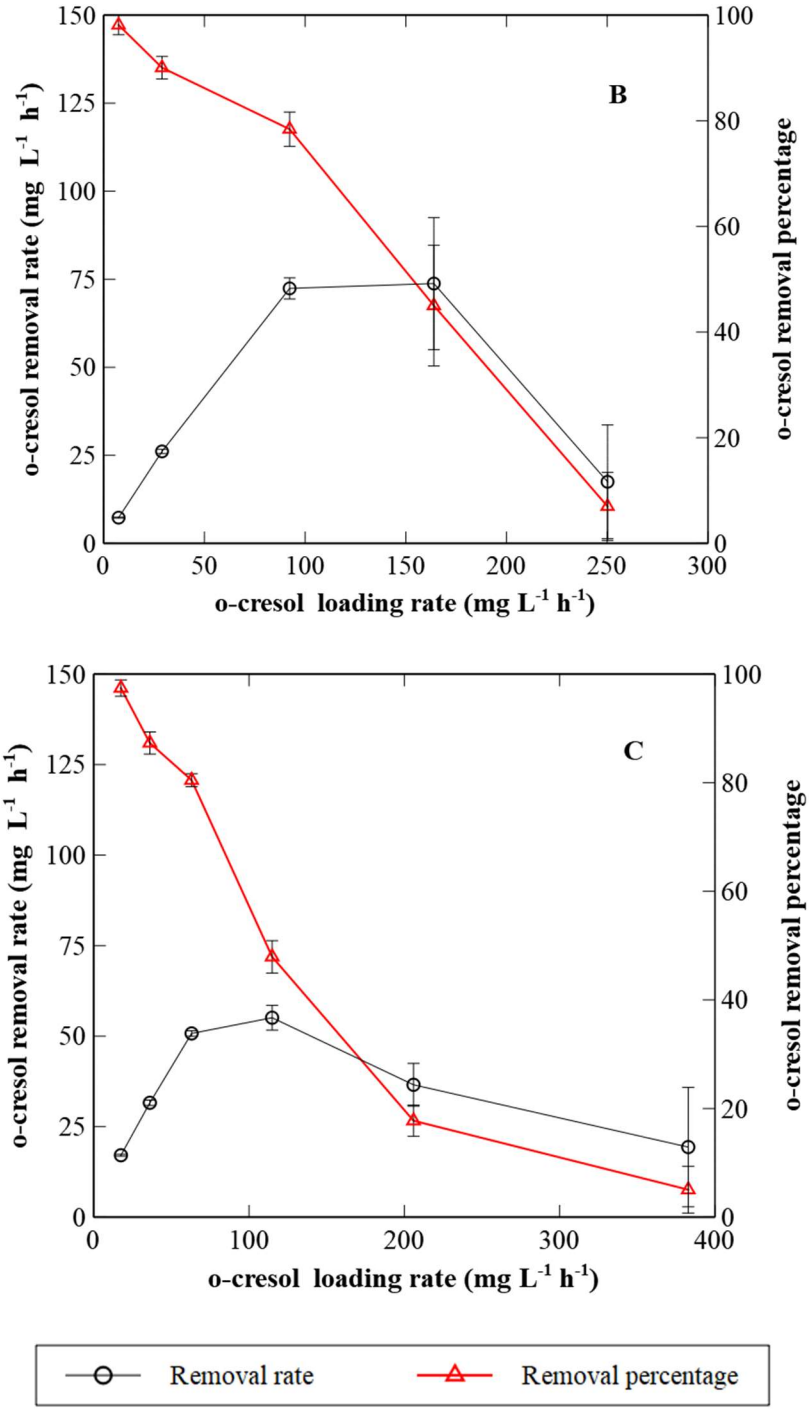

Figure 5.12 The effect of o-cresol loading rates on the performance of the CPBB. Panel (A): 95.6 ± 7.3 mg L^{-1} o-cresol, Panel (B): 302.6 ± 9.3 mg L^{-1} o-cresol, Panel (C): 506.9 ± 5.7 mg L^{-1} o-cresol. Each point represents the average value after the establishment of steady state. Error bars represent standard deviation and may not be visible in some cases.

The effect of o-cresol concentration in the effluent on the performance of CPBB is shown in Figure 5.13. Similar dependency between removal and loading rates were observed with all three applied concentrations. To be specific, application of higher loading rate (92.3 to more than 200 mg L^{-1} h^{-1}) as well as higher influent concentrations resulted in higher removal rates. For similar loading rates, the maximum removal rate was achieved when an influent o-cresol concentration of 302.6 ± 9.3 mg L^{-1} was used.

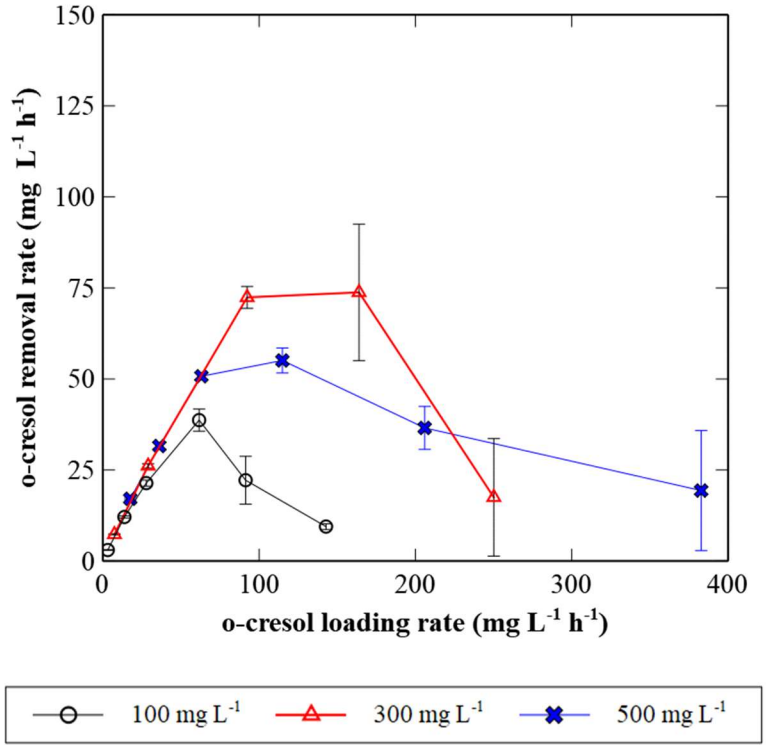

Figure 5.13 Comparison of o-cresol removal rate as a function of its loading rate with influents containing different o-cresol concentrations.

5.3.1 Toxicity Evaluation of Influent and Effluent

The results of toxicity test for biodegradation of o-cresol is represented in Figure 5.14. In terms of untreated influent, with 100, 300, and 500 mg L^{-1} the survival of shrimp larvae was only 40.5%, 0%, and 0% remained alive after 2 h exposure, respectively. This was clearly much lower than phenol and p-cresol and points to the high toxicity of o-cresol.

For treated effluent obtained with 95.6 ± 7.3 mg L^{-1} o-cresol in the influent, 93.3% shrimp larvae remained alive after 2 h. This effluent had obtained when loading rate, removal percentage, and removal rate were 61.6 mg L^{-1} h^{-1}, 64.1% and 38.7 mg L^{-1} h^{-1}, respectively. With an influent with 302.6 ± 9.3 mg L^{-1} o-cresol, the survival percentage of shrimp larvae in the treated effluent was 22.5%. This effluent represented a removal rate of 73.8 mg L^{-1} h^{-1} that obtained at the loading rate of 163.9 mg L^{-1} h^{-1} with removal percentage of 45.0%. When an influent concentration of 506.9 ± 5.7 mg L^{-1} was used, the survival of shrimp larvae exposed to the effluent was only 3.8%. This effluent had obtained when loading rate, removal percentage, and removal rate were 114.9 mg L^{-1} h^{-1}, 47.9% and 55.1 mg L^{-1} h^{-1}, respectively.

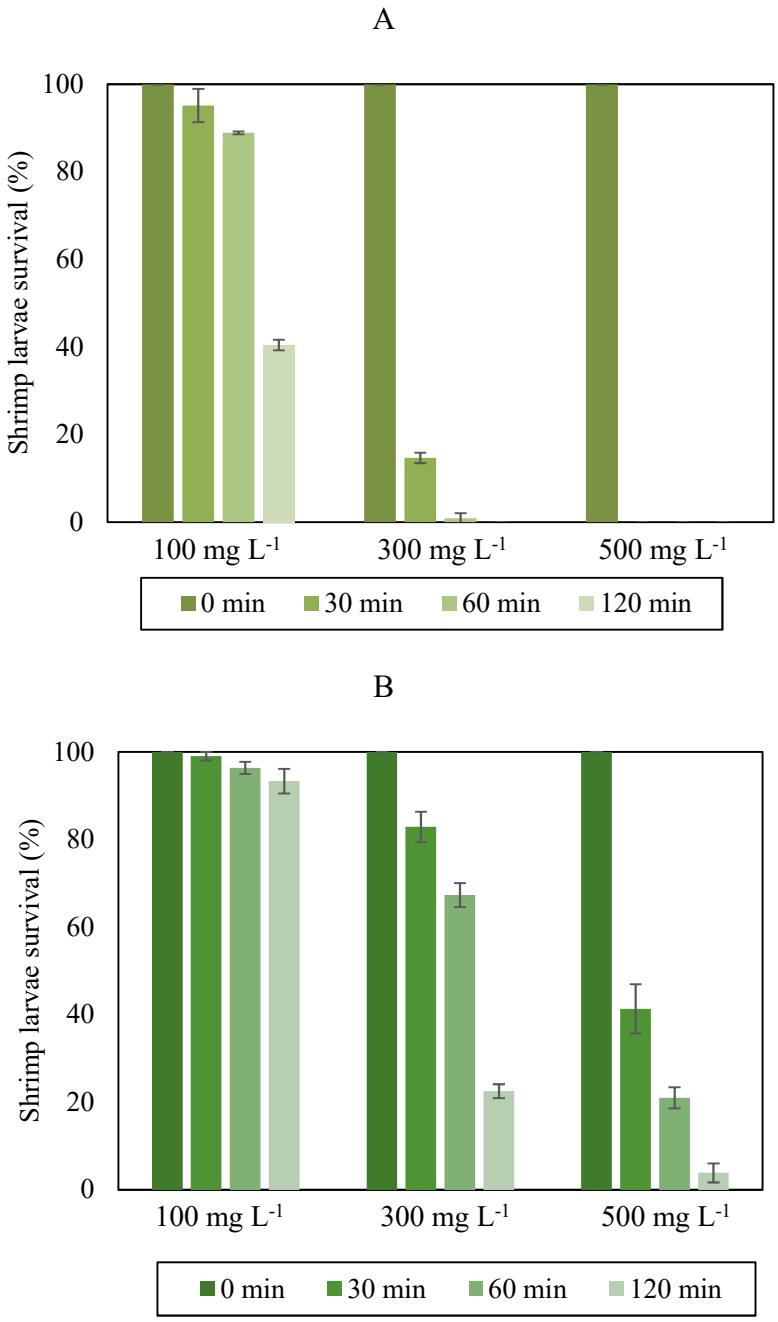

Figure 5.14 Results of o-cresol toxicity test. Panel (A): Influent toxicity; Panel (B): Toxicity results of effluents with the maximum removal rate. Error bars represent standard deviation and may not be visible in some cases.

The statistical significance of the toxicity results was examined in the same manner described and discussed for phenol and p-cresol. Boxplot of death percentage score difference at different exposure time, as shown in Figure 5.15, illustrated that the longer was the exposure time, the higher was the median. Based on the data presented in Figure 5.14, biodegradation of influent containing o-cresol in the bioreactor was less efficient in reducing the toxicity as the toxicity was still high in the effluent samples, especially when the influent concentration was high. Comparing the death percentage at the exposure time of 120 min point to clear reduction of toxicity in influent that contained lower o-cresol and that increase in influent concentration caused a marked rise in death percentage in the effluent samples when the bioreactor was operated at maximum removal rate. Table 5.3 shows the results of paired t-test for o-cresol toxicity reduction. The p-value of Shapiro test for the score difference at the exposure time of 30 min was very close to 0.05. It is highly likely the data do not follow normal distribution. As a result, only the paired t-test results for 60 min and 120 min is discussed here. In both cases the p values are less than 0.05, so the decrease in toxicity was statistically significant although the death percentage was still high.

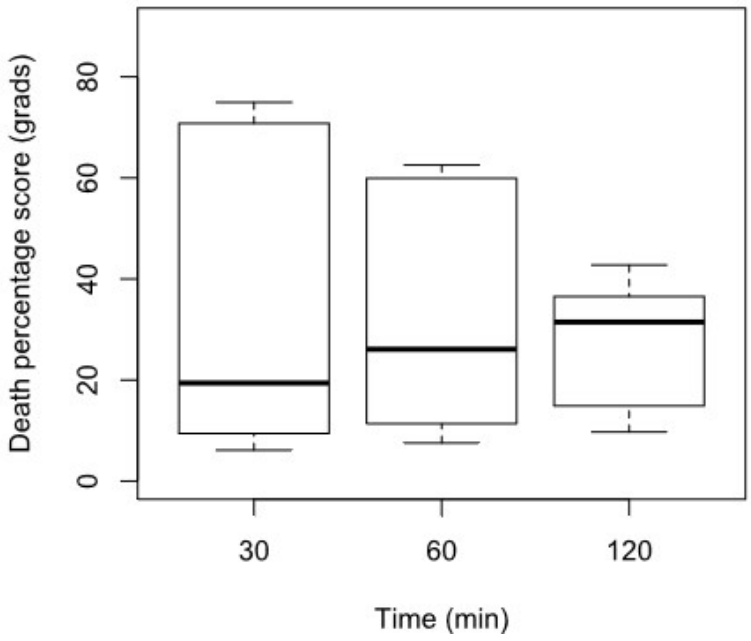

Figure 5.15 Boxplot of the difference of death percentage score between influent and effluent at different exposure time.

Table 5.3 Results of normality checking and paired t-test

Exposure time (min)	Shapiro test P value	t value	p value of t-test
30	0.051*	2.62	0.05
60	0.2302	3.30	0.02
120	0.4917	5.31	0.003

5.4 Comparison of Biodegradation of Phenol, p-cresol, and o-cresol

In this section, the performances of CPBB with influent containing individual phenolic compounds are compared. The removal rate profiles of phenolic compounds with different initial concentrations are presented in Figure 5.16. When substrate concentration was around 100 mg L^{-1} (Figure 5.16, Panel A), the CPBB had better capacity in removing phenol and p-cresol under a

wide range of loading rate (27.8 – 253.1 mg L^{-1} h^{-1}). Specifically, the removal rate profiles of phenol and p-cresol were very close to each other, especially for loading rates up to 80 mg L^{-1} h^{-1} but presented higher values than that of o-cresol. The maximum removal rate of p-cresol and phenol were also close but around 2.0 times higher than that of o-cresol. Application of higher loading rates (> 200 mg L^{-1} h^{-1}) made a distinct difference between phenol and p-cresol, with the latter having a much higher removal rate. The reason could be due to preferential use of p-cresol by the bacteria but the effect was certainly not as pronounced as that observed in the batch system.

When concentrations of these compounds in the influent were increased to 300 mg L^{-1} (Figure 5.16, Panel B), CPBB showed similar performance all three compounds and the removal rate profiles of phenol, p-cresol, and o-cresol including their maximum removal rates were close. This pattern was quite unexpected, as we observed that with 500 mg L^{-1} influent concentration, the profiles were consistent with those obtained with 100 mg L^{-1} whereby p-cresol and phenol displayed similar removal rate profiles and relatively close maximum removal rates. However, they reached much higher removal rates when compared to o-cresol.

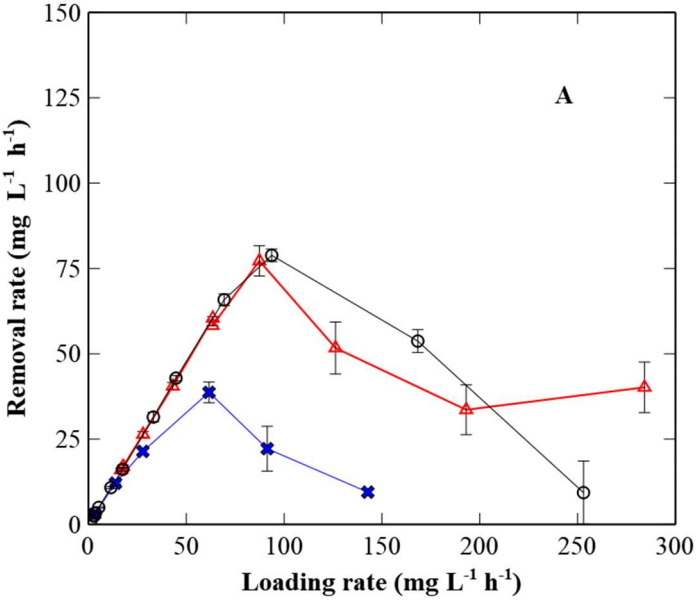
A
Removal rate (mg L-1 h-1)
Loading rate (mg L-1 h-1)
0
25
50
75
100
125
150
0
50
100
150
200
250
300

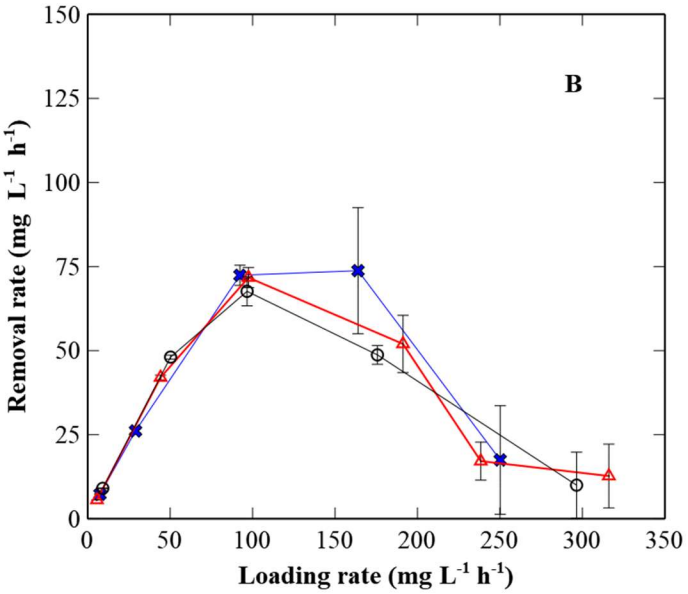
B
Removal rate (mg L-1 h-1)
Loading rate (mg L-1 h-1)
0
25
50
75
100
125
150
0
50
100
150
200
250
300
350

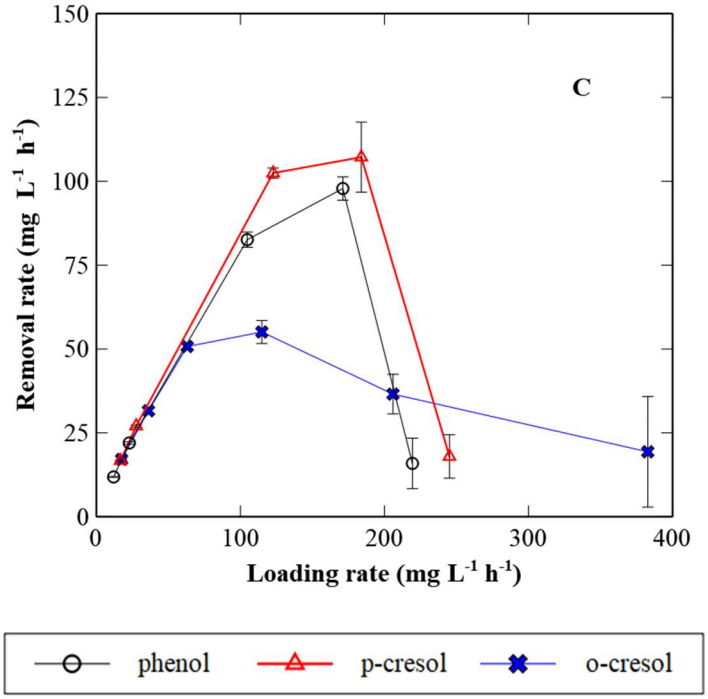

Figure 5.16 Removal rate as a function of loading rate in the CPBBs fed with different phenolic substrate with influent concentrations of (A): 100 mg L^{-1}; (B): 300 mg L^{-1}; and (C) 500 mg L^{-1}.

The toxicity of the influent and effluent for each phenolic compound are also compared and discussed in here. Figure 5.17 compares the toxicity of these compounds at different concentrations and exposure time. As seen in this figure, when the influent concentration was 100 mg L^{-1}, p-cresol is the compound with the highest toxicity, followed by o-cresol. Phenol had the lowest toxicity. On the contrary, higher concentrations (> 300 mg L^{-1}) of these substrates led to different toxicity, indicated by higher toxicity of o-cresol, followed by p-cresol, and then phenol with least toxicity.

Table 5.4 shows the toxicity of each substrate, presented in terms of shrimp larvae survival percentage after 2 h exposure, in the influent of different concentrations and effluents obtained under maximum removal rates. As seen the treatment of influents, regardless of phenolic

compound used, reduced the toxicity. The decrease in toxicity for all three compounds, presented as survival percentage of shrimp, at an influent concentration of 100 mg L^{-1} was the highest and close for all three compounds (>93%). This could be due to the fact that with a low influent concentration and a high removal efficiency in all three cases the residual concentration of phenolic compound in the treated effluent was low, leading to a low toxicity. Increase of influent concentration to 300 and 500 mg L^{-1}, however, made the distinction among the phenolic compounds clearer and as seen the decrease in toxicity of treated effluent was the highest for phenol followed by p-cresol and then o-cresol. This is quite interesting as the toxicity of treated effluent appears to be affected by the extent of biodegradation (removal rate and removal efficiency) as well as intrinsic toxic nature of phenolic compound. In other words, while biodegradation patterns (removal rates) of phenol and p-cresol were quite close, the more toxic nature of p-cresol when compared with phenol led to higher toxicity of the treated effluent (lower survival percentage) obtained with p-cresol. In a similar manner, o-cresol displayed less toxicity when compared to p-cresol but the less efficient biodegradation (lower removal rate) when compared with p-cresol led to an effluent that was more toxic than the one with p-cresol.

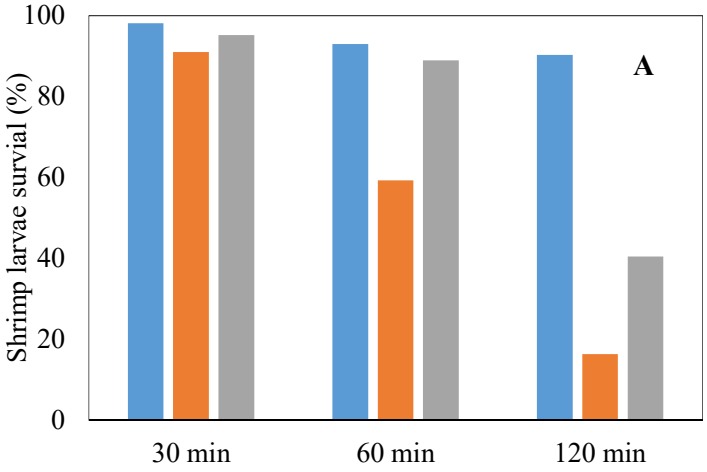
100
80
60
40
20
0
Shrimp larvae survial (%)
A
30 min
60 min
120 min

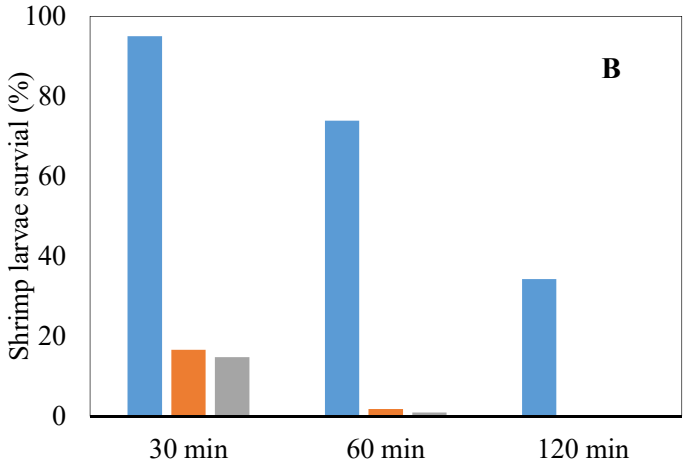
100
80
60
40
20
0
Shrimp larvae survial (%)
B
30 min
60 min
120 min

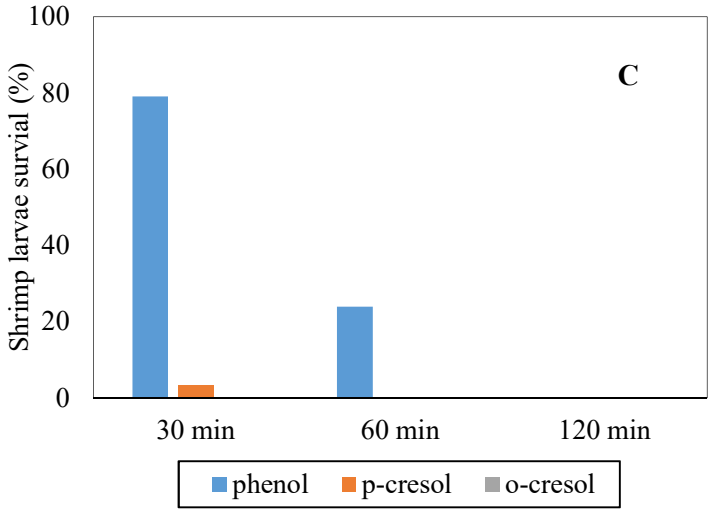

Figure 5.17 Toxicity comparison of phenolic compounds influent with different concentration: (A): 100 mg L^{-1}; (B): 300 mg L^{-1}; and (C) 500 mg L^{-1}.

Table 5.4 Comparison of toxicity of influent and effluents of various phenolic compounds after 2 h exposure

Initial concentration (mg L^{-1})	Shrimp survival (%) in Influent			Shrimp survival (%) in effluent		
	phenol	p-cresol	o-cresol	phenol	p-cresol	o-cresol
100	90.3	16.3	40.5	98.3	98.1	93.3
300	34.3	0	0	94.7	44.0	22.5
500	0	0	0	62.5	12.3	3.8

5.5 Co-biodegradation of Phenol and p-cresol

After completion of experiments studying the biodegradation of p-cresol as an individual substrate, the same bioreactors were used to examine the co-biodegradation of phenol and p-cresol. The effect of loading rates of phenol and p-cresol on residual concentration, removal percentage, and removal rate of each compound was assessed by varying the flow rate and influent concentration (only p-cresol). The specific flow rate and concentration was described in section 3.4.2.

Figures 5.18 shows the effect of loading rate on the residual concentration of phenol and p-cresol as a function of their respective loading rate. It is important to note that in this experiment concentration of phenol in the influent was kept around 500 mg L^{-1}, while p-cresol influent concentration was increased from 100 to 500 mg L^{-1}. As seen in the figures and similar to those observed with the individual compounds, an increase of loading rate caused the increase of residual concentration for both phenol and p-cresol. Comparing the residual phenol concentration profiles obtained in the presence of various concentrations of p-cresol revealed that phenol residual concentrations in the presence of 100 and 300 mg L^{-1} p-cresol were close but higher residual concentrations were observed with 500 mg L^{-1}. Based on these results, it appears that p-cresol did not have a marked effect on phenol biodegradation at least for concentrations up to 300 mg L^{-1}.

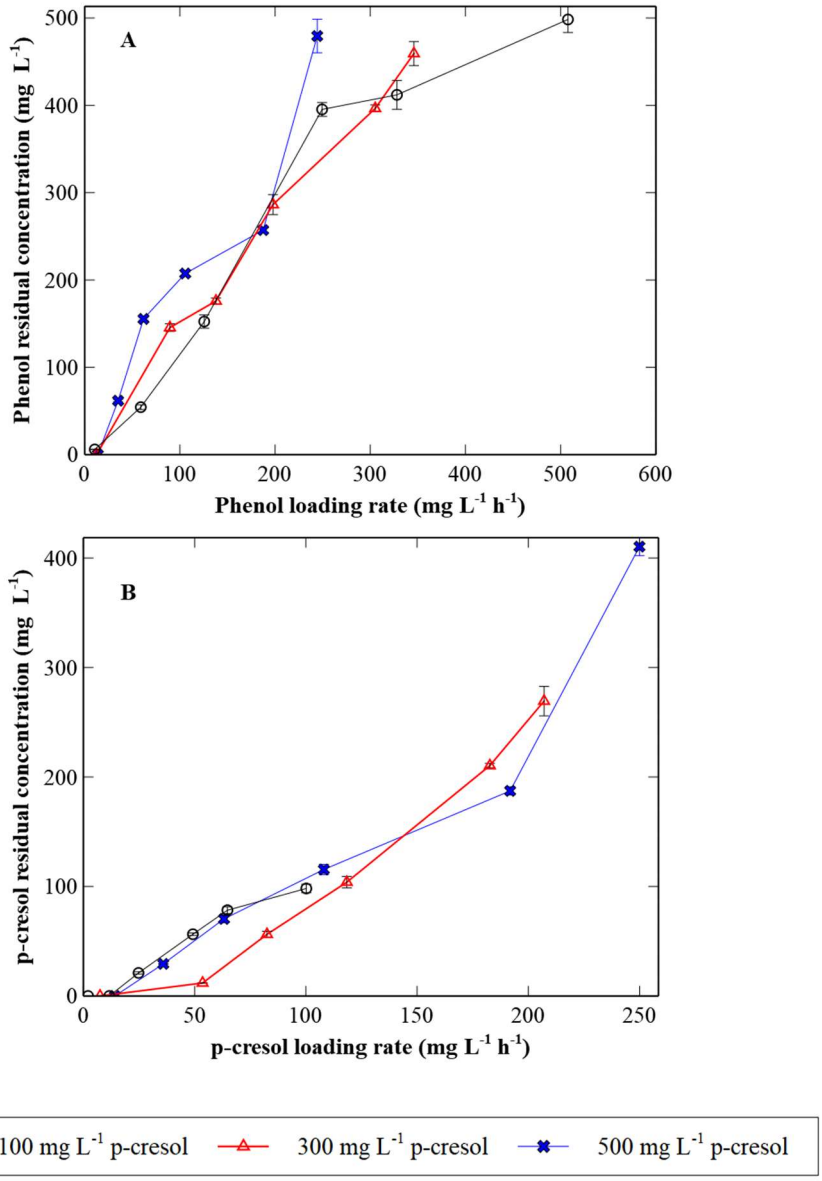

Figure 5.18 Residual concentration as a function of loading rate obtained with various combinations of phenol and p-cresol in the influent. Panel (A): phenol; Panel (B) p-cresol. Each point represents the average value of the data obtained after the establishment of steady state. Error bars represent standard deviation and may not be visible in some cases.

In case of p-cresol, the dependency of residual concentration on the loading rate showed a similar pattern in all influent concentrations (i.e., residual concentration increased as loading rate was increased). For the same loading rate, higher p-cresol influent concentration led to higher residual

concentrations, with the exception being the case of 100 mg L^{-1} whereby residual concentration, in this case, was high and close to those obtained with 500 mg L^{-1} p-cresol. This observed pattern could be attributed to the adaptation of biofilm to degradation of p-cresol, and the dependency of the biodegradation rate on substrate concentration and potential inhibitory effect of high concentration of p-cresol. In other words, the order at which the experiments were conducted with different influents concentration (100, followed by 300 and 500 mg L^{-1}) allowed adaptation of the biofilm to degrade p-cresol. The order also led to a better performance with 300 mgL^{-1} p-cresol. The inhibitory effect of p-cresol at a concentration of 500 mg L^{-1} then resulted in inferior performance when compared to that obtained with 300 mg L^{-1}.

Table 5.5 compiles the critical data obtained during co-biodegradation of phenol and p-cresol including the maximum removal rates of phenol and p-cresol under different operating conditions. The observed pattern is also presented in Figure 5.19.

Table 5.5 Experimental results for co-biodegradation of phenol and p-cresol with various initial concentration in CPBB under steady state conditions

Influent substrate concentration (mg L^{-1})		Flow rate (mL h^{-1})	HRT (h)	Effluent substrate concentration (mg L^{-1})		Loading rate (mg L^{-1} h^{-1})		Removal rate (mg L^{-1} h^{-1})		Removal percentage (%)	
phenol	**p-cresol**			**phenol**	**p-cresol**	**phenol**	**p-cresol**	**phenol**	**p-cresol**	**phenol**	**p-cresol**
498.47±9.97	98.36±4.92	9.56	47.07	5.92	0.00	10.59	2.09	10.46	2.09	98.81	100.00
		53.23	8.45	54.32	0.00	58.95	11.63	52.53	11.63	89.10	100.00
		113.39	3.97	152.39	21.01	125.58	24.78	87.18*	19.49	69.42	78.64
		225.19	2.00	395.32	56.37	249.40	49.22	51.57	21.01**	20.68	42.69
		296.17	1.52	412.01	78.31	328.00	64.74	56.84	13.20	17.33	20.38
		458.39	0.98	498.36	98.17	507.66	100.19	0.01	0.19	0.00	0.19
498.25±14.91	298.34±8.94	11.29	39.86	0.00	0.00	12.50	7.48	12.50	7.48	100.00	100.00
		80.83	5.57	145.48	11.84	89.52	53.58	63.39	51.46	70.81	96.03
		124.50	3.61	175.87	56.28	137.88	82.53	89.23*	66.96	64.71	81.13
		178.60	2.52	286.32	103.89	197.80	118.40	84.16	77.16**	42.55	65.15
		275.60	1.63	396.48	210.39	305.22	182.70	62.40	53.85	20.44	29.47
		312.26	1.44	459.31	269.31	345.82	207.07	27.10	20.13	7.84	9.72
498.38±9.75	509.88±20.43	12.50	36.00	0.00	0.00	13.84	14.16	13.84	14.16	100.00	100.00
		31.69	14.20	61.74	29.29	35.10	35.97	30.75	33.84	87.61	94.26
		55.78	8.07	155.35	70.38	61.78	63.20	42.52	54.48	68.83	86.20
		95.38	4.72	207.39	115.48	105.63	108.07	61.68	83.60	58.39	77.35
		169.30	2.66	257.17	187.32	187.50	191.83	90.75*	121.35**	48.40	63.26
		220.30	2.04	479.38	410.36	244.30	249.94	9.31	48.87	3.81	19.51

*: maximum removal rate of phenol; **: maximum removal rate of p-cresol

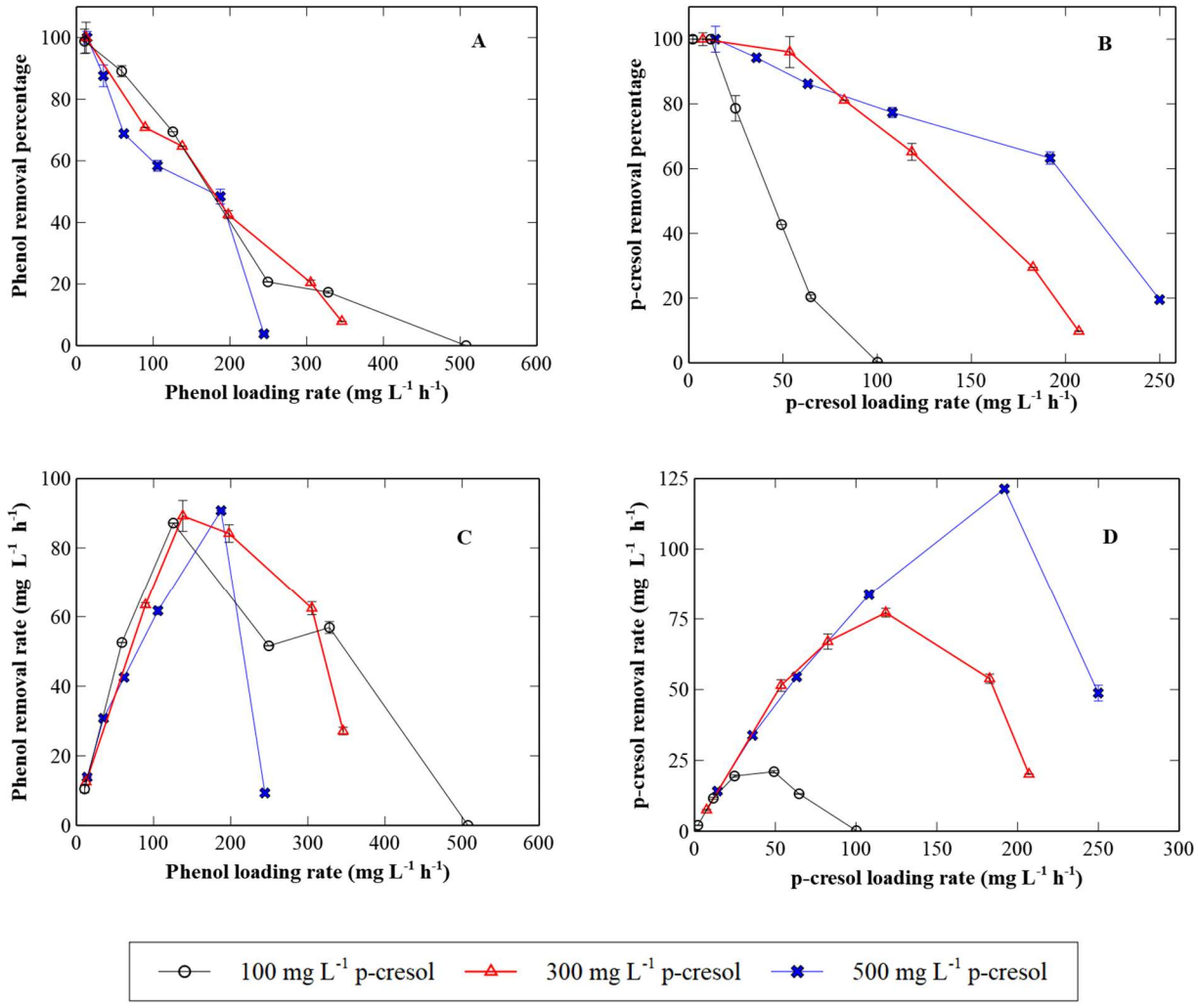

Figure 5.19 Removal percentages and removal rates and of phenol and p-cresol as a function of their respective loading rates in the CPBB fed with various combinations of phenol and p-cresol in the feed. Panel (A): phenol removal percentage vs. loading rate; Panel (B): p-cresol removal percentage vs. its loading rate; Panel (C): phenol removal rate vs. its loading rate; Panel (D): p-cresol removal rate vs. its loading rate. Each point represents the average value of the data obtained after the establishment of steady states. Error bars represent standard deviation and may not be visible in some cases.

As seen in Panels A and B in Figure 5.19 with both phenol and p-cresol the removal percentage gradually decreased as loading rate was increased. When loading rate was low (around 10 mg L^{-1} h^{-1}), the removal percentage of phenol was close to 100%. The presence of p-cresol at 100 and 300 mg L^{-1} did not have a marked effect on the removal percentage of phenol, but with 500 mg L^{-1},

slightly lower removal percentages were observed when the data were compared under similar loading rates. For p-cresol, the removal percentage remained high when loading rate was up to 89.5 mg L^{-1} h^{-1} and the further increase of loading rate led to a sharp decrease of removal percentage. Additionally, for similar loading rates, removal percentages with 300 and 500 mg L^{-1} were close and much higher than that with 100 mg L^{-1} p-cresol.

The removal rate of both compounds during the co-biodegradation followed a similar trend to that of individual compounds and an increase of loading rate increased the removal rate until it reached the maximum value and then started to decrease with further increase of loading rate. This pattern was regardless of p-cresol concentration in the influent. For phenol, an increase of p-cresol influent concentration had a slightly positive impact on the maximum removal rate, and the loading rate at which the maximum value observed, especially with 500 mg L^{-1} p-cresol. To be specific, the maximum removal rates with 100, 300 and 500 mg L^{-1} were 87.18, 89.23, and 90.15 mg L^{-1} h^{-1} and achieved at loading rates of 125.58, 137.88, 166.56 mg L^{-1} h^{-1}, respectively. However, further increase of phenol loading rate, however, made this difference more drastic. With 500 mg L^{-1} p-cresol, phenol had much lower removal rate. Interestingly, the presence of p-cresol with low initial concentration (around 100 mg L^{-1} and 300 mg L^{-1}) did not have a negative impact on the maximum removal rate of phenol when compared to the biodegradation rates obtained with phenol as a single substrate (Figure 5.2). The removal rates of phenol observed during co-biodegradation with 100 and 300 mg L^{-1} p-cresol were higher and only decreased when the p-cresol concentration of 500 mg L^{-1} was used. Specifically, the maximum removal rate of phenol as an individual compound with an influent concentration of 500 mg L^{-1} was 82.6 mg L^{-1} h^{-1}.

In case of p-cresol, an increase of influent concentration from 100 to 500 mg L^{-1} caused the maximum removal rate to increase by about 3.73 times and occurred at higher loading rates (shorter residence times). Compared to the results obtained with p-cresol as a single substrate (Figure 5.7), the presence of phenol negatively influenced the biodegradation of p-cresol. Phenol also decreased the maximum removal rate of p-cresol by about 3.61, 1.07, and 1.36 times when initial concentration of p-cresol was around 100, 300, and 500 mg L^{-1}, respectively.

Finally, consistent to the results observed in the batch system which singled out the p-cresol as the preferred substrate, the removal rate of phenol in the mixture was lower than that of p-cresol when concentrations of both substrates were 500 mg L^{-1} in influent.

5.5.1 Toxicity Assessment for Co-biodegradation of Phenol and p-cresol

The toxicity of influents of different compositions and treated effluent samples were compared to examine the efficiency of CPBB in reducing the toxicity. The treated effluent samples had been collected for two situations: 1) - CPBB was operating under phenol maximum removal rate; 2) - CPBB was operating under p-cresol maximum removal rate.

Figure 5.20 presents the toxicity results of the influent (Panel A), the toxicity of the effluent samples taken when phenol removal rate was maximum (Panel B), and the toxicity of the samples taken when p-cresol removal rate was maximum (Panel C). For influent, higher concentrations of p-cresol (or total concentration of phenolic compound) led to higher toxicity, manifested as lower survival percentage at shorter exposure times. Besides, as one could expect the toxicity of influent

containing both phenol and p-cresol were higher than those observed in the influents containing individual phenol or p-cresol. This pattern could be seen when the toxicity of single compounds presented in Figure 5.4 (A) for phenol and Figure 5.9 (A) for p-cresol was compared with that for the mixture in Figure 5.20 (A). For example, for the influent with 100 mg L^{-1} p-cresol only, after 120 min the shrimp larvae survival percentage was 16.3%, while in the mixture containing 500 mg L^{-1} phenol and 100 mg L^{-1} p-cresol, all shrimp larvae died after 120 min. In the same fashion with 500 mg L^{-1} phenol alone, the survival percentage after 120 min was 3.8% which means that toxicity was higher than the mixture (survival percentage: 16.3%).

The toxicity test results for effluent samples obtained when phenol removal rate was maximum in the CPBB is demonstrated in Figure 5.20 (B). In general, treatment of influents in the CPBB reduced the toxicity of resulting effluents. For instance, for an influent containing 500 mg L^{-1} phenol and 100 mg L^{-1} p-cresol, the survival percentage of live shrimp after 120 min exposure to the treated effluent was 68.59%, while in untreated influent, no shrimp larvae survived after 120 min. The decrease in toxicity of the treated effluent was also dependent on the concentration of p-cresol in the influent, where lower influent p-cresol concentrations resulting in effluents with lower toxicity. To be more specific, shrimp larvae survival percentage in the treated effluent generated with influents containing 500 mg L^{-1} phenol and 100, 300 and 500 mg L^{-1} p-cresol were 68.6%, 28.6%, 0%, respectively.

The effluent samples obtained under the maximum removal rate of p-cresol were also tested for toxicity (Figure 5.20, Panel C). The toxicity was substantially higher when compared to that when CPBB was operated under maximum removal rate of phenol as survival percentage of shrimp

larvae dropped to near zero after 120 min in all evaluated influent concentrations, though a slightly higher survival percentage of 5.5% was observed when the p-cresol influent concentration was 100 mg L^{-1}. The observed results indicate that although the removal rate of p-cresol was at the highest level the residual concentration of p-cresol in the treated effluent was high enough to impose severe toxicity. A high removal rate does not necessarily correspond to reduction in toxicity. The critical factor, as far as the toxicity of the treated effluent is concerned, is the removal efficiency (removal percentage) of p-cresol or any contaminant which affects the toxicity. After all, it is removal efficiency that determines the residual concentration of the toxic compound, thus, the level of toxicity. Therefore, one should consider both removal rate and removal efficiency when decides the proper operating condition for a treatment system such as CPBB. In other words, one might need to accept a lower removal rate that corresponds to a higher removal percentage in order to achieve an effluent with desired characteristics. It is also important to recognize that in some special cases such as treatment of industrial wastewater for the purpose of recycling in a process, the decrease in toxicity is not the main objective, and thus operating the treatment system at high removal rates and lower removal efficiency could satisfy the requirement.

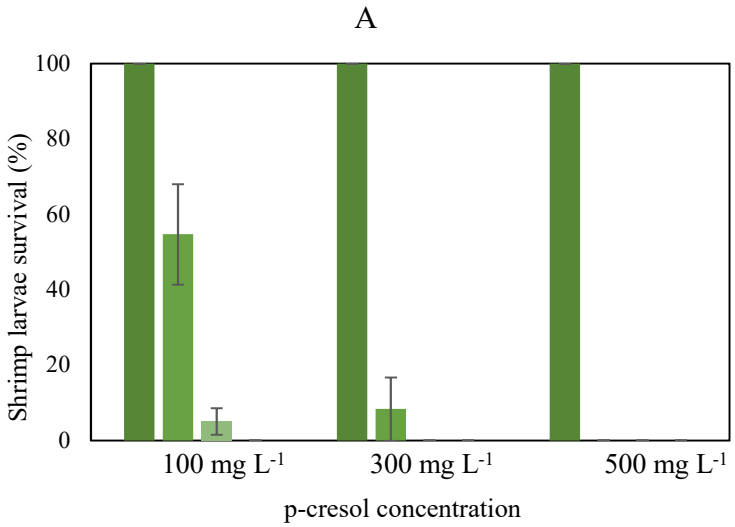

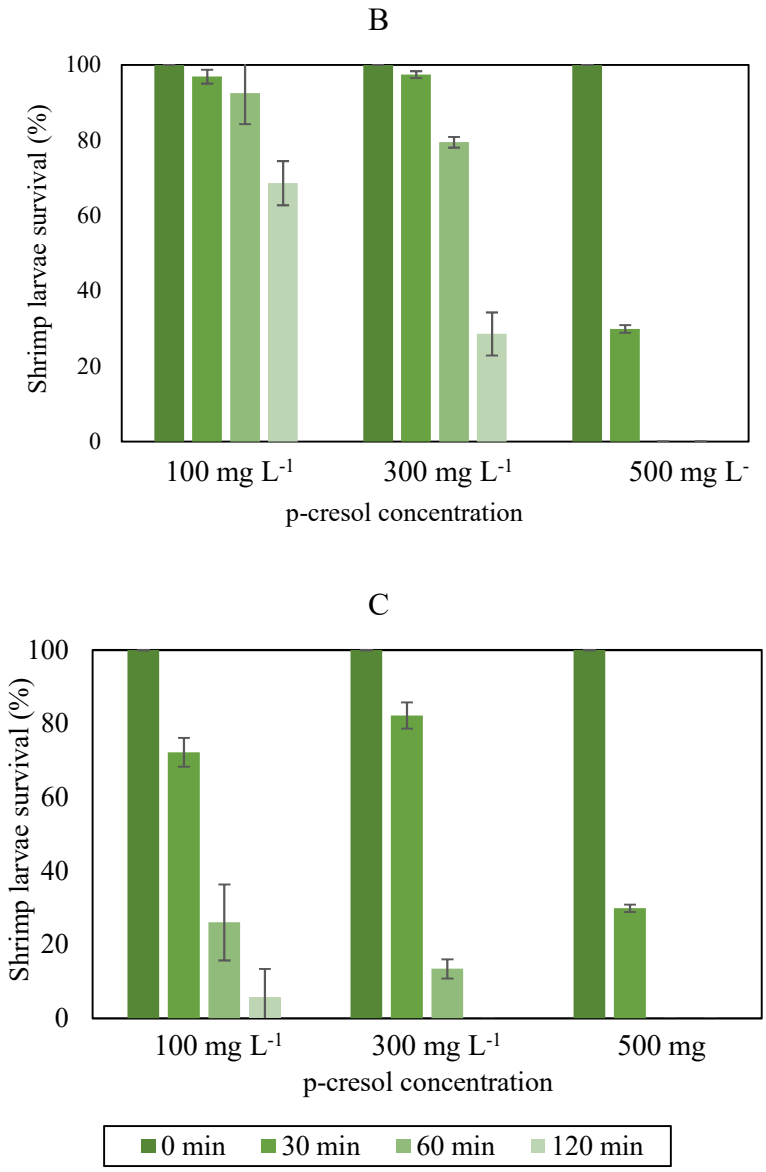

Figure 5.20 Results of toxicity test for co-biodegradation of binary-substrate (500 mg L^{-1} phenol and p-cresol). Panel (A): Toxicity of the influent solution (untreated); Panel (B): Effluents obtained with the maximum removal rate of phenol; (C): Effluents with the maximum removal rate of p-cresol. Error bars represent standard deviation of repeated tests and may not be visible in some cases.

5.6 Co-biodegradation of Phenol and o-cresol

Similar to phenol and p-cresol co-biodegradation, the effect of loading rate of phenol and o-cresol on residual concentration, removal rate, and removal percentage was evaluated.

Figure 5.21 represents the profile of steady state residual concentrations of phenol and o-cresol as a function of their loading rates. The concentration of phenol in the influent was kept around 500 mg L^{-1}, while o-cresol concentration was increased approximately from 100 to 500 mg L^{-1}. Consistent with the experimental observation with individual compounds, increase of loading rate led to an increase of residual concentration for both phenol and o-cresol. Comparing phenol residual concentration profiles in the presence of various concentration of o-cresol showed that in general, the higher the concentration of o-cresol in the influent, the higher the phenol residual concentration in the effluent. The exception was that at lower loading rate range (up to 67.6 mg L^{-1} h^{-1}), phenol residual concentrations were close for o-cresol influent concentrations of 100 and 300 mg L^{-1}. o-Cresol negatively impacted phenol biodegradation especially at both higher concentrations and higher loading rates, which was in contrast to p-cresol which did not actively influence the biodegradation of phenol, even at high concentrations.

Residual concentration of o-cresol was also increased as its loading rate was increased. For loading rates up to around 30 mg L^{-1} h^{-1}, the residual concentration was low regardless of o-cresol concentration in the influent. Above this loading rate, however, a similar pattern to that observed with phenol and p-cresol developed (Figure 5.18). In other words, for the same loading rate, residual concentrations with influents containing 100 and 500 mg L^{-1} o-cresol were close but higher than that with 300 mg L^{-1} o-cresol in the influent. Thus, the same effects described for the case of phenol and p-cresol could be in play for the phenol and o-cresol as well.

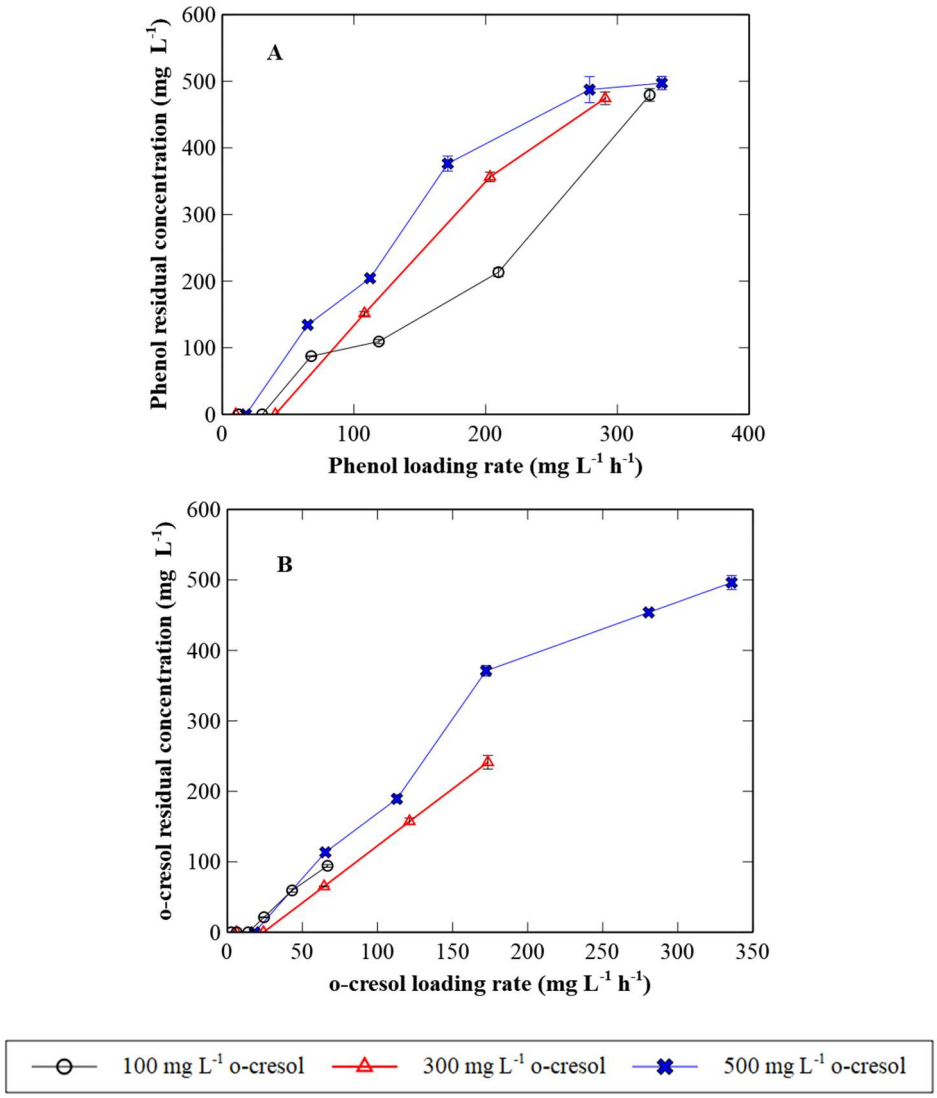

Figure 5.21 Residual concentrations of phenol and o-cresol as a function of their loading rate obtained with various combinations of phenol and o-cresol in the influent. Panel (A): phenol; Panel (B) o-cresol. Each point represents the average value of the data obtained after the establishment of steady state. Error bars represent standard deviation and may not be visible in some cases.

Table 5.6 summarizes the data obtained during co-biodegradation of phenol and o-cresol including the maximum removal rates of phenol and o-cresol under different operating conditions. Based on these results, Figure 5.22 was presented to show the effect of loading rate of phenol and o-cresol on their corresponding removal percentages and removal rates.

Panel A in Figure 5.22 indicates that removal percentage of phenol stayed close to 100% for a low range of loading rate up to 30 mg L^{-1} h^{-1}. At higher loading rate range, the presence of higher concentration of o-cresol led to lower removal percentage of phenol for similar loading rate. The difference of removal percentage became more noticeable when loading rate was higher than 100 mg L^{-1} h^{-1}. As seen in Panel B of Figure 5.22, o-cresol removal percentage also remained high and close to 100% when its loading rate was low (up to 20 mg L^{-1} h^{-1}). Further increase of loading rate caused a rather sharp decrease of removal percentage especially when the o-cresol influent concentration was 100 mg L^{-1}. Removal percentage profile of p-cresol in co-biodegradation with phenol had comparable patterns in which removal percentage was lower with 100 mg L^{-1} p-cresol in influent (Figure 5.19, Panel B).

The removal rates of phenol and o-cresol during co-biodegradation had a trend similar to that of individual compound. Irrespective of o-cresol concentration in the influent, an increase of loading rate initially led to the increase of removal rate until it reached maximum, then removal rate began to drop with further increase of loading rate. For phenol, an increase of o-cresol concentration in influent had an unfavorable effect on the maximum removal rate and the corresponding loading rate. To be more specific, the maximum removal rates of phenol in the presence of 100, 300, and 500 mg L^{-1} o-cresol were 119.94, 75.19, and 66.20 mg L^{-1} h^{-1} at the loading rate of 209.73, 107.99, and 112.22 mg L^{-1} h^{-1}, respectively (Figure 5.22, Panel C). The maximum removal rate decreased by about 44.8% when the influent concentration of o-cresol was increased from 100 to 500 mg L^{-1}. The presence of 100 mg L^{-1} o-cresol in the influent did not decrease the maximum removal rate of phenol when compared to the maximum removal rate with phenol as the sole substrate. The

maximum removal rate of phenol as an individual compound with an influent concentration of 500 mg L^{-1} was 82.6 mg L^{-1} h^{-1}. Therefore, the rates observed during the co-biodegradation of phenol and o-cresol were higher at a level of 119.94 mg L^{-1} h^{-1}. One could attribute the higher rate to prolonged operation of CPBB that had led to a higher biomass hold-up in the bioreactor. With 300 and 500 mg L^{-1} o-cresol, the observed rates were clearly lower than that observed with phenol alone even though the biomass hold-up could have been higher.

Comparing the phenol removal rates obtained with o-cresol and p-cresol revealed that high concentration of o-cresol had a more negative effect on phenol biodegradation than p-cresol. The maximal removal rate of phenol in the presence of 500 mg L^{-1} p-cresol was higher than that in the presence of 500 mg L^{-1} o-cresol in influent by about 60.2%, while at lower concentrations of 300 mg L^{-1} the corresponding values were 14.14%. At concentration of 100 mg L^{-1}, o-cresol, in contrast, had a more positive effect on the biodegradation of phenol than p-cresol. The maximum removal rate of phenol was 25.5% higher. In addition, similar to what was observed during co-biodegradation of phenol and p-cresol, only when o-cresol concentration in the influent was above 300 mg L^{-1}, maximum removal rate of phenol during co-biodegradation was lower than that during biodegradation of phenol alone (Figure 5.2).

Regarding o-cresol, an increase of influent concentration from 100 to 500 mg L^{-1} increased the maximum removal rate by about 3.6 folds and maximum rate was achieved at higher loading rates with a shorter residence time (Table 5.6 and Figure 5.22 (D)). Compare to the results with o-cresol as the sole substrate (Figure 5.12), the presence of phenol negatively affected the removal rate of o-cresol during the co-biodegradation. The maximum removal rate of o-cresol decreased by about

2.0, 1.3, 0.8 times for o-cresol initial concentrations of 100, 300, and 500 mg L^{-1}, respectively. Finally, when both of phenol and o-cresol had influent concentration of 500 mg L^{-1}, similar removal rates for phenol and o-cresol were observed. This is consistent with what was observed in the batch system, bacteria utilized phenol and o-cresol simultaneously.

Table 5.6 Experimental results for co-biodegradation of phenol and o-cresol with various initial concentration in CPBB under steady state

Influent substrate concentration (mg L^{-1})		Flow rate (ml h^{-1})	HRT (h)	Effluent substrate concentration (mg L^{-1})		Loading rate (mg L^{-1} h^{-1})		Removal rate (mg L^{-1} h^{-1})		Removal percentage (%)	
phenol	**o-cresol**			**phenol**	**o-cresol**	**phenol**	**o-cresol**	**phenol**	**o-cresol**	**phenol**	**o-cresol**
498.32±13.6	102.41±17.8	11.34	39.68	0.00	0.00	12.44	2.58	12.44	2.58	100.00	100.00
		27.39	16.43	0.00	0.00	30.05	6.24	30.05	6.24	100.00	100.00
		61.02	7.37	87.39	0.00	66.94	13.90	55.09	13.90	82.30	100.00
		107.36	4.19	109.31	21.38	117.77	24.45	91.69	19.35**	77.86	79.14
		189.37	2.38	213.36	59.37	207.74	43.13	117.75*	18.14	56.78	42.07
		293.04	1.54	479.38	94.31	321.46	66.73	9.29	5.32	2.89	7.97
498.64±9.6	297.43±11.6	9.26	48.60	0.00	0.00	10.39	6.12	10.39	6.12	100.00	100.00
		36.39	12.37	0.00	0.00	40.83	24.05	40.83	24.05	100.00	100.00
		97.51	4.61	151.36	65.10	109.41	64.44	76.61*	50.33	70.02	78.11
		183.58	2.45	356.32	157.39	205.99	121.32	60.63	57.11**	29.43	47.08
		262.50	1.71	474.39	241.24	294.54	173.48	17.82	32.75	6.05	18.88
498.36±15.4	501.40±23.6	16.30	27.61	0.00	0.00	18.50	18.16	18.50	18.16	100.00	100.00
		58.58	7.68	134.28	113.47	66.49	65.28	49.01	50.51	73.71	77.37
		101.33	4.44	204.37	189.37	115.01	112.92	68.99*	70.28**	59.99	62.24
		154.62	2.91	376.37	371.01	175.49	172.30	46.17	44.82	26.31	26.01
		251.82	1.79	487.32	453.84	285.81	280.62	13.11	26.65	4.59	9.50
		301.39	1.49	497.16	496.17	342.07	335.86	9.10	3.54	2.66	1.05

*: maximum removal rate of phenol; **: maximum removal rate of p-cresol

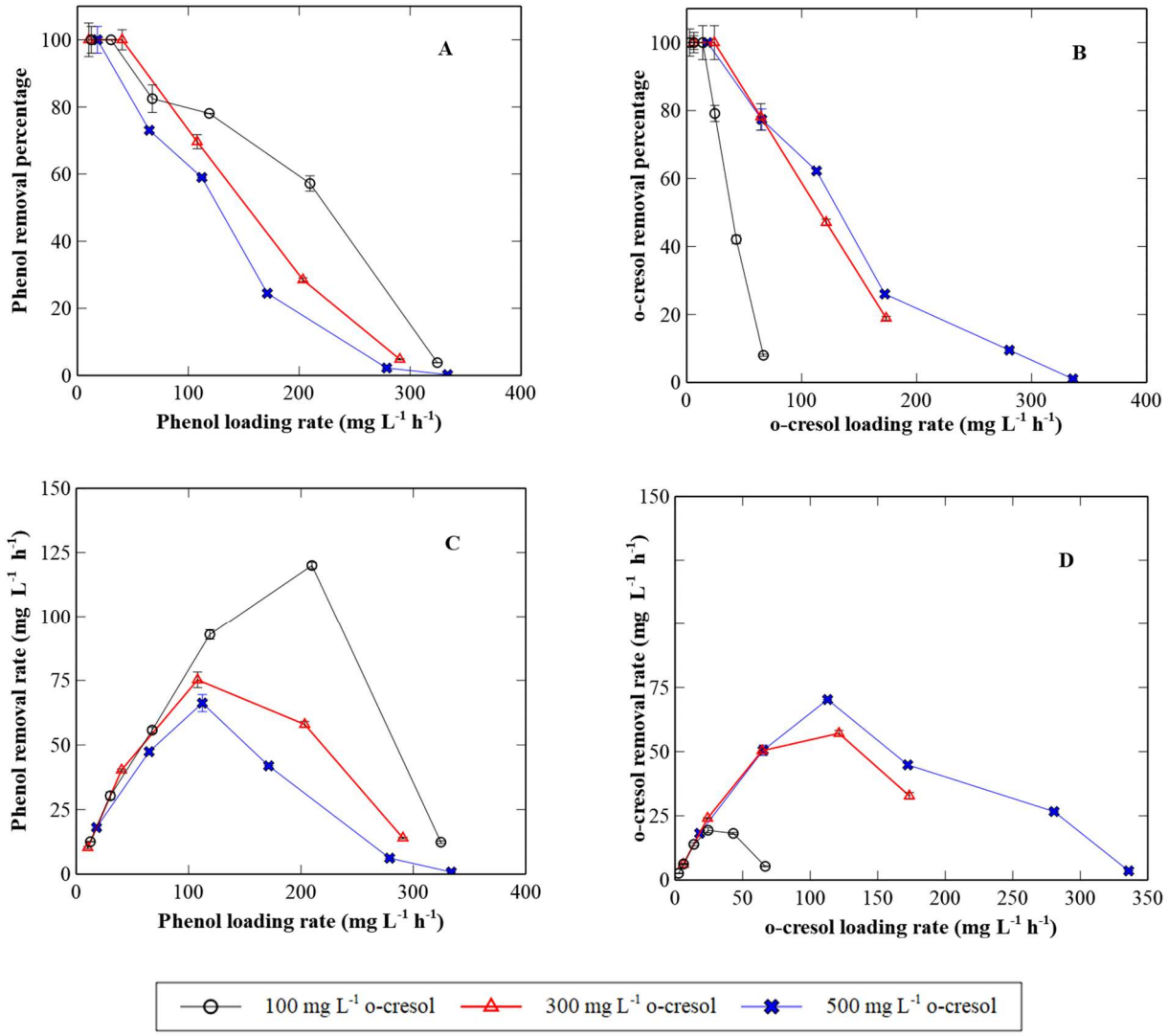

Figure 5.22 Removal percentages and removal rates and of phenol and o-cresol as a function of their respective loading rates in the CPBB fed with various combinations of phenol and o-cresol in the feed. Panel (A): phenol removal percentage vs. its loading rate; Panel (B): o-cresol removal percentage vs. its loading rate; Panel (C): phenol removal rate vs. its loading rate; Panel (D): o-cresol removal rate vs. its loading rate. Each point represents the average value of the data obtained after the establishment of steady state. Error bars represent standard deviation and may not be visible in some cases.

5.6.1 Toxicity Assessment for Co-biodegradation of Phenol and o-cresol

The toxicity of influent of different compositions and treated effluent samples collected when either phenol or o-cresol maximum removal rates were at the maximum level were assessed and compared to determine the efficiency of CPBB in decreasing toxicity.

Figure 5.23 presents the result of toxicity assessment of influent (Panel A), the toxicity of the effluent samples taken when phenol removal rate was maximum (Panel B), and the toxicity of the samples taken when o-cresol removal rate was maximum (Panel C). As expected, toxicity of samples with binary substrate (phenol and o-cresol) was higher than those with individual compound. The difference can be demonstrated via comparing the toxicity of single compound, presented in Figure 5.4 (A) for phenol and Figure 5.14 (A) for o-cresol with that for mixture in Figure 5.23 (A). Even when the o-cresol concentration in mixture was at the lowest level of 100 mg L^{-1}, the percentage of live shrimp larvae decreased to 0 within 30 min. By contrast, with 100 mg L^{-1} o-cresol alone, 40.5% shrimp larvae stayed alive after 120 min. With higher o-cresol concentrations of 300 and mg L^{-1}, either with or without phenol, the survival percentage was zero after 120 min, indicating the toxicity of o-cresol at high concentration in the aquatic environment.

Toxicity results of treated effluent samples obtained when phenol removal rate was at maximum, presented in Figure 5.23 (B) reveals that in general, the toxicity of the influent was reduced after treatment in CPBB. For example, with influent containing 500 mg L^{-1} phenol and 100 mg L^{-1} o-cresol, the percentage of live shrimp larvae after 60 min exposure to the treated effluent was 29.3%,

while in untreated influent no shrimp was live only after 30 min exposure. The toxicity of treated effluent samples increased as concentration of o-cresol in the influent increased, especially to 500 mg L^{-1}. To be more specific, shrimp larvae survival percentages in the treated effluent with influent containing 500 mg L^{-1} phenol and 100, 300, and 500 mg L^{-1} o-cresol after 60 minutes exposure were 0%, 14.3%, and 0%, respectively.

Treated samples taken under the maximum removal rate of o-cresol were also examined for toxicity (Figure 5.23, Panel C). When o-cresol concentration in the influent was around 100 mg L^{-1}, under its maximum removal rate (corresponding residual concentration for phenol and o-cresol: 109.31 mg L^{-1} and 21.38 mg L^{-1}), the toxicity of effluent samples was substantially lower than that of effluent samples taken under the maximum removal rate of phenol (residual concentration of phenol and o-cresol: 213.36 mg L^{-1} and 59.37 mg L^{-1}). Even after 120 min exposure, 78.44% shrimp larvae were alive in the samples taken under maximum removal rate of o-cresol. By contrast, samples taken under o-cresol maximum removal rate when o-cresol influent concentration was 300 mg L^{-1} were more toxic than those taken under phenol maximum removal rate with influent containing same concentration of phenol and o-cresol. This can be demonstrated that no shrimp larvae were alive after 60 min exposure to samples taken under o-cresol maximum removal rate, while 14.24% were still alive even after 120 min in samples taken under phenol maximum removal rate. The toxicity effect is directly associated with the residual concentration of phenols in effluent samples. The higher was the total concentration of phenol and o-cresol, the more toxic was the effluent (Table 5.6). When both phenol and o-cresol were 500 mg L^{-1} in influent, the toxicity was the same under experimental conditions because both substrates reached

maximum removal rate under the same flow rate, hence same total residual concentrations and same toxicity.

Finally, compared to phenol and p-cresol co-biodegradation (Panel B and C in Figure 5.20), the treated effluent obtained under phenol maximum removal rate for phenol and o-cresol co-biodegradation displayed more toxicity as the survival percentage even at low exposure time was very low. Compare to effluent toxicity obtained under p-cresol maximum removal rate during co-biodegradation, the toxicity of effluent samples obtained under o-cresol maximum removal rate was lower. The higher toxicity of p-cresol for shrimp larvae also contributed to overall toxicity.

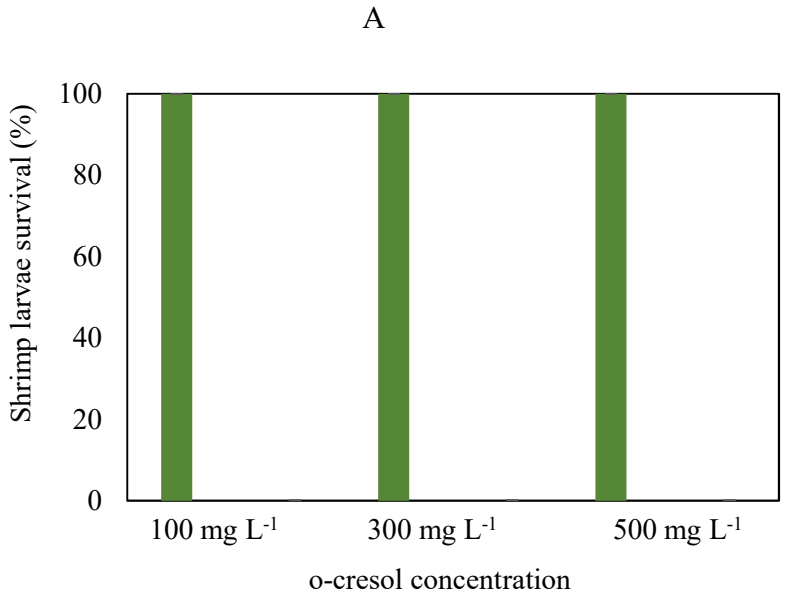

B

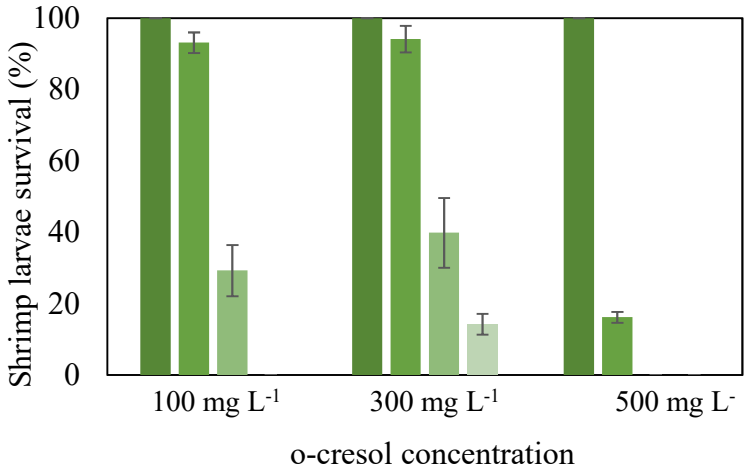

C

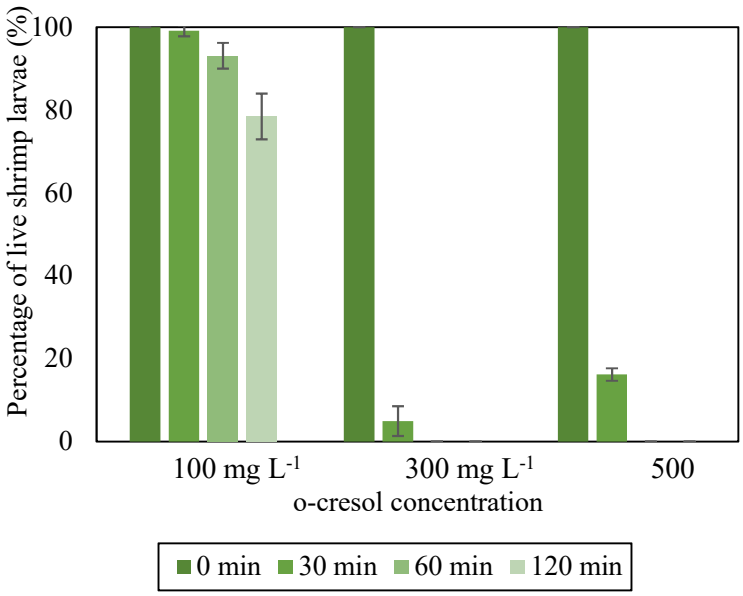

Figure 5.23 Results of toxicity test for co-biodegradation of 500 mg L^{-1} phenol and o-cresol of different concentrations. Panel (A): Toxicity of influent solution (untreated); Panel (B): Effluents obtained when the maximum removal rate of phenol was reached; (C): Effluents obtained when the maximum removal rate of o-cresol was reached. Error bars represent the standard deviation of repeated tests and may not be visible in some cases.

As indicated earlier, given the limited time and resources we carried out the toxicity tests to only two operating conditions where either phenol or cresol (ortho or para) removal rates were at the highest level. However, one could appreciate the complex nature of a co-biodegradation system. A thorough understanding of the treated effluent toxicity requires a much more extensive analysis under a variety of operating conditions (loading rate). The extensive analysis would involve different combinations of removal percentage and removal rate for each compound which subsequently might affect the toxicity of the treated effluent. This is certainly a major undertaking beyond the scope of current work. The task could be pursued as part of future work.

5.7 Ternary Biodegradation of phenol, p-cresol, and o-cresol

Following experiments exploring the co-biodegradation of phenols, CPBBs were utilized to study the ternary biodegradation of phenol, p-cresol, and o-cresol. Similar to previous cases, the effect of loading rate of these phenolic compounds on their residual concentration, removal percentage, and removal rate was examined through manipulating the influent flow rate and concentration (only p-cresol and o-cresol) as described in Section 3.4.2. This section is divided into three parts. The first part describes the results from the set of experiments with influent containing 500 mg L^{-1} phenol, 100 mg L^{-1} p-cresol, and various concentration of o-cresol (100, 300, and 500 mg L^{-1}). The second part focuses on the results obtained when influent contained 500 mg L^{-1} phenol, 300 mg L^{-1} p-cresol, and various concentration of o-cresol (100, 300, and 500 mg L^{-1}). The third one is results for influents containing 500 mg L^{-1} phenol, 500 mg L^{-1} p-cresol, and various concentrations of o-cresol (100, 300, and 500 mg L^{-1}).

Figure 5.24 presents the profiles of steady state residual concentrations of phenol, p-cresol, and o-cresol as a function of their loading rate. The concentration of phenol and p-cresol in the influent was kept around 500 and 100 mg L^{-1}, respectively, while the concentration of o-cresol in influent was increased from 100 to 500 mg L^{-1}. Similar to what was observed in cases of individual and binary substrate biodegradations, an increase of loading rate led to the increase of residual concentration for phenol, p-cresol, and o-cresol. Comparing the phenol residual concentration profiles in the presence of 100 mg L^{-1} p-cresol and various concentration of o-cresol (100 to 500 mg L^{-1}) showed that for the same loading rate, the higher residual concentration of phenol was observed when the o-cresol influent concentration was increased from 100 to 500 mg L^{-1}. For p-cresol, an increase of loading rate also led to the rise of residual concentration. For the same loading rate, the higher the influent concentration of o-cresol, the higher the residual concentration of p-cresol. These trends indicated the adverse effect of high concentration of o-cresol on biodegradation and removal of both phenol and p-cresol. For o-cresol, the lowest residual concentration was observed with the highest influent concentration of 500 mg L^{-1} and higher values were observed when lower concentrations of 100 and 300 mg L^{-1} were used. The reason for the observed pattern was that higher concentrations of substrate in influent led to higher biodegradation rate and thus lower residual concentration.

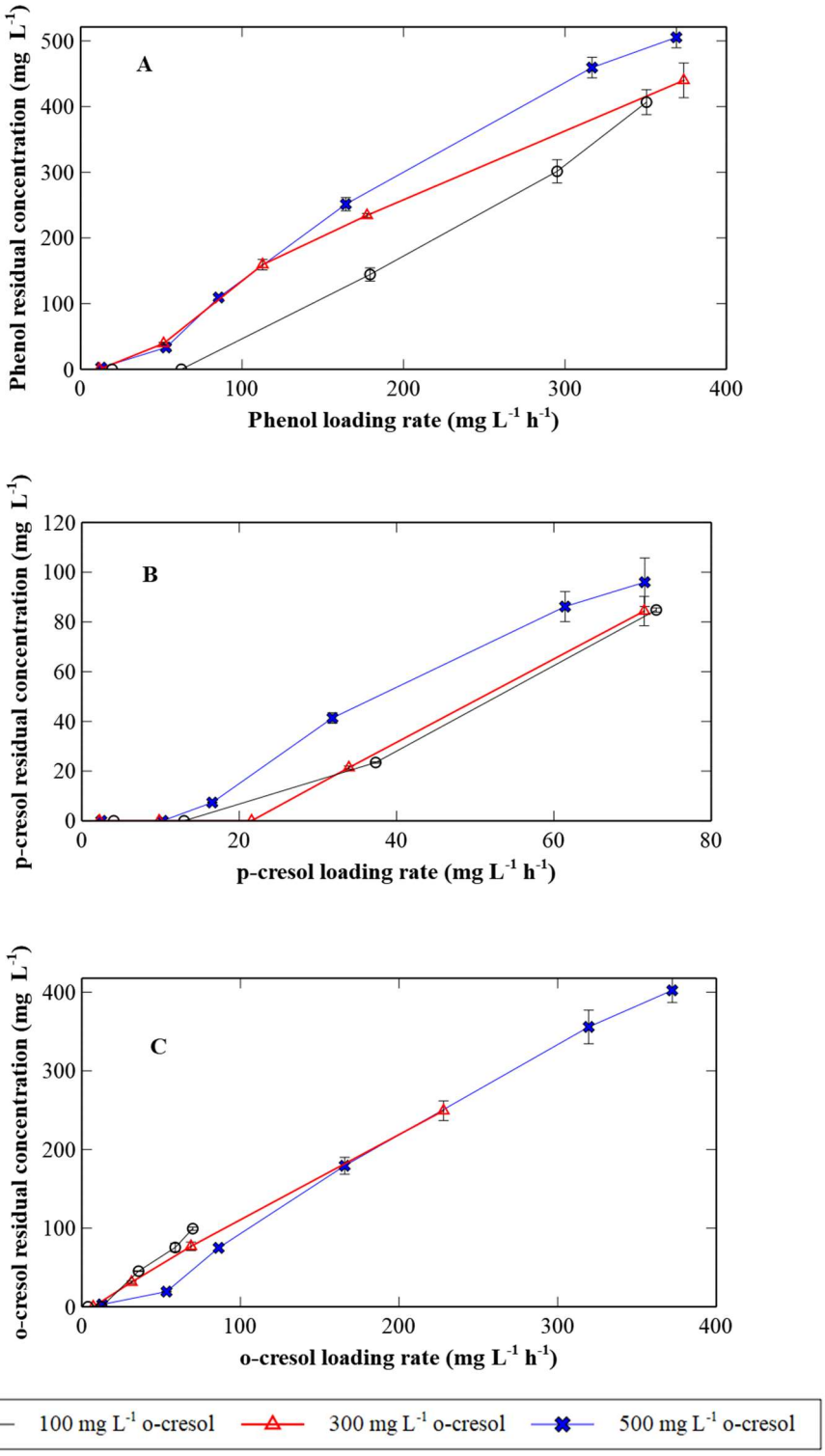

Figure 5.24 Residual concentration as a function of loading rate obtained with various combinations of phenol, p-cresol, and o-cresol influent concentrations. Panel (A): phenol; Panel (B) p-cresol; Panel (C): o-cresol. Each point represents the average value of the data obtained after the establishment of steady state. Error bars represent standard deviation and may not be visible in some cases.

Figure 5.25 presents the profiles of removal rate and removal percentage for each phenolic compound as a function of their loading rate as obtained in the first set of experiment. A summary of important data which includes the maximum removal rate of the three phenolic compounds and their corresponding removal percentages under different operating conditions are presented in Table 5.7.

As seen in Figure 5.25 (A, B, and C), an increase of loading rate led to the decrease of removal percentage of the three phenolic compounds. Removal percentage of phenol stayed close to 100% at loading rate up to 62.4 mg L^{-1} h^{-1}. Under similar loading rate (higher than 33.4 mg L^{-1} h^{-1}), the presence of higher concentration o-cresol besides p-cresol negatively influenced the removal percentage of phenol, indicated by lower phenol removal percentage when high concentrations o-cresol (300 and 500 mg L^{-1}) were present in influent. For the most part removal percentages of phenol with 300 and 500 mg L^{-1} o-cresol were close, and only at loading rate higher than ~200 mg L^{-1} h^{-1}, higher removal percentages were observed at 300 mg L^{-1} o-cresol. For p-cresol, under similar loading rate, removal percentage was higher when o-cresol concentration in influent was higher. In terms of o-cresol, removal percentage remained high (> 90%) for loading rate up to 31.4 mg L^{-1} h^{-1}. Under similar loading rate, removal percentage was higher when o-cresol concentration in influent was higher that again could be related to a positive effect of concentration on biodegradation where high concentration resulted in high biodegradation rates and thus lower residual concentrations and high removal percentages.

The removal rate of all three phenolic compounds during the ternary biodegradation process showed a comparable trend to that of individual and binary biodegradation. In another word, an increase of loading rate increased the removal rate and after it reached the maximum value, removal rate started to decrease with further increase of loading rate. This pattern was observed regardless of the concentration of o-cresol in the influent. For phenol, an increase of o-cresol influent concentration from 100 to 300 and 500 mg L^{-1} had a substantially negative effect on the removal rate. To be more specific, the maximum removal rates of phenol with 100, 300, and 500 mg L^{-1} were 129.16, 95.63, and 83.37 mg L^{-1} h^{-1}, which were achieved at the loading rates of 179.29, 177.08, and 164.29 mg L^{-1} h^{-1}, respectively (Table 5.7, Figure 5.25 (D)). This trend showed around 35.5% decrease in maximum removal rate when influent of o-cresol was increased from 100 to 500 mg L^{-1}. Compared to phenol biodegradation as sole substrate (Figure 5.2; maximum removal rate: 82.6 mg L^{-1} h^{-1}), the maximum removal rate of phenol in the ternary-substrates system was higher. The same is also true when comparing with binary-substrate biodegradation (phenol and o-cresol, Figure 5.19), whereby maximum removal rate of phenol was higher in ternary substrate system, regardless of o-cresol influent concentration.

In case of p-cresol, it can be observed that when the o-cresol influent concentration was increased from 100 to 500 mg L^{-1}, its removal rate decreased especially at loading rates higher than 33.4 mg L^{-1} h^{-1} (Figure 5.25 (E)). The decrease in removal rate was more drastic with an o-cresol influent concentration of 500 mg L^{-1}. For p-cresol loading rate lower than 20 mg L^{-1} h^{-1}, the removal rates were close and not impacted by the presence of o-cresol even at 500 mg L^{-1}. To be more specific, in ternary system, the maximum removal rate of p-cresol was 40.2, 26.0, and 18.54 mg L^{-1} h^{-1} at the loading rate of 61.5, 33.4, and 31.8 mg L^{-1} h^{-1}, respectively, showing 54.2% maximum removal

rate decrease when o-cresol was increased from 100 to 500 mg L^{-1} in influent (Table 5.7). Comparing the biodegradation of p-cresol (100 mg L^{-1}) in the ternary-substrate system with individual p-cresol biodegradation (Figure 5.7 (A)) showed that p-cresol maximum removal rate was higher during individual biodegradation (71.7 mg L^{-1} h^{-1}). Comparing with co-biodegradation (Figure 5.19 (D)) revealed that the addition of 500 mg L^{-1} o-cresol had a negative effect on p-cresol biodegradation while lower concentration (100 mg L^{-1}) of o-cresol enhanced p-cresol biodegradation. In the binary system, maximum removal rate of p-cresol was 21.0 mg L^{-1} h^{-1} at loading rate of 49.2 mg L^{-1} h^{-1}, while in the ternary system, the maximum removal rate was 18.5 mg L^{-1} at the loading rate of 31.8 mg L^{-1} h^{-1} when the o-cresol initial concentration was 500 mg L^{-1}. At lower o-cresol concentration, p-cresol maximum removal rate in the ternary system was higher (40.2 mg L^{-1} h^{-1}), possibly due to the enhanced enzymatic activity and less toxicity. (Table 5.7).

For o-cresol, an increase of influent concentration in generally led to higher rates, specifically the increase of influent concentration from 100 to 500 mg L^{-1} led to maximum removal rate to increase by about 4 folds and to occur at a higher loading rate of 165.72 mg L^{-1} h^{-1} (Table 5.7 and Figure 5.25 (F)). Comparing o-cresol maximum removal rate under ternary biodegradation with that under individual biodegradation (Figure 5.12) showed that the addition of both 500 mg L^{-1} phenol and 100 mg L^{-1} p-cresol reduced the efficiency of CPBB to degrade o-cresol as maximum removal rates of o-cresol was lower under ternary biodegradation. When the results were compared with binary-substrate biodegradation (Figure 5.22), it was observed that o-cresol maximum removal rate was higher in the ternary system by 53.7% when its influent concentration was 500 mg L^{-1}. When o-cresol influent concentration was 100 and 300 mg L^{-1}, maximum removal rate was similar

with the binary system. When 100 mg L^{-1} p-cresol was present with 500 mg L^{-1} phenol in the continuous system, the capability of CPBB to degrade o-cresol was enhanced. What's more, the influent did not have a strong inhibition on biofilm due to dilution of influent in contrast to the batch system. This is an advantage compared to the batch system.

Finally, comparing o-cresol maximum removal rate (when the o-cresol concentration in influent was 100 mg L^{-1}) with p-cresol indicated that o-cresol is more recalcitrant than p-cresol, as o-cresol had lower maximum removal rate than p-cresol by about 50.1% (when the concentration of both substrates was 100 mg L^{-1}). On the other hand, comparing o-cresol removal rate with phenol removal rate when the o-cresol concentration in influent was 500 mg L^{-1} revealed that o-cresol reached higher removal rate than phenol (by about 20%).

Table 5.7 Experimental results for ternary biodegradation of phenol, p-cresol, and o-cresol with various initial concentration in CPBBs under steady state

Inlet flow substrate concentration (mg L^{-1})			Loading rate (mg L^{-1} h^{-1})			Removal rate (mg L^{-1} h^{-1})			Removal percentage		
phenol	**p-cresol**	**o-cresol**	**phenol**	**p-cresol**	**o-cresol**	**phenol**	**p-cresol**	**o-cresol**	**phenol**	**p-cresol**	**o-cresol**
516.12	107.52	102.97	19.48	4.06	3.89	19.48	4.06	3.89	100.00	100.00	100.00
			62.38	13.00	12.45	62.38	13.00	12.45	100.00	100.00	100.00
			179.29	37.35	35.77	129.16	29.20	20.03	72.04	78.19	55.99
			295.12	61.48	58.88	122.80	40.17	15.77	41.61	65.35	26.78
			350.50	73.02	69.93	74.34	15.42	2.48	21.21	21.12	3.54
509.53	96.16	311.53	11.67	2.20	7.14	11.67	2.20	7.14	100.00	100.00	100.00
			51.31	9.68	31.38	47.35	9.68	28.22	92.28	100.00	89.95
			112.56	21.24	68.82	77.36	21.24	51.84	68.73	100.00	75.32
			177.08	33.42	108.27	95.63	25.98	44.23	54.00	77.76	40.85
			372.95	70.38	228.03	51.00	8.64	45.54	13.67	12.27	19.97
510.38	98.96	514.85	12.75	2.47	12.86	12.68	2.47	12.78	99.49	100.00	99.42
			52.93	10.26	53.40	49.49	10.26	51.40	93.50	100.00	96.26
			85.52	16.58	86.27	67.20	15.35	73.71	78.58	92.56	85.44
			164.29	31.85	165.72	83.37	18.54	108.00	50.74	58.21	65.17
			316.79	61.42	319.56	31.67	7.94	98.70	10.00	12.92	30.88
			369.01	71.55	372.24	3.63	2.15	81.33	0.98	3.01	21.85

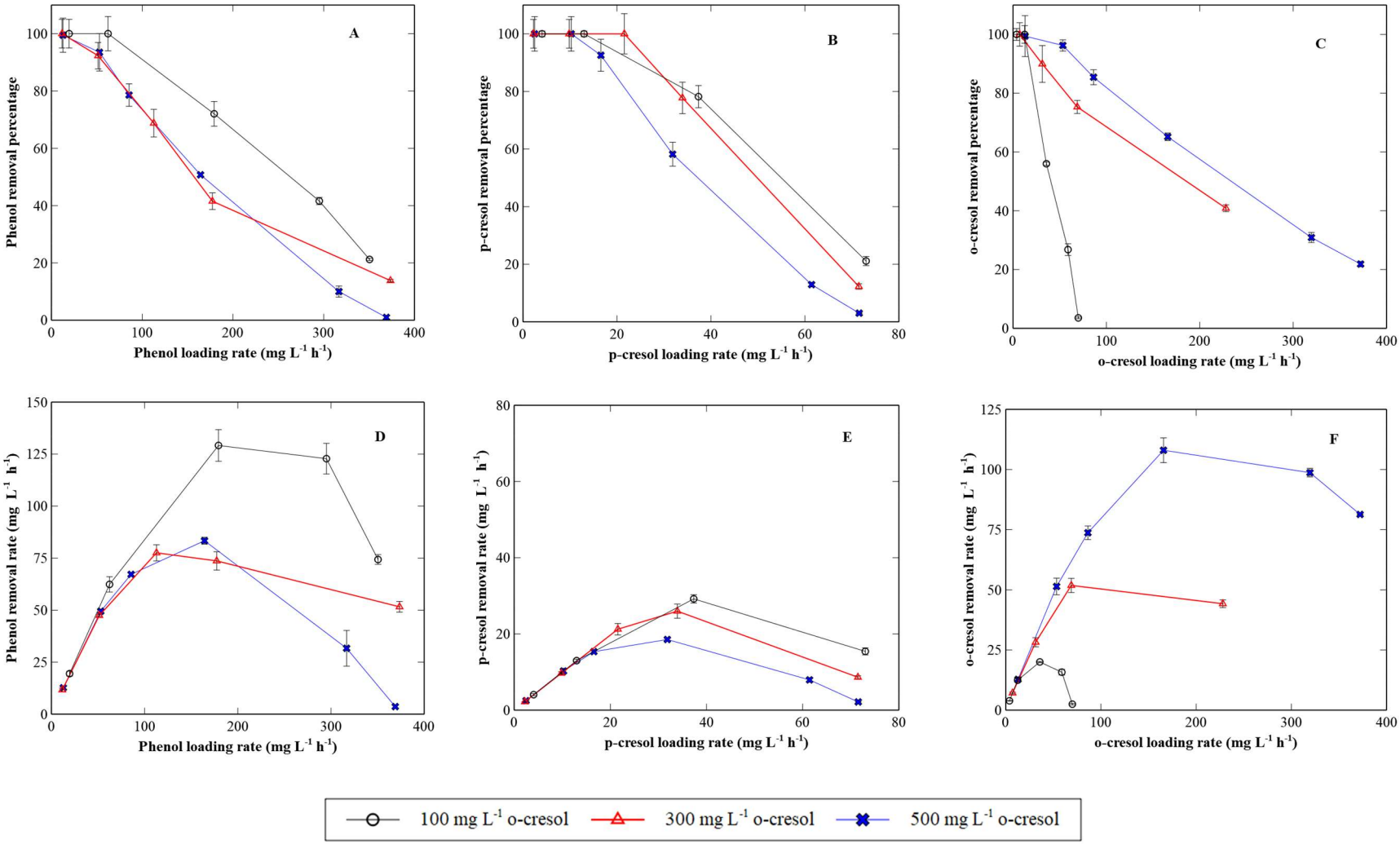

Figure 5.25 Removal percentages and removal rates of phenol, p-cresol and o-cresol as a function of their respective loading rates in the CPBB fed with 500 mg L^{-1} phenol and 100 mg L^{-1} p-cresol and various concentration of o-cresol in the influent. Panel (A): phenol removal percentage vs. its loading rate; Panel (B): p-cresol removal percentage vs. its loading rate; Panel (C): o-cresol removal percentage vs. its loading rate; Panel (D): phenol removal rate vs. its loading rate; Panel (E): p-cresol removal rate vs. its loading rate; Panel (F): o-cresol removal rate vs. its loading rate. Each point represents the average value of the data obtained after the establishment of steady states. Error bars represent standard deviation and may not be visible in some cases.

In this section, the results are presented and discussed for ternary biodegradation when the concentrations of phenol and p-cresol were kept around 500 and 300 mg L^{-1}, respectively. o-cresol concentration in influent was increased from 100 to 500 mg L^{-1}. Figure 5.26 presents the profiles of residual concentrations of each compound as a function of loading rate. Ann increase of loading rate led to an increase of the residual concentrations of all three compounds. At similar loading rates, phenol residual concentration was higher when concentration of o-cresol was higher in the influent. In terms of p-cresol, the residual concentration showed a similar pattern, whereby higher o-cresol influent concentration caused the higher residual concentration of p-cresol under similar loading rates. For loading rates higher than 50 mg L^{-1} h^{-1}, the residual concentration of o-cresol increased as o-cresol influent concentration was increased from 100 to 500 mg L^{-1}. At lower loading rate (lower than 37.9 mg L^{-1}), the dependency of residual concentration on o-cresol influent concentration was negligible.

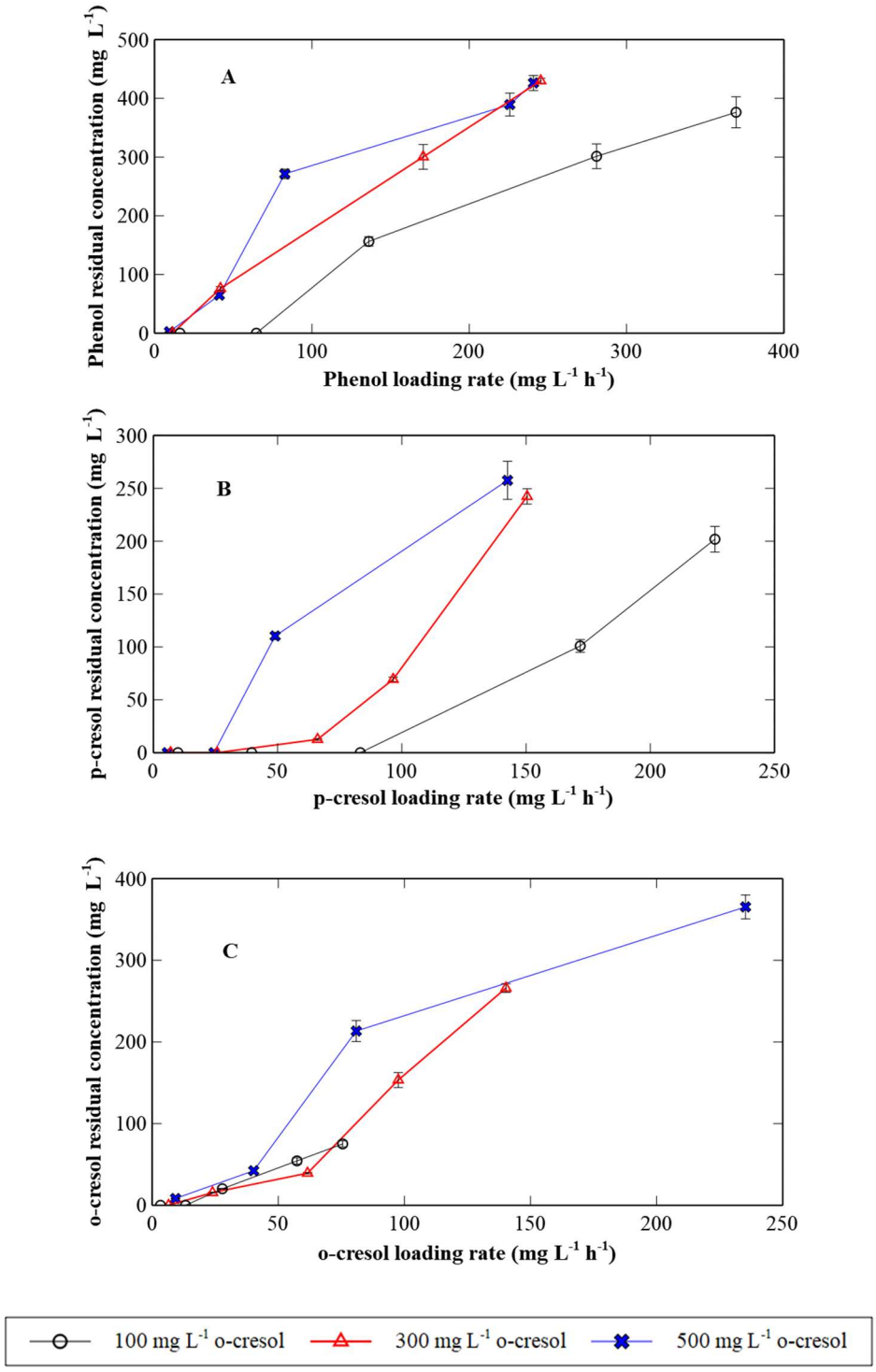

Figure 5.26 Residual concentration as a function of loading rate obtained with various combinations of phenol, p-cresol, and o-cresol influent concentrations. Panel (A): phenol; Panel (B) p-cresol; Panel (C): o-cresol. Each point represents the average value of the data obtained after the establishment of steady state. Error bars represent standard deviation and may not be visible in some cases.

Figure 5.27 presents the profiles of removal rate and removal percentage as a function of loading rate for each phenolic compound. Table 5.8 compiles main data obtained during ternary biodegradation when p-cresol concentration in the influent was 300 mg L^{-1}.

As seen in Panel A, B, and C in Figure 5.27, removal percentage decreased as loading rate was increased for all three phenolic compounds. For phenol, when the o-cresol influent concentration was 100 mg L^{-1}, phenol removal percentage kept near 100% for loading rate up to 64.7 mg L^{-1} h^{-1}. However, an increase of o-cresol influent concentration to 300 and 500 mg L^{-1} led to lower removal percentage of phenol under similar loading rate. The presence of high concentration of o-cresol in addition to 300 mg L^{-1} p-cresol had an obviously negative effect on biodegradation of phenol. For p-cresol, removal percentage was close to 100% even when loading rate was set as high as 82.3 mg L^{-1} h^{-1} when 100 mg L^{-1} o-cresol was in influent. Similar to phenol, the higher concentration of o-cresol in influent led to lower removal percentage of p-cresol. Lastly, o-cresol removal percentages were close at loading rates up to 60 mg L^{-1} h^{-1}. However, at higher loading rate, the dependency of o-cresol removal percentage on its initial concentration became positive.

The removal rate of the three phenolic compounds during ternary biodegradation showed a similar trend to that of the previous set of the experiment as well as those during biodegradation of individual compounds and binary substrate biodegradation. In other words, an increase of loading rate caused the removal rate to pass through a maximum and then decline. In case of phenol, at a lower range of loading rate, an increase of o-cresol concentration did not affect the removal rate. However, the negative impact of o-cresol on the phenol removal rate was observed at loading rate

above 136.2 mg L^{-1} h^{-1}. To be specific, the maximum removal rates of phenol with 300 mg L^{-1} p-cresol and 100, 300, and 500 mg L^{-1} o-cresol were 113.3, 88.0, and 51.3 mg L^{-1} h^{-1} and achieved at the loading rates of 280.9, 107.8, and 223.5 mg L^{-1} h^{-1}, respectively. 54.7% decrease in maximum removal rate was observed when influent concentration of o-cresol was increased from 100 to 500 mg L^{-1}. Comparing the results of phenol biodegradation with ternary biodegradation when 100 mg L^{-1} p-cresol was present revealed that the increase of p-cresol concentration from 100 mg L^{-1} to 300 mg L^{-1} led to a lower phenol biodegradation rate (Figure 5.25, Panel D), with the maximum phenol biodegradation rates in these two cases being 129.2, 95.6, and 83.3 mg L^{-1} as well as 113.3, 88.0, and 51.3 mg L^{-1} at the corresponding o-cresol influent concentration of 100, 300, and 500 mg L^{-1}, respectively.

In terms of the difference between phenol removal rate under this condition and under individual and binary biodegradation, the maximum removal rate of phenol in ternary system was higher than that in individual and binary biodegradation (Figure 5.2 and Figure 5.22). An increase of p-cresol concentration to 300 mg L^{-1} had a positive effect on phenol removal in CPBB, although the effect was less when compared to the case of 100 mg L^{-1} p-cresol in the influent. Due to more available substrates and enhanced capacity of biofilm to degrade phenols, CPBBs removed phenol more efficiently under ternary-substrate biodegradation.

In case of p-cresol, an increase of o-cresol concentration led to the decrease of removal rate especially at loading rate was higher than 83.3 mg L^{-1} h^{-1}. The maximum removal rate of p-cresol decreased by about 34.6% when the o-cresol concentration in influent was increased from 100 to

500 mg L^{-1}. Similar to the case of phenol at the lower range of loading rates up to 66.1 mg L^{-1} h^{-1} removal rate was not affected by the increase in o-cresol concentration. Comparing the result with p-cresol biodegradation as a single substrate (300 mg L^{-1} in influent; Figure 5.7), there is only 5.6% difference of maximum removal rate with 500 mg L^{-1} o-cresol. The difference suggests that the biodegradation of p-cresol (300 mg L^{-1}) was not negatively affected by the presence of both phenol and o-cresol. Comparing the result with those obtained with p-cresol and phenol under binary substrate biodegradation (Figure 5.19), the maximum removal rate varied by about 1.9% and 6.1% when the o-cresol concentration in the influent was 300 and 500 mg L^{-1}, respectively. Considering the standard deviation of measured results, this difference is not prominent. When o-cresol influent concentration was around 100 mg L^{-1}, p-cresol removal rate seemed to be higher under ternary biodegradation in CPBB.

For o-cresol, an increase of its influent concentration from 100 to 500 mg L^{-1} caused the maximum removal rate to increase by about 3.08 folds and occurred at higher loading rates. Comparing the results with those obtained during biodegradation of o-cresol as individual substrate (Figure 5.12) revealed that the presence of both 500 mg L^{-1} phenol and 300 mg L^{-1} p-cresol had negative influence on o-cresol biodegradation. For example, for o-cresol concentration of 300 mg L^{-1} under individual substrate biodegradation, the maximum removal rate is ~27.6% higher than that in ternary biodegradation. In addition, comparing the results with those obtained in binary biodegradation (Figure 5.21) revealed that the presence of additional 300 mg L^{-1} p-cresol in the influent influenced the biodegradation of o-cresol in a positive way. The maximum removal rates were increased by about 40.3% and 19.1% when initial concentration of o-cresol was 100 and 500 mg L^{-1}, respectively. For 300 mg L^{-1} o-cresol, the difference was not obvious. These results suggest

there was complex underlying interaction effect of metabolism for these phenolic compounds as substrates. Lastly, comparing the o-cresol maximum removal rate (Table 5.8) in the presence of 300 mg L^{-1} p-cresol with that in the presence of 100 mg L^{-1} p-cresol (Table 5.7) under ternary biodegradation revealed that an increase of p-cresol in ternary system did not strongly impact the biodegradation of o-cresol (up to 300 mg L^{-1}). However, a further increase of o-cresol to 500 mg L^{-1} led to a big drop of its removal rate by about 22.5%. The drop could be due to the higher toxicity. At the comparable influent concentration of 300 mg L^{-1}, the maximum removal rate of p-cresol was 1.5 times higher than o-cresol, indicating the better biodegradation property of p-cresol. When both o-cresol and phenol concentration in the influent were 500 mg L^{-1}, phenol reached higher maximum removal rate than o-cresol.

Table 5.8 Experimental results for ternary biodegradation of phenol, p-cresol, and o-cresol with various initial concentration in CPBB under steady state

Inlet flow substrate concentration (mg L^{-1})			Loading rate (mg L^{-1} h^{-1})			Removal rate (mg L^{-1} h^{-1})			Removal percentage		
phenol	**p-cresol**	**o-cresol**	**phenol**	**p-cresol**	**o-cresol**	**phenol**	**p-cresol**	**o-cresol**	**phenol**	**p-cresol**	**o-cresol**
			16.15	9.88	3.30	16.15	9.88	3.30	100.00	100.00	100.00
			64.68	39.56	13.22	64.68	39.56	13.22	100.00	100.00	100.00
504.95	308.82	103.18	136.18	83.29	27.83	94.02	83.29	22.37	69.04	100.00	80.37
			280.93	171.82	57.41	113.32	115.65	27.15	40.34	67.31	47.30
			369.58	226.03	75.52	94.22	78.30	20.53	25.50	34.64	27.18
			11.40	6.99	6.51	11.40	6.99	6.51	100.00	100.00	100.00
			41.89	25.68	23.94	35.76	25.68	22.69	85.35	100.00	94.75
519.79	318.58	297.03	107.80	66.07	61.60	87.96	63.47	53.45	81.59	96.05	86.76
			170.75	104.65	97.58	72.08	81.88	47.19	42.21	78.23	48.36
			245.45	150.44	140.27	42.49	36.01	14.68	17.31	23.94	10.46
			9.38	5.68	9.10	9.33	5.68	8.95	99.48	100.00	98.30
			40.78	24.73	39.59	35.55	24.73	36.17	87.18	100.00	91.37
505.29	306.35	490.52	81.99	49.71	79.59	37.97	31.80	44.97	46.30	63.98	56.50
			223.56	135.54	217.03	51.28	75.67	83.69	22.94	55.83	38.56
			238.41	144.54	231.44	37.33	23.03	59.07	15.66	15.93	25.52

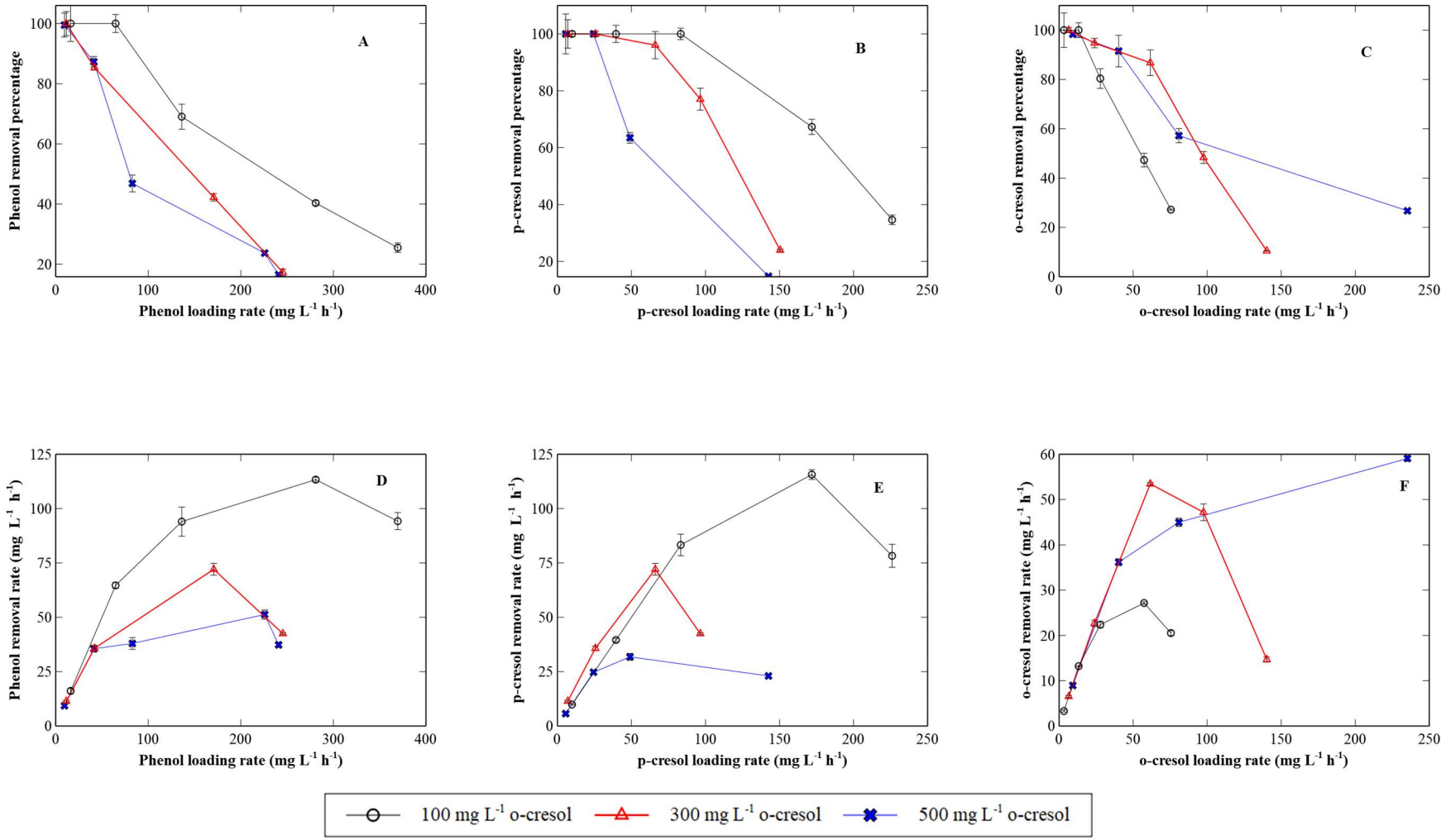

Figure 5.27 Removal percentages and removal rates and of phenol, p-cresol and o-cresol as a function of their respective loading rates in the CPBB fed with 500 mg L^{-1} phenol and 300 mg L^{-1} p-cresol and various concentration of o-cresol in influent. Panel (A): phenol removal percentage vs. its loading rate; Panel (B): p-cresol removal percentage vs. its loading rate; Panel (C): o-cresol removal percentage vs. its loading rate; Panel (D): phenol removal rate vs. its loading rate; Panel (E): p-cresol removal rate vs. its loading rate; Panel (F): o-cresol removal rate vs. its loading rate. Each point represents the average value of the data obtained after the establishment of steady states. Error bars represent standard deviation and may not be visible in some cases.

In this part, results are presented for ternary biodegradation when the o-cresol concentration in the influent was varied in the range 100 to 500 mg L^{-1} in the presence of both 500 mg L^{-1} phenol and 500 mg L^{-1} p-cresol. Figure 5.28 demonstrates the effect of loading rate on the residual concentration of the three phenolic compounds under harshest conditions (i.e. higher concentration of substrate in influent and hence more toxic environment). An increase of loading rate led to the increase of residual concentration in all three cases. For both phenol and p-cresol, under similar loading rate, higher concentrations of o-cresol resulted in higher residual concentrations. In case of o-cresol, its influent concentration did not seem to have any marked effect on the residual concentration, which could be attributed to faster degradation at higher initial concentrations. .

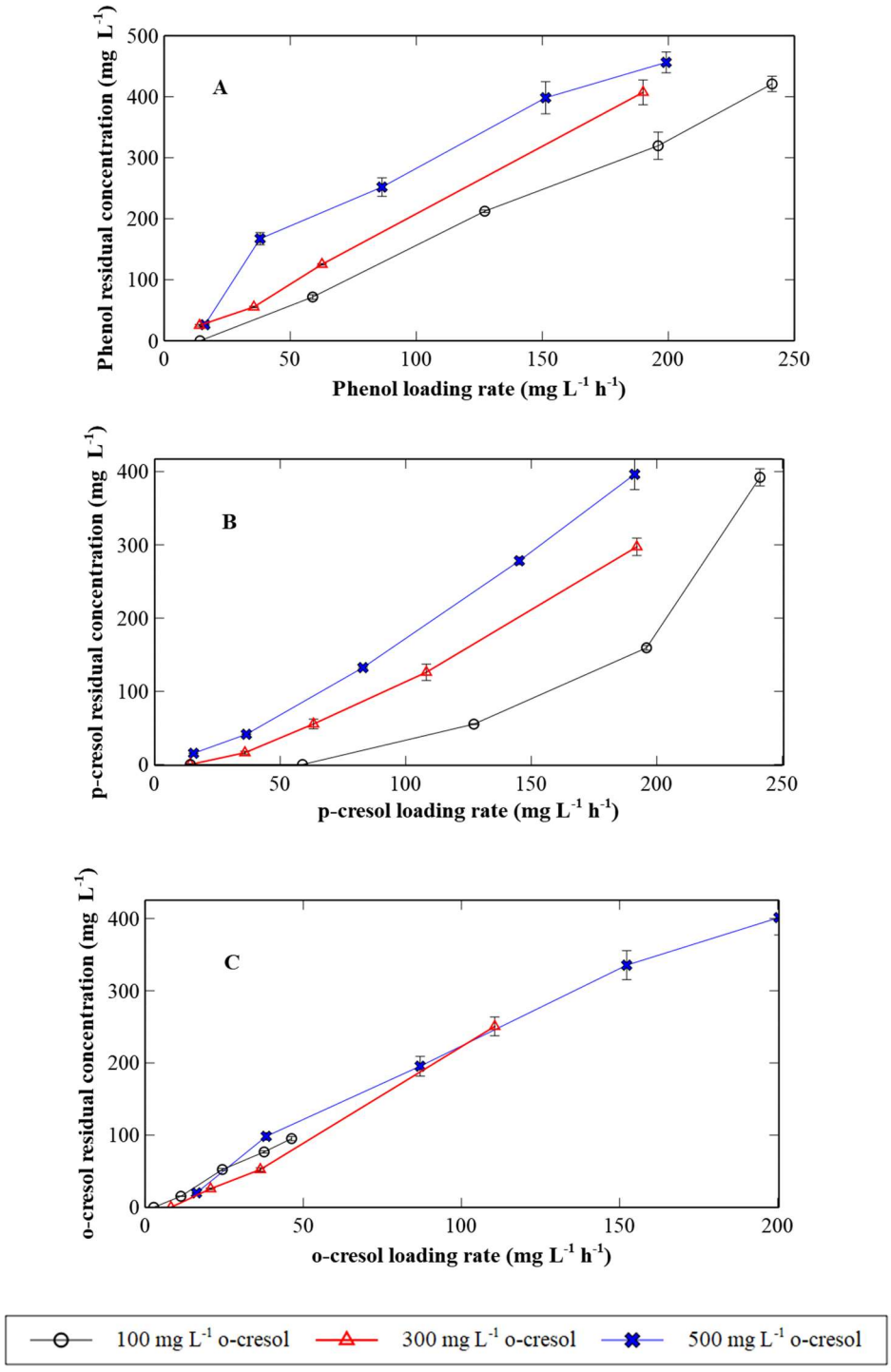

Figure 5.28 Residual concentration as a function of loading rate obtained with various combinations of phenol, p-cresol, and o-cresol influent concentrations. Panel (A): phenol; Panel (B) p-cresol; Panel (C): o-cresol. Each point represents the average value of the data obtained after the establishment of steady state. Error bars represent standard deviation and may not be visible in some cases.

Figure 5.29 showed the generated profiles of removal rate and removal percentage of each phenolic compound as a function of their respective loading rates. Table 5.9 compiles the important data for ternary biodegradation of these three phenolic compounds. When phenol loading rate was lower than 10 mg L^{-1} h^{-1}, the removal percentage was close to 100%. Similar to previous runs, an increase of o-cresol concentration negatively influenced phenol removal percentage. Higher concentration of o-cresol in the influent led to lower removal percentage of phenol at the same loading rate. The same results were also observed for p-cresol removal percentage, whereby a higher concentration of o-cresol in influent decreased the removal percentage of p-cresol at the same loading rate. The decrease was more drastic when loading rate was higher than 50 mg L^{-1} h^{-1}. For o-cresol, higher removal percentage was observed when the o-cresol influent concentration was 300 and 500 mg L^{-1} compared to that when the o-cresol influent concentration was 100 mg L^{-1}. In addition, when o-cresol concentration in influent was 300 and 500 mg L^{-1}, the removal percentages were close when its loading rates were lower than 38.3 mg L^{-1} h^{-1}.

The removal rates of these three compounds under ternary biodegradation (p-cresol concentration: 500 mg L^{-1}) showed similar trend as previous experiments (Figure 5.29, Panels D, E, and F). An increase of loading rate led to increase of removal rate until it reached maximum value, then removal rate began to decrease as loading rate was further increased. For phenol, a higher o-cresol concentration in the influent resulted in lower removal rate under the same loading rate. To be more specific, the maximum removal rates of phenol with 100, 300, and 500 mg L^{-1} o-cresol were 74.8, 47.1, and 44.2 mg L^{-1} h^{-1}, reached at the loading rate of 127.2, 63.3, and 82.9 mg L^{-1} h^{-1}, respectively. 40.9% decrease in maximum removal rate was shown when influent concentration of o-cresol was increased from 100 to 500 mg L^{-1}. Comparing with individual biodegradation

(Figure 5.2), phenol maximum removal rate decreased by about 9.5% even when the o-cresol concentration in influent was at the lowest level of 100 mg L^{-1}. The presence of higher concentration of o-cresol resulted in a much lower removal rate of phenol. Comparing phenol removal rate under co-biodegradation with o-cresol, the presence of 500 mg L^{-1} p-cresol led to decrease of maximum removal rate by 37.6%, 37.4%, and 33.2% when the o-cresol concentration in influent was 100, 300, and 500 mg L^{-1}, respectively. (Figure 5.22). Comparing the results with those in the presence of 100 and 300 mg L^{-1} p-cresol and various concentration of o-cresol, the maximum removal rate also decreased, indicating the negative effect of high concentration of p-cresol (also overall increased toxicity) in influent on phenol removal. For example, the maximum removal rate of phenol decreased by about 42.1%, 51.1%, and 47.0% when the o-cresol concentration was 100, 300, and 500 mg L^{-1} in the presence of 500 mg L^{-1} p-cresol compared to those in the presence of 100 mg L^{-1} p-cresol (Figure 5.25).

For p-cresol, an increase of o-cresol concentration in the influent from 100 to 500 mg L^{-1} caused the maximum removal rate to decrease by about 2 folds. Comparing the maximum removal rate of p-cresol under the ternary-substrate biodegradation with that of p-cresol as single substrate (Figure 5.7) showed that the maximum removal rate increased by about 26.3%. The presence of phenol and lower concentration of o-cresol in influent had somewhat positive effect on p-cresol biodegradation, which could be attributed to enzyme activity. However, further increase of o-cresol concentration led to a sharp drop of the maximum removal rate (lower than that of p-cresol under individual biodegradation). Comparing the result with p-cresol in binary substrate biodegradation (500 mg L^{-1} in influent) showed that maximum re7moval rate decreased by about 32.8% and 47.6% when o-cresol concentration in influent was 300 and 500 mg L^{-1}, respectively

(Figure 5.19). The presence of both high concentrations of o-cresol and phenol had a markedly negative impact on the removal rate of p-cresol in influent under ternary biodegradation.

In terms of o-cresol, it can be observed that in the presence of 500 mg L^{-1} phenol and 500 mg L^{-1} p-cresol, an increase of o-cresol influent concentration led to the increase of o-cresol maximum removal rate by about 4.7 times when o-cresol was increased from 100 to 500 mg L^{-1}. Comparing the result with individual biodegradation (Figure 5.12), the maximum removal rate decreased by 70.3%, 59.5%, and 1.7% when the o-cresol concentration in influent was 100, 300, and 500 mg L^{-1}, respectively. Comparing the results with binary biodegradation of o-cresol (with phenol) revealed that o-cresol maximum removal rate decreased by about 40.6%, 47.6%, and 22.9%, when its influent concentration was 100, 300, and 500 mg L^{-1} (Figure 5.22), respectively. In addition, comparing the result with that under ternary biodegradation in the presence of 300 mg L^{-1} p-cresol showed that maximum removal rate decreased by about 57.7%, 44.0%, and 35.2% when the o-cresol concentration in influent was 100, 300, and 500 mg L^{-1}, respectively (Figure 5.27).

When all the three-substrate concentration was 500 mg L^{-1} in the influent, the maximum removal rate of p-cresol was higher than phenol, while phenol maximum removal rate was higher than of o-cresol, indicating o-cresol was the most recalcitrant compound among the three phenolic compounds during ternary substrate biodegradation under highly stressful continuous mode operation.

Table 5.9 Experimental results for ternary biodegradation of phenol, p-cresol, and o-cresol with various initial concentration in CPBB under steady state

Inlet flow substrate concentration (mg L^{-1})			Loading rate (mg L^{-1} h^{-1})			Removal rate (mg L^{-1} h^{-1})			Removal percentage		
phenol	**p-cresol**	**o-cresol**	**phenol**	**p-cresol**	**o-cresol**	**phenol**	**p-cresol**	**o-cresol**	**phenol**	**p-cresol**	**o-cresol**
515.74	515.63	99.03	14.20	14.20	2.73	14.20	14.20	2.73	100.00	100.00	100.00
			58.90	58.88	11.31	50.70	58.88	9.56	86.09	100.00	84.49
			127.16	127.13	24.42	74.79	113.54	11.50	58.82	89.31	47.10
			195.93	195.89	37.62	74.49	135.35	8.49	38.02	69.09	22.56
			241.12	241.07	46.30	44.28	57.73	1.80	18.37	23.95	3.89
504.90	510.43	293.77	14.02	14.18	8.16	13.32	14.18	8.16	94.98	100.00	100.00
			35.56	35.95	20.69	31.66	34.81	18.88	89.04	96.83	91.24
			62.59	63.27	36.41	47.05	56.41	29.92	75.18	89.16	82.17
			107.02	108.19	62.27	33.84	81.49	18.53	31.62	75.32	29.76
			189.95	192.04	110.52	36.75	80.18	29.49	19.34	41.75	26.68
515.74	495.11	518.94	16.14	15.49	16.24	15.31	15.01	15.61	94.88	96.90	96.14
			38.04	36.52	38.28	25.70	33.48	31.03	67.56	91.66	81.05
			86.41	82.95	86.95	44.19	60.78	54.20	51.14	73.27	62.33
			151.30	145.24	152.23	34.44	63.64	53.85	22.76	43.81	35.37
			199.13	191.17	200.37	22.93	38.16	45.43	11.51	19.96	22.67

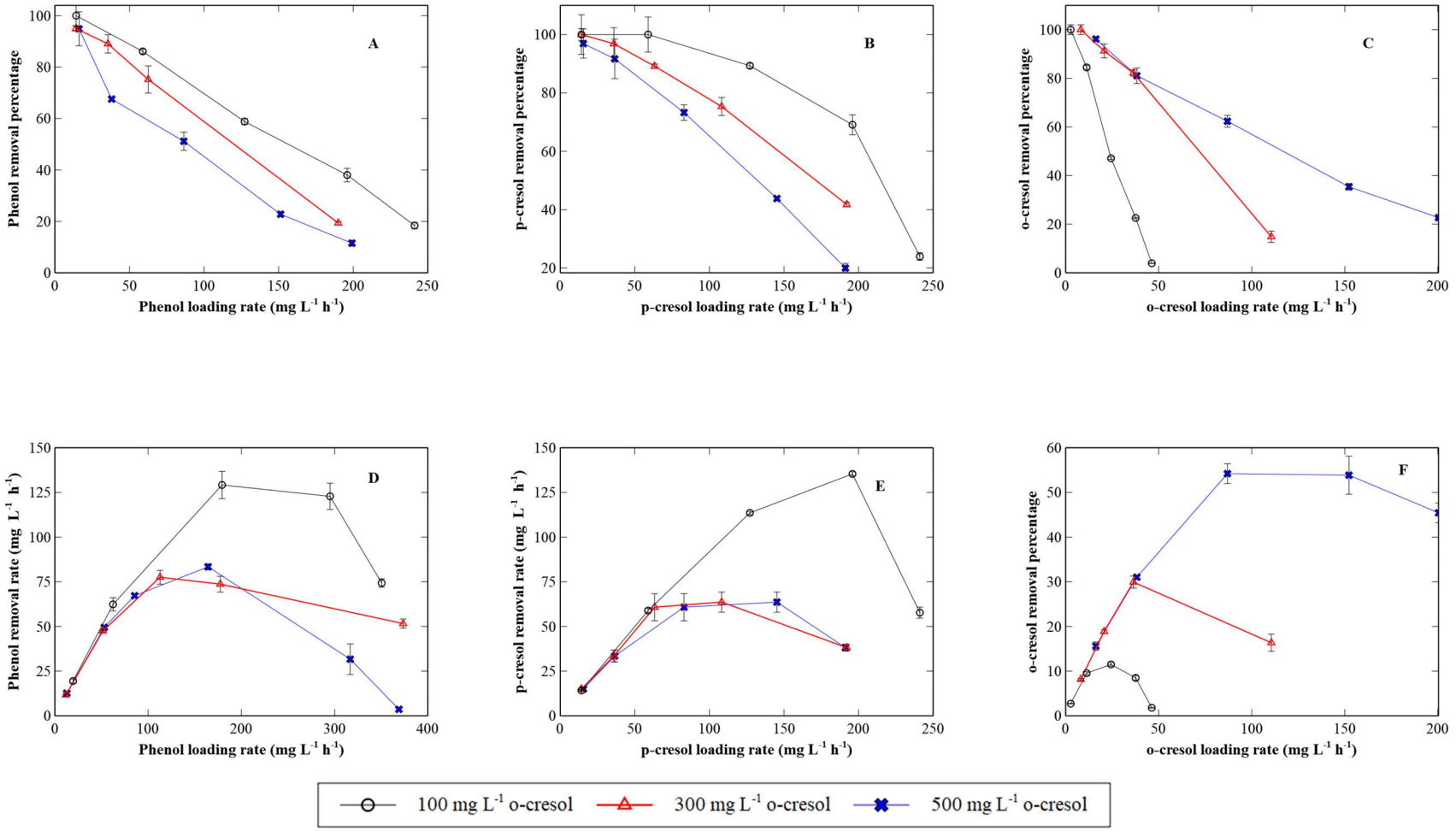

Figure 5.29 Removal percentages and removal rates and of phenol, p-cresol and o-cresol as a function of their respective loading rates in the CPBB fed with 500 mg L^{-1} phenol and 500 mg L^{-1} p-cresol and various concentration of o-cresol in influent. Panel (A): phenol removal percentage vs. its loading rate; Panel (B): p-cresol removal percentage vs. its loading rate; Panel (C): o-cresol removal percentage vs. its loading rate; Panel (D): phenol removal rate vs. its loading rate; Panel (E): p-cresol removal rate vs. its loading rate; Panel (F): o-cresol removal rate vs. its loading rate. Each point represents the average value of the data obtained after the establishment of steady states. Error bars represent standard deviation and may not be visible in some cases.

5.7.1 Toxicity Assessment for Ternary Biodegradation of Phenol, p-cresol, and o-cresol

The toxicity of influents with different composition of phenols and treated effluent samples were compared to examine the efficiency of CPBB in reducing the toxicity under ternary-substrate biodegradation. Similar to the previous case, the treated effluent samples had been collected for 3 conditions: 1) – CPBB was operating under phenol maximum removal rate; 2) – CPBB was operating under p-cresol maximum removal rate; 3) - CPBB was operating under o-cresol maximum removal rate. The results are also presented in three parts that correspond to the biodegradation sections.

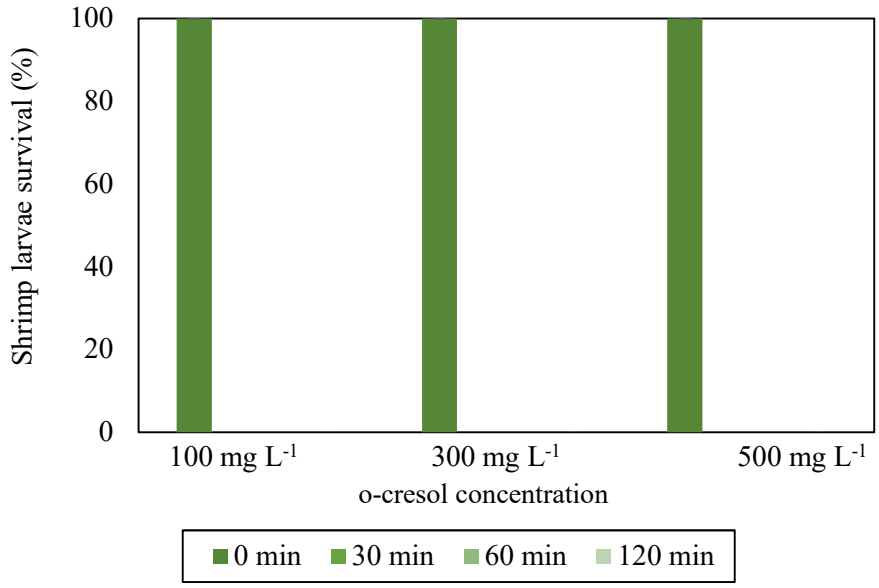

Figure 5.30 Toxicity results for influent containing 500 mg L^{-1} phenol, 100 mg L^{-1} p-cresol and various concentration of o-cresol.

Figure 5.30 presents the toxicity test results for influent containing 500 mg L^{-1} phenol, 100 mg L^{-1} p-cresol and various concentration of o-cresol (100, 300, and 500 mg L^{-1}). The toxicity of influents with three substrates of different compositions showed high toxicity. All shrimp larvae

died within 30 min exposure to influent samples. Further increase of p-cresol concentration would cause increased toxicity, which would have the identical result as the one presented here.

Figure 5.31 represents the toxicity results for the effluent obtained during the operation of CPBB with influent containing 500 mg L^{-1} phenol, 100 mg L^{-1} p-cresol and various concentration of o-cresol (100, 300, and 500 mg L^{-1}). Panels A, B, and C showed the results under maximum removal rate of phenol, p-cresol, and o-cresol, respectively. It can be observed that an increase of o-cresol in influent led to the increased toxicity of effluent samples under the maximum removal rate of the same substrate. For example, after 120 min exposure, shrimp larvae survival percentages under phenol maximum removal rates were 36.4% and 0% when o-cresol concentrations in the influent were 100 and 500 mg L^{-1}, respectively. Under p-cresol maximum removal rate, shrimp larvae survival percentages after 60 min were 20.1 and 0% when o-cresol concentrations in the influent were 100 and 500 mg L^{-1}, indicating the increased toxicity of effluent. For toxicity under o-cresol maximum removal rate, an increase of o-cresol concentration resulted in higher toxicity. The residual concentration of phenol, p-cresol, and o-cresol in effluent was 144.3, 23.45, and 20.0 mg L^{-1}, respectively when o-cresol initial concentration was 100 mg L^{-1}. The increased o-cresol initial concentration to 300 mg L^{-1} resulted in the residual concentration being 159.3, 0, and 76.9 mg L^{-1} for phenol, p-cresol, and o-cresol, respectively. The overall increased residual concentration contributed to the higher toxicity. But as indicated in the Figure 5.31, the performance of CPBB deteriorated with high concentrations of phenols.

A

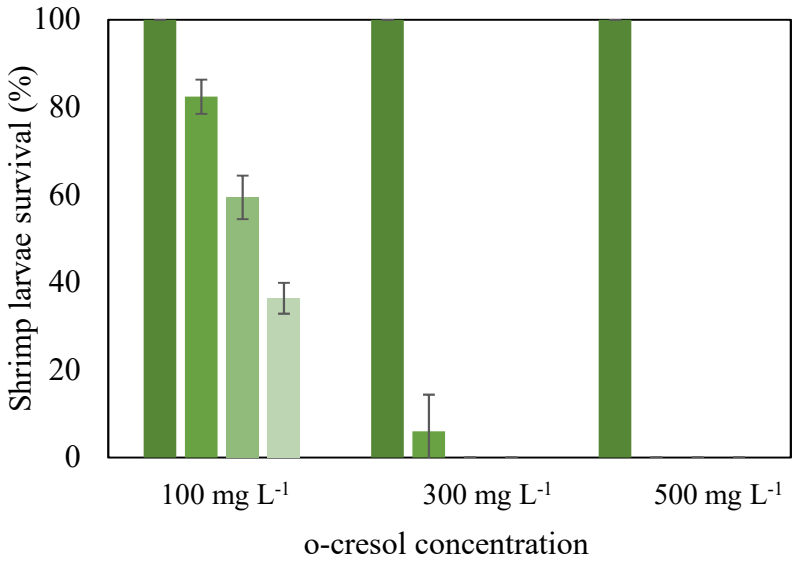
100
80
60
40
20
0
Shrimp larvae survival (%)
100 mg L-1
300 mg L-1
500 mg L-1
o-cresol concentration

B

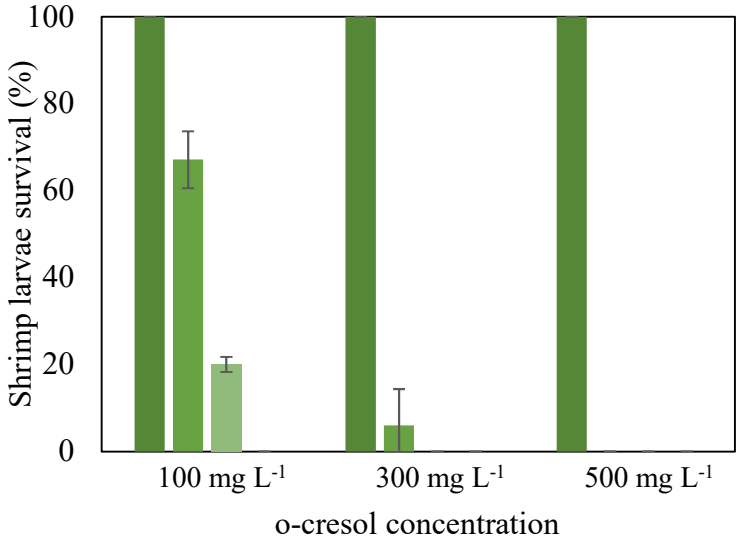
100
80
60
40
20
0
Shrimp larvae survival (%)
100 mg L-1
300 mg L-1
500 mg L-1
o-cresol concentration

C

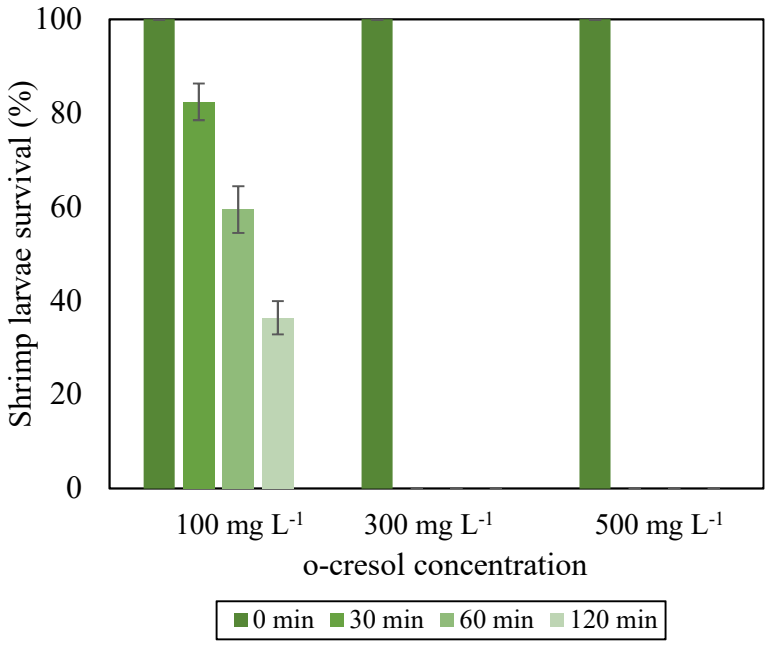

Figure 5.31 Toxicity of effluent samples when 500 mg L^{-1} phenol and 100 mg L^{-1} p-cresol was in influent. Panel (A): under phenol maximum removal rate; Panel (B): under p-cresol maximum removal rate; Panel (C): under o-cresol maximum removal rate. Error bars represent standard deviation and may not be visible in some cases. B in the bracket indicates best performance (under maximum removal rate) for the compound.

Figure 5.32 demonstrated the toxicity results when phenol and p-cresol concentrations in the influent were 500 and 300 mg L^{-1}, respectively and o-cresol concentration was in the range 100-500 mg L^{-1}. Similar to the previous set of experiment, when the o-cresol concentration was further increased to 500 mg L^{-1} in influent, effluent toxicity was also drastically increased. The observed pattern was that the higher was the o-cresol concentration, regardless which compound was under maximum removal rate, the higher was the toxicity. The overall residual concentration of phenols contributed to this increased toxicity (Table 5.8).

A

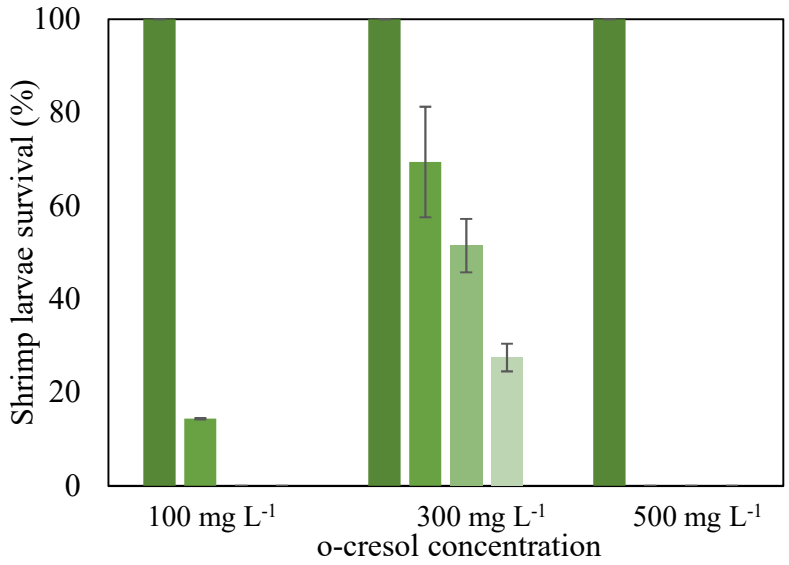
100
80
60
40
20
0
Shrimp larvae survival (%)
100 mg L-1
300 mg L-1
500 mg L-1
o-cresol concentration

B

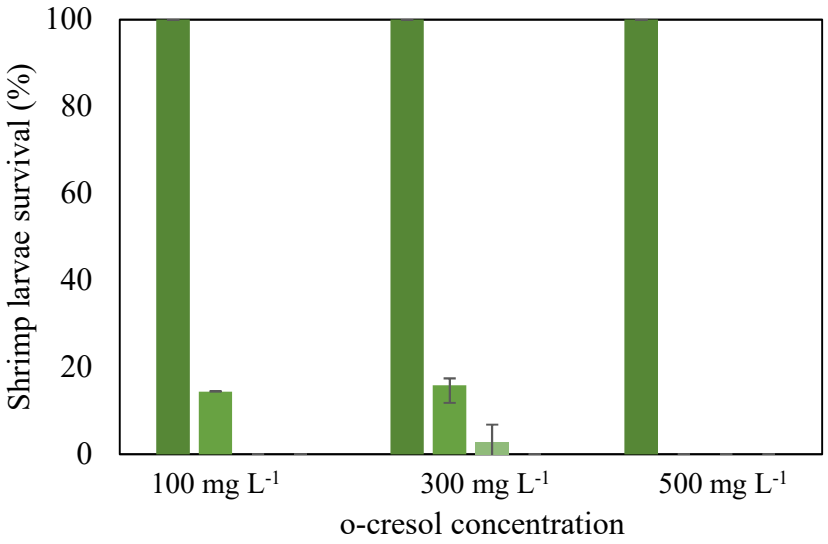
100
80
60
40
20
0
Shrimp larvae survival (%)
100 mg L-1
300 mg L-1
500 mg L-1
o-cresol concentration

C

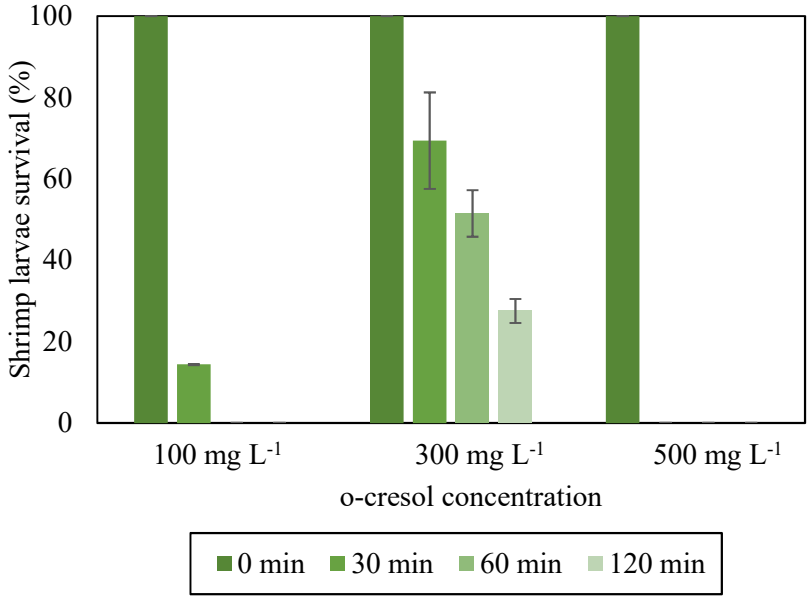

Figure 5.32 Toxicity of effluent samples when 500 mg L^{-1} phenol and 300 mg L^{-1} p-cresol was in influent. Panel (A): under phenol maximum removal rate; Panel (B): under p-cresol maximum removal rate; Panel (C): under o-cresol maximum removal rate. Error bars represent standard deviation and may not be visible in some cases. B in the bracket indicates best performance (under maximum removal rate) for the compound.

Figure 5.33 showed the toxicity results when both phenol and p-cresol influent concentration was set to 500 mg L^{-1} in influent and o-cresol concentration in influent was increased from 100 to 500 mg L^{-1}. It can be demonstrated that generally, the higher the o-cresol concentration in influent, the higher the toxicity. For example, for effluent samples taken under the o-cresol maximum removal rate, after 60 min exposure, the shrimp larvae survival percentage was 22.0% and 11.4% when the o-cresol influent concentration was 100 and 300 mg L^{-1}, respectively. However, CPBB also showed a limited capacity to degrade high concentration of phenols under ternary biodegradation

due to the fact that all shrimp larvae died after 120 min exposure, regardless the influent concentration in this case.

Similar to binary biodegradation in CPBB, if the overall goal of treatment of phenols is to reduce the total amount of compounds in influent, then CPBB should be operated under the maximum removal rate. However, if the goal is to reduce toxicity as much as possible, the bioreactor should be maintained at a low flow rate, which would yield a lower residual concentration in the effluent, therefore, reduce the overall toxicity.

A

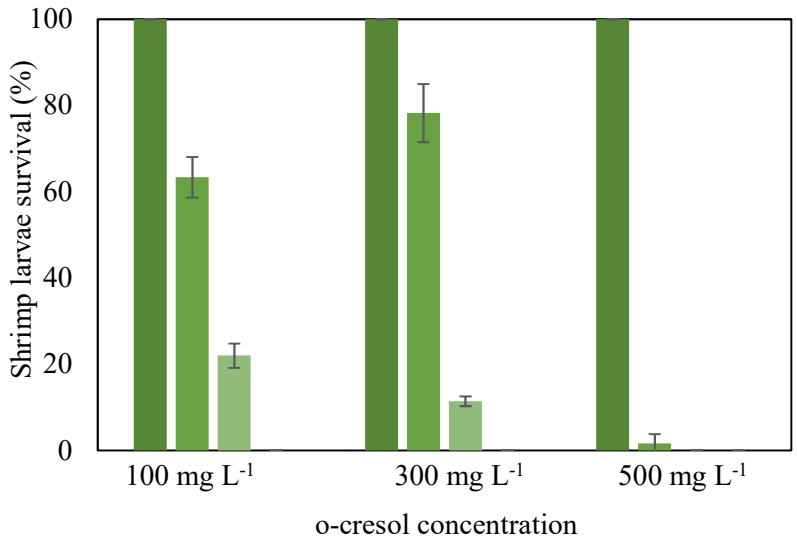

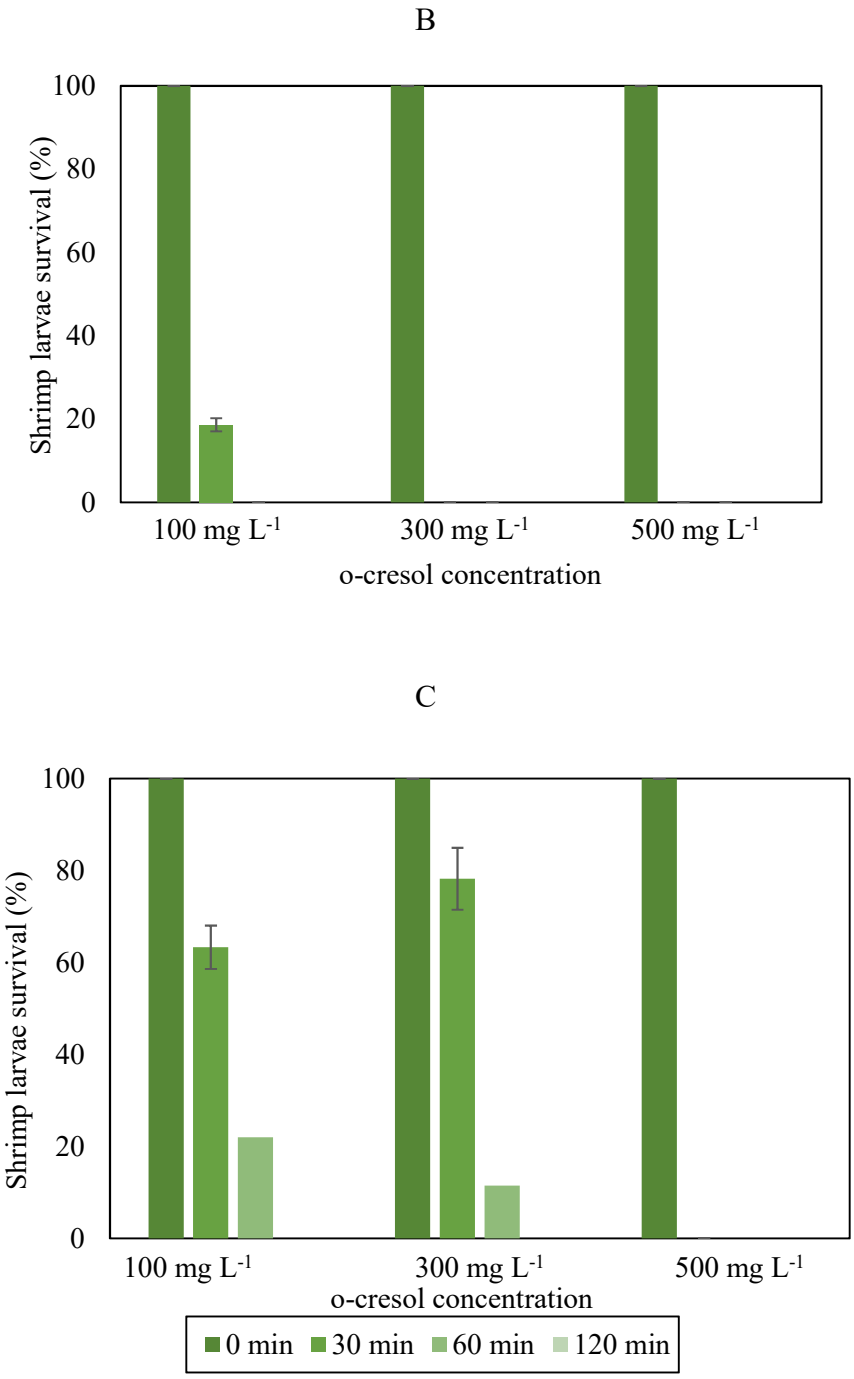

Figure 5.33 Toxicity of effluent samples when 500 mg L^{-1} phenol and 500 mg L^{-1} p-cresol was in influent. Panel (A): under phenol maximum removal rate; Panel (B): under p-cresol maximum removal rate; Panel (C): under o-cresol maximum removal rate. Error bars represent standard deviation and may not be visible in some cases. B in the bracket indicates best performance (under maximum removal rate) for the compound.

6 CONCLUSIONS

This study evaluated the biodegradation of phenolic compounds including phenol, p-cresol, and o-cresol in batch system and in continuous circulating packed-bad bioreactors and assessed the potential for application CPBBs to treat petroleum-originated and other wastewaters in the future and to take the intrinsic advantage of CPBB to increase the efficiency and feasibility for the treatment of these contaminated waters. To conclude the thesis, this chapter presents a summary of the findings in the order that corresponds the objectives of this research.

The first objective was to assess the biodegradation of phenols (mono-, binary-, and ternary-substrates) in batch system at varying initial substrate(s) concentration and various temperatures for gaining a better understanding of the effect of these parameters on the biodegradation process, as well as interaction of these compounds during their co-biodegradation. For mono-substrate system, increase in initial concentration from 100 to 500 mg L^{-1} had a positive effect on biodegradation rate of both o-cresol and p-cresol with the trend of this effect being linear. Biodegradation rate of p-cresol was slightly higher than that of o-cresol under the same initial concentration. Increase of temperature in the range 10 to 35 °C enhanced the biodegradation rate of p-cresol. By contrast, the highest biodegradation rate of o-cresol occurred at 25 °C. In addition, the bacterial culture used in this study was more efficient in degradation of p-cresol as shown by statistical analysis. During the co-biodegradation in binary mixture, addition of phenol increased the biodegradation rate of p-cresol when the initial concentration of p-cresol was in the range of 100 to 300 mg L^{-1}but did not increase o-cresol biodegradation rate markedly. The presence of o-cresol did not have a significant effect on phenol biodegradation rate when compared to p-cresol,

as confirmed by statistical analysis. For ternary-substrate co-biodegradation, using the generated experimental data three second order polynomial models were developed to describe biodegradation rates of phenol, p-cresol and o-cresol as determined under various compositions. It was shown that increase in p-cresol and o-cresol initial concentrations positively impacted the biodegradation rate of all three phenols but their interaction appeared to negatively impact the biodegradation rate (i.e. negative coefficient for interaction term in the polynomial model).

The second objective was to evaluate the performance of continuous flow CPBBs in treatment of phenolic compounds by investigating the effects of loading rate of phenols on their residual concentration, removal percentage, and removal rate through varying influent substrate(s) concentrations and influent flow rates. Experiments were conducted with mono-, binary-, and ternary-substrate systems. Regardless of tested phenol compound, its initial concentration or composition of influent, an increase of loading rate of phenolic compounds increased its residual concentration and decreased its removal percentage. Removal rate, however increased, reached maximum value, then started to decrease as a result of increase in loading rate. None of the phenolic compounds at evaluated concentrations (100 – 500 mg L^{-1}) imposed inhibitory effect microbial activity and biodegradation process. For both p-cresol and o-cresol at high loading rates (> 200 mg L^{-1} h^{-1}), higher influent concentrations led to higher removal rates. At lower loading rates the removal rates of three phenolic compounds were close but higher removal rates were obtained for phenol and p-cresol at higher loading rates when compare to o-cresol. During the biodegradation of individual phenols (100 – 500 mg L^{-1} initial concentration), the maximum removal rates for phenol, p-cresol, and o-cresol were 82.6, 107.2, and 73.8 mg L^{-1} h^{-1} at the loading rates of 104.7 (residence time: 4.7 h), 183.9 (residence time: 2.8 h), and 163.9 mg L^{-1} h^{-1} (residence

time: 1.8 h), respectively. The maximum removal rates of phenol and p-cresol during binary-substrate biodegradation were 89.2 and 78.4 mg L^{-1} h^{-1} at their respective loading rates of 137.9 and 123.9 mg L^{-1} h^{-1}, while the maximum removal rates of phenol and o-cresol during binary-substrate biodegradation were 119.9 and 70.3 mg L^{-1} h^{-1} at the respective loading rates of 209.8 and 112.9 mg L^{-1} h^{-1}. The presence of o-cresol had negative impact on phenol removal rate, while p-cresol did not show the same effect during binary-substrate biodegradation. When all three substrates were present in influent, the maximum removal rates of phenol, p-cresol, and o-cresol were 129.2, 135.3, and 108.0 mg L^{-1} h^{-1} at loading rates of 179.3, 195.9, and 165.7 mg L^{-1} h^{-1}. Consistent with the results of batch system p-cresol was the preferred substrate, followed by phenol and o-cresol.

The third objective in this research was to analyze toxicity of effluents obtained under various operating conditions and compare these with the toxicity of the respective influent to evaluate the effect of treatment in CPBB on the level of toxicity. For the influents, p-cresol was the most toxic substrate, followed by o-cresol and then phenol when concentration was 100 mg L^{-1}. Increase of concentration to higher or equivalent to 300 mg L^{-1}, on the other hand, indicated o-cresol as the most toxic, followed by p-cresol and then phenol. The presence of two or more phenolic compounds led to higher toxicity. The combination of phenol and o-cresol was more toxic than phenol and p-cresol. After biodegradation in CPBB, toxicity, regardless of substrate combination, was reduced, although the extent varied depending on the composition of influent. The higher the substrate concentration in influent, the more toxic the effluent. It was also shown that during binary substrate biodegradation CPBB reduced the toxicity more under phenol maximum removal rate compared to that under p-cresol maximum removal rate. The toxicity reduction efficiency for

phenol and o-cresol binary-substrate system varied depending on o-cresol concentration. The capability of CPBB to reduce the overall toxicity of influent with three phenolic compounds was limited when it was operated under maximum removal rate of any of three phenolic compounds. If the goal is to reduce toxicity as much as possible, the bioreactor should be maintained at low flow rate to achieve higher retention time.

As discussed in the last chapter, the batch system and CPBBs managed to remove phenolic mixture at a high rate. CPBBs were also used for removal of naphthenic acids (both linear and cyclic) and benzoquinone in previous studies (D'Souza, 2012; Kumar, 2010; Huang, 2011). The continuous system managed to achieve the biodegradation rate up to 401.1, 209.0, and 246 mg L^{-1} h^{-1} for octanoic acid, trans-4MCHCA, and 1,4 – benzoquinone, respectively (D'Souza, 2012; Kumar, 2010; Huang, 2011). The results are comparable to this study. CPBBs are versatile to multiple groups of organic contaminants. Therefore, it is promising to use this bioreactor for petroleum wastewater treatment. The obtained results indicated that *P. putida* has the potential to be employed for removal of phenolic mixtures with naphthenic acids even under highly toxic environment. Compared to other systems, CPBBs achieved a high biodegradation rate of overall phenols, which proved the efficiency. We also assessed the toxicity of effluent samples from CPBBs under selected conditions. The resulted make us believe CPBBs could be used in combination with other systems for achieving a lower residual concentration in the effluent samples under maximum removal rate. Else it should be operated under low flow rate. However, it is important to note that our current understating of CPBBs are mostly based on synthetic wastewater. The presence of heavy metals or PAHs might have a negative impact on the efficiency of organic contaminants in CPBBs. It is critical to understand these influences. In the future,

petroleum wastewater collected from real contaminated sites could be used as influent in order to thoroughly test the potential application of CPBBs for wastewater treatment. A more holistic investigation, such as scale-up and cost analysis, could be included in the future research.

Chemical pollution is one of the proposed planetary boundaries, yet the values of the threshold for chemical pollution is more difficult to determine than other boundaries (Rockstrom et al., 2009). Before a universal consensus was reached for the threshold of chemical pollution, it is imperative to control the contamination. Other than political, social, and economic strategies, the scientific strategy is a key to remediate existing contaminated sites and to prevent future pollution. The results of present of study revealed that the continuous flow circulating packed-bed bioreactors can be successfully used to treat waters contaminated with phenolic compounds that are produced in a variety of industrial processes. Thus, the results of present study not only contribute in development of control measures for a sever environmental problem, it could also assist the industry in achieving a sustainable approach as far as the use of water in the industrial processes is concerned through the effective treatment of generated wastewater and reuse of treated effluent. The realization of this technology in practical applications, however, required additional work with real wastewaters, modeling and CPBB scale-up studies and other efforts as listed in the recommendation section of this thesis.

7 RECOMMENDATIONS FOR FUTURE WORK

Given the scope of this study and restricted timeline, this study only focused on biodegradation of three phenolic compounds individually and in mixtures of different composition. The biodegradation of other phenolic compounds such as m-cresol or chlorophenol together with these three compounds in batch and continuous systems could be further studied. What's more, the effect of temperature that was only investigated for biodegradation of individual phenols could be evaluated on co-biodegradation of binary and ternary mixtures. Also, pH is another important variable that affect the biodegradation and its effect needs to be evaluated.

The use of bacterial cultures isolated from petroleum contaminated sites (especially with high concentration of phenols), as well as bacterial consortium adapted to biodegradation of phenolic compounds in the laboratory over an extended period could also contribute in enhancing the bioremediation of waters contaminated with phenols. In those cases, community analysis based on 16s rRNA sequence, especially in case of biofilms developed in the CPBB would be very helpful to gain better understanding of the dynamic of microbial community and get a better understanding of changes associated with phenols biodegradation.

Another important undertaking which is more relevant to engineering aspects of bioremediation process is the use of extensive experimental data generated in the batch system and to develop comprehensive kinetic expressions for biodegradation of phenol and cresols as individual or in a

mixture (i.e. multi-substrate kinetic expressions). The developed biokinetic expressions then can be used in mathematical modeling and simulation of biodegradation process in the CPBBs. The resulting information then will have beneficial applications in the design, scale up, and control of biodegradation process. In addition, the study of process parameters such as the circulation rates, air flow rates, pressure drop, liquid holdup, and initial residence time for early stages of microbial activities is recommended for future work.

Given that understanding of biodegradation of individual and mixture of phenolic compounds were the main focus of this study, the conducted toxicity evaluations were limited in scope and conducted under specified conditions. A more comprehensive toxicity study that give us a better understanding about the toxicity of effluents generated under various conditions, especially high removal percentages that do not necessary correspond to high removal rates, is recommended. This study that could be done by simulated effluents or those obtained during the operation of CPBB under various conditions should utilize other toxicity evaluation methods. Toxicity tests were performed in the presence of salt. Therefore, the results may not be relevant to freshwater organisms because of the potential interaction between the salt and the compounds and different environmental conditions (high Ph in saline water). In addition, these tests were acute tests. The long-term chronic effect may not be directly related to acute toxicity. Therefore, it is recommended in the future, a freshwater toxicity test should be performed and a long-term toxicity should be evaluated (Landis et al., 2010).

Finally, a feasibility assessment of bioremediation process in CPBBs including scaling up the bioreactor, and applying real industrial wastewater, as well as a detailed cost analysis and comparison with other existing treatment systems are also recommended.

REFERENCE LIST

Agency for Toxic Substances & Disease Registry (2015, Jan 21) Toxic substances portal – phenol. Retrieved from https://www.atsdr.cdc.gov/toxprofiles/tp.asp?id=148&tid=27. Accessed on Aug 29, 2017

Agency for Toxic Substances & Disease Registry (2015, Jan 21) Toxic substances portal – methylene chloride. Retrieved from https://www.atsdr.cdc.gov/toxprofiles/tp.asp?id=234&tid=42. Accessed on Aug 29, 2017

Agarry, S. E., Durojaiye, A. O., & Solomon, B. O. (2008). Microbial degradation of phenols: a review. *International Journal of Environment and Pollution*, *32*(1), 12-28.

Ahmaruzzaman, M., & Sharma, D. K. (2005). Adsorption of phenols from wastewater. *Journal of Colloid and Interface Science*, *287*(1), 14-24.

Aksu, Z., & Bülbül, G. (1998). Investigation of the combined effects of external mass transfer and biodegradation rates on phenol removal using immobilized *P. putida* in a packed-bed column reactor. *Enzyme and Microbial Technology*, *22*(5), 397-403.

Alexieva, Z., Gerginova, M., Manasiev, J., Zlateva, P., Shivarova, N., & Krastanov, A. (2008). Phenol and cresol mixture degradation by the yeast *Trichosporon cutaneum*. *Journal of Industrial Microbiology & Biotechnology*, *35*(11), 1297-1301.

Allen, E. W. (2008). Process water treatment in Canada's oil sands industry: I. Target pollutants and treatment objectives. *Journal of Environmental Engineering & Science*, 7(2), 123-138.

Alslaibi, T. M., Abustan, I., Ahmad, M. A., & Foul, A. A. (2013). A review: production of activated carbon from agricultural byproducts via conventional and microwave heating. *Journal of Chemical Technology and Biotechnology*, *88*(7), 1183-1190.

Atlas, R. M., & Bartha, R. (1998). *Microbial Ecology: Fundamentals and Applications*. Don Mills, ON: Addison-Wesley Publishing Company.

Bajaj, M., Gallert, C., & Winter, J. (2008). Biodegradation of high phenol containing synthetic wastewater by an aerobic fixed bed reactor. *Bioresource Technology*, *99*(17), 8376-8381.

Balasubramanian, A., & Venkatesan, S. (2012). Removal of phenolic compounds from aqueous solutions by emulsion liquid membrane containing ionic liquid [BMIM] + [PF 6] − in tributyl phosphate. *Desalination*, *289*, 27-34.

Bansal, V. K., Kumar, R., Prasad, R., & Prasad, S. (2008). Catalytic chemical and electrochemical wet oxidation of phenol using new copper (II) tetraazamacrocycle complexes under homogeneous conditions. *Journal of Molecular Catalysis A: Chemical*, *284*(1), 69-76.

Basha, K. M., Rajendran, A., & Thangavelu, V. (2010). Recent advances in the biodegradation of phenol: a review. *Asian Journal Experimental Biological Sciences*, *1*(2), 219-234.

McNeil, B., & Harvey, L. (Eds.). (2008). *Practical Fermentation Technology*. West Sussex, England: John Wiley & Sons.

Box, G. E., Hunter, J. S., & Hunter, W. G. (2005). *Statistics for Experimenters: Design, Innovation, and Discovery*. New York City, NY: Wiley-Interscience.

Brar, S. K., Verma, M., Surampalli, R. Y., Misra, K., Tyagi, R. D., Meunier, N., & Blais, J. F. (2006). Bioremediation of hazardous wastes—a review. *Practice Periodical of Hazardous, Toxic, and Radioactive Waste Management*, *10*(2), 59-72.

Brundtland, G. H. (1987). Report of world commission on environment and development: our common future. *World Commission for Environment and Development*. Retrieved from http://www.un-documents.net/our-common-future.pdf. Accessed on Aug 29, 2017

Busca, G., Berardinelli, S., Resini, C., & Arrighi, L. (2008). Technologies for the removal of phenol from fluid streams: a short review of recent developments. *Journal of Hazardous Materials*, *160*(2), 265-288.

Canadian Council of Ministers of the Environment. Canadian Water Quality Guidelines for the Protection of Aquatic Life – Phenols. Retrieved from: http://ceqg-rcqe.ccme.ca/download/en/204?redir=1517512522. Accessed on Feb 01, 2018.

Carberry, J. B., & Wik, J. (2001). Comparison of ex situ and in situ bioremediation of unsaturated soils contaminated by petroleum. *Journal of Environmental Science and Health, Part A*, 36(8), 1491-1503.

CBC news (2016, Nov 17). Husky's oil pipeline broke due to ground movement, report says. Retrieved from http://www.cbc.ca/news/canada/saskatchewan/husky-energy-north-saskatchewan-river-pipeline-break-1.3855871. Accessed on Aug 29, 2017

Cerniglia, C. E. (1984). Microbial metabolism of polycyclic aromatic hydrocarbons. *Advances in Applied Microbiology*, *30*, 31-71.

Chapelle, F. H. (1999). Bioremediation of petroleum hydrocarbon-contaminated ground water: the perspectives of history and hydrology. *Groundwater*, *37*(1), 122-132.

Chen, H. C., & Hu, Y. C. (2006). Bioreactors for tissue engineering. *Biotechnology Letters*, *28*(18), 1415-1423.

Christi, M. Y., 1989. *Airlift Bioreactors*. Essex, England: Elsevier.

Clark, W. C. (2007). Sustainability science: a room of its own. *Proceedings of the National Academy of Sciences*, 104(6), 1737.

Dąbrowski, A., Podkościelny, P., Hubicki, Z., & Barczak, M. (2005). Adsorption of phenolic compounds by activated carbon—a critical review. *Chemosphere*, *58*(8), 1049-1070.

Das, N., & Chandran, P. (2010). Microbial degradation of petroleum hydrocarbon contaminants: an overview. *Biotechnology Research International*, *2011*.

Das, S. (Ed.). (2014). *Microbial Biodegradation and Bioremediation*. Waltham, MA: Elsevier.

D'Souza, L., Sami, Y., Nemati, M., & Headley, J. (2014). Continuous co-biodegradation of linear and cyclic naphthenic acids in circulating packed-bed bioreactors. *Environmental Progress & Sustainable Energy*, *33*(3), 835-843.

Dutta, N. N., Borthakur, S., & Baruah, R. (1998). A novel process for recovery of phenol from alkaline wastewater: laboratory study and predesign cost estimate. *Water Environment Research*, *70*(1), 4-9.

El-Naas, M. H., Al-Zuhair, S., & Alhaija, M. A. (2010). Removal of phenol from petroleum refinery wastewater through adsorption on date-pit activated carbon. *Chemical Engineering Journal*, *162*(3), 997-1005.

El-Naas, M. H., Alhaija, M. A., & Al-Zuhair, S. (2017). Evaluation of an activated carbon packed bed for the adsorption of phenols from petroleum refinery wastewater. *Environmental Science and Pollution Research*, *24*(8), 7511-7520.

Erdogan, E. E., & Karaca, A. (2011). Bioremediation of crude oil polluted soils. *Asian Journal of Biotechnology*, *3*(3), 206-213.

Environment and Climate Change Canada (2016, May). Internationally classified substance grouping – cresol (phenol, methyl-) substances. Retrieved from https://www.ec.gc.ca/ese-ees/default.asp?lang=En&n=6ED0027C-1. Accessed on Aug 29, 2017

Fazal, S., Zhang, B., Zhong, Z., Gao, L., & Chen, X. (2015). Industrial wastewater treatment by using MBR (membrane bioreactor) review study. *Journal of Environmental Protection*, *6*(06), 584.

Flox, C., Arias, C., Brillas, E., Savall, A., & Groenen-Serrano, K. (2009). Electrochemical incineration of cresols: a comparative study between PbO_2 and boron-doped diamond anodes. *Chemosphere*, *74*(10), 1340-1347.

Fortuna, M. E., Simion, I. M., & Gavrilescu, M. (2011). Sustainability in environmental remediation. *Environmental Engineering & Management Journal*, *10*(12).

García, J. A. L., Grijalbo, L., Ramos, B., Fernández-Piñas, F., Rodea-Palomares, I., & Gutierrez-Mañero, F. J. (2013). Combined phytoremediation of metal-working fluids with maize plants inoculated with different microorganisms and toxicity assessment of the phytoremediated waste. *Chemosphere*, *90*(11), 2654-2661.

Gogoi, B. K., Dutta, N. N., Goswami, P., & Mohan, T. K. (2003). A case study of bioremediation of petroleum-hydrocarbon contaminated soil at a crude oil spill site. *Advances in Environmental Research*, *7*(4), 767-782.

Gonzalez, G., Herrera, M. G., Garcıa, M. T., & Pena, M. M. (2001). Biodegradation of phenol in a continuous process: comparative study of stirred tank and fluidized-bed bioreactors. *Bioresource Technology*, *76*(3), 245-251.

Gupta, V. K., Nayak, A., Agarwal, S., & Tyagi, I. (2014). Potential of activated carbon from waste rubber tire for the adsorption of phenolics: effect of pre-treatment conditions. *Journal of Colloid and Interface science*, *417*, 420-430.

Haddadi, A., & Shavandi, M. (2013). Biodegradation of phenol in hypersaline conditions by *Halomonas sp*. strain PH2-2 isolated from saline soil. *International Biodeterioration & Biodegradation*, *85*, 29-34.

Hank, D., Azi, Z., Hocine, S. A., Chaalal, O., & Hellal, A. (2014). Optimization of phenol adsorption onto bentonite by factorial design methodology. *Journal of Industrial and Engineering Chemistry*, *20*(4), 2256-2263.

Harwood, C. S., & Parales, R. E. (1996). The β-ketoadipate pathway and the biology of self-identity. *Annual Reviews in Microbiology*, *50*(1), 553-590.

Head, I. M., Singleton, I., & Milner, M. G. (Eds.). (2003). *Bioremediation: a Critical Review*. Summerville, SC: Horizon Scientific.

Hill, G. A., & Robinson, C. W. (1975). Substrate inhibition kinetics: phenol degradation by *Pseudomonas putida*. *Biotechnology and Bioengineering*, *17*(11), 1599-1615.

Hopper, D. J., & Taylor, D. G. (1977). The purification and properties of p-cresol-(acceptor) oxidoreductase (hydroxylating), a flavocytochrome from *Pseudomonas putida*. *Biochemical Journal*, *167*(1), 155-162.

Hoque, A., & Clarke, A. (2013). Greening of industries in Bangladesh: pollution prevention practices. *Journal of Cleaner Production*, *51*, 47-56.

Huang, L. Y. (2011). Bioremediation of naphthenic acids in a circulating packed bed bioreactor. M.Sc. Thesis, Univ. of Saskatchewan, Saskatoon, Canada.

Huang, J., Nemati, M., Hill, G., & Headley, J. (2012). Batch and continuous biodegradation of three model naphthenic acids in a circulating packed-bed bioreactor. *Journal of Hazardous Materials*, *201*, 132-140.

Jemaat, Z., Suárez-Ojeda, M. E., Pérez, J., & Carrera, J. (2014). Partial nitritation and o-cresol removal with aerobic granular biomass in a continuous airlift reactor. *Water Research*, *48*, 354-362.

Jemaat, Z., Suárez-Ojeda, M. E., Pérez, J., & Carrera, J. (2014). Sequentially alternating pollutant scenarios of phenolic compounds in a continuous aerobic granular sludge reactor performing simultaneous partial nitritation and o-cresol biodegradation. *Bioresource Technology*, *161*, 354-361.

Jernberg, C., & Jansson, J. K. (2002). Impact of 4-chlorophenol contamination and/or inoculation with the 4-chlorophenol-degrading strain, *Arthrobacter chlorophenolicus* A6L, on soil bacterial community structure. *FEMS Microbiology Ecology*, *42*(3), 387-397.

Jiang, L., Ruan, Q., Li, R., & Li, T. (2013). Biodegradation of phenol by using free and immobilized cells of *Acinetobacter* sp. BS8Y. *Journal of Basic Microbiology*, *53*(3), 224-230.

Johnson, P. C., Johnson, R. L., Bruce, C. L., & Leeson, A. (2001). Advances in in-situ air sparging/biosparging. *Bioremediation Journal*, *5*(4), 251-266.

Jordan, W., van Barneveld, H., Gerlich, O., Kleine-Boymann, M., & Ullrich, J. (1985). *Ullmann's Encyclopedia of Industrial Chemistry*. Weiheim, Germany: VCH.

Kapałka, A., Fóti, G., & Comninellis, C. (2009). The importance of electrode material in environmental electrochemistry: formation and reactivity of free hydroxyl radicals on boron-doped diamond electrodes. *Electrochimica Acta*, *54*(7), 2018-2023.

Karigar, C. S., & Rao, S. S. (2011). Role of microbial enzymes in the bioremediation of pollutants: a review. *Enzyme Research*, *2011*.

Kaushik, N., Biswas, S., & Singh, J. (2014). Biocatalysis and biotransformation processes–an insight. *The Scitech Journal*, *8*, 15-22.

Kavitha, V., & Palanivelu, K. (2005). Destruction of cresols by Fenton oxidation process. *Water Research*, *39*(13), 3062-3072.

Kiezyk, P. R., & Mackay, D. (1971). Waste water treatment by solvent extraction. *The Canadian Journal of Chemical Engineering*, *49*(6), 747-752.

Klamklang, S. (2007). Restaurant wastewater treatment by electrochemical oxidation in continuous process. Ph.D Thesis, Chulalongkorn University, Bangkok, Thailand.

Klinkow, N., Oleksy-Frenzel, J., & Jekel, M. (1998). Toxicity-directed fractionation of organic compounds in tannery wastewater with regard to their molecular weight and polarity. *Water Research*, *32*(9), 2583-2592.

Komiyama, H., & Takeuchi, K. (2006). Sustainability science: building a new discipline. *Sustainability Science*, 1-6

Koukkou, A. I. (Ed.). (2011). *Microbial Bioremediation of non-Metals: Current Research*. Summerville, SC: Horizon Scientific.

Krastanov, A., Alexieva, Z., & Yemendzhiev, H. (2013). Microbial degradation of phenol and phenolic derivatives. *Engineering in Life Sciences*, *13*(1), 76-87.

Krishna, I. M., & Manickam, V. (2017). *Environmental Management: Science and Engineering for Industry*. Oxford, England: Butterworth-Heinemann.

Kumar, P., Nikakhtari, H., Nemati, M., Hill, G., & Headley, J. (2010). Oxidation of phenol in a bioremediation medium using chlorine dioxide. *Journal of Chemical Technology and Biotechnology*, *85*(5), 720-725.

Landis, W., Sofield, R., Yu, M. H., Landis, W. G., & Sofield, R. M. (2010). *Introduction to environmental toxicology: Molecular substructures to ecological landscapes*. Boca Raton, FL: CRC Press.

Li, P., Sun, T., Stagnitti, F., Zhang, C., Zhang, H., Xiong, X., & Allinson, M. (2002). Field-scale bioremediation of soil contaminated with crude oil. *Environmental Engineering Science*, *19*(5), 277-289.

Li, Z., Wu, M., Jiao, Z., Bao, B., & Lu, S. (2004). Extraction of phenol from wastewater by N-octanoylpyrrolidine. *Journal of Hazardous Materials*, *114*(1), 111-114.

Lin, S. H., & Juang, R. S. (2009). Adsorption of phenol and its derivatives from water using synthetic resins and low-cost natural adsorbents: a review. *Journal of Environmental Management*, *90*(3), 1336-1349.

Liu, J., Xie, J., Ren, Z., & Zhang, W. (2013). Solvent extraction of phenol with cumene from wastewater. *Desalination and Water Treatment*, *51*(19-21), 3826-3831.

Loh, K. C., & Liu, J. (2001). External loop inversed fluidized bed airlift bioreactor (EIFBAB) for treating high strength phenolic wastewater. *Chemical Engineering Science*, *56*(21), 6171-6176.

Lynch, J. M., & Moffat, A. J. (2005). Bioremediation–prospects for the future application of innovative applied biological research. *Annals of Applied Biology*, *146*(2), 217-221.

Mahesh, S., Prasad, B., Mall, I. D., & Mishra, I. M. (2006). Electrochemical degradation of pulp and paper mill wastewater. Part 2. Characterization and analysis of sludge. *Industrial & Engineering Chemistry Research*, *45*(16), 5766-5774.

Marrot, B., Barrios-Martinez, A., Moulin, P., & Roche, N. (2006). Biodegradation of high phenol concentration by activated sludge in an immersed membrane bioreactor. *Biochemical Engineering Journal*, 30(2), 174-183.

Masunaga, S., Urushigawa, Y., & Yonezawa, Y. (1986). Biodegradation pathway of o-cresol by heterogeneous culture phenol acclimated activated sludge. *Water Research*, *20*(4), 477-484.

Medel, A., Bustos, E., Esquivel, K., Godínez, L. A., & Meas, Y. (2012). Electrochemical incineration of phenolic compounds from the hydrocarbon industry using boron-doped diamond electrodes. *International Journal of Photoenergy*, *2012*, 681875

Meng, A. X., Hill, G. A., & Dalai, A. K. (2002). Hydrodynamic characteristics in an external loop airlift bioreactor containing a spinning sparger and a packed bed. *Industrial & Engineering Chemistry Research*, *41*(9), 2124-2128.

Merchuk, J. C. (2003). Airlift bioreactors: review of recent advances. *The Canadian Journal of Chemical Engineering*, *81*(3-4), 324-337.

Mohee, R., & Mudhoo, A. (2012). *Bioremediation and Sustainability: Research and Applications*. Hoboken, NJ: John Wiley & Sons.

Moreno, L., Nemati, M., & Predicala, B. (2018). Biodegradation of phenol in batch and continuous flow microbial fuel cells with rod and granular graphite electrodes. *Environmental technology*, 39(2), 144-156.

Moss, B. (2008). The Water Framework Directive: total environment or political compromise? *Science of the Total Environment*, *400*(1), 32-41.

Mulligan, C. N., Fukue, M., & Sato, Y. (2009). *Sediments Contamination and Sustainable Remediation*. Boca Raton, FL: CRC Press.

Nakada, N., Tanishima, T., Shinohara, H., Kiri, K., & Takada, H. (2006). Pharmaceutical chemicals and endocrine disrupters in municipal wastewater in Tokyo and their removal during activated sludge treatment. *Water research*, 40(17), 3297-3303.

Nemati, M., & Webb, C. (1996). Effect of ferrous iron concentration on the catalytic activity of immobilized cells of *Thiobacillus ferrooxidans*. *Applied Microbiology and Biotechnology*, *46*(3), 250-255.

Nemati, M., & Webb, C. (2011). Immobilized Cell Bioreactors. *Comprehensive Biotechnology (2nd Ed.)*. Amsterdam, the Netherland: Elsevier

Olejniczak, J., Staniewski, J., & Szymanowski, J. (2005). Extraction of phenols and phenyl acetates with diethyl carbonate. *Analytica Chimica Acta*, *535*(1), 251-257.

Olmez-Hanci, T., & Arslan-Alaton, I. (2013). Comparison of sulfate and hydroxyl radical based advanced oxidation of phenol. *Chemical Engineering Journal*, *224*, 10-16.

Otero, M., Rozada, F., Calvo, L. F., Garcıa, A. I., & Moran, A. (2003). Elimination of organic water pollutants using adsorbents obtained from sewage sludge. *Dyes and Pigments*, 57(1), 55-65.

Paslawski, J. C., Headley, J. V., Hill, G. A., & Nemati, M. (2009). Biodegradation kinetics of trans-4-methyl-1-cyclohexane carboxylic acid. *Biodegradation*, 20(1), 125-133.

Palma, M. S. A., Paiva, J. L., Zilli, M., & Converti, A. (2007). Batch phenol removal from methyl isobutyl ketone by liquid–liquid extraction with chemical reaction. *Chemical Engineering and Processing: Process Intensification*, *46*(8), 764-768.

Pandey, J., Chauhan, A., & Jain, R. K. (2009). Integrative approaches for assessing the ecological sustainability of in situ bioremediation. *FEMS Microbiology Reviews*, *33*(2), 324-375.

Pilato, L. (Ed.). (2010). *Phenolic Resins: a Century of Progress*. New York City, NY: Springer.

Praveen, P., & Loh, K. C. (2012). Two-phase biodegradation of phenol in a hollow fiber membrane bioreactor. *Journal of Environmental Engineering*, *139*(5), 654-660.

Praveen, P., Nguyen, D. T. T., & Loh, K. C. (2015). Biodegradation of phenol from saline wastewater using forward osmotic hollow fiber membrane bioreactor coupled chemostat. *Biochemical Engineering Journal*, *94*, 125-133.

Puzyn, T., & Mostrag-Szlichtyng, A. (2012). *Organic Pollutants Ten Years after the Stockholm Convention-Environmental and Analytical Update*. Rijeka, Croatia: InTech.

Qiao, J. Q., Yuan, N., Tang, C. J., Yang, J., Zhou, J., Lian, H. Z., & Dong, L. (2012). Determination of catalytic oxidation products of phenol by RP-HPLC. *Research on Chemical Intermediates*, *38*(2), 549-558.

Rao, N. N., Singh, J. R., Misra, R., & Nandy, T. (2009). Liquid–liquid extraction of phenol from simulated sebacic acid wastewater. *Journal of Scientific & Industrial Research*, 68, 823-828.

Reis, M. T. A., de Freitas, O. M., Ismael, M. R. C., & Carvalho, J. M. (2007). Recovery of phenol from aqueous solutions using liquid membranes with Cyanex 923. *Journal of Membrane Science*, *305*(1), 313-324.

Richardson, C. J. (2008). *The Everglades Experiments*. New York City, NY: Springer.

Rittmann, B. E. (1994). *In situ Bioremediation*. Park Ridge, NJ: Taylor & Francis.

Rockström, J., Steffen, W., Noone, K., Persson, Å., Chapin III, F. S., Lambin, E. F., ... & Nykvist, B. (2009). A safe operating space for humanity. *nature*, 461(7263), 472.

Romeela, M., & Ackmez, M. (2012). Energy from biomass in Mauritius: overview of research and applications. *Waste to Energy*. London, England: Springer.

Rubin, H., Rubin, E., & Schüttrumpf, H. Modeling and implementation of sustainable remediation based on bioventing. *Bioremediation and Sustainability: Research and Applications*, 317-366.

Sabarunisha Begum, S., & Radha, K. V. (2014). Hydrodynamic behavior of inverse fluidized bed biofilm reactor for phenol biodegradation using *Pseudomonas fluorescens*. *Korean Journal of Chemical Engineering*, *31*, 436-445.

Saravanan, P., Pakshirajan, K., & Saha, P. (2008). Biodegradation of phenol and m-cresol in a batch and fed batch operated internal loop airlift bioreactor by indigenous mixed microbial culture predominantly *Pseudomonas sp*. *Bioresource Technology*, *99*(18), 8553-8558.

Sarkar, M., & Acharya, P. K. (2006). Use of fly ash for the removal of phenol and its analogues from contaminated water. *Waste Management*, *26*(6), 559-570.

Schmidt, K. R., Gaza, S., Voropaev, A., Ertl, S., & Tiehm, A. (2014). Aerobic biodegradation of trichloroethene without auxiliary substrates. *Water Research*, *59*, 112-118.

Schügerl, K., & Bellgardt, K. H. (Eds.). (2012). *Bioreaction Engineering: Modeling and Control*. Berlin, Germany: Springer.

Shuler, M. L., Kargi, F., & Kargi, F. (2002). *Bioprocess Engineering: Basic Concepts*. Upper Saddle River, NJ: Prentice Hall.

Sdiri, A., Higashi, T., Hatta, T., Jamoussi, F., & Tase, N. (2011). Evaluating the adsorptive capacity of montmorillonitic and calcareous clays on the removal of several heavy metals in aqueous systems. *Chemical Engineering Journal*, *172*(1), 37-46.

Şentürk, M., Gülçin, İ., Daştan, A., Küfrevioğlu, Ö. İ., & Supuran, C. T. (2009). Carbonic anhydrase inhibitors. Inhibition of human erythrocyte isozymes I and II with a series of antioxidant phenols. *Bioorganic & Medicinal Chemistry*, *17*(8), 3207-3211.

Singh, J., Kaushik, N., & Biswas, S. (2014). Bioreactors–technology & design analysis. *The Scitech Journal*, 28-36.

Singh, R., Paul, D., & Jain, R. K. (2006). Biofilms: implications in bioremediation. *Trends in Microbiology*, *14*(9), 389-397.

Stanier, R. Y., & Ornston, L. N. (1973). *Advances in Microbial Physiology*. London, England: Academic Press

Thomashow, M. (1996). *Ecological identity: Becoming a Reflective Environmentalist*. London, England: the MIT Press.

Tišler, T., & Zagorc-Končan, J. (1997). Comparative assessment of toxicity of phenol, formaldehyde, and industrial wastewater to aquatic organisms. *Water, Air, & Soil Pollution*, *97*(3), 315-322.

Toussaint, M. W., Shedd, T. R., van der Schalie, W. H., & Leather, G. R. (1995). A comparison of standard acute toxicity tests with rapid-screening toxicity tests. *Environmental Toxicology and Chemistry*, *14*(5), 907-915.

Trigo, A., Valencia, A., & Cases, I. (2008). Systemic approaches to biodegradation. *FEMS Microbiology Reviews*, *33*(1), 98-108.

Tyagi, M., da Fonseca, M. M. R., & de Carvalho, C. C. (2011). Bioaugmentation and biostimulation strategies to improve the effectiveness of bioremediation processes. *Biodegradation*, *22*(2), 231-241.

United States Environmental Protection Agency (2017, Aug 28). Primer for municipal wastewater treatment systems. Retrieved from https://www.epa.gov/npdes/municipal-wastewater Accessed on Aug 29, 2017

United States Environmental Protection Agency (2016). IRIS assessment – phenol. Retrieved from https://cfpub.epa.gov/ncea/iris2/chemicalLanding.cfm?substance_nmbr=88. Accessed on Aug 29, 2017

United States Environmental Protection Agency (1993, Mar 15). Reference dose (RfD): description and use in health risk assessments. Retrieved from https://www.epa.gov/iris/reference-dose-rfd-description-and-use-health-risk-assessments. Accessed on Aug 29, 2017

Verschueren, K. (2001). *Handbook of Environmental Data on Organic Chemicals: Vol. 1 (Ed. 4).* New York City, NY: John Wiley and Sons

Wang, X., Huang, S., Zhu, L., Tian, X., Li, S., & Tang, H. (2014). Correlation between the adsorption ability and reduction degree of graphene oxide and tuning of adsorption of phenolic compounds. *Carbon*, *69*, 101-112.

Webb, C., & Dervakos, G. A. (1996). *Studies in Viable Cell Immobilization*. New York City, NY: Academic Press.

World Energy Council (2017, Aug 28). World energy resources. Retrieved from https://www.worldenergy.org/wp-content/uploads/2017/03/WEResources_Oil_2016.pdf. Accessed on Aug 29, 2017

Yang, C., Qian, Y., Zhang, L., & Feng, J. (2006). Solvent extraction process development and on-site trial-plant for phenol removal from industrial coal-gasification wastewater. *Chemical Engineering Journal*, *117*(2), 179-185.

Yavuz, Y., Savaş Koparal, A., & Öğütveren, Ü. B. (2011). Electrochemical oxidation of Basic Blue 3 dye using a diamond anode: evaluation of colour, COD and toxicity removal. *Journal of Chemical Technology and Biotechnology*, *86*(2), 261-265.

Zhao, H., Xia, S., & Ma, P. (2005). Use of ionic liquids as 'green' solvents for extractions. *Journal of Chemical Technology and Biotechnology*, *80*(10), 1089-1096.

APPENDICES

Appendix A Conference Contribution

This research has been presented in the following two conferences:

1. 66th Canadian Chemical Engineering Conference.
2. 10th World Congress of Chemical Engineering.

Manuscripts of this study are also being prepared.

Appendix B Sample Calculations

Hydraulic residence time (HRT), loading rate, removal rate, and removal percentage of phenolic compounds, for CPBB were calculated using the following procedures:

Hydraulic residence time = working volume of CPBB / flow rate

For example, at a flow rate of 30 mL h^{-1} for CPBB, with a working volume of 450 mL, CPBB had a hydraulic residence time of 15 h.

Loading rate = substrate influent concentration / hydraulic residence time

For example, at a phenol influent concentration of 500 mg L^{-1} for CPBB, with a HRT of 15 h, CPBB had a phenol loading rate of 33.3 mg L^{-1} h^{-1}.

Removal rate = (influent concentration – residual concentration) / HRT

For example, at a phenol influent concentration of 500 mg L^{-1} and a residual phenol concentration of 54.3 mg L^{-1} for CPBB, with a HRT of 15 h, CPBB had a phenol removal rate of 29.7 mg L^{-1} h^{-1}.

Removal percentage = (influent concentration – residual concentration) / influent concentration * 100%

For example, at a phenol influent concentration of 500 mg L^{-1}, and a residual concentration of 54.3 mg L^{-1} for CPBB, CPBB had a removal percentage of 89.1%.

Appendix C HPLC Chromatogram

Figure C.1 shows the elution time of phenol, p-cresol, and o-cresol using HPLC. The elution time was 4.6, 6.8, and 7.2 minutes for phenol, p-cresol, and o-cresol, respectively in this chromatogram.

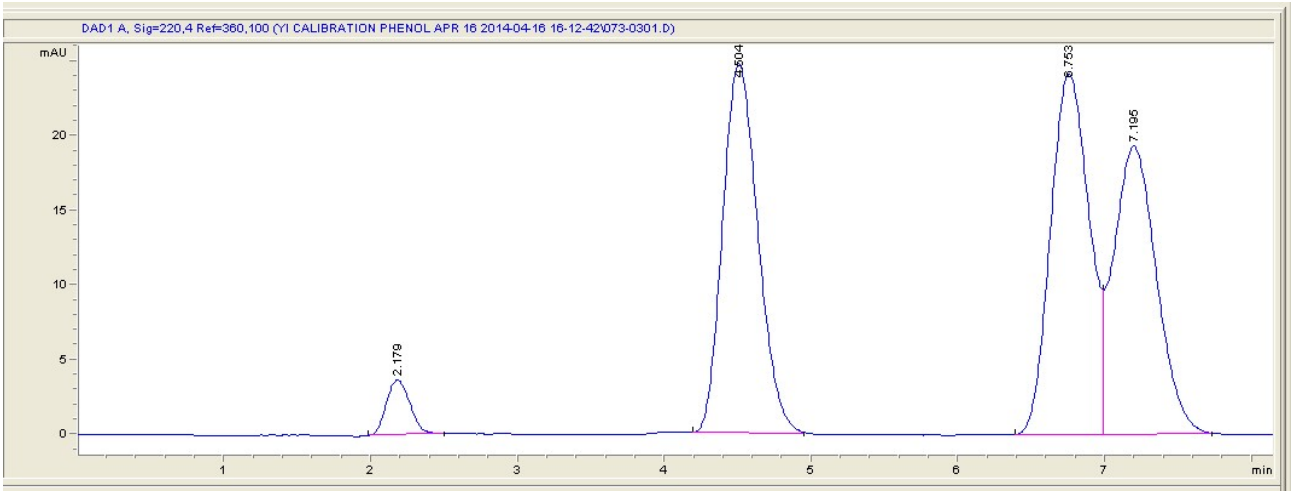

Figure C.1 The representative HPLC chromatogram of phenols.

Appendix D Calibration Curves and Experimental Data Uncertainties

D1 Biomass Calibration Curve

Optical Density (OD) of the samples was measured to monitor the growth of bacteria for batch experiment using spectrophotometer at a wavelength of 620 nm. Dry weight of the biomass for the culture was measured using one batch experiment with 500 mg L^{-1} phenol, 300 mg L^{-1} p-cresol, and 300 mg L^{-1} o-cresol at the end of exponential phase. A 90 mL sample was taken to determine the biomass concentration in terms of dry weight per volume and 10 mL sample was diluted 2, 4, 6, and 8 times to determine OD and their corresponding biomass concentration. The linear relationship between OD and biomass dry weight is shown in Figure D.1.

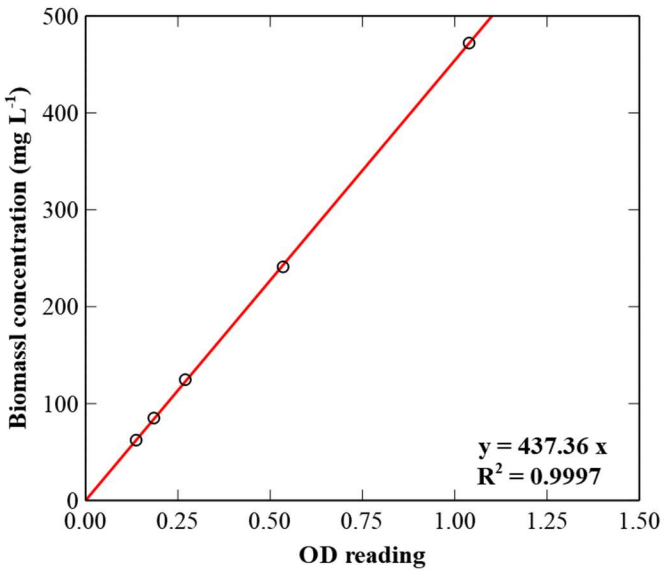

Figure D.12 Biomass calibration curve.

D2 Phenols Calibration Curve (Spectrophotometric method)

For concentration measurement of individual phenolic compound in batch and continuous system, spectrophotometer was used. For phenol, calibration curve was generated using 6 standard solutions (0, 10, 12.5, 25, 50, and 100 mg L^{-1}) in sterilized modified Mckinney's medium. The wavelength was set at 269 nm (Figure D.2).

For p-cresol, calibration curve was generated using 5 standard solutions (0, 25, 50, 75, and 100 mg L^{-1}) in sterilized modified Mckinney's medium. The wavelength was set at 277 nm (Figure D.3).

For p-cresol, calibration curve was generated using 5 standard solutions (0, 12.5, 25, 50, and 125 mg L^{-1}) in sterilized modified Mckinney's medium. The wavelength was set at 269 nm (Figure D.4).

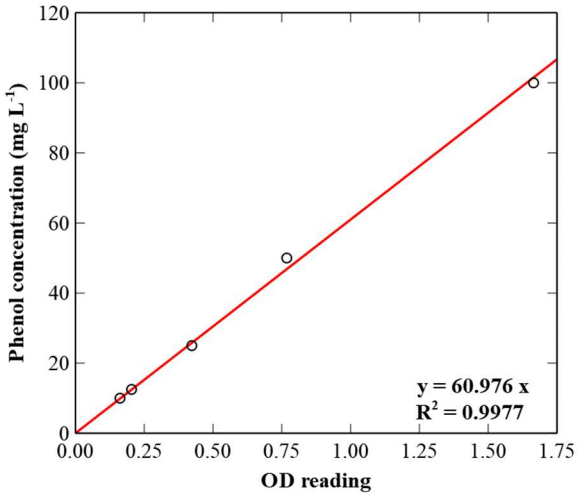

Figure D.3 Calibration curve developed for various phenol concentrations.

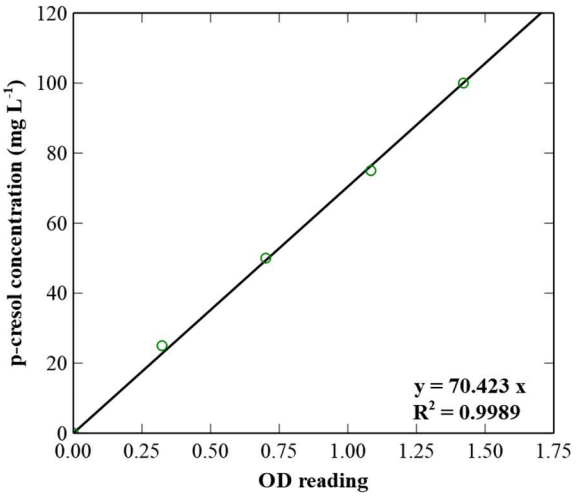

Figure D.4 Calibration curve developed for various p-cresol concentrations.

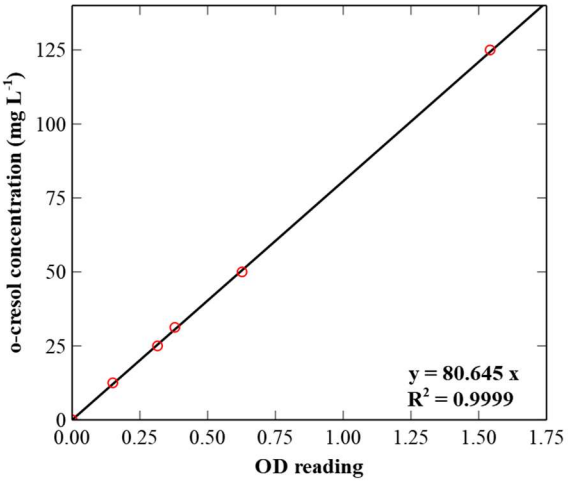

Figure D.5 Calibration curve developed for various o-cresol concentrations.

D3 HPLC Calibration Curves

The concentration measurement of phenolic compounds in mixture, HPLC was used. The calibration curves for phenol, p-cresol, and o-cresol were developed using 5 standard solutions (0, 12.5, 25, 50, and 125 mg L^{-1}) in sterilized Mckinney's medium (Figure D.5).

A

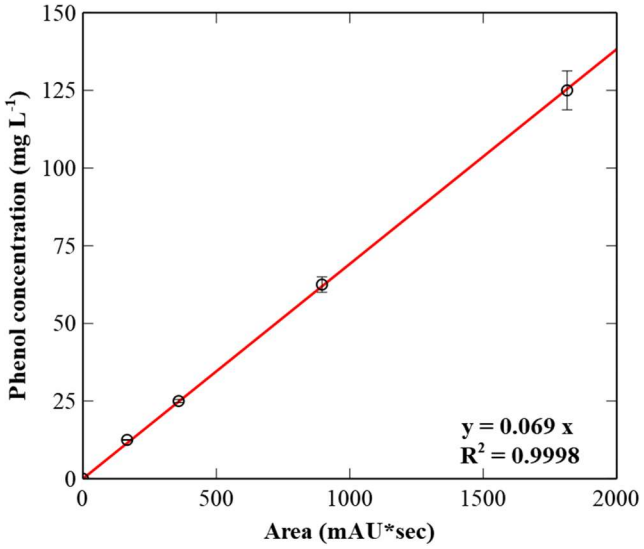

B

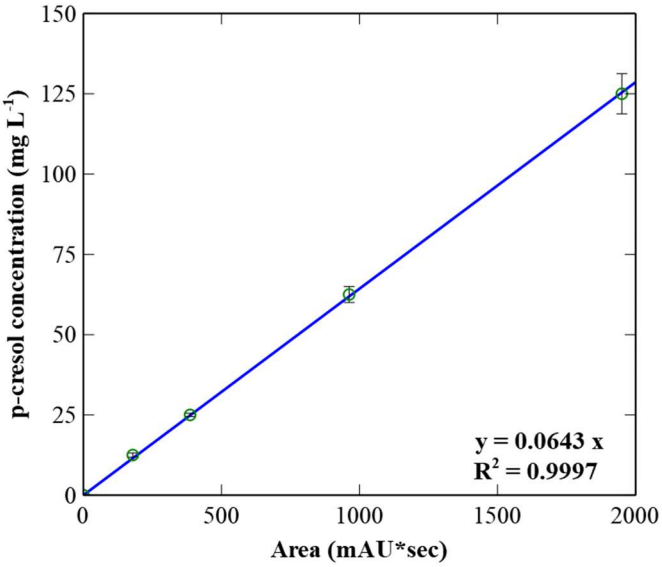

C

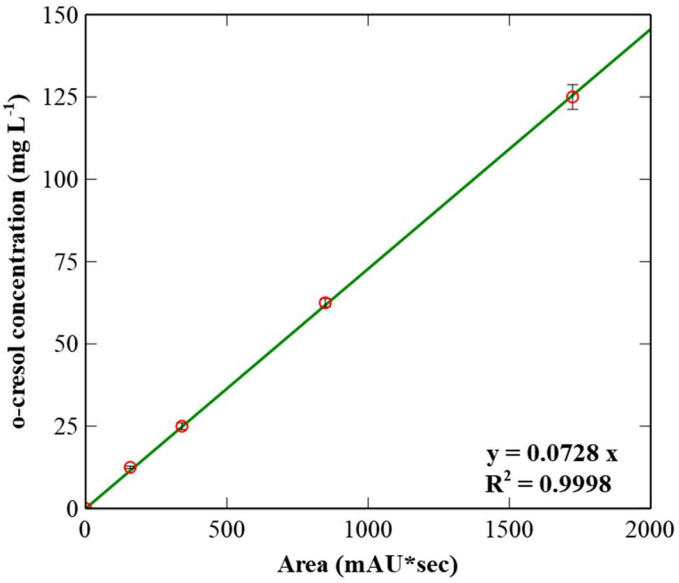

Figure D.5 HPLC calibration curve for phenol (A), p-cresol (B), and o-cresol (C)

D4 Control Experiments and Calculation of Data Uncertainty

As described in Methodology, control experiments were conducted in the batch system using McKinney's medium containing either 500 mg L^{-1} phenol, or p-cresol, or o-cresol (Figure D.6). The generated data clearly showed that the abiotic biodegradation in all cases was negligible and even after 350 h of experiments, the measured concentration was still very close to the initial concentration. Monitoring of OD (an indication of biomass concentration) revealed that the procedure followed was stringent enough to prevent microbial contamination.

A

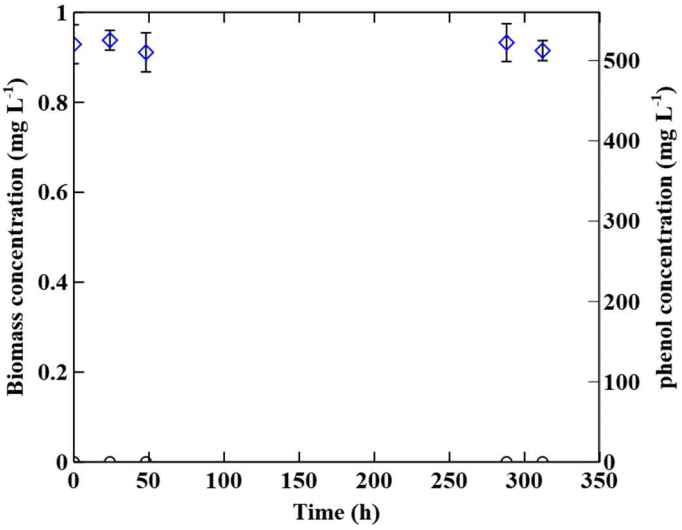

B

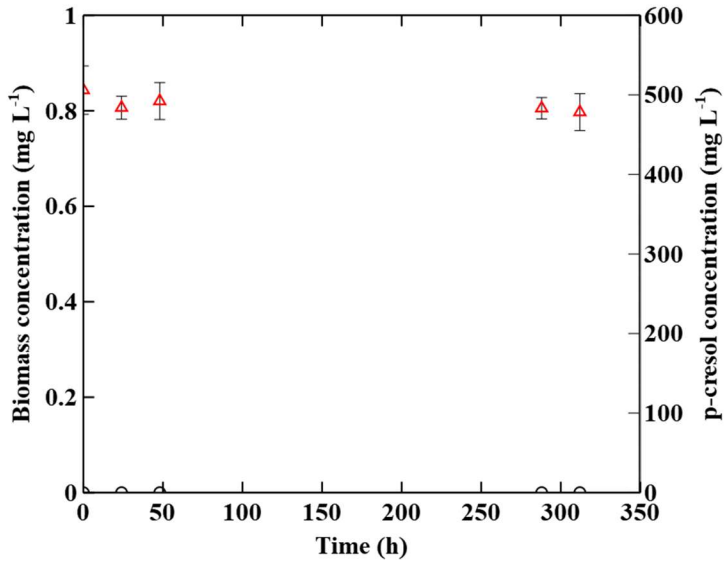

C

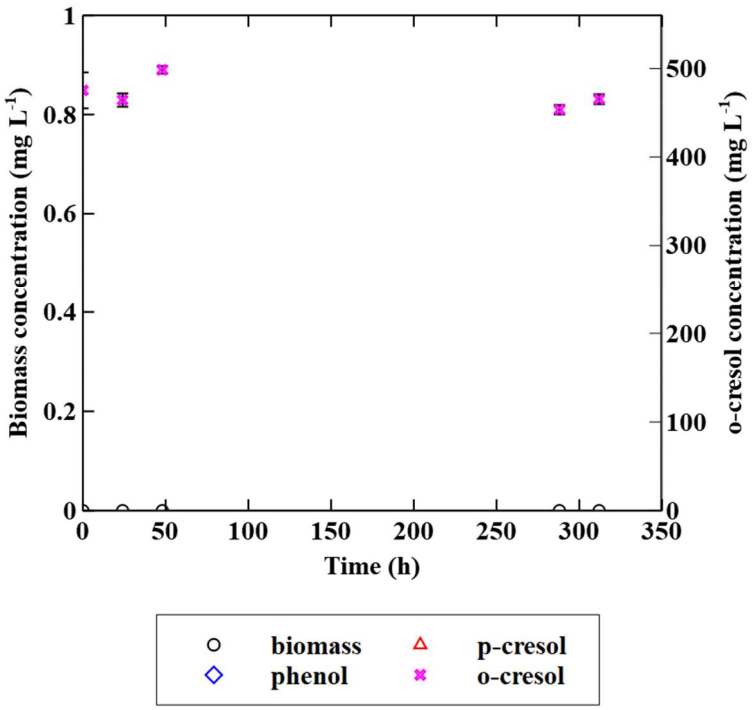

Figure D.6 Control experiments results: (A) phenol; (B) p-cresol; (C) o-cresol

For uncertainties calculation, two tables are presented below as examples for the batch (Table D.1) and the continuous systems (Table D.2). In batch system, the standard deviation of biomass concentration was calculated via multiplying the standard deviation of optical density by the biomass calibration curve coefficient. The procedure was based on error propagation. The same procedure was applied to calculate the standard deviation of substrate concentration in case of mono-substrate experiments. The standard deviation of phenolic compounds concentrations in case of multi-substrate system was calculated using three concentration readings that HPLC provided directly.

Table D.1 Standard deviation calculation for biomass concentration

Measurement No.	Optical density	Average	Standard deviation	Biomass standard deviation (mg L^{-1})
1	0.22			
2	0.21	0.22	0.01	4.73
3	0.23			

For continuous system, the uncertainty calculation is shown below. The standard deviations of loading rate, removal rate, and removal percentage were calculated using three set of data obtained after establishment of steady state conditions at each operating condition. Each set has an influent sample and an effluent sample. The concentrations were in mg L^{-1}. The example shown is p-cresol concentration when CPBB was used for phenol and p-cresol binary-biodegradation.

Table D.2 Standard deviation calculation for circulating packed bed bioreactor data

Measurement No.	Influent samples (mg L^{-1})	Effluent samples (mg L^{-1})	HRT (h)	Loading rate (mg $L^{-1}h^{-1}$)	SD	Removal rate (mg $L^{-1}h^{-1}$)	SD	Removal percentage	SD
1	302.32	63.23	3.61	83.74		66.22		0.790851	
2	294.42	55.43	3.61	81.55	1.44	66.20	2.38	0.811732	0.02
3	304.24	50.3	3.61	84.27		70.34		0.83467	

For toxicity assessment, standard deviations were calculated using duplicated results. For example, the toxicity of influent containing 300 mg L^{-1} phenol was tested using 4 watch glasses. Two of the watch glasses were used to test the toxicity of the influent samples. Another two were used for control experiments. All shrimp larvae remained alive in the control experiments after 2 h exposure. Therefore, survival percentages were 100% and 100%. On the other hand, the survival percentages of shrimp larvae subjected to the exposure to the influent samples were 0.41 and 0.28. Thus, the standard deviation was 0.1.